Development of an Extended Environmental Multimedia Modeling System (EEMMS)

Jing Yuan

A Thesis

in

The Department

of

Building, Civil and Environmental Engineering

Presented in Partial Fulfillment of the Requirements for the Degree of Doctor of Philosophy (Civil Engineering) at

Concordia University

Montreal, Quebec, Canada

December 2009

Your file Votre référence
ISBN: 978-0-494-67381-2
Our file Notre référence
ISBN: 978-0-494-67381-2

ABSTRACT

All pollutant contamination problems have both short and long term impacts on ambient air, water, and soil environments. Previous environmental pollution control programmes mainly focused on a single environmental medium (e.g., groundwater). Traditional environmental multimedia models (EMM) usually simulate pollutants' fate and transport in separate zones, based on one-dimensional, first-order mechanisms. This may lead to biased results and simulation errors.

In this study, firstly, a new extended environmental multimedia model system (EEMMS) was set up, which includes four sub-modules (sources, air quality, unsaturated zone, groundwater) on a regional spatial-temporal scale. Three different approaches were evaluated for solving multi-dimensional coupled pollutants equations using experimental data from the literature: a) EEMMS/FEM (numerical finite element method); b) EEMMS /FDM (numerical finite difference method); and, c) EEMMS /analytical method. Furthermore, three validations related to the three approaches are conducted. First, experimental results from a pilot scale landfill were used to verify the spatial temporal accuracy of predicted emission fluxes and concentrations in both numerical spatial and temporal scale. Further systematic model validations were implemented and tested comparing with the dual domain mass transfer model and 2-D analytical model. Complicated 3-D real site validation was conducted through the Trail Road Sanitary Landfill site. 3-D reasonable results have been obtained through the comparisons of

analytical and numerical solutions (FDM and FEM) in non-uniform and unsteady conditions. Implementing the EEMMS/FEM solution in the above three validations was found to be better than that of EEMMS/FDM, and EEMMS /analytical solutions. EEMMS/FEM solution also provided more stabilization technique, a better mesh that minimizes the error or even a faster solution. In addition, given a large amount of uncertainties associated with EMMS practices, sensitivity analyses approach such as retardation factor, Peclet number (Pe), hydraulic conductivity, bulk density, porosity, were embedded into the developed EEMMS. Lastly, the new EEMMS model containing both new environmental multimedia system (EMS) and Monte Carlo Method (MCM) was developed to an integrated tool for the risk assessment of contaminants.

The new EEMMS would serve as a risk assessment tool to address the fate and transport of the pollutants in complex, multimedia environments and subsequently to help in the management of the resulting environmental impacts.

Acknowledgements

Reflecting back on these enjoyable and painful years of Ph.D study, I would like to express my gratitude to all those people who helped, supported and accompanied me.

First of all, I would like to express my great appreciation to my advisor, Dr. Maria Elektorowicz. As my teacher and mentor, she guided me into the wonderful world of scientific research. I feel very fortunate to sit in her class on the first day of my study. Her guidance on numerical modeling is critical for completing this dissertation. Her support and suggestions on my life and future plans are invaluable. I will always remember her encouragement and trust for me. Her good personality will affect my whole life.

I would like to thank my advisor, Dr. Zhi Chen, for supporting me, and for providing motivation and guidance throughout my dissertation research. I am indebted to him for his availability, inspiration, criticism, and optimism. His technical and editorial advice is essential to the completion of this dissertation.

My thanks also go to Drs. Pascale Biron, Andreas Athienitis and Paul P. Fazio for serving on my dissertation committee, for contributing their time and offering valuable comments on my research work.

Last, but not least, I am greatly indebted to my devoted family, especially my son, Zhenghao Huang. I appreciate their strong confidence in my ability to accomplish my research goals. Their encouragements and supports have been the true origins of completing this work. Their love forms the root of my happiness.

This dissertation is supported in part through a grant from the Natural Sciences and Engineering Research Council of Canada (NSERC).

Table of Content

List of Tables.......................... xiii

List of Figures.......................... xv

List of Acronyms.......................... xxii

Chapter 1 Introduction.......................... 1

1.1 Definition.......................... 1

1.2 Challenges in Modeling of Multimedia Environmental Issues.......................... 1

1.2.1 Multidimensional Dispersing.......................... 2

1.2.2 Multiphase.......................... 2

1.2.3 Complex Characteristics.......................... 3

1.2.4 Complex Processes.......................... 8

1.3 Review of Related Research.......................... 11

1.4 New Study.......................... 16

1.5 Research Goals.......................... 19

1.6 Research Objectives and Steps.......................... 20

1.7 Organization of the Dissertation.......................... 22

1.8 Summary.......................... 24

Chapter 2 Literature Review.......................... 25

2.1 Literature Survey of Existing Single-Media Models.......................... 26

2.2 A Literature Survey of Existing Environmental Multimedia Models.......................... 33

2.2.1 CalTOX 33

2.2.2 MEPAS 35

2.2.3. MMSOILS 37

2.2.4. ISMCM 39

2.3 Risk Assessment Associated With the Multimedia Pollution Problems 42

2.3.1 FRAMES-HWIR 43

2.3.2 TRIM 43

2.3.3 MIMS 44

2.3.4 3MRA. 44

2.3.5 CHARM (chemical hazard assessment and risk management) 45

2.3.6 Monte Carlo Method (MCM) 45

2.4 Summary 47

Chapter 3 Methodology of the Study 51

3.1 Modeling Approach 52

3.2 Development of the General Governing Equations of EEMMS 53

3.2.1 The Conceptual Model and Governing Equations 59

3.2.2 Source Module and Governing Equations 60

3.2.3 Unsaturated Zone Module and Governing Equations 63

3.2.4 Saturated Zone (Groundwater) Module and Governing Equations 64

3.2.5 Air Module and Governing Equations 65

3.3 Initial and Boundary Conditions 66
3.3.1 Initial and Boundary Conditions in 1-D 66
3.3.2 Initial and Boundary Conditions in 2-D 67
3.3.3 Initial and Boundary Conditions in 3-D 70
3.4 Integrated Model Flux Transfer 72
3.4.1 Integrated Model Flux Transfer in 1-D 72
3.4.2 Integrated Model Flux Transfer in 2-D and 3-D 74
3.5 Integrated Risk Assessment 76
3.5.1 Description of the Integrated Risk Assessment Approach 77
3.5.2 Strategy for Deciding on Sample Size 78
3.5.3 Monte Carlo Method to Assess Model Uncertainty 79
3.5.4 Characterization of the Risk 80
3.6 Solutions Techniques for Multidimensional Equations 82
3.7 Consideration of Fate Mechanisms in the EEMMS 83
3.7.1 Different Processes in the EEMMS 83
3.7.2 Sensitivity Analysis in the EEMMS 87
3.8 Model Input and Output 92
3.9 Summary 94
Chapter 4 Systematic Model Verification in 1-D through Analytical and Numerical Comparison with Extensive Data from the Literature 96

4.1 A Complete Case Study ... 98

4.1.1 Introduction ... 98

4.1.2 Modeling Flux Results ... 101

4.1.3 Comparison with Literature Data ... 105

4.2 Model Validation ... 107

4.3 Discussion ... 112

4.4 Summary ... 113

Chapter 5: Systematic Model Verification in 2-D through Analytical and Numerical Comparison with Extensive Data from the Literature ... 114

5.1 Systematic Model Verification in 2-D: Case Study 1 ... 115

5.1.1 Introduction ... 115

5.1.2 Numerical Modeling Approach ... 116

5.1.3 Results ... 118

5.1.4 Discussion ... 127

5.1.5 Summary ... 127

5.2 Validation in 2-D: Case Study 2 ... 128

5.2.1 Introduction ... 128

5.2.2 Problem Description ... 130

5.2.3 Basic Results ... 132

5.2.4 Discussion ... 143

5.2.5 Summary ... 144

5.3 Discussion ... 144

5.4 Summary ... 145

Chapter 6 Validation of EEMMS through Analytical and Numerical Comparison with Field-Scale Data for Benzene Dispersion ... 148

6.1 Introduction the Dispersion of Benzene at Trail Road Landfill Site ... 148

6.1.1 Site Information of the Trail Road Landfill Site ... 148

6.1.2 Geological Condition of the Trail Road Landfill Site ... 150

6.1.3 Climate Conditions of the Trail Road Landfill Site ... 151

6.2 Data Collections ... 152

6.2.1 Collections and Estimation of Model Data ... 152

6.2.2 Collections of Pollutants' Physical-Chemical Properties ... 156

6.3 Simulation Results of Benzene and Comparison with Observed Data at Trail Road Landfill Site in 3D ... 157

6.3.1 Model Setting and Topography ... 157

6.3.2 Current Groundwater Flow Direction and Water Table ... 159

6.3.3 Concentration Comparison Based on Current Data ... 161

6.4 Discussion ... 164

6.5 Summary ... 165

Chapter 7 Sensitivity Analysis and Integrated Risk Assessment ... 166

7.1 Introduction 166

7.2 Sensitivity Analysis 167

7.2.1 Peclet Number (Pe) 167

7.2.2 Retardation Factor 171

7.3 Integrated Risk Assessment for the Trail Road Landfill Site 173

7.3.1 Monte Carlo Simulation for Uncertainty Analysis and Risk Assessment 173

7.3.2 Risk Quotient (RQ) Evaluation 179

7.4 Integrated Risk Assessment Results 180

7.5 Summary 186

Chapter 8 Discussion 188

8.1 Discussion of Numerical Method's Sensitivity 188

8.2 Discussion of Integrated Risk Assessment 195

8.3 Other Factors Affecting the Pollutants' Transport 201

Chapter 9 Conclusion, Contribution and Future Work 203

9.1 Conclusions 203

9.2 Research Contributions 207

9.3 Recommendations for Future Work 210

References 212

Appendix 235

A: Finite-Difference Method (FDM) 235

B: Finite-Element Method (FEM) 237

C: Finite-Difference Method (FDM) for Two Dimensional Model 240

D: Partial Matlab Code 246

List of Tables

Table 2-1 A survey of the related modeling methods 26

Table 2-2 Comparison of single-media model software 30

Table 2-3 Comparison of multi-media models 41

Table 3-1 Initial and boundary conditions 69

Table 3-2 Four typical scenarios with different processes 83

Table 4-1 Input parameters for air module (Stephenw and Karsten, 2003) 99

Table 4-2 Input parameters for landfill module (Lin and Hildemann, 1995) 99

Table 4-3 Input parameters of unsaturated zone module (Domenico, 1987) 100

Table 4-4 Input parameters of saturated groundwater module (Carnahan and Remer, 1984)

.... 100

Table 4-5 Modeling flux outputs results to compare the traditional and new EEMMS . 102

- 102

Table 4-6 Input parameters for modeling the mass flux of benzene (Rickabaugh, 1990)

.... 109

Table 4-7 Comparison of the flux results generated from the EEMMS using the numerical (FEM and FDM) and analytical approaches and Rickabough's(1990) experimental results

.... 111

Table 5-1 Input parameters for modeling the mass flux of a point source (Zheng and Wang,

1998) 116

Table 5-2 2D EEMMS/FEM model flux results at depth = 200 m at different times after a contaminant spill 127

Table 5-3 Mesh and grid details.... 131

Table 5-4 Summary of wind direction and pollutant coefficient.... 139

Table 5-5 Modeling tritium flux outputs results of EEMMS at different times 142

Table 6-1 Climate information of landfill site 152

Table 6-2 Physical properties and environmental conditions in the landfill site.... 153

Table 6-3 Input parameters related to pollutants' chemical properties 157

Table 6-4 Comparison of modeling results and observed benzene.... 162

Table 6-5 Groundwater quality standard for benzene.... 165

Table 7-1 Summary of risk assessment results 181

List of Figures

Figure 1-1 Generalized phases in the generation of landfill gases (I=initial adjustment, II= transition phases, III= acid phase. IV= methane fermentation. And V= maturation phase. (George et al., 1993; Pohland, 1994) 6

Figure 1-2 Sources of pollutants of groundwater 9

Figure 3-1 Comparison of the traditional and extended multimedia models........ 51

Figure 3-2 Flow chart depicting the elements of the proposed approach 52

Figure 3-3 EEMMS conceptual model 60

Figure 3-4 A schematic diagram of a 2-D modeling domain........ 68

Figure 3-5 A schematic diagram of a 3-D modeling domain........ 70

Figure 3-6 Integrated multimedia box model on non-uniform conditions 73

Figure 3-7 Deterministic analysis (Kamboj et al., 2002)........ 77

Figure 3-8 Integrated risks used in EEMMS 77

Figure 3-9a Normalized “a” scenario for benzene contamination........ 85

Figure 3-9b Normalized “b” scenario for benzene contamination 85

Figure 3-9c Normalized “c” scenarios for benzene contamination 85

Figure 3-9d Normalized “d” scenario for benzene contamination 86

Figure 3-10 2-D point source contaminant plume at bulk density=500 kg m^{-3} 89

Figure 3-11 2-D point source contaminant plume at bulk density=2000 kg m^{-3} 89

Figure 3-12 2-D point source contaminant plume at bulk density=4000 kg m^{-3} 90

Figure 3-13 2-D point source contaminant plume at hydraulic conductivity =0.11 m d^{-1} 91

Figure 3-14 2-D point source contaminant plume at hydraulic conductivity =0.22 m d^{-1} 91

Figure 3-15 2-D point source contaminant plume at hydraulic conductivity =0.44 m d^{-1} 92

Figure 3-16 Modeling outline and the expected outcomes 93

Figure 4-1 Validation framework chart of the EEMMS 97

Figure 4-2 Type of site modeled 98

Figure 4-3 EEMMS numerical and analytical solutions in four zones 101

Figure 4-4 Distribution of uniform vertical fluxes (mg m^{-2} d^{-1}) 104

Figure 4-5 Distribution of non-uniform vertical fluxes (mg m^{-2} d^{-1})............................ 104

Figure 4-6 Comparison of different models' prediction of subsurface flux for benzene 105

Figure 4-7 Benzene concentration profile at the bottom of the unsaturated zone 106

Figure 4-8 Benzene concentration profile at the bottom of the saturated zone 107

Figure 4-9 Landfill leachate and gas composition experimental setup.......................... 108

Figure 4-10 Comparisons between numerical, analytical, and experimental results.......110

Figure 5-1 Definition of the point source transport problem 115

Figure 5-2 Finite element meshes for 2-D point source case study 118

Figure 5-3 2-D point source contaminant plume at time=30 days.................................119

Figure 5-4 2-D point source contaminant plume at time=60 days..................................119

Figure 5-5 2-D point source contaminant plume at time=100 days............................... 120

Figure 5-6 3-D point source contaminant plume at time=100 days 120

Figure 5-7 Comparison of the 2D EEMMS numerical and analytical concentrations ... 122

(mg m^{-3}) results at 30 days from a continuous point source 122

Figure 5-8 Comparison of the 2D EEMMS numerical and analytical concentrations ... 123

(mg m^{-3}) results at 60 days from a continuous point source 123

Figure 5-9 Comparison of the 2D EEMMS numerical and analytical concentrations ... 123

(mg m^{-3}) results at 100 days from a continuous point source 123

Figure 5-10 2D EEMMS/FEM model calculations of total flux relative to a point source at different times after a spill 125

Figure 5-11 2D EEMMS/FEM model calculations of dispersive solute flux relative to a point source at different times after a contaminant spill 125

Figure 5-12 2D EEMMS/FEM model calculations of advective solute flux relative to a point source at different times after a contaminant spill 126

Figure 5-13 Definition of the environmental multimedia transport problem 130

Figure 5-14 Finite element grids for environmental media 131

Figure 5-15 Geometry used for numerical simulation and the relevant coordinate system 132

Figure 5-16 2-D EEMMS/FEM point source contaminant plume at time=328 days 133

Figure 5-17 2-D EEMMS/FEM point source contaminant plume at time=1080 days ... 134

Figure 5-18 2-D EEMMS/FEM point source contaminant plume at time=1440 days ... 134

Figure 5-19 2-D EEMMS/FEM point source contaminant plume at time=1800 days... 135

Figure 5-20 Simulated tritium plume at 328 days after injection with the analytical solutions at MADE site (Feehley et al., 2000) 135

Figure 5-21 2-D point source hydraulic head and stream function solutions (EEMMS/FEM) 137

Figure 5-22 Contour of hydraulic head and observed heads at MADE site (Sudicky, 1989; Zheng and Jiao, 1998) 137

Figure 5-23 Wind direction roses diagram 140

Figure 5-24 Pollutant coefficient roses diagram 140

Figure 5-25 Concentration contour of tritium gas from the MADE site (unit: pCi mL^{-1}) 141

Figure 6-1 Location and map of Trail Road landfill in Ottawa 149

Figure 6-2 Leachate collection systems of Trail Road landfill in Ottawa 150

Figure 6-3 North to south cross section of site (Dillon et al., 2002 and 2005)............... 151

Figure 6-4 3D model grid of the site in study area 158

Figure 6-5 3D bottom topography of the site in study area 159

Figure 6-6 Contour of flow on the Trail Road landfill (EEMMS/FEM) 160

Figure 6-7 Contours of water table, velocity vector and its cut-section velocity 161

Figure 6-8 Concentration EEMMS /FEM contours of benzene from 2002-2006 (g m^{-3}) 163

Figure 6-9 Concentration of 3D EEMMS /FEM contours of benzene (g m^{-3}, 10 years) 163

Figure 6-10 Concentration 3D EEMMS /FEM contours of benzene (μg L^{-1}, 10 years) 164

Figure 7-1a Comparison, at indicated times, of the performance of multimedia models using different numerical and mathematical solutions for Pe=0.1 168

Figure 7-1b Comparison, at indicated times, of the performance of multimedia models using different numerical and mathematical solutions for Pe =0.5 169

Figure 7-1c Comparison, at indicated times, of the performance of multimedia models using different numerical and mathematical solutions for Pe =5 169

Figure 7-1d Comparison, at indicated times, of the performance of multimedia models using different numerical and mathematical solutions for for Pe =10........................... 170

Figure 7-2 EEMMS numerical and analytical solutions in four zones for different retardation factor values... 172

Figure 7-3 Graphical output from EEMMS probabilistic analysis of hydraulic conductivity at (1400m, 1800m) in 2016: (a) probability distribution and (b) cumulative probability distribution 176

Figure 7-4 EEMMS probabilistic analysis of bulk density at (1400m, 1800m) in 2016: (a) probability distribution and (b) cumulative probability distribution 177

Figure 7-5 EEMMS probabilistic analysis of recharge at (1400m, 1800m) in 2016: (a) probability distribution and (b) cumulative probability distribution 178

Figure 7-6 EEMMS output probabilistic analysis of benzene concentration (kg m^{-3}) at

(1400m, 1800m) in 2016 182

Figure 7-7 EEMMS output from probabilistic analysis of benzene concentration (kg m^{-3}) at (1400m, 1800m) in 2026 183

Figure 7-8 Uncertainty predictions contour maps of 95 percentile concentrations in 2016 185

Figure 7-9 Uncertainty predictions contour maps of 5 percentile concentrations in 2016 186

Figure 8-1 Subsurface concentration profile of benzene as function of depth 189

Figure 8-2 Analytical concentration results of benzene as function of depth 191

Figure 8-3 Numerical concentration results of benzene as function of depth 191

Figure 8-4 FEM concentration contour when solving the problems in point sources 193

Figure 8-5 FDM concentration contour when solving the problems in point sources 194

Figure 8-6 Concentration contour for standard C=20 (pCi mL^{-1}) for tritium after 1800 days 197

Figure 8-7 Concentration contour for standard C=1 μg L^{-1} after five years 198

Figure 8-8 95-percentile risk quotients associated with the benzene criterion issued by the Health Canada (1 μg L^{-1}) in 2016, the shaded area is RQ $\geq$ 6.2 200

Figure 8-9 5-percentile risk quotients associated with the criterion issued by the Health Canada (1 μg L^{-1}) in 2016, the shaded area is RQ $\geq$ 1 201

Figure A-1 Grid used to obtain a numerical solution to the continuity equation 235

Figure C-1 Finite difference algorithm for two-dimensional equations 241

List of Acronyms

3MRA:	Multimedia, Multipathway, and Multireceptor Risk Assessment
CalTOX:	California Department of Toxic Substance Control's Multimedia Risk Computerized Model
CAEAL:	Accutest laboratories Ltd. of Canadian Association for Environmental
CHARM:	Chemical Hazard Assessment and Risk Management
CNRC:	Canada National Research Council
DOE:	Department of Energy
DTSC:	Department of Toxic Substance Control
EEMMS:	Extended Environmental Multimedia Model System
EMMS:	Environmental Multimedia Model System
EPA:	Environmental Protection Agency
HDPE:	High Density Polyethylene
ISMCM:	Integrated Spatial Multimedia Compartment Model
LFG:	Landfills Produce Gas
LSSMM:	Linked Spatial Single-Media Models
MC	Monte Carlo
MCM:	Monte Carlo Methods
ME:	Multimedia Environment

MEPAS: Multimedia Environmental Pollutant Assessment System

MIMS: Multimedia Integrated Modeling System

MMSOILS: The Multimedia Contaminant Fate, Transport, and Exposure Model

NAPLS: Non-Aqueous Phase Liquids

PCE Tetrachloroethylene

PME: Pollutant Multimedia Environment

TRIM: Total Risk Integrated Methodology

USGS: United States Geological Survey

Symbols used in the modules of EEMMS

θ : Porosity [dimensionless]

Ω : Area of contamination, defined in equation [3.21], [L^2]

α_x : Dispersivity in the x coordinate directions [L]

α_y : Dispersivity in the y coordinate directions [L]

α_z : Dispersivity in the z coordinate directions [L]

D_x : Dispersion coefficient in x coordinate direction [$L^2 T^{-1}$]

D_y : Dispersion coefficient in y coordinate direction [$L^2 T^{-1}$]

D_z : Dispersion coefficient in z coordinate direction [$L^2 T^{-1}$]

C_α^k : Concentration of the non-inert α component in p-phase expressed as the mass of α per phase volume in the k^{th} layers [ML^{-3}]

$J^{k}_{\alpha i}$: Mass flux density of α per porous media cross section in the i-direction [$ML^{-1}T^{-1}$]

R^{k}_{α}: Net mass transfer rate per porous medium volume of species α into (+) or out (-)[ML^{-3}]

λ_{α}: Apparent first–order decay coefficient [dimensionless]

S^{k}: Saturation in the k layer [dimensionless]

$D^{k}_{\alpha ij}$: Dispersion tensor [$L^{2}\,T^{-1}$]

V^{k}_{i}: Seepage or linear pore water velocity [$L\,T^{-1}$]

C_{α}: Contaminant concentration of the different α components [ML^{-3}]

m_{0}: Rate of release of the solute from the point source at time zero [$M\,T^{-1}$]

$\psi_{1}(y,t)$: Pollution flux rate per unit area, defined in Equation [3.21] [$ML^{-1}T^{-1}$]

a: Volumetric air content of the soil [dimensionless]

A: Area of the plane of diffusion [L^{2}]

A_x: Length parallel to groundwater flow [L]

A_y: Length orthogonal to groundwater flow [L]

C_a: Mass of contaminant absorbed [$M\,L^{-3}$]

C_d: Mass of contaminant dissolved in the aqueous phase [$M\,L^{-3}$]

d: Thickness of landfill cover [L]

D_g: Gaseous diffusion coefficient [$L^{2}\,T^{-1}$]

D_g^a: Gaseous diffusion coefficient in air [L^2 T^{-1}]

D_l: Diffusion coefficient [L^2 T^{-1}]

D_l^w: Liquid diffusion coefficient in water [L^2 T^{-1}]

D_T: Coefficient of transverse dispersion [L^2 T^{-1}]

D_{xx}, D_{yy}, D_{zz}: Principal components of the dispersion tensor [L^2T^{-1}]

D_{xy}, D_{xz}, D_{yx}: Cross terms of the dispersion tensor [L^2T^{-1}]

D_{yz}, D_{zx}, D_{zy}: Cross terms of the dispersion tensor [L^2T^{-1}]

F_a: Aqueous and gaseous phase advective flux [M L^{-2} T^{-1}]

F_g: Diffusive vapour flux [M L^{-2} T^{-1}]

F_l: Diffusive flux of dissolved solute [M L^{-2} T^{-1}]

f_{ocsat}: Organic carbon fraction [dimensionless]

F_t: Total of diffusive and advective fluxes in gaseous and dissolved phases released from landfill [M L^{-2} T^{-1}]

h: Hydraulic head [L]

H: Aquifer mixing zone thickness [L]

k : Overall mass transfer coefficient through the top cover [L T^{-1}]

K_d : Distribution coefficient [dimensionless]

K_H Henry's law constant [dimensionless]

K_i: Principal component of the hydraulic conductivity tensor [LT^{-1}]

K_{oc}: Organic carbon partition coefficient [L^3 M^{-1}]

k_t: Mass transfer coefficient in the air-soil boundary layer [L T^{-1}]

L: Total depth of landfill, constant [L]

n: Volumetric water content at field capacity [dimensionless]

Pe: Peclet number [dimensionless]

R: Retardation factor [dimensionless]

$t_{1/2}$: Half-life [T]

v: Mean velocity of fluid [L T^{-1}]

v_G: Gaseous velocity [L T^{-1}]

v_L: Liquid velocity [L T^{-1}]

V_x,: Seepage velocity in x coordinate direction [L T^{-1}]

V_y: Seepage velocity in y coordinate direction [L T^{-1}]

V_z: Seepage velocity in z coordinate direction [L T^{-1}]

Z: Landfill depth, variable [L]

z_{wt}: Water table depth [L]

ρ_b: Bulk density [M L^{-3}]

ρ_{unsat}: Bulk density of unsaturated zone [M L^{-3}]

φ_{un}: Porosity of unsaturated zone [dimensionless]

Symbols used in the algorithm equations

A_{ik}:	Interpolation functions, or basis functions at nodal point k
A_{jl}:	Interpolation functions, or basis functions at nodal point l
C_{kj}:	Concentration function at nodal point k
C_{li}:	Concentration function at nodal point l
FDM:	Finite difference method
FEM:	Finite element method
HQ:	Hazard quotient
KEC:	Known environmental criteria
N_x:	Total number of nodes on x-axis
N_y:	Total number of nodes on y-axis
ODEs:	Ordinary differential equations
PDF:	Parameter probability density function
Pe:	Peclet number
PEC:	Predicted environmental concentration
PNEC:	Predicted no effect concentration
PRA:	Probabilistic risks assessment
RQ:	Risk quotient
t:	Time interval [T]
Δx:	Grid spacing [L]
z:	Space interval [L]
Δt :	Step sizes of the variables t [T]
Δz:	Step sizes of the variable [L]

Chapter 1 Introduction

1.1 Definition

The Canada National Research Council (NRC) (2005) created a definition of "multimedia source zone" as a saturated and unsaturated zone containing hazardous substances, pollutants, or contaminants that act as a reservoir that sustains a contaminant plume in groundwater, surface water (landfill), soil or air, or acts as a source for direct exposure. Its volume is or has been in contact with separate multiphase contaminant (liquid, air, and solid).

1.2 Challenges in Modeling of Multimedia Environmental Issues

Modeling of multimedia environmental issues is extremely complex due to the intricacy of the systems with the consideration of many factors. In this research, typical challenges associated with multimedia environmental systems, include spatial and temporal scale effects, dimensionality, different processes, data insufficiency, model's rationality, variability, uncertainty, error analysis, and risk analysis (Coulibaly et al., 2004). Whereas, this research is needed to acquire further knowledge and understanding of different types of factors (e.g., different characteristics, different processes, multimedia, multiphase, multidimensional solutions) inherent in environmental multimedia environmental issues, how these factors affect the systems, how rational the model tools, and how is the error and risk analysis. However, as models become more complex to better represent integrated environmental multimedia systems, achieving this goal becomes more difficult. Due to the limited time, only some of the important issues that need to be addressed in relation to the incorporation of environmental multimedia modeling are discussed.

1.2.1 Multidimensional Dispersing

Most of the traditional environmental multimedia models are one-dimensional models. Even the multidimensional models have a static structure with members of dimensions computed in a unique way, such as analytical mesh dispersing or finite difference mesh way. However, multidimensional data is often characterized by descriptors that can be obtained by various computation modes, such as FEM (Jang and Aral, 2007; Cooke and Kerry, 2008). In this research, the definitions of multi-species multidimensional (i.e. 2D or 3D) models include other solution methods such as finite element methods.

1.2.2 Multiphase

Multiphase can also affect transportation of the pollutants. For example, recharge of the surface layer during rain events can lead to dissolution of solid phase explosives and subsequent transfer of explosives' mass to soil pore water and perhaps groundwater media (Ferguson and Kaddouri, 2004). This highlights that there are interactions occurring between phases; consequently, more inter-media transfers should be considered.

1.2.3 Complex Characteristics

In the present paper, the characteristics of multimedia contaminants in multiphase and in transportation and transformation models are investigated to determine how contaminants are distributed within the multimedia zone. Considering the range of contaminant transport, fate and behavior in the environment, and the environmental behavior of inorganic and organic chemicals in multimedia environments, including water, air, sediment and biota, the characteristics of the pollutant-releasing source are extremely complicated (Coulibaly et al., 2004). In this research, the focus is on the site characteristics, source characteristics and surrounding environment and the characteristics of contaminants such as reactivity and partitioning behavior in environmental media. Among this, source characteristics and the characteristics of contaminants are the two main considerations.

Pollutants sources, such as landfill, which was mainly used in this research, can be defined as the engineered deposit of waste into land in such a way that the pollution or the harm to the environment is minimized and through restoration, providing additional land for other purposes. Al-Yousfi (1998) classified landfills into three general categories according to their content: sanitary, secure and controlled landfills. Sanitary landfills are the most common and contain municipal solid wastes. Secure landfills are designed to hold hazardous waste, and the controlled landfills are designed for leachate and gas management with the possibility of co-disposal of municipal, industrial as well as hazardous wastes.

A sanitary landfill is a land disposal site employing the method of disposing solid waste on land in a manner that minimizes environmental hazard by spreading the solid wastes to the smallest practical volume, and applying and compacting cover material at the end of each operating day (Zacharof and Butler, 2004b). Accordingly, sanitary landfills involve two conditions of operation. Firstly, it requires a minimum daily cover of soil or an inert material in order to conserve the space available for filling. Secondly, it needs pollution prevention measures of the surface or ground waters, air and other environmental elements in the surrounding setting.

The main environmental problems associated with land filling of wastes are the production of leachate and landfill gases (CO_2, CH_4, and H_2S). At most large landfills, carbon dioxide (CO_2) and methane (CH_4) are the principal gases and represent over 95% of landfill gas (USEPA, 1995; Kortegast and Ampurch, 1997). Leachate is any liquid that has percolated through or drained from hazardous or solid waste and has extracted the dissolved or suspended materials from it. This liquid may progressively contain high concentrations of organic and inorganic materials, including toxic compounds and heavy metals. Leachates can cause environmental problems if allowed to flow out of the landfill into the surrounding soil, and perhaps to surface and groundwater bodies, thus, it has to be managed.

Another potential environmental risk caused by landfill practice is the production and migration of decomposition gases (CO_2, CH_4, and H_2S) due to the anaerobic digestion of solid wastes (Fadel et al., 1996). Carbon dioxide is a green house gas, while methane accounting for about 60% of the total gas production in a landfill is a flammable gas and can explode when present with sufficient amounts of oxygen. Carbon dioxide is sparingly soluble in water, thus forming carbonic acid causing mineralization of groundwater. Other potential risks linked to landfill practice include dissolution of heavy metals in groundwater and odor problems caused from hydrogen sulphides production.

The stabilization process in a landfill consists of a sequence of physical, chemical and biological reactions. Organic matters in the landfill decompose either aerobically or anaerobically. Aerobic bacteria actively decompose these materials in the presence of oxygen. In the absence of (or depleted) oxygen, the degradation process proceeds anaerobically, to produce, as end product, a mixture of gas containing mainly carbon dioxide, CO_2, and methane, CH_4, in varying proportions. Another consequence of the degradation process is the settlement of the waste. At the end of fermentation process, the residual content is referred to as residual matter. Both aerobic and anaerobic biological activities occur in landfills, which result in stabilization. Oxygen concentration is rapidly exhausted at the initial stages of stabilization. Thus anaerobic biological processes play a key role in landfill stabilization. The anaerobic processes, which lead to landfill stabilization, were described in five phases by George et al. (1993) and Pohland (1994) (Picture 1-1). These phases are: initial adjustment, transition, acid formation, Methane formation and final maturation.

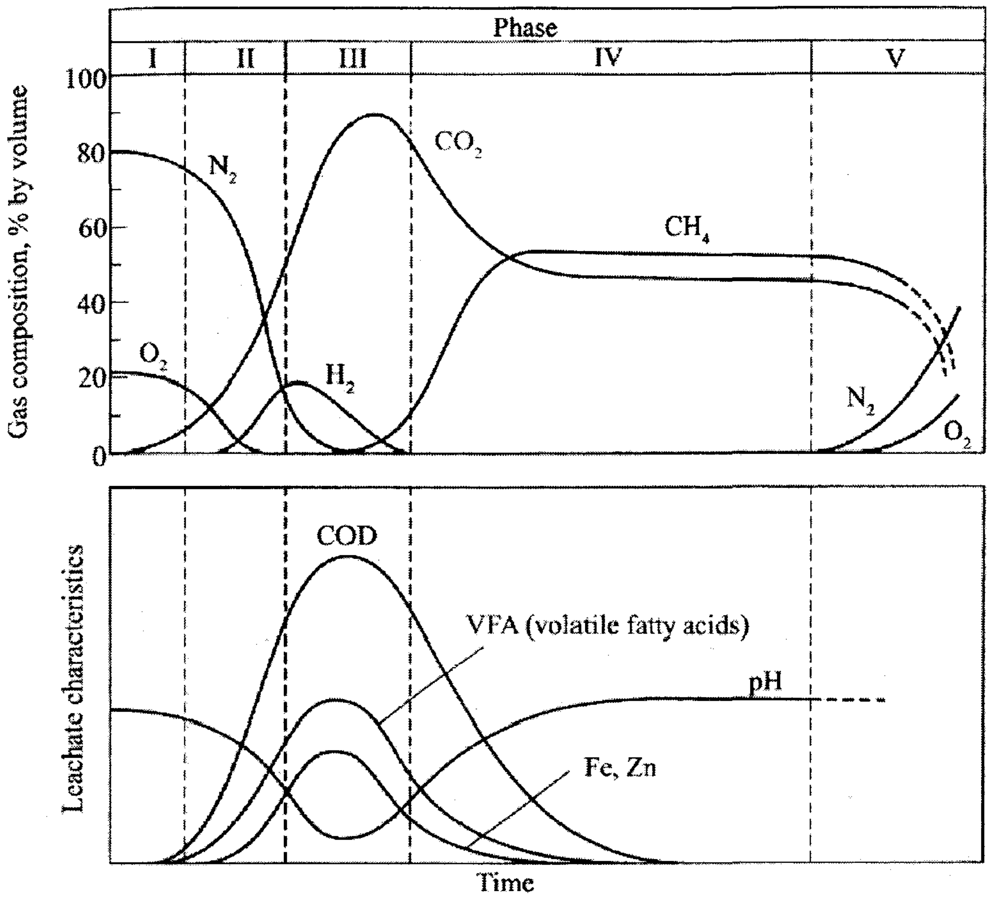

Figure 1-1 Generalized phases in the generation of landfill gases (I=initial adjustment, II= transition phases, III= acid phase. IV= methane fermentation. And V= maturation phase. (George et al., 1993; Pohland, 1994)

Benzene will be chose the main contaminants of this research. The main characteristics of it are: clear, colorless, volatile, highly flammable liquid with a characteristic sickly, sweet odor. Benzene is chemically characterized by six carbon atoms linked in a planar symmetrical hexagon (equal C-C bond lengths) with each carbon atom attached to a hydrogen atom. The electronic structure of that geometry makes benzene unusually stable. It does react with other compounds mainly by the substitution of a hydrogen atom (USEPA, 1993b). Benzene is soluble in water and miscible with alcohol, chloroform, ether, carbon disulfide, carbon tetrachloride, glacial acetic acid, acetone, and oils. Benzene is easily vaporized, especially in high temperature. Benzene occurs in nature as emissions from volcanoes and forest fires, and as a natural constituent of crude oil and plant volatiles (HSDB, 1995). Indoor benzene sources include tobacco smoke, heating and cooking systems, evaporation from various products used in a home or work area, and drift from outdoor automobile exhaust. The predominant sources of total benzene emissions in the atmosphere are gasoline fugitive emissions and gasoline motor vehicle exhaust. Mobile sources contribute 85% and industry-related stationary sources 15% of the emissions. Approximately 70% of mobile source benzene emissions can be attributed to on-road motor vehicles, with the remainder attributed to non-road mobile sources (USEPA, 1993b).

The office of environmental health hazard assessment reviews risk assessments submitted under the air toxics "hot spots" program (OEHHA). Of the risk assessments reviewed as of April 1996, benzene was the major contributor to the overall cancer risk in 85 of the approximately 550 risk assessments reporting a total cancer risk equal to or greater than 1 in 1 million and contributed to the total cancer risk in 284 of the these risk assessments. Benzene was also the major contributor to the overall cancer risk in 16 of the approximately 130 risk assessments reporting a total cancer risk equal to or greater than 10 in 1 million, and contributed to the total cancer risk in 92 of these risk assessments (OEHHA, 1996a). For non-cancer health effects, benzene contributed to the total hazard index in 52 of the approximately 89 risk assessments reporting a total chronic hazard index greater than 1. Benzene also contributed to the total hazard index in 5 of the approximately

107 risk assessments reporting a total acute hazard index greater than 1 (OEHHA, 1996b). Probable routes of human exposure to benzene are inhalation and ingestion of drinking water (USEPA, 1994a). Benzene can sensitize the myocardium to the arrythmogenic effects of epinephrine. Workers chronically exposed to benzene have shown alterations in serum levels of immunoglobulin (USEPA, 1993b);

1.2.4 Complex Processes

Lastly, to achieve successful remediation of contaminated groundwater, it is critical for engineers and scientists to possess a clear understanding of the complex transfer processes that may occur in the multimedia environment. The presence of physical and chemical heterogeneity of multimedia systems, as well as the inherent complexity associated with the transfer processes, provide for significant challenges to accurately predict the fate and transport of chemical constituents within the multimedia environment (Mccoy and Rolston, 1992). In this research, physical, chemical, and biological processes will be considered. For example, once contaminants are in the multimedia environment, processes such as non-diffusive and diffusive transfers, advection, sink, sorption, radioactive decay and biodegradation transformation will be considered. However, in the real case study, some processes do not need to be considered. For instance, Thomson et al. (1997) only considered groundwater-table fluctuation, gas density, infiltration, and temperature and exclude sorption and potential biological transformation when examining the effect of density-driven transport of volatile organic compounds using one- and two-dimensional environmental subsurface transport models.

Multimedia pollutant transports are determined not only by advection and transformation, but also by other inter-media transfers such as non-diffusive and diffusive transfers, sink, sorption, radioactive decay and biodegradation in the multi-layers, as shown in Figure1. Diffusion itself can be divided into two phenomena, diffusion with one medium (i.e. dilution) and diffusion between two adjacent media (i.e. volatilization). In the real environment, the diffusive transport is very slow and difficult to quantify. This process (diffusive in a single medium and diffusive across two media) has been and continues to be the focus of scientific investigation.

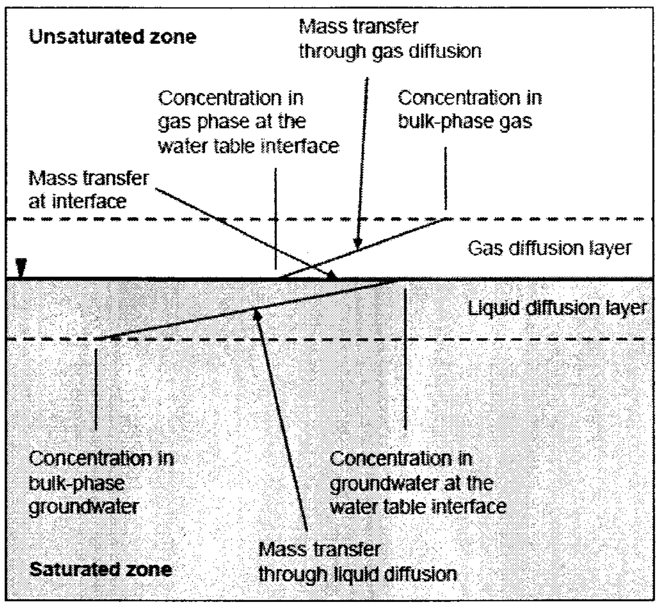

Figure 1-2 Sources of pollutants of groundwater

There are five sources of pollutants of groundwater:

1. Diffusion within a single compartment. This type of diffusive transfer is driven by the presence of a concentration gradient and is generally termed "molecular diffusion with

a phase". This process is the result of the continuous movement and mixing of the molecules from one distribution to another.

2. Diffusion between phases

This type of diffusion represents the advantage of the multimedia approach over the spatial approach in environmental modeling. Although it is often difficult to characterize, many analogies exist in other engineering fields. Processes that are described by inter-phase diffusion include volatilization (air-water transfer), sorption and desorption (water-sediment), absorption (soil-air), and water to aquatic biota transfers. While diffusion in a single medium has been described using a concentration gradient, the case is not true for inter-phase diffusion. The diffusion (i.e. volatilization) between water and air can be completed without the need for the concentrations to be equal. However, at this non-equilibrium state, the fugacity in both water and air will be equal. Thus, the inter-media diffusion is driven by the fugacity gradient and not by the concentration gradient.

(1) Air-water transfers

The volatilization of certain contaminants from water to the atmosphere is significant. Oxygen transfer between the atmosphere and the ocean is considered to have the highest overall mass transfer coefficient in nature in the order of 20 cm h^{-1} (Schnoor, 1996). There are other contaminants that readily volatilize from water to air: they include PCBs and dieldrin.

(2) Soil-air transfers

The volatilization and absorption from and to surface soils can be modeled using the inter-media diffusion. This process is important for chemicals with high vapor pressures such as TCE (trichloroethylene).

(3) Sediment-water transfers

This includes the re-diffusion of contaminants from the buried sediment layers to the water column. A major concern that arises in dredging water bodies is not only the re-suspension of sediment particles but also the availability of buried contaminant for back diffusion to the water compartment.

(4) Biota-water transfers

This relates to the diffusion of contaminant across the skin, stomach and gills of aquatic biota (Clark, 1990). Through this process a low concentration of a contaminant becomes concentrated in fish tissues (usually several orders of magnitude for chemicals with high K_{ow}). This phenomenon is referred to as bio-concentration.

1.3 Review of Related Research

Before the formal definition, efforts to assess human exposure from multiple media date back to the 1950s (Eisenbud, 1987; Whicker and Kirchner, 1987), when the need to assess human exposure to global fallout led rapidly to a framework that included transport both through and between air, soil, surface water, and groundwater. Efforts to apply such a framework to organic and inorganic toxic chemicals have been more recent and have not as yet achieved the same level of sophistication. In response to the need for the complex multimedia models in exposure assessment, a number of multimedia transport models have recently appeared. The first widely used multimedia compartment modelling for organic chemicals were the "fugacity" models proposed by Mackay (1991) and Mackay and Paterson (1982). Cohen and Ryan (1985) applied the concept of multimedia compartment modelling as a screening tool by developing the multimedia compartment model, followed by the linked spatial single-media models (LSSMM) (McDonald and Gelston, 1998), and more recently the integrated spatial multimedia compartment model (ISMCM) (Cohen and Cooter, 2002).

Given their simplicity and ease of use, compartmental mass-balance models have been widely used over the last decade. However, such models assume uniformity of compartments, a condition which obviously does not hold when the model must consider spatial-temporal variations to accurately perform risk assessment for single point contaminant sources, particularly those where the point source is located in soil. Furthermore, such models are invalid on a small scale.

A typical fugacity model, called CalTOX was one of the earliest multimedia models to explicitly address human exposure. It was developed by the office of scientific affairs in the California department of toxic substances control (McKone and Enoch, 2002). The principal representatives of LSSMM are MEPAS (McDonald and Gelston, 1998); MMSOIL (USEPA, 1988), etc. MEPAS, for instance, was developed at the U.S. Department of Energy's (DOE) Pacific Northwest laboratory to assess risks from mixed wastes at DOE facilities.

LSSMM integrates serially linked single-medium transport models for air, water, soil and other media of interest. Compared to other types of multimedia models, it can provide fine spatial and temporal resolutions, which are significant features in evaluating the risk level for exposure to hazardous contaminants. However, previous implementations of LSSMM have suffered from certain limitations: (i) an empirical algorithm was used to estimate gaseous emissions from the surface of a contaminated site, (ii) gaseous advection in the polluted soil was not considered, and (iii) leachate release from the contaminated soil was modeled to occur in a steady state.

ISMCM considers all media, biological and non-biological, in one integrated system. ISMCM includes both spatial and compartmental modules to account for complex transport of pollutants through the ecosystem. ISMCM is able to predict transport based on a sound mechanistic description of environmental processes, including estimation of inter-media transfer factors. One of the limiting factors with the ISMCM system is that it is not structured to incorporate uncertainty/variability directly into the model operation. Another limitation of the ISMCM model is the fact that the links and compartments (spatial configuration) of this model are predetermined. ISMCM was apparently not designed from the start with the necessary flexibility. Having this flexibility is not a trivial thing to request if the system is to be fully integrated. Furthermore, ISMCM includes both "well-mixed" and spatial compartments integrated through inter-media physical boundary conditions. The atmosphere and water compartments are treated as uniform multiple compartments. Soil is expressed as a spatial compartment. Thus a greater resolution can be gained in soil, but the spatial resolution for the air and water compartments falls short. Detailed summaries and evaluations of each of the multimedia models discussed above are given in Chapter 2.

Based on the models, the risk assessment and solutions are developed. For example, exposure to toxic chemical contaminants/pollutants is a significant risk factor for biological organisms (USEPA, 1996). Pollutant emissions impact on the surrounding air, water and soil, referred to collectively as the multimedia environment (ME). Characterization of the natural behavior of chemical contaminants/pollutants in the environment by computer pollutant multimedia environment (PME) modeling has been an important step towards environmental pollutant risk assessment and management (Labieniec et al., 1996a; Labieniec et al., 1996b). PME models can provide insight and information when data is missing, insufficient or unavailable (Droppo at al., 1993; Hsieh and Ouimette, 1994).

Early studies on PME modeling included the application of advective-dispersive transport equations (Bear, 1960; Harleman and Ramur, 1962; Bachmat and Bear, 1964). Coats and Smith (1964) incorporated a mass-transfer equation into the advective-dispersive equations that provided analytical solutions. More development and applications of PME models have been reported since the early 1980s to address major environmental pollution issues, such as superfund sites) (Mackay, 1991; Cowan et al., 1995). Most of the previous studies were based on one-dimensional (1D) analytical solutions (compartmental models) (Droppo et al., 1989; Mackay, 1991).

In the past two decades, mathematicians, engineers and hydrogeologists have successfully developed several PME analysis risk assessment systems to better understand contaminant transport in porous media (Morris and Mustafa, 2004; Jang and Mustafa, 2005). These models use analytical solutions (Carnahan and Remer 1984; Lin and Hildemann 1995) or finite difference methods (FDM) (Delshad et al., 1996; Jang and Aral, 2005; Kindlein et al., 2006; Maslia et al., 2007a). For example, Lin and Hildemann (1995) generated a general mathematical model to predict emissions of volatile organic compounds from hazardous landfills in unsaturated subsurface media. Carnahan and Remer (1984) implemented analytical solutions for the three-dimensional axisymmetric problem of solute transport in a steady field of groundwater mass transport. Delshad et al. (1996) developed the UTCHEM model/FDM numerical approach to solve the migration and dissolution of the non-uniform phase liquids. This method has not been widely accepted due to the limitations of complex boundary conditions.

The current PME models/analytical approaches often ignored temporal and spatial effects and errors that are introduced through computation and limited consideration of boundary conditions. Simple analytical approaches require assumptions to be made.

Finite difference methods (FDM) approaches to PME problems are limited, due to the complexity of the problems, the sophistication of the mathematical formulas, as well as difficulty in their implementation. Furthermore, the lack of a fixed grid or fixed coordinates can lead to numerical instability and computational difficulties, particularly in ME and complex boundary conditions (Yeh, 1990).

Finite element method (FEM) approaches to PME problems attempt to overcome the above disadvantages of the FDM approach. It is believed that FEM will eliminate the geometric constraints (i.e. complex problem domain or boundary) that are usually approximated by FDM. In addition, numerical dispersion is expected to be reduced due to the reduced discretization error. FEM has long been studied in other fields (Aulisa et al., 2006; Sun et al., 2006; Wang, 2007) and has recently been used in the analysis of multimedia field applications (Ekrem et al., 2006; Halder et al., 2006). For example, Ekrem et al. (2006) used the FEM (COMSOL Multiphysics) approach to simulate the transport of inert colloidal particles at the pore scale within an unsaturated micro-model consisting of sand grains and air bubbles. However, finite-element based computer code for solving the ME fate and transport problem in a multimedia environment is still at an early stage, and no publications were found on this subject.

1.4 New Study

Considering these current pollutant multimedia environment (PME) modeling have a lot of limitations, such as its model's rationality, its error and risk analysis, in order to mitigate these limitations and to extend previous studies on environmental multimedia models, a new extended environmental multimedia modeling system (EEMMS) was developed with verification by both numerical and mathematical methods. The developed EEMMS includes sever main improvement: (1) the consideration of flux integrated associated with multimedia transportation to make model more rational. It is useful for simulating mass transfer and fate-and-transport of chemical contaminants/pollutants. (2) The development of appropriate risk assessment based on Monte Carlo methods, which will save more time to get more field data. (3) The improvement of solutions accuracy through the use of different method approaches (e.g., FEM, FDM and analytical solutions), including model divergence correction. (4) Incorporating adaptive case validation involving the different processes including advective, dispersive transport, sink, sorption, radioactive decay and biodegradation and so on. Field validations with data from the literature case studies using several approaches (FDM, FEM, analytical) for current simulation are conducted, further systematic model validations were implemented and tested comparing with the dual domain mass transfer model (Feehley et al., 2000) and 2-D analytical model (Dmity et al., 1999). Complicated 3-D real site validation was conducted through the Trail Road Sanitary Landfill site (Dillon et al., 1995, 2002, and 2005). (6) The development of integrated frameworks for comprehensively addressing uncertainty as part of the environmental multimedia environmental modeling issues. Error analysis will be discussed too. (7) Finally, an integrated risk assessment approach based on EEMMS and Monte Carlo method is used to evaluate the long-term environmental risk impacts. The development of approaches and strategies for increasing the computational efficiency of integrated models, optimization methods, and methods for estimating risk-based performance measures will improve its risk analysis.

Normally, each of the issues needs to be researched in detail. However, when we considered the whole multimedia environmental modeling systems, some of the issues do not need to be considered in detail. For example, for a real case study validation, some detailed process such as biodegradation will be ignored according to the real site situation. The key point for this case study is to integrate the framework of the systems and to indicate its concentration and flux transportation in the multimedia environment in a multidimensional dispersing way (Thomson et al., 1997).

In summary, preliminary modeling efforts have been reported over past decades. The traditional environmental multimedia model (EMM) is often based on a one-dimensional and first-order assumption, which may cause numerical errors in the simulation results. However, more knowledge is required, especially with regard to possible long-term adverse effects risk assessments. This study presents an extended EMM (EEMMS) with an incorporation of numerical analysis. The developed EEMMS includes four component modules: an air module, a landfill module, an unsaturated zone module, and a saturated zone (groundwater) module. The modules are solved within the EEMMS framework using both FEM (finite element) and FDM (finite difference) methods. The new EEMMS is first examined through comparisons with analytical solutions for the analysis of pollutant multimedia transport under non-uniform and unsteady conditions. Sensitivity analysis is also conducted for the modeling process. The developed EEMMS will be a risk assessment tool to address the fate and transport of the pollutants in complex multimedia environments and to help the subsequent management of the resulting environmental impacts.

1.5 Research Goals

The main goals of this study are the development of Extended Environmental Multimedia Modeling System (EEMMS), based on extensions of FEM and FDM adapted to the specific research needs identified within this dissertation. The EEMMS will facilitate a more accurate prediction of the fate and transport of contaminants in multimedia environments, which

(i) allows mass conservation: pollutant mass will be conserved, and the systems will model the movement of pollutant mass over time, through a user defined, and bounded system;

(ii) will have multimedia assessment capabilities and can perform pollutant assessments in multiple media, and with multiple exposure pathways in non-uniform conditions;

(iii) will be flexible in temporal and spatial scales in multidimensional dispersing way; and

(iv) will be able to explicitly address uncertainty and variability.

The EEMMS then should be solved with analytical, numerical techniques FEM (finite element method) and FDM (finite difference method). The results obtained from EEMMS should be validated through comparison with various the field sites data and literature experiment data. At last, an integrated risk assessment approach based on EEMMS and MCM is anticipating to be applied in this thesis to demonstrate an advance application of a new system.

1.6 Research Objectives and Steps

Based on the aforementioned goals, the following three objectives with several sub-objectives are proposed. The objectives of this research can be itemized as follows:

(i) Based on the data obtained, establish a new extended environmental multimedia modeling system with acceptable accuracy which is delineated into three tasks:

(i-1). This EEMMS will include an air dispersion module, a source module, an unsaturated media module and a saturated media module. The four modules would quickly predict the indices related to waste transportation risk and lower experimental cost according to the transport parameters, landfill configuration, and interior or exterior environmental conditions;

(i-2). Examine three methodologies [finite element method (FED), finite difference method (FDM) and a mathematical method] in solving the EEMMS. To search for the near optimal parameters and to choose the best method with the minimum cost and the ability to assess the potential risk to the environment more accurately;

(i-3). Compare the new modeling with field observation and experimental data, visualize the multidimensional dispersion of pollutants in the multimedia, and include a non-uniformed input source for an unsaturated zone module.

(ii) Use the results of computational simulations to assess the potential risk to the water quality and identify the important parameters that influence the groundwater design case;

Develop an integrated risk assessment method (including Monte Carlo method) to conduct long-term risk assessment. To characterize the risk level by combining EEMMS and risk models to provide decision makers with a clear view of the risks of pollutant sources.

To find appropriate solutions, a systematic approach should be adopted. This involves four main steps.

(i) General problem definition: during this step, the chemical(s) to be modeled and the initial spatial features of the areas are determined. It will be necessary at this step to specify various types of data, or simply the sources of the data (e.g., a remote database). Data types include spatial information about the modeling areas, chemical-specific environmental data (e.g., degradation rates in various domain types), and data for the specified domain instances (e.g., soil bulk densities and organic carbon content for soil domains).

(ii) The foundation of the problem is to accurately predict the system response to the input information. Those parameters examined in the first step which greatly influence the problem objectives, will be chosen as the input variables into a simplified system model. The independent variables and process reactions used to evaluate the accuracy of the model outputs will also be examined. Once the model is established based on all the information obtained in first step, it will be able to precisely represent system characteristics, and thus accurately determine required site remediation and associated environmental assessments cost according to any input data sets.

(iii) Finding the solution to this multimedia-modeling problem is another key issue. Based on the model generated in the second step, certain optimization algorithms can be applied to search for the best set of input data, which can minimize (or maximize) the objective function. In the present study, verification is conducted by two main methods: analytical and numerical prediction. Field observation and experimental data are used to validate the results.

(iv) An important aspect of the EEMMS is the integration of sensitivity and uncertainty analyses methods into the model framework. Sensitivity analysis serves to identify important inputs with respect to outcome variance. Many of the parameters used in modeling systems are uncertain or variable. It is critical to confront sources and ranges of parameter variance for several reasons. Among them are the need to determine the range of possible outcomes of the model, and the need to determine what parameters are the important contributors to the range of outcome values generated by the model.

1.7 Organization of the Dissertation

This dissertation is organized into nine chapters. The following detailed chapters of this thesis are as follows.

Chapter 1 includes an introduction to the research topic, its significance to environmental multimedia problems, and the stated hypotheses and objectives.

Chapter 2 provides a literature review of existing environmental multimedia models, of solution methods and of risk assessment studies of transportation in multimedia area.

Chapter 3 describes the methodology developed in the present research, including the EEMMS, risk assessment method and the analytical, numerical algorithms such as governing equations, boundary considerations, and structure of the computations for the EEMMS.

Chapter 4 introduces the preliminary 1-D systematic model verification approach and sample analysis results through analytical and numerical comparison with extensive data from the literature.

Chapter 5 introduces 2-D complete case study validation combining several literatures, which use several approaches (FDM, FEM, analytical) for current simulation.

Chapter 6 presents a further field-scale validation through analytical and numerical comparison with experiment of the dispersion of benzene for Trail Road landfill site. In this chapter, the considerations of the boundary conditions in the study area, the validation of the current field data, and 3D simulation results for the study area are presented. Detailed model settings, 3D validation for the developed EEMMS.

Chapter 7 presents the risk assessment results for the Trail Road landfill site. Sensitivity analysis and integrated risk analysis are presented in this chapter too.

Chapter 8 describes the numerical derivations, validations, stability and accuracy analysis, and successful applications of EEMMS. It also discusses the factors affecting the EEMMS prediction and integrated risk assessment results.

Chapter 9 summarizes the main conclusions from the dissertation, addresses contribution to knowledge and defines future areas of research.

1.8 Summary

In summary, this chapter consists of seven sections providing an extensive review of the background and theories related to this research. It then summarizes current research big challenge and efforts, and highlights the specific research objectives and organization of this study. Finally, an integrated risk assessment approach based on EEMMS and Monte Carlo method is used to evaluate the long-term environmental impacts.

Chapter 2 Literature Review

A variety of previous studies investigated multi-media pollutant transport problems, either through single-media models or by applying analytical prediction strategies. However, since previous research was mainly focused on single-media, studies related to verify multi-media pollutant transport under non-uniform conditions are relatively sparse.

This chapter first offers the big challenges in modeling of environmental issues since it involved so many complicated factors. It introduces a general review of the background behind modeling studies related to the multimedia model systems. Finally, the chapter includes a detailed literature survey of environmental multimedia models. This survey identified several models/approaches for multimedia, multi-pathway modeling for pollution evaluation. These include the California Department of Toxic Substance Control's multimedia risk computerized model (CalTOX), the multimedia environmental pollutant assessment system (MEPAS), a kind of typical LSSMM, and the integrated spatial multimedia compartmental model (ISMCM). The findings can be used as guidance for the new extended multimedia model system being developed.

The limitations of former verification works make the numerical method a promising alternative. FEM and FDM simulation, as widely recognized, are two of the most applicable numerical methods for multimedia pollutants research. The literature survey establishes the need for the development of new approaches to implement risk assessment and management of large volumes of multimedia environmental problems.

2.1 Literature Survey of Existing Single-Media Models

Since there are so many challenges on multimedia modeling systems research, in order to simplify the problems, the single-media models that only consider one media would be considered firstly.

Considerable effort has been devoted to the media problems. The model in most cases first focuses on single-media transport processes. The structures of existing single-media models are summarized and compared in Table 2-1. Specially, Table 2-1describes the different contaminant transport and natural attenuation processes, and the solution methods.

Table 2-1 A survey of the related modeling methods

Author and Time	Description	Simulation Tool	Objectives
Harbaugh and McDonald (2004)	Unsteady-state groundwater flow and transport modeling	MODFLOW-2004 UTCHEM model—numerical model	Transient ground-water flow
Jonatham and Kindlein (2006); AL-Thani et al.(2004); Zheng and Wang (1998); Delshad et al. (1996); Fadel et al. (1996)	Several numerical models are available for a wide range of applications related groundwater flow and contaminant transport	MT3DMS — numerical model	Simulation of the fate and migration
Masters (1998); Faye (In press 2007b)	Computation of concentration of PCE in drinking water from the Tarawa Terrace WTP using results from fate and transport modeling	Materials mass balance model using principles of conservation of mass and continuity	PCE concentration in WTP finished water

Author and Time	Description	Simulation Tool	Objectives
Jang and Aral (2005)	Three-dimensional simulation of the fate, degradation	TechFlowMP — numerical in groundwater	Fate and transport and degradation
Wang and Aral (2007)	Analysis to assess impact of schedule variation of water-supply well operations on arrival of PCE at wells	Numerical; optimization	Early and late arrival of PCE at WTP
Doherty (2005); Maslia et al. (In press 2007b)	Assessment of parameter sensitivity, uncertainty, and variability associated with model simulations of ground-water flow	PEST; Monte Carlo simulation; probabilistic	Parameter uncertainty and variability
Rossman (2000); Sautner et al. (In press 2007)	Simulation of hydraulics and water quality in water-distribution system	EPANET 2; numerical	Distribution of PCE in drinking water
Morris and Mustafa (2004)	Analytical contaminant transport analysis system--ACTS.	ACTS model; analytical	Saturated and unsaturated zone
Lin and Hildemann (1995)	Analytical contaminant transport analysis in landfill	Physical analytical model	Landfill zone
Arystanbekova (2004)	Gaussian model; steady- and unsteady-state; three-dimensional; uniform and steady wind direction;	Gaussian model; analytical	Air dispersion
Jury et al. (1990) Zacharof and butler (2004);	One-dimensional, unsteady; uniform and steady infiltration rate; linear phase partitioning;	Unsaturated zone model; analytical	Unsaturated zone
Domenico (1987)	One and two-dimensional transport;	Unsaturated zone model; analytical	Unsaturated zone
Carnahan and Remer (1984)	One and two-dimensional transport;	Saturated zone model; analytical	Saturated zone

Fadel et al. (1996) introduced a one-dimensional numerical model for the generation and transport of gas and heat, in which landfill cells were treated as homogeneous media. Based on Fadel's work, Helmig (1997) conducted detailed investigations of numerical procedures and discretization techniques of fate and transport equations for subsurface modeling. In 2002, Islam and Singhal extended the model from one-component to a linear reactive multi-component transport model. Domenica (1987) suggested a mathematical model for a finite source in saturated single media environment. In 2004, Mulligan and Yong extended Dominica's work to three dimensions and considered many other factors such as decay for either radionuclides or biodegradable organics. With respect to the multimedia model's solution, traditional mathematical modeling within multimedia models has long been studied and developments have become relatively mature. For example, Morris and Mustafa (2004) implemented analytical solutions for the three-dimensional axis symmetric problem of solute transport in a steady field of groundwater mass transport. Zacharof and Butler (2004) generated a general mathematical model to predict emissions of volatile organic compounds from hazardous landfill in unsaturated subsurface media. Such traditional models assume that the solute concentration does not affect the fluid density, viscosity or the soil's hydraulic conductivity, and they do not consider the sink or sorption or adsorption. Based on those assumptions, multimedia models usually solve the four media (air, landfill, unsaturated, saturated) flow and contaminant transport separately.

However, with the addition of the multiple and inter-phase mass transfer processes to the multimedia flow and solute transport, the mathematics becomes more complicated and highly non-linear. Many numerical models have attempted to address these issues. For example, numerical modeling of 3-D groundwater flow and contaminant migration in the saturated zone has long been studied and its development has become relatively mature. Zhang and Wang (2004) gave compilations of phenomena, equations and solutions to groundwater flow and transport problems. Schroeder et al. (1994 a, b) , AL-Thani et al. (2004), Jang and Aral (2005), Doherty (2005), Jonatham and Kindlein (2006), Sautner et al. (2007), and Wang and Aral (2007)also provided several numerical models that were available for a wide range of applications related to groundwater flow and contaminant transport. However such numerical models cannot handle more complicated problems since they do not capture processes occurring, due to the presence of non-aqueous phases, sink sorption, radioactive decay and biodegradation. However such numerical models have experienced some numerical difficulties. The limitations to simulate complex boundary conditions prevent it from being widely accepted. Furthermore, it can cause excessively long execution time when a lengthy simulation is desired.

However, some single-media models software are developed, such as unsaturated zone models software, subsurface transport models software and surface water models software described here exist for a variety of applications. The structures of the reviewed single-media model software are summarized in Table 2-2.

Table 2-2 Comparison of single-media model software

Type of model	Landfill model	Air model	Unsaturated zone models			Saturated zone models	
Author, time /software	Garg A. et al (2006,2007)	Gaussian plume model (2004)	Harper et al. (2003)	Healy (1996/VS2 DT)	Schroeder et al. (1994/HELP)	Zhang and Wang (2004/ MODFLOW)	Yeh and Ward (1987/ FEMWATER)
Developer	University of Calgary	Arystanbekova	University of Guelph	USGS	USEPA	USGS	USEPA
Media	Air and water	Air	Air and water			Groundwater	
Methodology	Fuzzy synthetic	Analytical	Mass transfer Model	FDM	FDM	FDM	FDM
Dimension	1-D	3-D	2-D	2-D	2-D	3-D	3-D
Main application field	LFG (Landfills producing gas)	Simulates air pollution at instantaneous emissions	Water and solute movement in variably saturated porous media and leachate production			Groundwater flow	
Model validation	Yes	Yes	-	-	-	Kling et al. (2004)	Yes
Calibration (sensitivity analysis)	Yes	Yes	-	-	-	Yes	Yes

Note: USEPA: U.S environmental protection agency; USGS: U.S geological survey

From Tables 2-1 and 2-2 on the solutions to those single models or software, most of the numerical methods used in the early 1990's to solve the advection-dispersion equation could be classified as finite different methods (FDM) (Yeh and Ward, 1987; Schroeder et al., 1994; Delshad et al., 1996; Fadel et al., 1996; Healy, 1996; Zheng and Wang (1998); AL-Thani et al., 2004; Zhang and Wang, 2004; Jonatham and Kindlein, 2006). In FDM, the transport equation is solved in a fixed spatial grid. FDM method, which works well in flow and mass simulation, were among the earliest methods applied to transport modeling and they are still commonly used today. Finite element methods (FEM) offer the advantage and convenience of a fixed grid, are generally mass conservative, and handle dispersion-dominated problems both accurately and efficiently. They are also easy to program and implement. In FDM, the partial differential equation governing solute transport is not directly solved. Instead, a large number of moving particles are used to approximate both advection and dispersion. It is only effective in advection-dominated problems, as it essentially eliminates numerical dispersion (Tompson and Gelhar, 1990). However, the lack of a fixed grid or fixed coordinates multimedia and complex boundary conditions can lead to numerical instability and computational difficulties in FDM (Diersch and Kolditz, 2002). However, some commonly used analytical procedures, such as the method of characteristics or complex boundary conditions, do not guarantee mass conservation. In addition, FDM is usually not as computationally efficient as FEM or purely analytical methods. FEM attempts to combine the advantages of the FDM and analytical methods. The FEM approach is conceptually attractive and simulators based on this approach have recently seen a wide application in the media fate and transportation applications (Zheng and Wang, 1998). For example, Cooke and Kerry (2008) described a 2D model for predicting clogging of a landfill leachate collection system and subsequent leachate surface position (mounding). In this paper, FEM methods were first used in the single media environment problems. Jang and Aral (2007) also use a 3D finite-element-based numerical model to test the effects of density-driven advection, infiltration, and permeability on contaminant plume evolution and natural attenuation of VOCs in the subsurface system. Also, FEM was used to overcome mass-balance errors. For example, the method has been successfully applied by Rathfelder and Abriola (1994) and Lehmann and Ackerer (1998) to both the unsaturated and saturated zones in one-dimensional environmental subsurface. There are other FEM case studies that have recently been used in the analysis of multimedia field applications (Aulisa et al., 2006; Ekrem et al., 2006; Halder et al., 2006; Sun et al., 2006; Wang, 2007). All those previous outcomes gave the good examples for solving this EEMMS research work.

In conclusion, even though individual models that perform individual functions do exist, none of these, separately or in combination with other models, provide an integrated system that could function to meet the modeling needs for the system being studied.

2.2 A Literature Survey of Existing Environmental Multimedia Models

At the same time that single media models or software are developed, some simple environmental multimedia models have been developed. These multimedia models make different assumptions to simplify the problems and the challenges mentioned in Chapter 2.1. For the purpose of comparison, a brief summary of some existing environmental multimedia models are evaluated for their applicability to the EMS effort.

2.2.1 CalTOX

First issued in 1993 and updated in 1995, with continual enhancements underway, California Department of Toxic Substance Control's multimedia risk computerized model (CalTOX) was developed as a spreadsheet model for California's Department of Toxic Substance Control (DTSC), to assist in human health risk assessments that address contaminated soils and the contamination of adjacent air, surface water, sediment, and groundwater (McKone and Enoch, 2002). CalTOX consists of two component sub-models: a multimedia transport model, which is based on both conservation of mass and chemical equilibrium; and, a multi-pathway human exposure model that includes ingestion, inhalation and dermal uptake exposure routes. CalTOX is a fully mass balancing model and also includes additions to quantify uncertainty and variability. The multimedia transport model is a dynamic model that can be used to assess time-varying concentrations of contaminants introduced initially to soil layers or for contaminants released continuously to air, soil, or water. The CalTOX multimedia model is a seven-compartment regional and dynamic multimedia fugacity model. The seven compartments are (i) air, (ii) ground surface soil, (iii) plants, (iv) root-zone soil, (v) the unsaturated zone soil below the root zone, (vi) surface water, and (vii) sediment. The air, surface water, ground surface soil, plants and sediment compartments are assumed to be in quasi-steady state with the root zone soil and unsaturated zone soil compartments. Contaminant inventories in the root zone soil and unsaturated soil zone are treated as time-varying state variables. Contaminant concentrations in groundwater are based on the leachate from the unsaturated zone soil. The multi-pathway exposure model encompasses 23 exposure pathways, which are used to estimate average daily doses within a human population in the vicinity of 3 or 4 hazardous substances release sites. The exposure assessment process consists of relating contaminant concentrations in the multimedia model compartments to contaminant concentrations in the media with which a human population has contact (personal air, tap water, foods, household dusts/soils, etc.). The explicit treatment of differentiating environmental media pollutant concentration and the pollutant concentration to which humans are exposed favorably distinguishes CalTOX from many other exposure models. In addition, all parameter values used as inputs to CalTOX are distributions, described in terms of mean values and a coefficient of variation, rather than as point estimates or plausible upper values such as most other models employ. This stochastic approach allows both sensitivity and uncertainty to be directly incorporated into the model operation. As indicated in the literature review reports, the CalTOX model appears to be the most promising existing model for application. Several of the mathematical concepts and derivations used by the developers of CalTOX can be directly applied. However, CalTOX does have several limitations. These limitations result from going beyond intended applications for CalTOX; for example, for landscapes in which there is a large ratio of land area to surface water area, for a limited range of chemicals (e.g., non-ionic organic chemicals in a liquid or gaseous state). As a result, the model does not provide adequate flexibility in environmental settings and chemical classes (e.g., volatile metals such as mercury). The most significant of these limitations is the fact that the CalTOX model, as it currently exists, does not allow spatial tracking of a pollutant.

2.2.2 MEPAS

The Pacific Northwest laboratory developed the multimedia environmental pollutant assessment system (MEPAS) (McDonald and Gelston, 1998). The model can be used for sites that release radionuclide or toxic chemicals from a variety of different sources. In addition to allowing the input of an atmospheric source term, MEPAS can estimate volatilization from surface impoundments, spills, contaminated soils, ponds and landfills.

The emission of particle-bound contaminants from surface storage sites, contaminated soils and roads is also allowed. A budget of all sources is maintained and checked against the chemical inventory at the site to ensure that the total emissions do not surpass the available material.

The atmospheric module of MEPAS is a variation of the Gaussian plume model. Plume depletion due to dry and wet deposition is accounted for, though the model does not allow for the dynamic simulation of rainfall events, depending instead on mean values of the deposition fluxes. Degradation and radioactive decay in the atmosphere are accounted for through the use of first order rate coefficients.

The surface water module of MEPAS allows for the simulation of rivers and wetland environments. Transport in rivers is modelled using an analytical solution of a one dimensional convective diffusion equation. Though this equation is modified to account for first order reaction of the chemical, volatilization and sedimentation processes are neglected.

Contaminant concentrations in the unsaturated soil zone can serve as input for the case of an initially contaminated soil or calculated using source terms given by the user. MEPAS models contaminant transport in the saturated soil zone using a one-dimensional convective, three dimensional diffusive transport equation. This transport equation includes a term to account for chemical degradation and assumes uniform flow, a linear adsorption isotherm and constant hydraulic conductivity in each different soil layer. Using these equations, water concentrations at various receptor wells can be calculated for use in the exposure module.

The exposure module in MEPAS considers ingestion, inhalation and dermal contact pathways. Calculations for the exposure due to these different pathways are made using well-established EPA formulations. The concentrations provided by the model for the purpose of exposure assessment are assumed to represent seventy-year means. Mean activity levels for the exposed population are also used. One disadvantage to this approach is that the mean values used may not reflect the exposed populations at certain sites.

MEPAS is a user-friendly model with online help and an extensive database of chemical properties. The various modules that constitute the model are based on well-known approaches from the contaminant transport literature. These modules allow for spatial discrimination and incorporate a number of important transport pathways. From a multimedia perspective, MEPAS has the following deficiencies:

(i) The model requires the input of a large number of input parameters due to the site-specific character of some of its constituent modules.

(ii) Because the modules for the individual compartments are not linked through appropriate boundary conditions, a true dynamic global mass conservation is not guaranteed.

(iii) The use of mean concentrations and fluxes precludes the determination of dynamic effects. (rainfall events, temperature changes, etc.).

(iv) The method used to calculate volatilization does not incorporate possible effects of wind speed, temperature variation and moisture profile variation in the unsaturated zone.

2.2.3. MMSOILS

The U.S. EPA (1988) developed MMSOILS for the evaluation of hazardous waste sites.

MMSOILS is capable of modelling toxic chemicals emitted from contaminated soils, landfills, lagoons and ponds. Sources to the atmospheric module of MMSOILS include volatilization from contaminated soil and water as well as re-suspension of contaminated soil particles via wind re-suspension or mechanical disturbance. These emissions are the source term for a box model used to calculate air concentrations within 100 m of the emission site.

A sector-averaged Gaussian plume model is then used to calculate air concentrations at the site of the exposed human population. The plume model accounts for deposition fluxes but not for atmospheric degradation. The MMSOILS model can simulate small lakes and streams near the contaminated site. Streams are modelled using an analytical solution of a one dimensional convective diffusion equation. This equation contains a first order term to account for losses due to sedimentation, volatilization and chemical reaction. Sources to streams include dissolved and particle bound contaminant in runoff as well as groundwater flow. Lakes are modelled as spatially uniform with mass transfer at the sediment/water and water/air interfaces. Only runoff-borne dissolved and particle-bound contaminants are considered as contaminant sources to lakes. Contaminant transport in the saturated soil zone is modelled using a one-dimensional convective, three dimensional diffusive transport equation similar to the equation used in MEPAS. A mixing zone analysis is used to determine transport at the boundary of the saturated and unsaturated soil zones. The MMSOILS exposure module employs standard USEPA formulations to calculate the exposure of local populations. Concentrations used for the exposure analysis are the seventy-year mean concentrations calculated by the model, though it is possible to consider one-time "accidental" exposures.

In summary, MMSOILS can model a variety of scenarios involving toxic chemical releases to soils with state-of-the-art precision. It is also capable of more limited modelling of air and water emissions. The model incorporates a large database of chemical properties and is user-friendly. Disadvantages of the MMSOILS model include:

(i) Global mass conservation is not guaranteed because the modules for the individual compartments are not linked through appropriate boundary conditions.

(ii) The model cannot account for the transport of non-aqueous phase liquids (NAPLS) in the unsaturated soil zone.

(iii) MMSOILS neglects some transport pathways that could be important (i.e. volatilization and sedimentation processes in rivers, etc.).

2.2.4. ISMCM

Integrated spatial multimedia compartmental model (ISMCM) has been under development by the school of engineering and applied science at university of California Los Angeles for approximately 15 years. A newer version of ISMCM, called MEND-TOX, is currently under evaluation by the USEPA's office of research and development national exposure research laboratory. ISMCM considers all media, biological and non-biological, in one integrated system. ISMCM includes both spatial and compartmental modules to account for complex transport of pollutants through the ecosystem. Assuming mass conservation, ISMCM is able to predict transport based on a sound mechanistic description of environmental processes, including estimation of inter-media transfer factors. One of the limiting factors with the ISMCM system is that it is not structured to incorporate uncertainty/variability directly into the model operation. One of the limitations of the ISMCM model within the context of the goals is the fact that the links and compartments (spatial configuration) of this model are predetermined. ISMCM was apparently not designed from the start with the necessary flexibility. Having this flexibility is not a trivial thing to request, if the system is to be fully integrated. The structures of the reviewed multimedia models are summarized and compared in Table 2-3.

Comparing Tables 2-2 and 2-3, it shows that most multimedia models are evaluated in one dimension and verified using FDM more than FEM. However, for single-media model, it is only necessary to consider one media and whether its boundary conditions are uniform. Consequently, it is very simple to solve them using FEM, so most of them are evaluated in two or three dimensions. Furthermore, it could be noted that some multimedia models are based on the linking of detailed single media models. MEPAS is one example. However, it is extremely difficult to impose strict mass balance relationships, implement thermodynamics of partition processes, and carry out comprehensive sensitivity and uncertainty analyses with these "linked-model" systems. On the basis of literature reviews, the new EEMMS will retain the advantages of both single media and the traditional multimedia models.

Table 2-3 Comparison of multi-media models

Author, time/software	CalTOX (2002)	Chen and Ma (2006/MMSOILS)	ChemRange (2002)	ChemCAN (2003)	Di Guardo, et al. (1994/SoilFug)	Mepas(1998)
Developer	The California Department of Toxic Substances Control	USEPA	Swiss Federal Institute of Technology, Zürich	Canadian Environmental Modeling Center	University of Milan at Varese	Pacific Northwest Laboratory
Media	Mainly air	Air, soil and water	Air and water	Air or water	Soil, water and air	Soil, water and air
Methodology	FDM	Monte Carlo analysis	FDM	FEM	FDM	FDM
Dimension	0-D	1-D	1-D	1-D	3-D	0-D
Main application field	Hazardous waste sites	A surface soil, considers potential degradation reactions	Spatial area of organic chemicals	Assist human exposure assessment, designed for use in Canada	Surface water pollution by pesticide on agricultural fields.	Sites that release radionuclides or toxic chemicals for a different sources
Temporal resolution	Steady state	Steady state	Steady state	Steady state	Unsteady state	Steady state
Emission media	Air, water, surface soil, root soil, any combination	Air, water and soil, any combination	Air, water and soil, any combination	Air, water, soil, sediment, any combination	Air, water, soil, sediment, any combination	Air, water, soil, sediment, any combination
Model validation	Yes	Yes	No	Yes	Yes	Yes
Sensitivity analysis	Yes	Liu Zhi quan et al. (2007)	No	Yes	Yes	Yes
Output format	Excel tables	Excel tables	Excel tables	Excel tables	Excel tables	Excel tables

2.3 Risk Assessment Associated With the Multimedia Pollution Problems

Early environmental decision-making was based on qualitative descriptions of the effects of pollutant disperse on organisms and the environment, with some reliance on the assumption that the protection of human health would also ensure an adequate protection of the environment. Current information and environmental regulations suggest a need for a more quantitative risk-based approach to decision-making for environmental protection. A consultative risk assessment approach is necessary to evaluate the scale of potential hazardous environmental impacts on the ecology and human health. The benefit of risk assessment is to assist the decision-making and planning framework for management of a given region. In recent years, much more research work which integrated with multimedia models has been concentrated on the human and risk assessments. Several representative risk assessment modeling systems are: the hazardous waste identification rule frameworks (FRAMES-HWIR) (USEPA, 1999), the total risk integrated methodology (TRIM) system (USEPA, 1996), and the multimedia integrated modeling system (MIMS) (Johnston et al., 2000). The finite-source multimedia, multipathway, and multireceptor risk assessment (3MRA) (USEPA, 2003), CHARM (chemical hazard assessment and risk management) (Thatcher et al., 1999) and Monte Carlo Method (USEPA, 1996a; Luo and Yang, 2007; Liu et al., 2007). These risk assessment modelling systems consist of characterising the risk that a substance poses to human and non-human organisms by considering its inherent toxicity and the potential for exposure. For each compartment of the environment, the calculation of a predicted concentration, or exposure value, is compared to an effect concentration. Here we present some current models in detail:

2.3.1 FRAMES-HWIR

FRAMES-HWIR is a software system, which is applied to the technical assessment of exposures and risks relevant to the hazardous waste identification rule (HWIR). The software system automates this assessment to the framework for risk analysis in multimedia environmental systems (FRAMES). The HWIR is designed to determine quantitative criteria for allowing a specific class of industrial waste streams to no longer require disposal as a hazardous waste (USEPA, 1999).

2.3.2 TRIM

An expanded multimedia compartmental model that improves spatial resolution by using multiple sub-compartments per given medium is the total risk integrated model (TRIM). TRIM is a time series modeling system with multimedia capabilities for assessing human health and ecological risks. The first TRIM module accounts for movement of a chemical through a comprehensive system of discrete compartments (e.g., media and biota) that represent possible locations of the chemical in physical and biological environments of the modeled ecosystem and provides an inventory, over time, of a chemical throughout the entire system.

2.3.3 MIMS

In the development of TRIM, existing models and tools are relied upon where possible. For example, USEPA has incorporated TRIM into USEPA's MIMS, a modeling framework that accommodates linkages among multiple models and the sharing of common tools and data.

2.3.4 3MRA

The finite-source multimedia, multipathway, and multireceptor risk assessment modeling system (3MRA) is intended to be one of EPA's next generations of multimedia exposure and risk models, capable of modeling multimedia, multipathway, and multireceptor exposures. The 3MRA modeling system models multimedia exposures by simulating releases of a constituent to air, soil, and ground water, and then modeling the transport and fate of the constituent in each of these media and in the food webs associated with them. It models multipathway exposures by calculating simultaneous exposures of a receptor through multiple pathways, such as the ambient air, soil, food items, and drinking water, and summing them, when appropriate. It models multireceptor exposures by simulating a set of human receptors and a set of ecological receptors that characterize the receptor populations and behaviors of those receptors within an area of interest (AOI). (USEPA, 2003)

2.3.5 CHARM (chemical hazard assessment and risk management)

Chemical hazard assessment and risk management model is a tool that supports the environmental evaluation of the use of production chemicals on the basis of available data on these production chemicals and platform-related conditions. CHARM does not assess any potential harm caused during the production and transport of chemicals or the handling of unused remainders. It only produces information on the potential harm that occurs in the marine environment. The CHARM model comprises a set of rules that calculate the internationally accepted hazard quotient (HQ), which represents the ratio of the predicted environmental concentration (PEC) to the predicted no effect concentration (PNEC). The user has to define the criteria for using CHARM and the basis for which decisions are to be made on the results of CHARM, as it is a decision support tool and not a decision imposing method. All the rules are described in the CHARM User Guide (Thatcher et al., 1999, 2001).

2.3.6 Monte Carlo Method (MCM)

The estimation of risks to the natural environment requires explicit description of uncertainties in assumptions, models and parameters and the incorporation of these uncertainties into the final expression of risk. The most widely used approach to characterize uncertainty in risk assessment studies is the Monte Carlo (MC) simulation (USEPA, 1996a). In a Monte Carlo analysis, a sample from the distribution of an input parameter is placed into a simulation run to interact in a model with samples from other input parameters. A number of previous studies on the risk assessment of environmental multimedia assessment using the Monte Carlo method to conduct probabilistic analysis have been carried out. Although MC simulation has its limitations, as insufficient or imprecise informative data are difficult to analyze (Lee, 1996), there is still a small, but growing, number of multimedia environmental fate models that perform stochastic simulations by including both the uncertainty in chemical parameters and spatial and temporal variability within the environment (Bennett et al., 1999; Liu et al., 1999; MacLeod et al., 2002). Most of the former existing probability analyses in the multimedia environmental fate models consider only the uncertainties in the chemical properties (Citra, 2004; Fenner et al., 2004). However, owing partly to the CPU high improvement and the size of the database, it is possible to estimate uncertainties using this traditional Monte Carlo methods simulation. For instance, Quan et al. (2007) describes the application of MMSOILS model to predict health risk and distributions of those predictions generated using Monte Carlo methods. With the increasing computational power of personal computers, probability distributions are used in place of discrete values, and appropriate Monte Carlo analysis is currently the major technique for quantifying uncertainty in environmental assessments (Chen and Ma, 2006; Quan et al., 2007; Luo and Yang, 2007).

From reviewing the literatures on the integrated risk assessment, it is found that previous risk assessment based on environmental multimedia system modeling does not fully consider all the factors that have an impact on the result when using the MCM. This inadequacy may lead to an incorrect assessment of the risk level. Therefore, there is a need and necessity to develop a new model approach containing both new EEMMS and MCM to an integrated tool for the risk assessment of contaminants.

2.4 Summary

The literature review can be summarized as follows:

(1). Current multimedia models can be divided into three basic categories, each with its own advantages and disadvantages: "linked" model systems, fugacity models, and compartmental models: (i) multimedia compartmental ("well-mixed" media) models, (ii) linked spatial single-media models (LSSMM), and (iii) integrated spatial-multimedia-compartmental models (ISMCM). The identified limitations were considered critical, and therefore, deemed unacceptable for incorporating such models into multimedia use. "Linked" model systems (e.g., MEPAS) generally utilize a one-way process through a series of linked models that mathematically describe distinct environmental media or processes (e.g., aquatic environment). These types of models can never be truly mass conserving and cannot address feedback loops and secondary pollutant movement (e.g., re-volatilization and transport). Fugacity models (e.g., CalTOX) typically are compartment models without an explicit spatial scale (zero dimensional); thus, they do not provide the ability to spatially track pollutant movement. They are also applicable only to a limited range of chemical classes,e.g. inappropriate to model volatile metals (e.g., mercury). Compartmental models are also zero dimensional and do not allow for spatial tracking of pollutant movement and concomitant exposures. Spatial compartmental models (ISMCM) represent the closest current models to an extended integrated multimedia system. However, as previously described, it also does not meet the design goals for a flexible architecture. In general, none of the current models present a sufficiently coupled multimedia model or accounts for inherent "feedback" loops or secondary emissions (i.e., re-emission of deposited pollutants) or releases to specific media, or provides the temporal and spatial resolution critical in estimating exposures. While the degree to which modeled results would differ between current models and a truly coupled multimedia model is unknown, models that are not truly coupled have been considered to lack scientific credibility. Therefore, it was necessary to undertake efforts to develop a new extended multimedia model that will combine the benefits of both the ISMCM and LSSMM.

(2). The previous approaches have many limitations:

(i) Single modules are not integrated and can only be used separately. Traditional multimedia models do not consider spatial-temporal variations.

(ii) The atmosphere and water compartments are treated as uniform multiple compartments. An assumption of uniformity is made for individual multimedia zones.

(iii) Soil is expressed as a spatial compartment in the unsaturated part (not including the landfill part). Thus a more elaborate resolution can be gained in soil, but the approach for air and water compartments still falls short of spatial resolution.

(iv) There is no consideration of whole mass balance among the different media.

(v) There is no consideration of other inter-media mass transfers such as non-diffusive and diffusive transfers, sink, sorption, radioactive decay and biodegradation.

(vi) The use of a single method. There are no comparisons among the FEM, FDM, and analytical methods. The results are less accurate than the results of numerical solutions.

(3). With the recent progress towards a better understanding of the dynamics and complexities of environmental multimedia pollution issues, and due to the increased availability of numerical and computational tools, it is possible to extend previous efforts on environmental multimedia modeling in the domain of multidimensional accuracy.

(4). As for risk assessment, few studies were found for quantifying system uncertainties and predicting the risks of leachate. Therefore, in the present thesis study, the MCM is used for uncertainty analysis involved in the risk assessment. A HQ factor derived from the CHARM model is incorporated to quantify the possible risk levels. The detailed solution is described in Chapter 3.

In conclusion, it is expected that the new EEMMS incorporates numerical analysis techniques to characterize the spatial and temporal dynamics involved in the typical environmental multimedia problems. The new EEMMS with numerical solutions should address the transport of pollutants in an environmental multimedia system such as the sorption and decay mechanisms. Furthermore, the new EEMMS incorporates the MCM and sensitivity analysis to illustrate the risks associated with pollutant dispersion into the multimedia environment.

Chapter 3 Methodology of the Study

In 2002, Cohen and Cooter suggested that serially linked single-medium transport models for air, water, soil and other media should be integrated. Aiming to mitigate the limitations and challenges summarized in Chapter 2 and to extend on previously studies on multimedia models, a new EEMMS will be developed in this study. It will provide fine spatial and temporal resolutions to estimate time-varying and spatial-varying pollutant concentrations in air, soil, and groundwater, which are significant features in evaluating the risk level for exposure to hazardous contaminants. It will also be used to evaluate the potential risk to human health presented by contaminants released from a pollution site. The comparison between the traditional multimedia model and an extended multimedia model is illustrated in Figure 3-1.

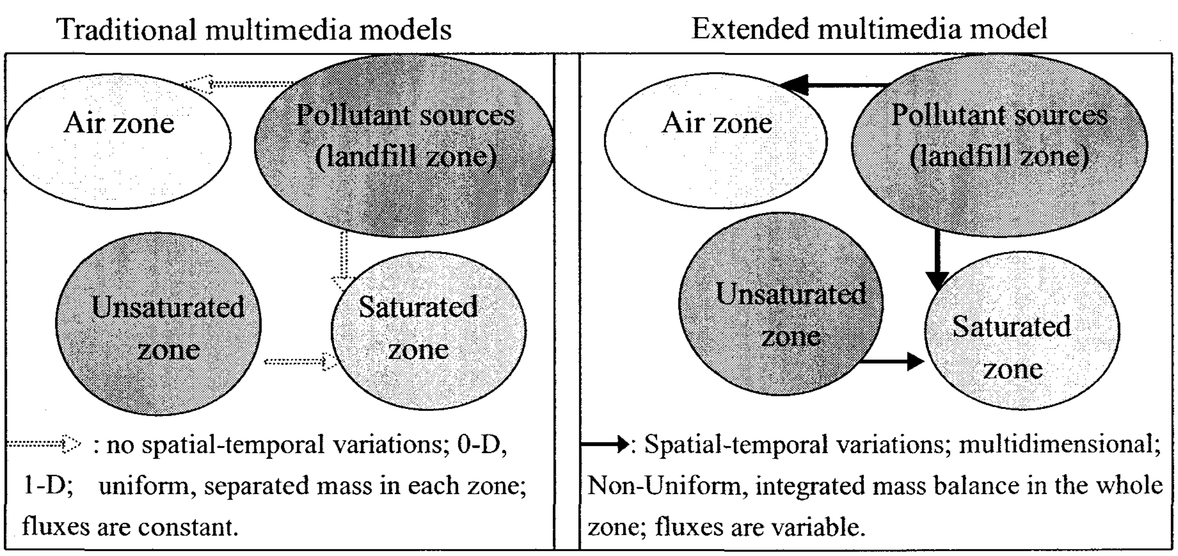

Figure 3-1 Comparison of the traditional and extended multimedia models

For example, the new-extended multimedia models provide a strict mass balance relationship, use mass balance between media to implement mass transfer, and provide a traceable and scientifically defensible framework for assessing pollutant behavior in complex systems. Based on this comparison, a new integrated modeling approach (EEMMS) is developed in the present chapter. Furthermore, the MCM is further incorporated with EEMMS to quantify the risks associated with pollutants dispersion into the multimedia environment.

3.1 Modeling Approach

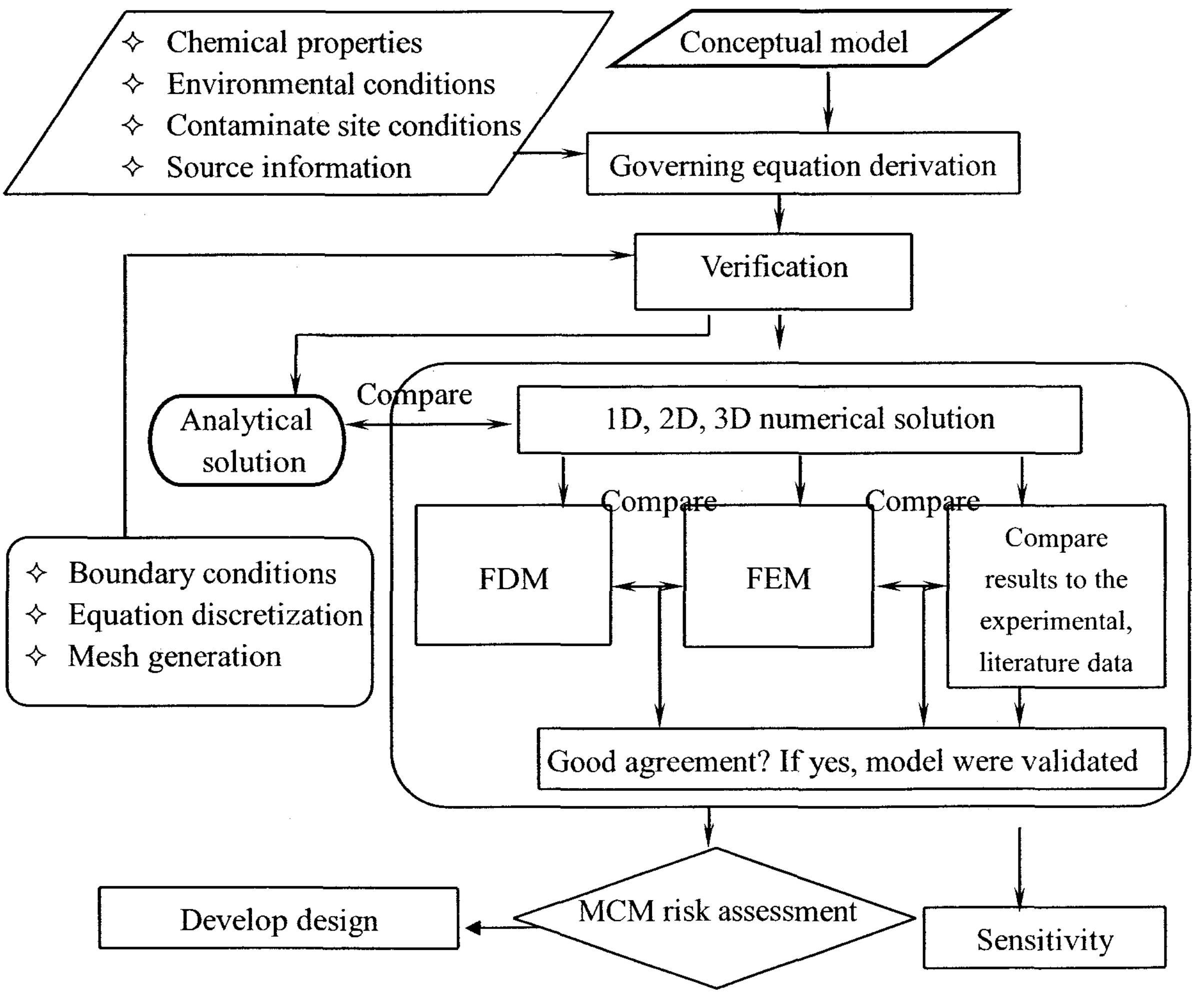

Figure 3-2 Flow chart depicting the elements of the proposed approach

An integrated risk assessment approach based on the EEMMS and MCM is proposed to quantify system uncertainties and to evaluate the environmental risks associated with the pollutants dispersion in the multimedia environment. The EEMMS method includes three major components: data input part, model verification, and MCM risk assessment and sensitivity analysis. The framework of the developed EEMMS approach is presented in Figure 3-2.

Figure 3-2 shows the computational process of the integrated risk-assessment method. Details of the numerical algorithm are described in the following sections. Figure 3-2 gives a brief outline of the implementation plan of the above proposed research methodology, which will ensure the validity of the new EEMMS.

3.2 Development of the General Governing Equations of EEMMS

Based on the research work of Parker (1989), the multimedia model equation is developed. Then, the following governing multimedia model equation for pollutant fate and transport become:

$$\theta_\alpha^k R_\alpha^k \frac{\partial C_\alpha^k}{\partial t} = -\frac{\partial^2 J_{\alpha i}^k}{\partial x_i} + Q_\alpha^k - \theta_\alpha^k R_\alpha^k \lambda_\alpha^k C_\alpha^k \tag{3.1}$$

where,

C_α^k : concentration of the non-inert α component in the k^{th} layers [ML^{-3}],

$J_{\alpha i}^k$: mass flux density of α per porous media cross section in the i-direction [$ML^{-1}T^{-1}$],

R_α^k : retardation factor,

Q_α^k : net mass transfer rate per porous medium volume of species α into (+) or out (-)[ML^{-3}],

θ_α^k : porosity, and

λ_α^k : apparent first-order decay coefficient, usually given in terms of the half-life;

$$\lambda_\alpha^k = (\ln 2)/t_{\alpha\ 1/2}^k \tag{3.2}$$

where,

$t_{\alpha\ 1/2}^k$: half-life of radioactive or biodegradable materials, i.e., the time required for the concentration to decrease to one-half of the original value.

The mass flux density of component α in k layer due to convection, diffusion and mechanical dispersion is described as follows:

$$J_{\alpha i}^k = \theta_\alpha^k C_\alpha^k V_i^k - \theta_\alpha^k D_{\alpha ij}^k \frac{\partial C_\alpha^k}{\partial x_j} \tag{3.3}$$

where,

$D_{\alpha ij}^k$: dispersion tensor, and

V_i^k : seepage or linear pore water velocity in the k layer.

The latter is related to the specific discharge (Urquiza et al., 2008).

$$V_i = \frac{q_i}{\theta} = -\frac{k_i}{\theta}\frac{\partial h}{\partial x_i} \tag{3.4}$$

where,

k_i : principal component of the hydraulic conductivity tensor, (LT^{-1}), and

h : hydraulic head, (L).

Combining the phase continuity Equation (3.1) and the mass flux Equation (3.3) for transport of component α in the k layer, one expands the first and third terms using Equation 3.3, employing the Darcy continuity Equation (3.4), and assuming density derivative terms to be of second order importance within a given time step:

$$\underbrace{\frac{\partial C_{\alpha}^{k}}{\partial t}}_{time\ variation} = \frac{1}{\theta_{\alpha}^{k} R_{\alpha}^{k}} \left(\underbrace{\frac{\partial}{\partial x_i} [\theta_{\alpha}^{k} D_{\alpha ij}^{k}] \frac{\partial C_{\alpha}^{k}}{\partial x_j}}_{Dispersion} - \underbrace{\frac{\partial (\theta_{\alpha}^{k} C_{\alpha}^{k} V_i^{k})}{\partial x_i}}_{advective} + \underbrace{Q_{\alpha}^{k}}_{sources/sinks} \right) - \underbrace{\lambda_{\alpha}^{k} C_{\alpha}^{k}}_{reaction} \tag{3.5}$$

Note that in the transport governing equations described above, assumptions are made on advection, dispersion, sink, sorption, radioactive Decay and biodegradation. The details are as follows:

(1) Advection: The advection describes the transport of miscible contaminants at the same velocity. For many field-scale contaminant transport problems, the advection term dominates over other terms. To measure the degree of advection domination, a dimensionless Peclet number is usually used.

(2) Dispersion mechanism: dispersion in porous media refers to the spreading of contaminants over a greater region than would be predicted solely from the average velocity vectors. Dispersion is caused both by mechanical dispersion, a result of deviations of actual velocity on a micro-scale from the average groundwater velocity, and by molecular diffusion driven by concentration gradients, which is called diffusion-dispersion. Molecular diffusion is generally secondary and negligible compared to the effects of mechanical dispersion, and becomes important only when

velocity is very low.

(3) The total mass transfer rate, Q_α^k, it may be noted, is related to the individual component mass transfer rates.

Mass transfer is an essential part of many environmental processes within natural or engineered systems, such as water and wastewater treatment, air emissions control, and groundwater and soil remediation systems. In this research, our focus is on the mass transfer processes from the sources to the air, soils and groundwater. Mass transfer processes include phenomena affecting the movement of constituents in the bulk of a system and across its boundaries such as advection, dispersion, diffusion and sorption processes that occur primarily at interfaces between different media (Weber and DiGiano, 1996). Processes involved in mass transfer can be classified as (Brusseau and Rao, 1989; Brusseau and Rao, 1990; Weber et al., 1991; Brusseau, 1998): (i) advective-dispersive transport from bulk solution to the boundary layer of a soil or sediment particle; (ii) film diffusion across the adsorbed water to the surface of a pollutant; and (iii) sorption across the adsorbed water to the surface of a pollutant. Since these processes act in series, the slowest process will represent the rate-limiting step. The different media are also complicated by the presence of variable fluid flow patterns, causing transitions between laminar and turbulent flow. Although fluid flow in groundwater is generally laminar in nature, the flow pattern and the residence times of fluid elements within the system may also influence the time available for mass transfer.

Initially, due to the slow movement of groundwater, it is assumed that local sorption equilibrium should prevail, i.e., local equilibrium assumption. Numerous studies (Karickoff and Brown, 1978; Freeman and Cheung, 1981; Di Toro and Horzempa, 1982; Ball, 1989; Harmon, 1992; Carroll et al., 1994; Farrell and Reinhard, 1994; Weber and Huang, 1996; Werth and Reinhard, 1997; Werth and Reinhard, 1997; Werth and Hansen, 2002), however, cast doubt on the local equilibrium assumption applications through the observation of long term sorption/desorption processes following an initial fast uptake. The resulting influence on these mass transfer phenomena is asymmetrical breakthrough curves, with earlier breakthrough and tailing.

This two-stage sorption-desorption phenomena can be attributed to many factors (Brusseau et al., 1989; Brusseau, 1994), including transport related factors (e.g., different advection pattern) and sorption related factors (e.g., chemical non-equilibrium reactions, and intrasorbent diffusion). Attempts to capture sorption kinetics can be classified into two types of mass transfer models, i.e., first order reaction based and diffusion model based, both of which strive to include transport-related factors in the model. Among these three regions, the fluid sink/source and chemical reactions based on the one-dimensional landfill model is added.

The sinks term represents solute mass entering the model domain through sources, or solute mass leaving the model domain through sinks. Sinks or sources may be classified as a well distributed or point sinks or sources. Boundaries in the flow model are also treated as point sinks or sources because they function in exactly the same fashion as wells, drains, or rivers in the transport model. For sources, it is necessary to specify the concentration of source water. For sinks, the concentration of sink water is generally equal to the concentration in the aquifer at the sink location and cannot be specified. However, there is one exception where the concentration of sinks may differ.

(4) Chemical reactions include equilibrium-controlled linear or non-linear sorption, non-equilibrium (rate-limited) sorption, and first-order reaction that can represent radioactive decay or provide an approximate representation of biodegradation. The general formulation designed to model rate-limited sorption can also be used to model kinetic mass transfer between the mobile and immobile domains in a dual-domain advection-diffusion model. More sophisticated chemical reactions can be modeled through add-on reaction packages. Sorption refers to the mass transfer process between the contaminants dissolved in aqueous phase and the contaminants sorbed on the porous medium (solid phase). It is generally assumed that equilibrium conditions exist between the aqueous-phase and solid-phase concentrations and that the sorption reaction is fast enough relative to liquid phase velocity so that it can be treated as instantaneous. The functional relationship between the dissolved and sorbed concentrations under a constant temperature is referred to as the sorption isotherm. Equilibrium-controlled sorption isotherms are generally incorporated into the transport model through the use of the retardation factor. Three types of equilibrium-controlled sorption isotherms are considered in the transport model: linear, Freundlich and Langmuir.

(5) Radioactive decay or biodegradation, λ_{α}^{k}: the first-order irreversible rate reaction term represents the mass loss of both the dissolved phase and the sorbed phase. The rate constant

is usually given in terms of the half-life, the time required for the concentration to decrease to one-half of the original value. For radioactive decay, the reaction generally occurs at the same rate in both phases. For biodegradation, however, it has been observed that certain reactions occur only in the dissolved phase. That is why two different rate constants may be needed.

The overall governing equation will be used in the four zones. However, there are still some differences between them. For example, the landfill is basically a specific type of unsaturated zone, so we can use the same equations in the unsaturated module that are used in landfill module. However, there remain some differences between the landfill and the unsaturated zone. First, the media is changed from being landfill to soil. So, we could use the same equations but C_α^k, R_α^k, and λ_α^k are changed so as to be soil-specific. The same principle will be used in the saturated zone, where the major change in the equations will be porosity, which is equal to 1 in the saturated zone. Considering all the factors above, the governing Equation 3.5 can be written in the different formats when they are used in the different dimensions.

3.2.1 The Conceptual Model and Governing Equations

Once a contaminant is released into the environment from a pollution source, such as an oil spill or at a solid waste site-landfill, it will migrate into all connected environmental media and may eventually lead to human exposure. Figure 3-3 illustrates such a typical contamination site in one-dimensional environment, namely a waste site, in which basic environmental media are contaminated: the air, the soil and the groundwater. The conceptual model is visualized in Figure 3-3.

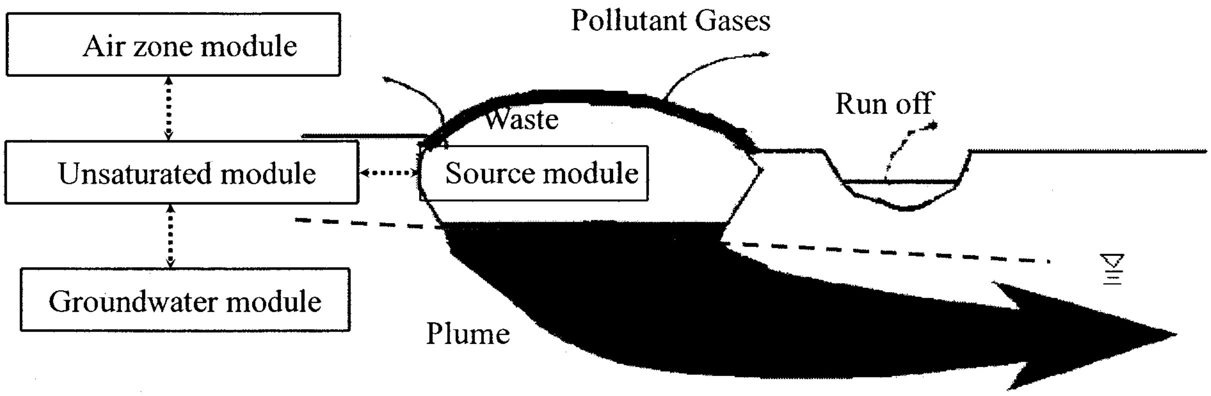

Figure 3-3 Conceptual application of EEMMS

Based on the concept shown in Figure 3-3, the EEMMS proposed in the research will consists of four modules: a source module, an air module, an unsaturated zone module and a saturated groundwater zone module.

3.2.2 Source Module and Governing Equations

The source module is used to simulate the dynamics of the solid waste in the waste zone, and to compute the mass emission rate upwards to the air and the leachate release rate down to the unsaturated zone. Considering one pollutant (p=1), the governing equation 3.5 can be written as:

$$\frac{\partial C_\alpha^k}{\partial t}=\frac{1}{\theta_\alpha^k R_\alpha^k}\left[D_x^k\frac{\partial^2 C_\alpha^k}{\partial x^2}+D_y^k\frac{\partial^2 C_\alpha^k}{\partial y^2}+D_z^k\frac{\partial^2 C_\alpha^k}{\partial z^2}-V_x^k\frac{\partial C_\alpha^k}{\partial x}-V_y^k\frac{\partial C_\alpha^k}{\partial y}-V_z^k\frac{\partial C_\alpha^k}{\partial z}\right]-\lambda_\alpha^k C_\alpha^k \tag{3.6}$$

When k is unsaturated-zone soil medium, seepage velocity is not considered along the y-axis, z-axis. This allows both numerical and analytical solutions for Equation (3.6) to be obtained. The numerical solution uses FDM and FEM as noted in Appendix A, B and C. The analytical solution (Equation 3.7) is derived below for the comparison studies discussed later (Dmitry and Victor, 1999):

$$C_a^k = \frac{x}{4B\sqrt{\pi D_x^{'}}}\int_0^t C_{a0}^k(\tau)\frac{1}{(t-\tau)^{\frac{3}{2}}}\exp\left\{-\lambda_a^k(t-\tau)-\frac{(x-v_x^{'}(t-\tau))^2}{4D_x^{'}(t-\tau)}\right\}$$

$$\cdot\left[\begin{array}{l}\left[erfc\left\{\dfrac{y-y_0}{2\sqrt{D_y^{'}(t-\tau)}}\right\}-erfc\left\{\dfrac{y+y_0}{2\sqrt{D_y^{'}(t-\tau)}}\right\}\right]\cdot \\ \left[(z_2-z_1)+\dfrac{2B}{\pi}\displaystyle\sum_{n=1}^{\infty}\frac{1}{n}\left[\sin(\frac{n\pi z_2}{B})-\sin(\frac{n\pi z_1}{B})\right]\cos(\frac{n\pi z}{B})\exp\left\{-D_z^{'}\frac{n^2\pi^2}{B^2}(t-\tau)\right\}\right]\end{array}\right]d\tau \tag{3.7}$$

where, $v_x^{'}=\frac{V_x^k}{R_\alpha^k}$, $D_x^{'}=\frac{D_x^k}{R_\alpha^k}$, $D_y^{'}=\frac{D_y^k}{R_\alpha^k}$, $D_z^{'}=\frac{D_z^k}{R_\alpha^k}$; B is the thickness of the aquifer, $C_{a0}^k(t)$ is the arbitrary time-varying function, y_0 is the half-width of source, z_1 is the bottom of source, z_2 is the top of source, τ is integral variate. In Equation 3.7, the dispersion coefficients are defined as the sum of mechanical dispersion and diffusion coefficients:

$$D_x^k = \alpha_L^k V^k + D^{k*} \tag{3.8}$$

$$D_y^k = \alpha_{TH}^k V^k + D^{k*} \tag{3.9}$$

$$D_z^k = \alpha_{TV}^k V^k + D^{k*} \tag{3.10}$$

where, α_L^k is the longitudinal dispersivity in the k layer [L]; α_{TH}^k is the horizontal transverse dispersivity in the k layer [L]; α_{TH}^k = vertical transverse dispersivity [L]; and $D*$ = effective dispersion coefficient [L^2 T^{-1}]. Specifically, a partial differential equation is formulated and solved to address the processes in the source zone and the releases out of the source liner system in the one-dimensional problems (Parker, 1989; Lin and Hildemann, 1995):

$$\frac{\partial C_\alpha}{\partial t} = D_\alpha \frac{\partial^2 C_\alpha}{\partial x^2} - V_\alpha \frac{\partial C_\alpha}{\partial x} - \mu_\alpha C_\alpha \tag{3.11}$$

where,

$$D_a = \frac{a \times K_H \times D_g}{\theta \times R} + \frac{D_L}{R} \tag{3.12}$$

$$R = 1 + k_d \frac{\rho_b}{\theta} + \frac{\alpha K_H}{\theta} \tag{3.13}$$

$$\mu_\alpha = ln2/ t_{1/2} \tag{3.14}$$

and, a is volumetric air content (L^3 L^{-3}), k_d is the distribution coefficient (L^3 M^{-1}), C_α is the contaminant concentration of the different α components (M L^{-3}), D_a is the dispersion coefficient of the different α components (L^2 T^{-1}), D_g is the diffusion coefficient of the vapor-phase contaminant in landfill (L^2 T^{-1}), D_L is the diffusion/dispersion coefficient of the dissolved-phase contaminant in landfill (L^2 T^{-1}), K_H is the dimensionless Henry's Law Constant (dimensionless), R is the total retardation factor (dimensionless), $t_{1/2}$ is the half-life of radioactive or biodegradable materials (T), V_a is the seepage velocity of the different α components (L T^{-1}), θ is porosity (dimensionless), ρ_b is bulk density (M L^{-3}), and μ is the effective first-order decay rate constant (d^{-1}). Both numerical and analytical solutions to Equation (3.11) are developed in this study. The numerical solution uses FEM (finite element methods) and FDM (finite difference methods). The analytical solution is derived below for the comparison studies introduced later:

$$C_a = \frac{C_0}{2} \, exp \, \left(\frac{V_a \times x}{2 \times D_a} \right) \{exp \left[-\frac{x}{2D_a} \sqrt{(V_a)^2 + 4\mu_a D_a} \right] erfc \left[\frac{x - \sqrt{(V_a)^2 - 4\mu_a D_a t}}{2\sqrt{D_a t}} \right] + exp$$

$$\left[\frac{x}{2D_a} \sqrt{(V_a)^2 + 4\mu_a D_a} \right] erfc\left[\frac{x + \sqrt{(V_a)^2 - 4\mu_a D_a t}}{2\sqrt{D_a t}} \right]\} \tag{3.15}$$

where, erfc is the complementary error function (Vogel, 1970).

3.2.3 Unsaturated Zone Module and Governing Equations

The unsaturated zone module simulates the fate and transport of leachate contaminants in the soils from the base of the landfill to the lower unsaturated/saturated zone boundary and computes the contaminant flux as input to the saturated zone (groundwater) module. The governing three-dimensional equations for the unsaturated zone soil medium are given (Carnahan and Remer, 1984) as:

$$\frac{\partial C_\alpha}{\partial t} = \frac{D_T}{R}\left(\frac{\partial^2 C_\alpha}{\partial x^2} + \frac{\partial^2 C_\alpha}{\partial y^2}\right) + \frac{D_L}{R}\frac{\partial^2 C_\alpha}{\partial z^2} - \frac{v}{R}\frac{\partial C_\alpha}{\partial z} - \mu_\alpha C_\alpha \tag{3.16}$$

where, D_L is the coefficient of longitudinal dispersion ($L^2 T^{-1}$), D_T is the coefficient of advective transport ($L^2 T^{-1}$), v is the velocity of the flow ($L T^{-1}$), and other parameters are the same as in Equation (3.7). The analytical solution to Equation (3.16) is given by Carnahan and Remer (1984):

$$C_\alpha = \frac{m_0 \exp[-(\gamma + \mu_t)t]}{4\pi\eta D_T D_L^{1/2}} \exp\left(\frac{vz}{2D_L}\right) erfc\left[0.5\eta\left(\frac{R}{t}\right)^{1/2}\right] \tag{3.17}$$

where, m_0 is the rate of release of the solute from the point source at time zero ($M T^{-1}$), and

$$\eta = \left(\frac{r^2}{D_T} + \frac{z^2}{D_L}\right)^{1/2} \tag{3.18}$$

$$r^2 = x^2 + y^2 \tag{3.19}$$

$$\gamma = \frac{v^2}{4D_L R} \tag{3.20}$$

3.2.4 Saturated Zone (Groundwater) Module and Governing Equations

The governing equation for the saturated zone groundwater is given as follows (Carnahan and Remer, 1984):

$$\frac{\partial C_\alpha}{\partial t} = \frac{1}{R}\left[D_x \frac{\partial^2 C_\alpha}{\partial x^2} + D_y \frac{\partial^2 C_\alpha}{\partial y^2} + D_z \frac{\partial^2 C_\alpha}{\partial z^2} - V_x \frac{\partial C_\alpha}{\partial x} - V_y \frac{\partial C_\alpha}{\partial y} - V_z \frac{\partial C_\alpha}{\partial z}\right] - \mu_\alpha C_\alpha \quad (3.21)$$

where, C_a is the contaminant concentration, equal to the mass of contaminant per unit volume of ground water (M L^{-3}), V_x, V_y, V_z are the components of the seepage velocity (L T^{-1}), D_x, D_y, D_z are the components of the dispersion coefficient (L^2 T^{-1}), and other parameters being similar to those in Equation (3.11).

The analytical solution to Equation (3.21) can be obtained for comparison analysis introduced later (Domenico, 1987):

$$C_\alpha(x,y,t) = \frac{C_{\alpha 0}}{8}\exp\left(\frac{x}{2\alpha_x}\left[1-\left(1+\frac{4\mu_{sat}\alpha_x}{V_d/R}\right)^{1/2}\right]\right) erfc\left(\frac{x-(V_d t/R)(1+4\mu_a\alpha_x R/V_d)^{1/2}}{2(\alpha_x V_d t/R)^{1/2}}\right)$$

$$\left\{erf\left[\frac{y+A_y/2}{2(\alpha_y x)^{1/2}}\right]-erf\left[\frac{y-A_y/2}{2(\alpha_y x)^{1/2}}\right]\right\}\left\{erf\left[\frac{z+H}{2(\alpha_z x)^{1/2}}\right]-erf\left[\frac{z-H}{2(\alpha_z x)^{1/2}}\right]\right\} \quad (3.22)$$

where, H is the aquifer-mixing zone thickness (L). It is the vertical thickness of this plume within the aquifer at the point where the plume passes beneath the contamination site (Solhotra et al., 1995), and V_d is the seepage velocity (LT^{-1}), and α_x, α_y, α_z are the dispersivity in the coordinate directions, and are defined as the dispersion coefficient divided by the mean seepage velocity:

$$\alpha_x = \frac{D_x}{V_d} \quad (3.23)$$

$$\alpha_y = \frac{D_y}{V_d} \tag{3.24}$$

$$\alpha_z = \frac{D_z}{V_d} \tag{3.25}$$

where, D_x, D_y and D_z are the dispersion coefficients in x, y, and z directions, respectively ($L^2\ T^{-1}$). Other parameters are similar to those in the Equation (3.14).

3.2.5 Air Module and Governing Equations

The air module zone is one of the principal pollutant transport vehicles through which volatile organic compounds (VOCs) and toxic chemicals volatilising from waste sites may reach living organisms. This air module simulates the transport and diffusion of constituents in the form of volatilized gases emitted from area sources into the air. According to the research of Tsuang and Chao (1997), the governing equation for the air-zone is given as follows:

$$\frac{\partial C_\alpha}{\partial t} = D_x \frac{\partial^2 C_\alpha}{\partial x^2} + D_y \frac{\partial^2 C_\alpha}{\partial y^2} + D_z \frac{\partial^2 C_\alpha}{\partial z^2} - V \frac{\partial C_\alpha}{\partial x} - P\Lambda C \tag{3.26}$$

where, D_x, D_y, D_z are eddy diffusivity in the x direction, y direction, and y direction, respectively ($m^2 s^{-1}$). V is wind speed. And Λ is a scavenging coefficient (s^{-1}), which ranges from 0.4×10^{-5} to 3×10^{-3} s with a median value of $1.5\times10^{-4}\ s^{-1}$ for particle (McMahon and Denison, 1979). P is the proportion of time raining ($s\ s^{-1}$).

Specifically, the governing equation for the air zone in the one-dimensional environment is given as follows (Stephen and Karsten, 2003):

$$\frac{\partial C}{\partial t} = D_a \frac{\partial^2 C}{\partial^2 Z} \tag{3.27}$$

where, t is time (T), C is the concentration (mg m) in dimensions of Z (L), D_a is the diffusion coefficient in dimensions of (L^2 T^{-1}) and Z is the length along the study direction (L). The resulting flux can be derived from Fick's First law:

$$F_a = AD_a \frac{\partial C}{\partial Z} \tag{3.28}$$

where A is the area of plane of diffusion (L^2), D_a is the diffusion or turbulent coefficient of molecular (L^2 T^{-1}), and F_a is the mass flux (M L^{-2} T^{-1}).

3.3 Initial and Boundary Conditions

Governing equations have been proposed along with derived analytical solutions for the four modules of the EEMMS. The initial and boundary conditions among the four governing equations serve as the bases that introduce the integrated development of the new EEMMS. The detailed initial and boundary conditions are described in the following subsections.

3.3.1 Initial and Boundary Conditions in 1-D

The following equations give the integrated initial and boundary solution algorithm for solving representing Equations 3.11, 3.16, 3.21, and 3.27 within an EEMMS framework using FDM and FEM at one-dimensional conditions:

$$C(z,0) = C_0 \quad if\ 0 < z < L \tag{3.29}$$

$$if\ z > L,\ t=0,\ C_1=0,\ C_2=0;\ t=+\infty,\ C_1=0,\ C_2=0 \tag{3.30}$$

$$C_a(x,t)\Big|_{t=0} = C_0(x) \tag{3.31}$$

$$-D_a \frac{\partial C_a}{\partial X} + V_a C_a \Bigg|_{t>0, X=0} = kC_0 \tag{3.32}$$

$$-D_a \frac{\partial C_a}{\partial X} + V_a C_a \Bigg|_{t>0, X=L} = kC_{out} \tag{3.33}$$

where, L is the length of the simulated Landfill depth (L), in which C_0 is the background concentration in landfill. The upper boundary condition is shown as Equation (3.34):

$$F_t(0,t) = -kC_G(0,t) \tag{3.34}$$

where, F_t is pollution flux; C_G is the concentration on the upper boundary (the bottom of the aquifer) that is considered the plane (z=0); k is the overall mass transfer coefficient through the top cover (L T^{-1}) and is estimated by (Zhang et al., 2003):

$$\frac{1}{k} = \frac{d}{D_g} + \frac{1}{k_t} \tag{3.35}$$

in which k_t is the mass transfer coefficient in the air-soil boundary layer (L T^{-1}), D_g is the gaseous diffusion coefficients ((L^2 T^{-1})) in the soil (Millington and Quirk, 1961), and d is the thickness of landfill cover (L).

3.3.2 Initial and Boundary Conditions in 2-D

The initial concentrations of the pollutants in four different zones are set to zero within the domain. As boundary conditions for the sources, the pollutants source is conceptualized as two-dimensional; one part of the contaminant mass emitted up into the air and another released leachate down into soil beneath the sources. It simultaneously achieves the mass balance between the source and all affected media. The parameters of mass balance and the transfer rules used here are given in Table 3-1. The other initial and boundary conditions are given in the Figure 3-4. Ψ is referred to the flux. C is referred to the concentration. Some other parameters such as the groundwater table elevation, first-order rate coefficients for dissolution, water-gas partitioning and volatilization are inputted into the FEM solvers. Finally, the model solvers will output the results like the domain grid nodes and elements that were discretized with uniform grid spacing in x-direction and z-direction. In order to evaluate the risk of exposure to the contaminants released from an influential source and its effects of density-driven advection, infiltration, and permeability on contaminant plume evolution in a two-dimensional system, detailed case studies will be shown in the later chapters.

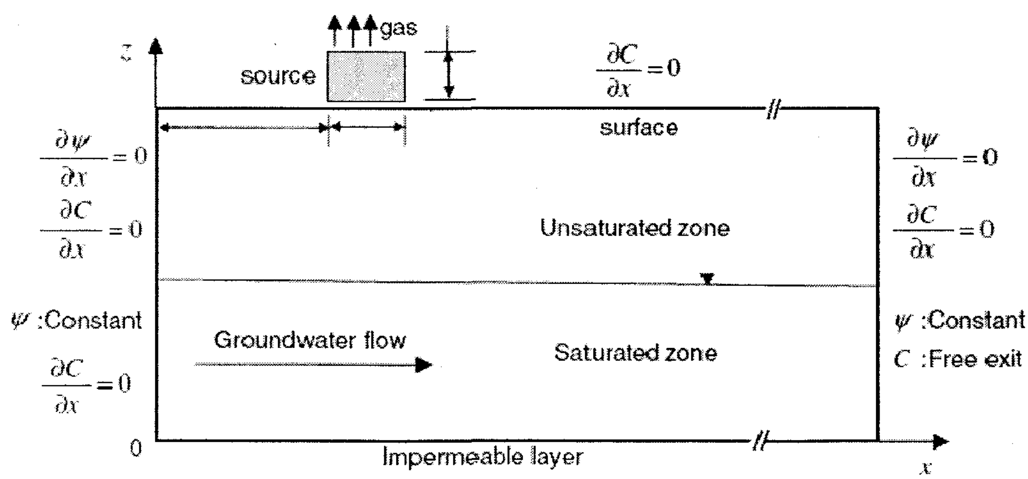

Figure 3-4 A schematic diagram of a 2-D modeling domain

In Figure 3-4, the following transport processes are of primary consideration.

1) The aquifer is semi-infinite in the longitudinal direction ($0 \leq x < \infty$).

2) Ground water flow is steady. Flow is uniform and one-dimensional along the x-axis.

3) The following transport processes are considered: advection, dispersion, transformation reactions and sorption.

4) Dispersion is assumed to be a Fickian process.

5) The principal axes of the dispersion tensor are assumed to coincide with the directions parallel and transverse to ground water flow.

6) Transformation reactions are represented by a first-order decay/production reaction.

7) Sorption is assumed to be instantaneous and reversible, governed by a linear isotherm.

Table 3-1 Initial and boundary conditions

Boundary	Condition	Variable
Vertical side of the zones (right and left sides)	Axial symmetry	-
Intersection between the sources to unsaturated zones; Intersection between the unsaturated to saturated zones;	Advective flux	-
Sources zone	Flux	F_0
Sources zone	Volatilization	d
The highest top of the air zone and the lowest layer of the saturated zone	No flux/symmetry	-
Saturated zone	Flow boundary	-

3.3.3 Initial and Boundary Conditions in 3-D

The 2D domain shown in Figure 3-4 is extended to a 3D domain with dimensions in x, y, and z directions, respectively. The initial and boundary conditions are similar as in 2D domain. The main difference is the y direction.

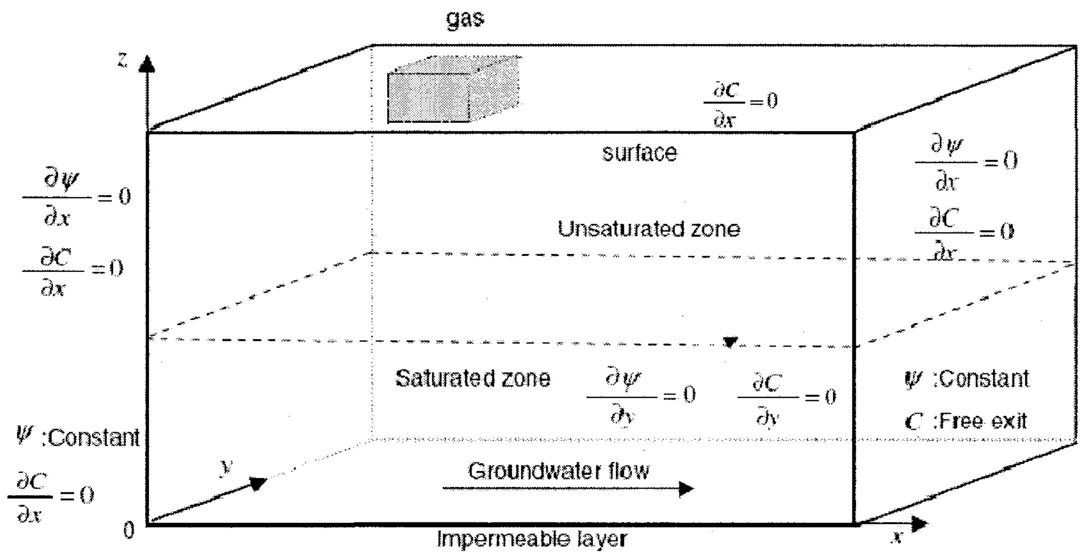

Figure 3-5 A schematic diagram of a 3-D modeling domain

In Figure 3-5, density-driven advection of gas phase in a three-dimensional domain is needed for more realistic scenarios. The pollutant sources will describe the pollutants fate and transport in a porous medium, in which the sorption, degradation, advection and diffusion processes are considered more complicated in three dimensions. From the source output, the contaminant mass will emit to the air and atmosphere. It will use the simplified Gaussian plume 3-D model. Air zone outputs will represent the concentration in the ambient atmosphere above ground. Another part of the mass will be emitted as leachate migrating vertically through the unsaturated zone from landfill and finally reaches the saturated groundwater. The 3-D outputs include the contaminant concentration in the water table and the mass flux entering into the groundwater that is used by the saturated zone as the contaminant source. The contaminant coming from the unsaturated zone is presumed to be uniformly mixed in the groundwater to form a mixing zone, which serves as the source term of the saturated zone dispersion. The saturated zone simulates the fate and transport of dissolved contaminants from the water table to the down gradient with an FEM numerical solution to three-dimensional groundwater. The outputs are the groundwater contaminant concentrations in the potential receptors. Those are used to determine whether the concentrations of concerned pollutants exceed the water standard at the downstream receptors. The initial and boundary conditions are as follows:

The aquifer is initially devoid of contaminants; $C\ (x, y, z, 0) = 0$, contaminants enter the aquifer through a rectangular source of specified concentration located on the upstream boundary. The concentration on the remaining portion of the upstream boundary is zero. The top and bottom boundaries (z=0, z=B) are zero mass flux boundaries. The details are as follows:

1) Along the x-direction, aquifer is semi-infinite in extent

$$C(\infty, y, z, t) = 0 \tag{3.36}$$

2) Along the y-direction, aquifer is infinite in extent

$$C(x, -\infty, z, t) = 0 \tag{3.37}$$

$$C(x, \infty, z, t) = 0 \tag{3.38}$$

3) Along the z-direction, aquifer is finite in extent

$$\frac{\partial c}{\partial z}C(x,y,0,t)=0,\text{ when } z=0 \tag{3.39}$$

$$\frac{\partial c}{\partial z}C(x,y,B,t)=0,\text{ when } z=B \tag{3.40}$$

3.4 Integrated Model Flux Transfer

Such integration is based on the consideration of mass balance, box model concept, and numerical analysis techniques (Mackay, 1991; Cowan et al., 1995). Mathematically and physically defined Equations 3.11, 3.16, 3.21, and 3.27 for the four media zones share the same general fate and transport mechanisms. They are concerned not only with the pollutants penetrating the advection and transformation inside a particular medium but also with the inter-media mass transfers. Furthermore, reactions like sink, sorption, radioactive decay and biodegradation are included in those equations that consider the multimedia impacts associated with a complex pollution problem. Integrating the entire system consisting of four zones, non-uniform and non-steady conditions will be considered.

3.4.1 Integrated Model Flux Transfer in 1-D

In this study, a two step-approach (Figure 3-6) is followed, using emission characteristics and a simple box model, to characterize the major fate pathway. Then the fate of the chemical in a spatial way is re-calculated, using a water, air or soil model, as appropriate. From Figure 3-6, it can be noted that, basically, Equations (3.11), (3.16), (3.21) and (3.27) are uniform in the separated zone, but the different zones have different *C, V, R*, and λ values. That means the whole multimedia system should be non-uniform.

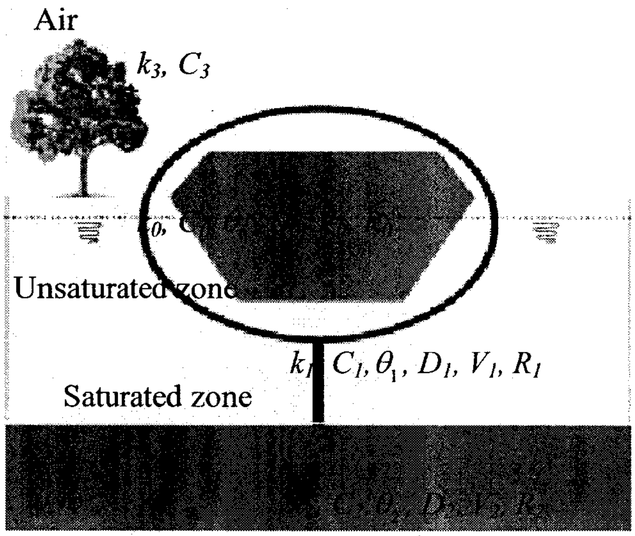

Figure 3-6 Integrated multimedia box model on non-uniform conditions

For all zones concerned pollutants penetrate into them not only by advection and transformation, but also through other inter-media transfers such as non-diffusive and diffusive transfers. Furthermore, reactions like sink, sorption, radioactive decay and biodegradation are included in those equations as well. The major difference among the four equations is that Equation (3.11) is assumed to be one-dimensional with the vertical parameters, Equation (3.16) is assumed to be three-dimensional only with respect to the dispersion coefficient, Equation (3.21) is assumed to be three-dimensional with either dispersion or seepage velocity components, and Equation (3.27) only considers the diffusion coefficient. When integrating the whole zones, non-uniformity of the individual zones should be considered.

The chemical flux F_t (M L^{-2} T^{-1}) is the sum of the vapor flux and the flux of dissolved solute. The total mass flux is the sum of the flux above, calculated by:

$$F_t(z,t) = F_g(z,t) + F_l(z,t) + F_a(z,t) \tag{3.41}$$

where, F_g is the gas phase diffusive flux, F_l is the aqueous phase diffusive flux, and F_a is the aqueous and gaseous phase advective flux.

The analyses above make it possible for the governing equations of all four modules to be solved within one scheme and to generate coherent simulation results for air, landfill, unsaturated, and saturated media. Both steady and unsteady flow effects are considered in the proposed EEMMS. The outputs of the EEMMS include (i) gaseous emission flux out of landfill cover, (ii) a spatial concentration distribution profile of waste species in a landfill chamber in the surrounding soil media, and in the adjacent groundwater system. Both finite difference and finite element methods are examined to give numerical solutions for the developed EEMMS. More solution algorithm schemes are provided in Appendices A, B and C.

3.4.2 Integrated Model Flux Transfer in 2-D and 3-D

According to the mass balance and box model (Figure 3-6), we could find that the area of contaminant penetrating into the aquifer is approximated as a rectangle $\Omega = \{(x,y): x_1 \le x \le x_2, y_1 \le y \le y_2\}$ on the upper boundary, then the flux transfer should be represented by the equation:

$$-D_z\frac{\partial C}{\partial X}+V_zC=F(x,y,t)=\begin{cases}\psi(t),(x,y)\in\Omega\\0, \quad ,(x,y)\notin\Omega\end{cases} \tag{3.42}$$

$$F_0(x,y,t)=-D_{z,1}\frac{\partial C_1}{\partial X}+V_{z,1}C_1 \tag{3.43}$$

So that the initial concentration is defined as:

$$C_0=\begin{cases}F_0(x,y,t)/V_{z,1} & inside\,\Omega\\0 & outside\,\Omega\end{cases}. \tag{3.44}$$

In the bottom boundary (the top of the aquifer) section (z=L), where L is the simulated landfill depth, we set the pollution flux percolating down through the section equal to the pollution flux F_1 into the aquifer:

$$F_0(x,y,t)=-D_{z,1}\frac{\partial C_1}{\partial X}+V_{z,1}C_1\bigg|_{z=L} \tag{3.45}$$

To solve the mass flux, we use the following formula for the pollution flux rate per unit area:

$$\psi_1(y,z,t)=\begin{cases}V_xC(0,y,z,t) & x=0\\V_x\int_{-\infty}^{+\infty}\int_0^{+\infty}C(0,y,z,t)dzdy & x\neq 0\end{cases} \tag{3.46}$$

In two-dimensional cases, the governing Equation (3.46) can be rewritten into following forms:

$$\psi_1(y,t)=\begin{cases}V_xd_0\bar{C}(0,y,t) & x=0\\V_xd_0\int_{-\infty}^{+\infty}\bar{C}(0,y,t)dy & x\neq 0\end{cases} \tag{3.47}$$

where,

$\bar{C}$ is the mean concentration across depth (mg m^{-3}), and

d_0 is the mean aquifer thickness (m).

When the flux transferred from one zone to another, the total flux F_t (g m^{-2} d^{-1}) is the sum of the air flux and the flux to the leachate. F_t (g m^{-2} d^{-1}) is the sum of this two:

$$F_t(x,y,z,t) = F_{air}(x,y,z,t) + F_{leachate}(x,y,z,t) \tag{3.48}$$

The cumulative air mass lost from the landfill surface per unit area of contamination site, M_{air} (g m^{-2}), is as follows (Jury et al. 1990).

$$M_{air}(t) = \int_0^t -F_{air}(0,t)dt \tag{3.49}$$

And the cumulative leachate flux (g m^{-2}) is predicted by using:

$$M_{leachate}(z,t) = \int_0^t F_{leachate}(z,t)dt \tag{3.50}$$

Finally, the total cumulative flux (g m^{-2}) is calculated by

$$M_t(z,t) = M_{air}(z,t) + M_{leachate}(z,t) \tag{3.51}$$

3.5 Integrated Risk Assessment

Lowrance (1976) defines risk as a measure of the probability and severity of adverse effects. In order to quantify risks, it is necessary to specify the spatial and temporal distribution of contaminants in the environment, the uncertainties in the system, and the method of risk evaluation. In the present study, EEMMS predictions that examine the contaminant transport in the multimedia environment, in conjunction with the environmental guidelines for protection of groundwater, will be used to quantify the risk of environmental impacts. The Monte Carlo method will be used to analyze the system uncertainties. What follows will introduce the integrated risk assessment approach developed in the present research.

3.5.1 Description of the Integrated Risk Assessment Approach

To analyze cases involving uncertainty and variability of input parameters, the MCM differs from single-valued output, where "single-point" values are specified for model parameters and results are obtained in terms of single-valued output (Figure 3-7) (Kamboj et al., 2002). In the MCM analysis model, input parameters may be characterized in terms of statistical distributions. Results are obtained in terms of distributed value output that can be used to characterize uncertainty and variability for conducting probabilistic analyses (Figure 3-8). Once the parameter probability density function (PDF) for an input parameter has been generated (Figure 3-8), a specific value within the MCM -generated PDF range of values can be selected as the input-parameter value for the EEMMS.

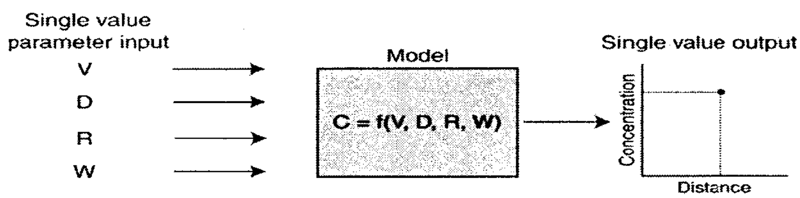

Figure 3-7 Deterministic analysis (Kamboj et al., 2002)

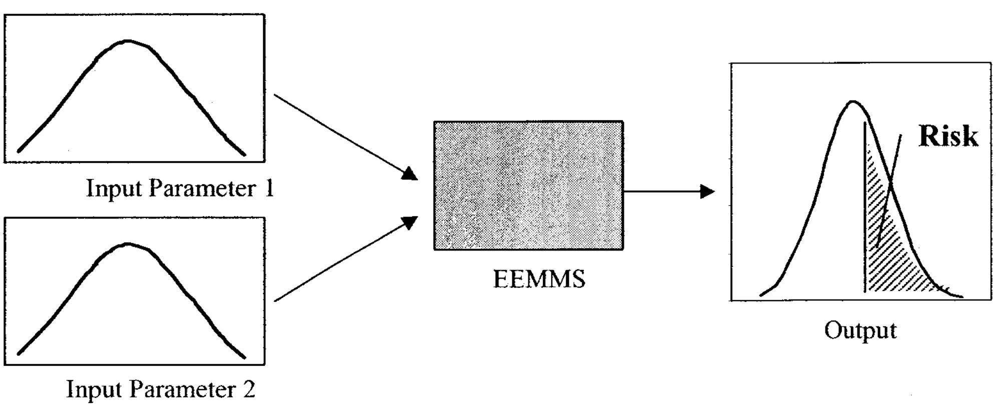

Figure 3-8 Integrated risks used in EEMMS

The following illustrative steps are given to show how to quantify the risk level based on the EEMMS under published environmental guidelines:

(i) Generation of parameter probability density functions (PDF) for dispersivity coefficient, hydraulic conductivity, and bulk density, retardation and porosity coefficient.

(ii) Implementation of the new EEMMS to simulate pollutant transport for each set of coefficients generated in Step (i);

(iii) Generation of outputs from step (ii) for each set of data which will be stored until the chosen sample size of simulations is finished;

(iv) Selection of a point of concern, generation of statistics for simulation outputs and conducting of an uncertainty analysis;

(v) Identification of pollutants standards to calculate the risk level; and

(vi) Obtaining a complete set of risk-level predictions using RQ evaluation methods.

3.5.2 Strategy for Deciding on Sample Size

One of the first problems encountered when applying the MCM is to decide on the number of samples. Several criteria are examined to determine sample size. The first criterion is that parameter and standard error biases do not exceed 10 percent for any parameter in the EEMMS. The second criterion is that the standard error bias for the parameter for which power is being assessed does not exceed 5 percent. The third criterion is that coverage remains between 0.91 and 0.98. Once these three conditions are satisfied, the sample size is chosen to keep power close to 0.80. The value of 0.80 is used because it is a commonly accepted value for sufficient power. In the present paper, the sample size of MCM is derived by Equation (3.52) (Mendenhall, 1994) as follows:

$$n = \left[\frac{S_{\alpha/2}\sigma_{stv}}{E} \right]^2 \tag{3.52}$$

Where, n is the sample size, E is the percent error with respect to the mean; $S_{\alpha/2}$ is known as the critical value, the positive S value that is at the vertical boundary for the area of $\alpha/2$ in the right tail of the standard normal distribution; σ_{stv} is the population standard deviation.

3.5.3 Monte Carlo Method to Assess Model Uncertainty

Recent emphasis in the risk analysis has focused on uncertainty in the risk assessment process (Michael et al., 2004). To perform risk assessment, model uncertainty and data uncertainty should be taken into account. "uncertainty" can be described as a lack of knowledge regarding the true value of a parameter. Since a lack of knowledge does not imply total ignorance, it is possible to characterize the relative likelihood of different values for a parameter. MCM is used for quantifying system uncertainties, with the modeling outputs serving as the basis for risk quantification.

Considering the uncertain parameters in the EEMMS, hydraulic conductivity, K, bulk density, ρ_b or porosity, θ are the key input variables in the simulations. It has been reported that the mixing coefficient resulted in generally normal distributions. Using the MCM approach, the values of those parameters are generated from a uniform distribution. The normal generators can be simply expressed as follows:

$$u = F(\sigma_u, \mu_u) \tag{3.53}$$

where, u = hydraulic conductivity, K, bulk density, ρ_b or porosity, θ; $F(\sigma_u, \mu_u)$ represents a normal distribution function of σ_u and μ_u ; σ_u = standard deviation of x; and μ_u = the mean value of u. It should be noted that the results of the uncertainty analysis depend directly on the distributions assumed for each of the parameters. Hence, good representative data are required to obtain reliable estimates of uncertainty.

After generating certain sets of random samples for each parameter, the distribution of predicted concentrations for each grid square can be calculated by the EEMMS. The distribution results can then be used to define 5 and 95 percentile concentrations, and an uncertainty factor is calculated as the ratio of the 95 and 5 percentile concentrations.

3.5.4 Characterization of the Risk

In the study, two methods were used to study the levels of risks or adverse effects associated with multimedia pollutants transportation, the risk quotient (RQ) and Probabilistic risk assessment (PRA).

More specifically, risk quotient is the ratio of a measured or estimated level of concentration to a benchmark concentration. RQ evaluation will be derived from the CHARM model. The RQ quotient evaluation is carried out based on the comparison of the predicted environmental concentration (PEC) to the known environmental criteria (KEC), which refer to local environmental guidelines for a species.

The RQ factor is calculated as follows:

$$RQ = \frac{PEC}{KEC} \tag{3.54}$$

Probabilistic risk assessment (PRA) often refers to the generation of distributions of exposure or risk representing uncertainty or variability or both. In this way, Environmental risk associated with the transportation of multimedia pollutants could be expressed as the probability of a pollutant's concentration (denoted as C) exceeding local environmental guidelines (denoted as $C_{standard}$), i.e., $R = P\ (C > C_{standard})$, R denotes risk. Thus, the risk can be quantified as follows (NRC, 2007):

$$R = P(C > C_{\text{standard}}) = \int_{C_{\text{standard}}}^{\infty} f_C(C)dC \tag{3.55}$$

The integrated risk simulation calculates numerous scenarios of a model by repeatedly picking values from a probability distribution for the uncertain variables and using those values for the model. These probabilities are propagated through the EEMMS, and an output distribution describing the probability of various outcomes is generated (Figure 3-8).

The MCM will be used to analyze system uncertainties. Recent emphasis on risk analysis has focused on uncertainty in the risk assessment process (Schuhmacher et al., 2001). To perform risk assessment, model uncertainty and data uncertainty should be taken into account. "uncertainty" can be described as a lack of knowledge regarding the true value of a parameter. Since a lack of knowledge does not imply total ignorance, it is possible to characterize the relative likelihood of different values for a parameter. MCM is used to quantify system uncertainties, with the modeling outputs serving as a basis for risk quantification. MCM for the integrated risk assessment includes three main parts: parameter probability density function (PDF), model outputs for PDF and the risk quotient evaluation. In the MCM analysis mode, results are obtained in terms of distributed value output that can be used to characterize uncertainty and variability for conducting probabilistic analyses (Figure 3-8). Once the parameter probability density function (PDF) for an input parameter has been generated (Figure 3-8), a specific value within the MCM -generated PDF range of values can be selected as the input-parameter value for the EEMMS.

3.6 Solutions Techniques for Multidimensional Equations

Based on the review of previous literature above (Chapter 2), it can be concluded that the mathematical methods available for the prediction of multimedia mass transport have serious shortcomings. Therefore, the present investigation has been directed to develop numerical models using the finite-difference method and finite-element method to simulate the problem stated, taking into consideration the parameters mentioned in Equations (3.6-3.27). Appendix A, B, C and D show the calculation details and the part code.

Numerical models using the finite-difference method and finite-element method to simulate the problem stated were also used in this research. Analytical models will be compared to assess differences between the methods. In addition, some of the parameters' uncertainty analysis associated with the finite-difference method and finite-element method for solving the multimedia pollutants are illustrated.

3.7 Consideration of Fate Mechanisms in the EEMMS

3.7.1 Different Processes in the EEMMS

Many factors influence contaminant transport dynamics in multi-zone (landfill, unsaturated saturated) systems (Table 3-2). While reaction processes depend on advection and transport; transport is driven, to a certain extent, by the other reactions.

For example, linear equilibrium sorption, linear equilibrium liquid-vapor partitioning, and decay rate, and even retardation will affect the plume. There are four typical scenarios (Table 3-2).

Table 3-2 Four typical scenarios with different processes

Scenarios	Simulated processes				
	Advection	Diffusion /dispersion	Vapor partition Vapor-phase diffusion	Sorption	Decay
a	√	√			
b	√	√			√
c	√	√		√	√
d	√	√	√	√	√

Usually researchers will consider the very simple case, scenario “a”, which describes only advection and diffusion/dispersion of a dissolved-phase conservative contaminant ($R=1$; $\mu=0$) under steady-state flow conditions (V=constant, 0.05m d^{-1}, D_l=constant, 88.1×10^{-6} m^2 d^{-1}). If the decay is added to the advection-dispersion problem, the result is scenario “b”. Considering sorption and decay process (R=1.4776; μ=0.001899), the outcome is scenario “c”. Based on scenarios “c” and taking into account of the vapor-phase contaminant (D_g=0.752 m^2 d^{-1}), the result is scenario “d”.

When the multimedia pollutant transport increases in complexity and difficulty by considering advection and dispersion, other process such as sink, sorption, radioactive decay and biodegradation (scenario “d”) should also be included. There is very little recent research relate to scenario “d” and their relations to each other.

Based on a review of literature, it was found that in the multimedia contaminant transport governing equations described earlier, the influence of advection and dispersion have been well researched, whereas retardation, sink, sorption, radioactive decay and biodegradation have just begun to be addressed. Vapor reaction sink/source and chemical reactions were added and differences in scenarios (Table 3-2) can be clearly seen in Figure 3-9a to Figure 3-9d.

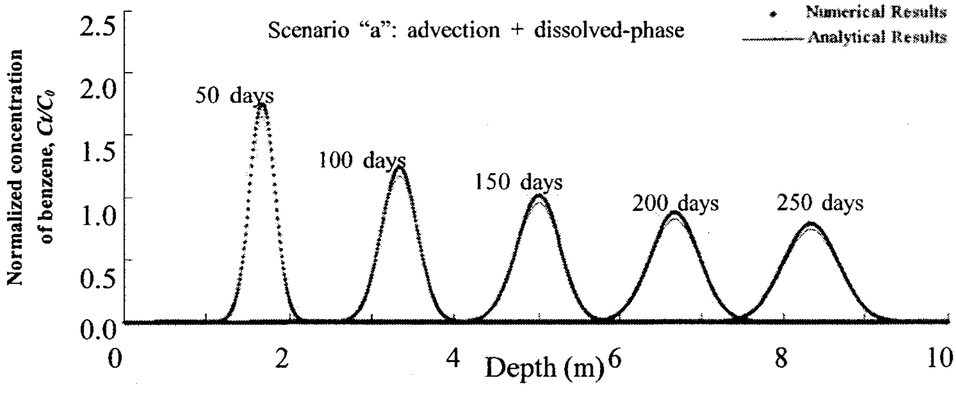

Figure 3-9a Normalized "a" scenario for benzene contamination

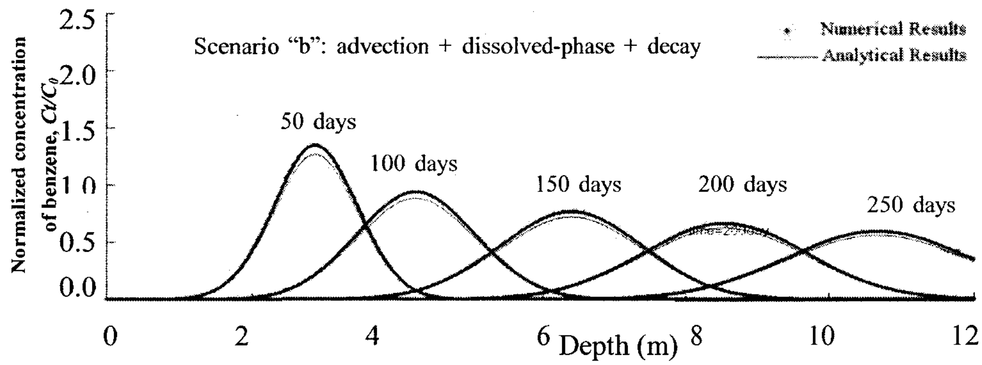

Figure 3-9b Normalized "b" scenario for benzene contamination

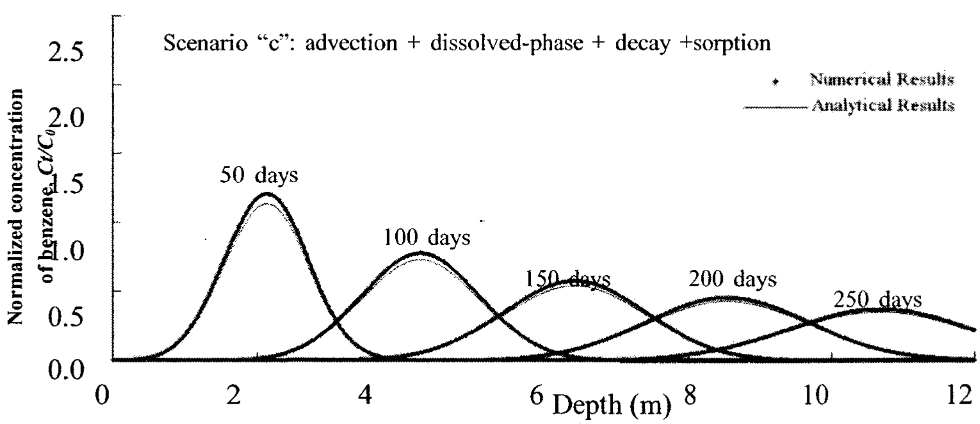

Figure 3-9c Normalized "c" scenarios for benzene contamination

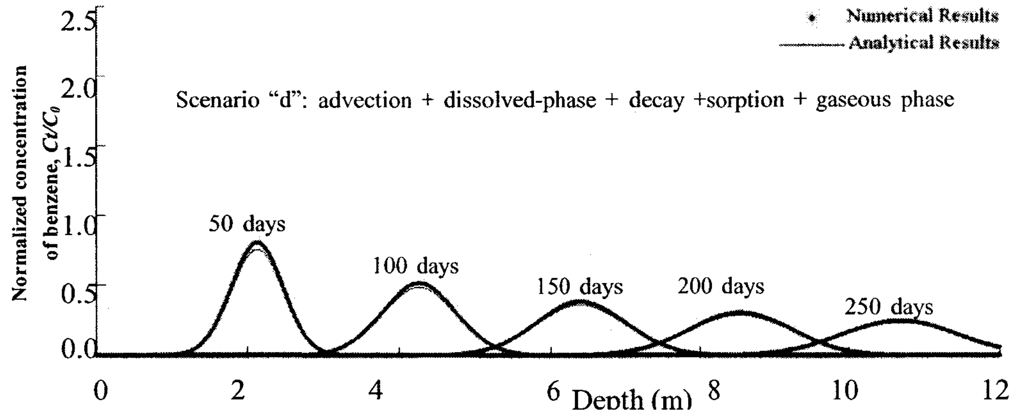

Figure 3-9d Normalized "d" scenario for benzene contamination

From Figure 3-9a to Figure 3-9d it can be seen under scenario "b" the simulated benzene concentrations are smaller than that in scenario "a" due to the decay process. Inclusion of the sorption process (scenario "c") not only lowers the contaminant levels along the soil profile but also results in a time shift of the spatial distribution of concentrations due to an increase in the retardation factor. In scenario "d" diffusion of the vapor-phase, decay of the vapor-phase contaminant and elevated retardation cause the concentration curves of the contaminant transport problem to be stretched and the values become much smaller. In conclusion, in the improved multimedia model the addition of retardation, sink, sorption, radioactive decay and biodegradation will make the predicted contaminant levels smaller than those predicted by equations that only consider advection and dispersion.

3.7.2 Sensitivity Analysis in the EEMMS

Sensitivity analysis is also conducted to evaluate the applicability and performance of various uncertainty analysis techniques to this new EEMMS. Since there are so many uncertainties, the real cases usually are much more complex, it is reasonable to consider all the factors together.

Sensitivity analysis is used to determine how "sensitive" a model is to changes in the value of the parameters of the model and to changes in the structure of the model. In this paper, we focus on parameter sensitivity such as hydraulic conductivity, bulk density and porosity. Parameter sensitivity is usually performed as a series of tests in which the modeler sets different parameter values to see how a change in the parameter causes a change in the dynamic transportation. By showing how the model behavior responds to changes in parameter values, sensitivity analysis is a useful tool in model building as well as in model evaluation.

Sensitivity analysis helps to build confidence in the EEMMS by studying the uncertainties that are often associated with parameters in the EEMMS. Many parameters represent quantities that are very difficult, or even impossible to measure to a great deal of accuracy in the real case study. Furthermore, when building the EEMMS, there are some uncertainties on the parameter values. Sensitivity analysis could determine what level of accuracy is necessary for a parameter to make the model sufficiently useful and valid. If the tests reveal that the model is insensitive, then it may be possible to use an estimate rather than a value with greater precision. Sensitivity analysis can also indicate which parameter values are reasonable to use in the EEMMS. If the model behaves as expected from real case observations, it gives some indication that the parameter values reflect, at least in part, the “real case”.

Sensitivity tests help the modeler to understand dynamics of the EEMMS. Experimenting with a wide range of values can offer insights into the behavior of a system in extreme situations. Discovering that the system behavior greatly changes for a change in a parameter value can identify a leverage point in the model, parameter whose specific value can significantly influence the behavior mode of the EEMMS.

For example, the different bulk density shown in Figure 3-10, 3-11, 3-12 was designed using the FEM (COMSOL Multiphysics). Figure 3-10 shows the x–y plane of the evolution of the contaminant plume at 100 days when bulk density is 500 kg m^{-3}. Figures 3-11 and 3-12 respectively present results of the evolution of the contaminant plume at bulk density are 2000 kg m^{-3} and 4000 kg $m^{-3}$of the model. From Figures 3-10, 3-11, 3-12, we find that the higher the bulk density, the lower the concentration dispersion.

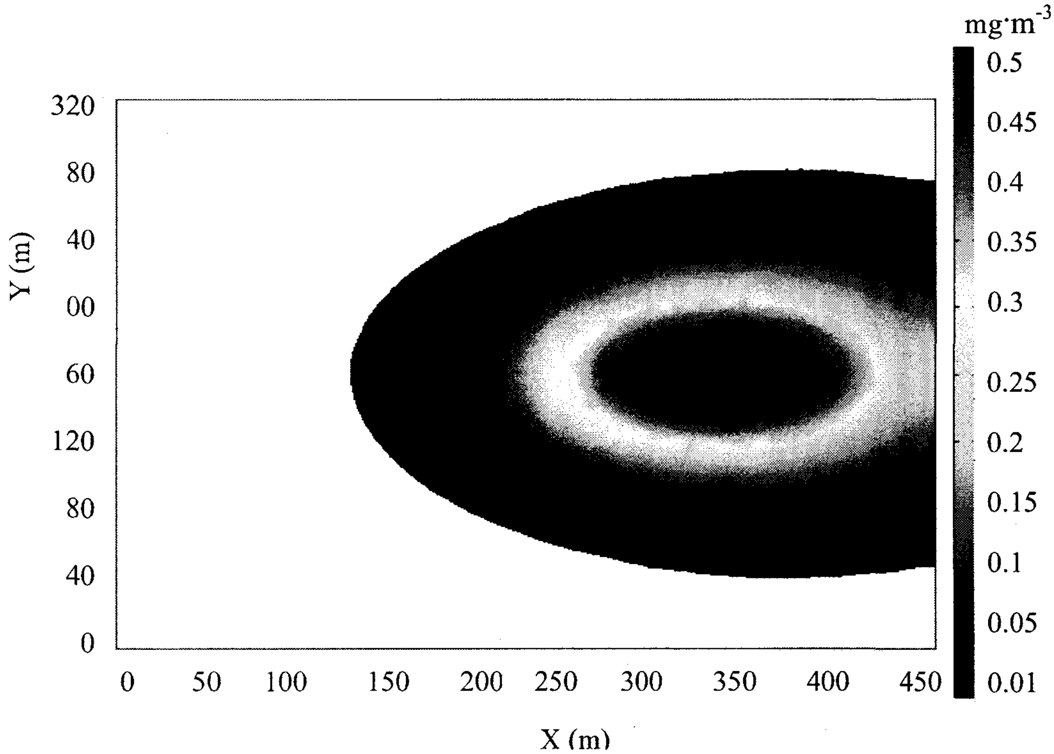

Figure 3-10 2-D point source contaminant plume at bulk density=500 kg m^{-3}

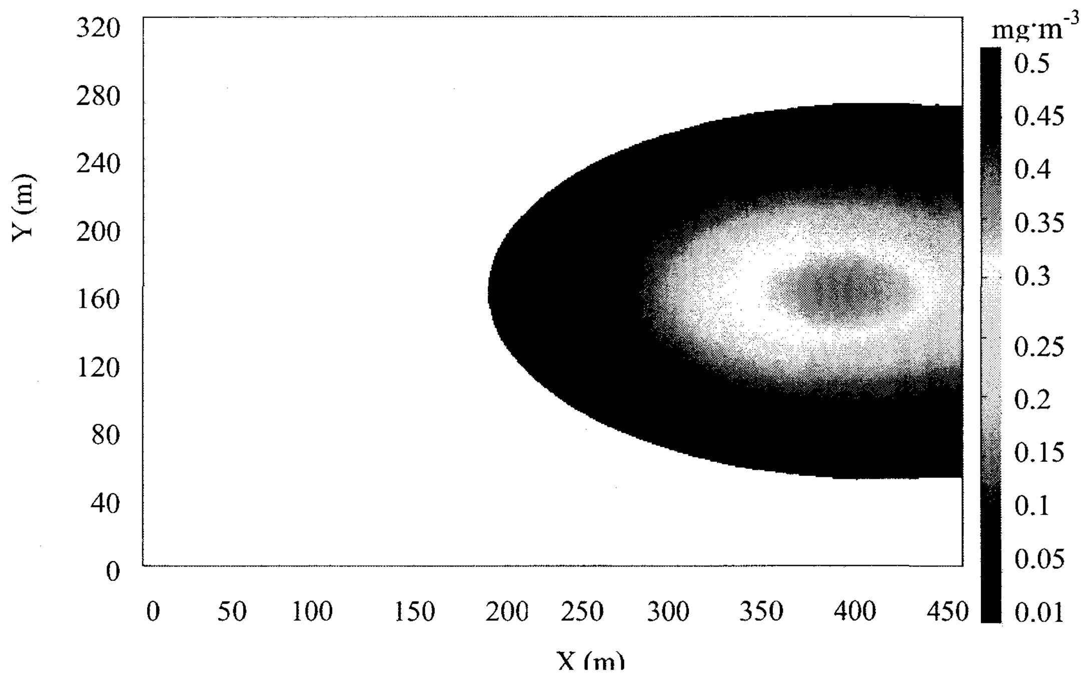

Figure 3-11 2-D point source contaminant plume at bulk density=2000 kg m^{-3}

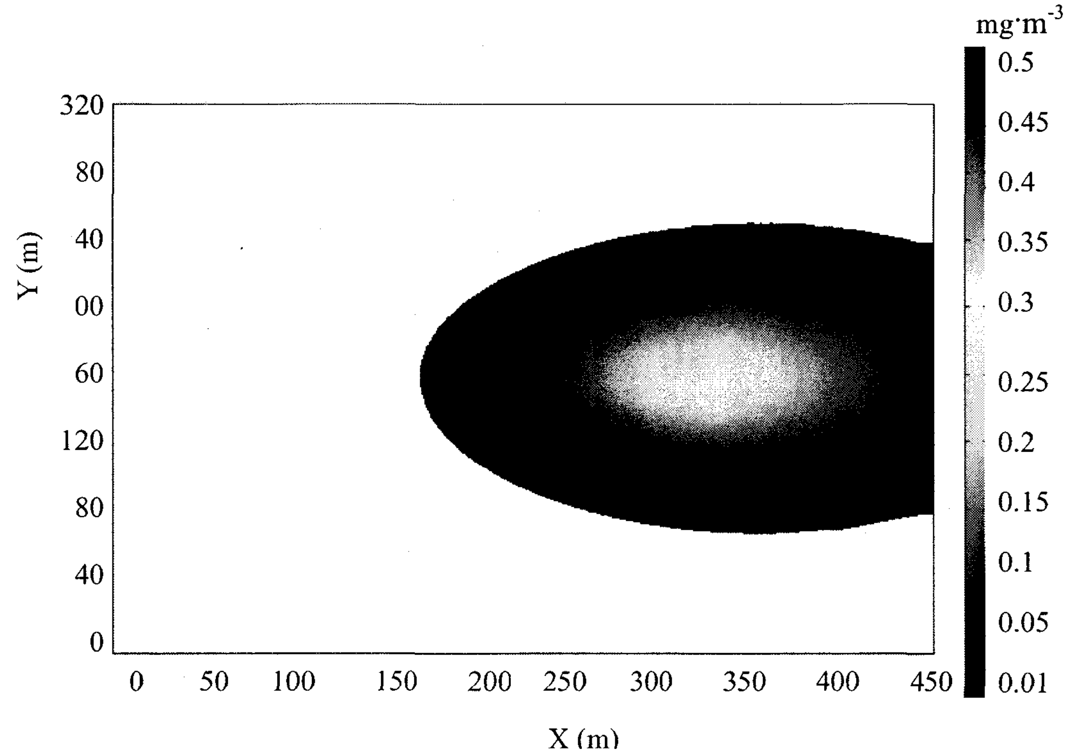

Figure 3-12 2-D point source contaminant plume at bulk density=4000 kg m^{-3}

Hydraulic conductivity, symbolically represented as *K*, is a property of soil or rock, which describes the ease with which water can move through pore spaces or fractures. It depends on the intrinsic permeability of the material and on the degree of saturation. So different soil has different hydraulic conductivity, Figures 3-13, 3-14, and 3-15 shown here give results along the time t = 100 days at hydraulic conductivity equal to 0.11, 0.22, and 0.44 m d^{-1}. From the Figure 3-13 to Figure 3-15, It was found that the higher the hydraulic conductivity, the higher the concentration dispersion.

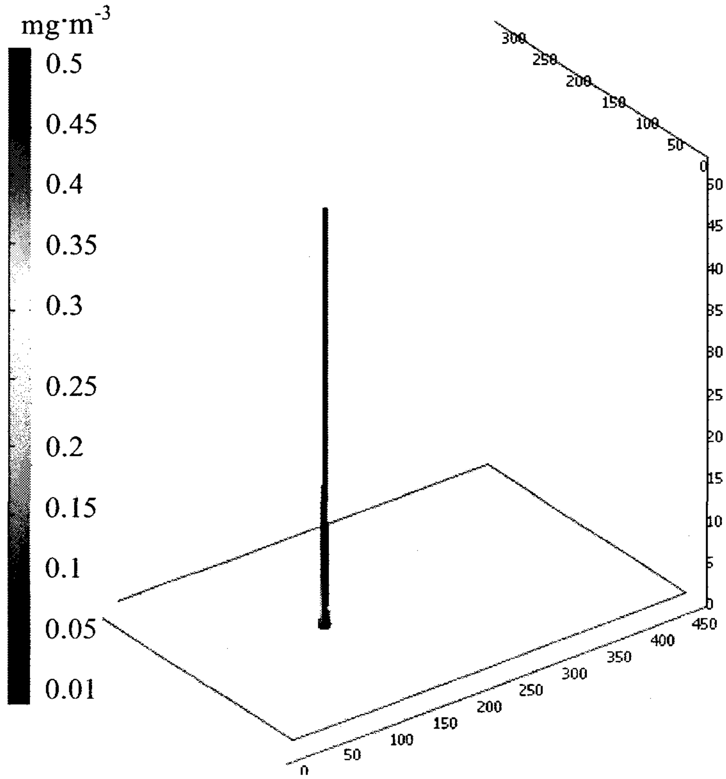

Figure 3-13 2-D point source contaminant plume at hydraulic conductivity =0.11 m d^{-1}

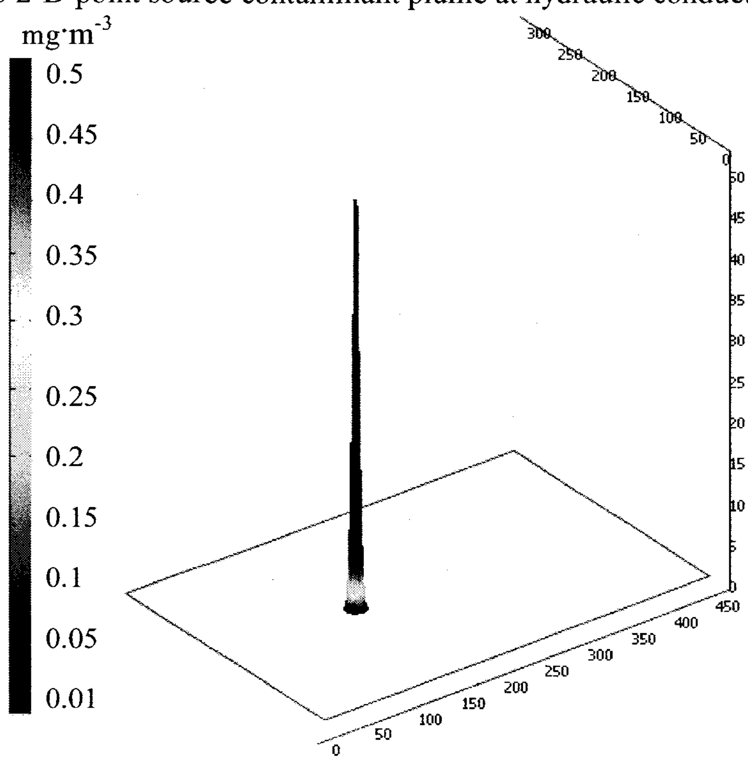

Figure 3-14 2-D point source contaminant plume at hydraulic conductivity =0.22 m d^{-1}

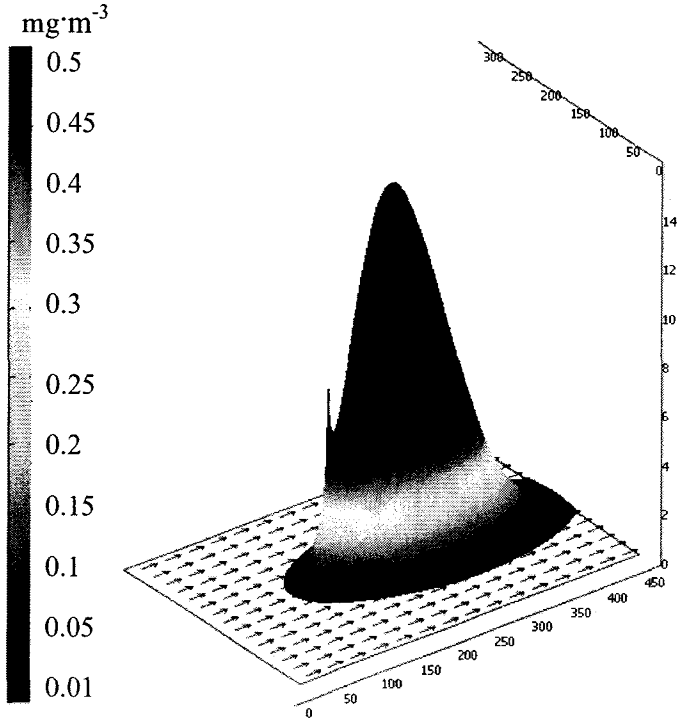

Figure 3-15 2-D point source contaminant plume at hydraulic conductivity =0.44 m d^{-1}

3.8 Model Input and Output

This study is directed to the prediction of the transport of multimedia pollutants. For this purpose, the EEMMS will be developed to simulate the problem stated. The improved multimedia model presented in this report is divided into four key modules: a source module, an unsaturated zone module, a saturated zone module, and an air dispersion module. The modeling outline and the expected outcomes are summarized in Figure 3-16.

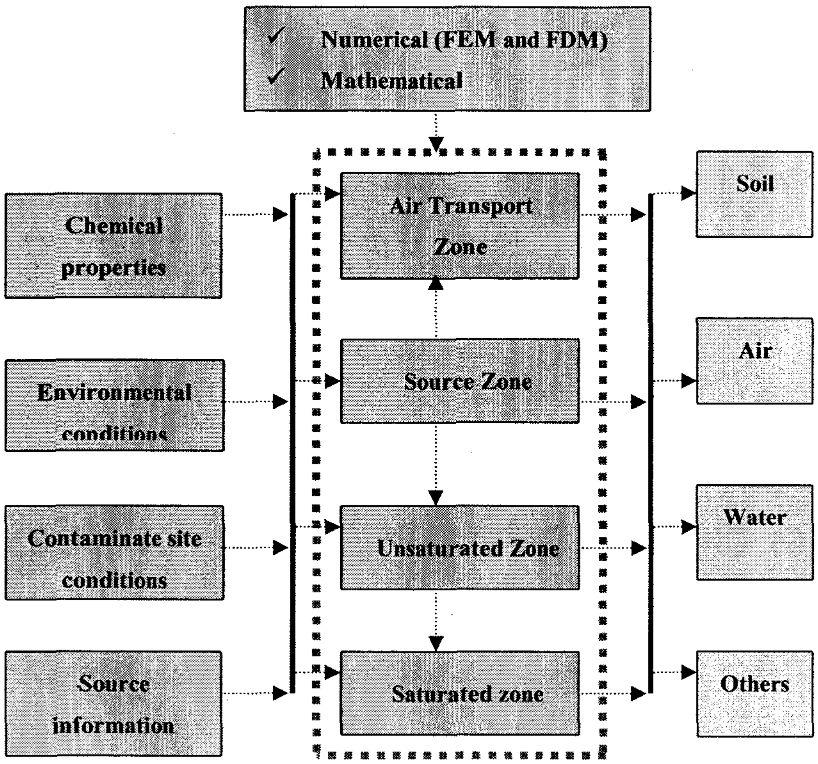

Figure 3-16 Modeling outline and the expected outcomes

The input is subdivided into the chemical properties, environmental conditions, contaminate site conditions and source information. Three basic environmental media, air, soil and water are treated as contaminant transport pathways integrated within the integrated multimedia model to predict potential risks at exposure sites. The model will simulate the internal dynamics of the polluting source area (e.g. landfill); compute emission fluxes up to the air and atmosphere and down to the soil and groundwater from the polluting source zone. It will also estimate the subsequent dispersion of pollutants in the ambient atmosphere, the concentration profiles in the connected soil and groundwater systems, and will consider not only physical transport but also the decay evolution in multiple dimensions.

3.9 Summary

The methodology used in the present study can be summarized as follows:

(1). A new modeling approach (EEMMS), which followed the MCM, has been developed to simulate the multi-dimensional transportation of contaminants in the multimedia environment.

(2). The numerical methods such as FEM and FDM have proven to be a powerful technique to solve a variety of science and engineering problems. In the present study, those numerical techniques were used to model the new EEMMS and their methodologies in this research were discussed in detailed 1-D, 2-D and 3-D situations.

(3). EEMMS is introduced in details as a three-dimensional, multimedia, fate and transport model. Its governing equations and computational scheme with a full consideration of boundary conditions are presented in this chapter.

(4). Considering the uncertainty parameters in the EEMMS, the MCM has been chosen to assess model uncertainties and to provide the probability distribution of predicted concentrations for each grid square. The results from the MCM approach will serve as the bases for the environmental risk assessment.

(5). Two methods for quantifying risks have been presented and incorporated with

EEMMS in this chapter: the PRA and the RQ factor. Mapping of the possible risk severities based on these two methods is demonstrated in the Chapter 7.

Chapter 4 Systematic Model Verification in 1-D through Analytical and Numerical Comparison with Extensive Data from the Literature

After the numerical model is constructed through the appropriate input files, it is generally necessary to calibrate the model. Calibration is a process in which model input parameters are adjusted until model output variables (or dependent variables) match field-observed values to a reasonable degree. The new EEMMS integrates information on emissions, chemical properties, environmental characteristics, and transport processes into a comprehensive framework for assessing the distribution of pollutants entering the environment. Comparison against monitoring data provides one means of arriving at some understanding of the strengths and limitations of these models. The process for validation was defined as one that "requires applying a calibrated model to a new scenario and then evaluating the agreement between model predictions and observed data" (Cowen et al., 1995). Validation of complex environmental models is a daunting task and the subject has received a significant amount of attention recently (Beck et al., 1997). Different approaches liken numerical verification and experimental validation have been performed in several studies (Mackay and Paterson, 1991; Devillers et al., 1995; Gobas et al., 1998)

In Chapter 4, testing of the new EEMMS against a complete case study has been undertaken, and a comparison was made between analytic and numerical results. The simulation results were also compared with data from the literature. Thus, model validation was conducted through comparing simulated or predicted model output to measured output such as literature data, field sites data or a pilot experimental data. The detailed flow chart of the model validation process is presented in Figure 4-1.

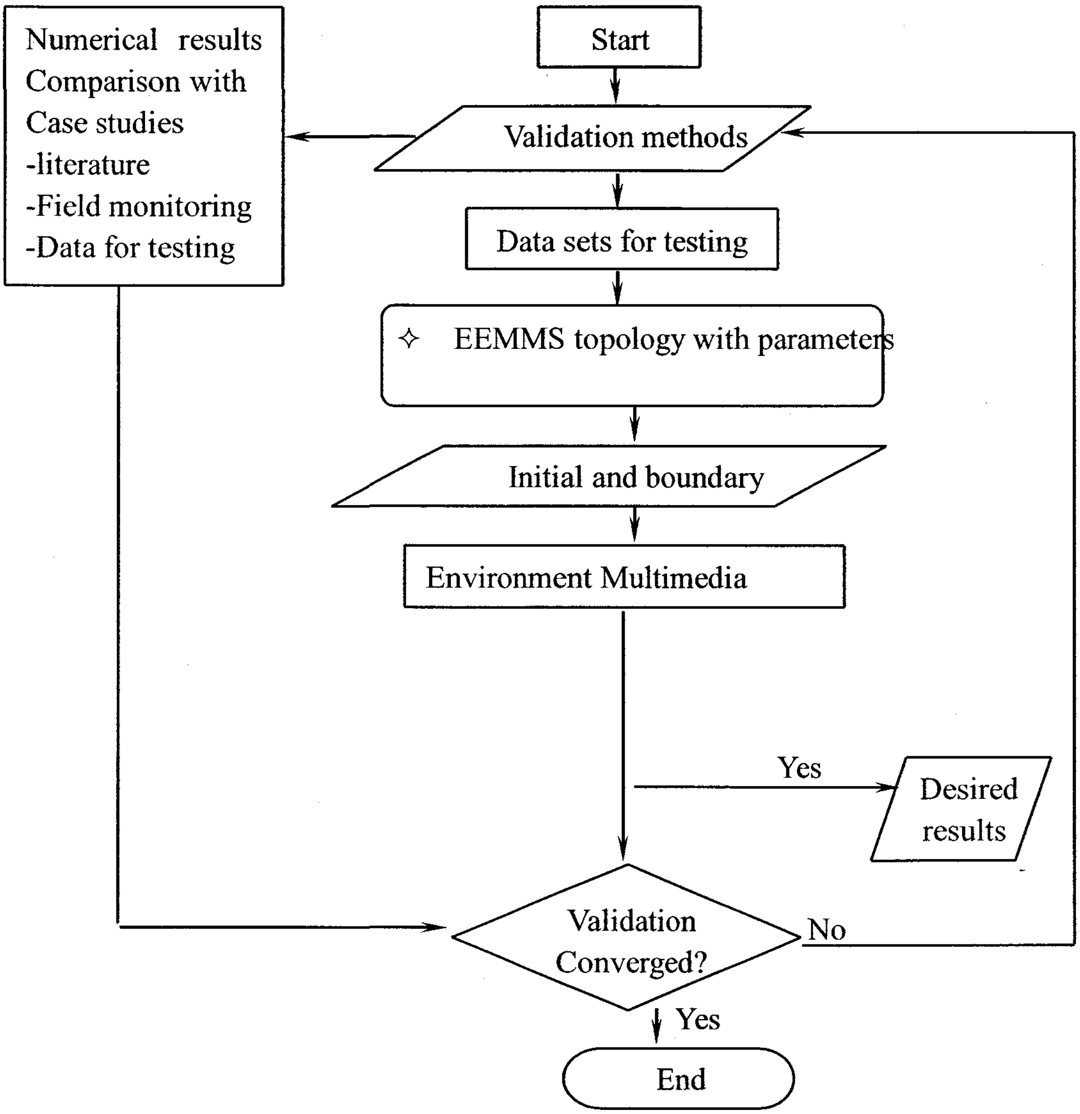

Figure 4-1 Validation framework chart of the EEMMS

4.1 A Complete Case Study

4.1.1 Introduction

The developed EEMMS was applied to a representative multimedia environment with a landfill source (Figure 4-2), so as to assess the impact of the landfill on surrounding soil and groundwater systems resulted from benzene emissions. The site data are modified from Carnahan and Remer (1984), Domenico (1987), Lin and Hildemann (1995), and Stephenw and Karsten (2003). The site, is approximately $100m \times 100m$ in area and 1 m in depth, and is surrounded by an area of farms, forest and industry. Moreover, a residential area is located 500 m downstream from the landfill where the residents use the groundwater (Figure 4-2).

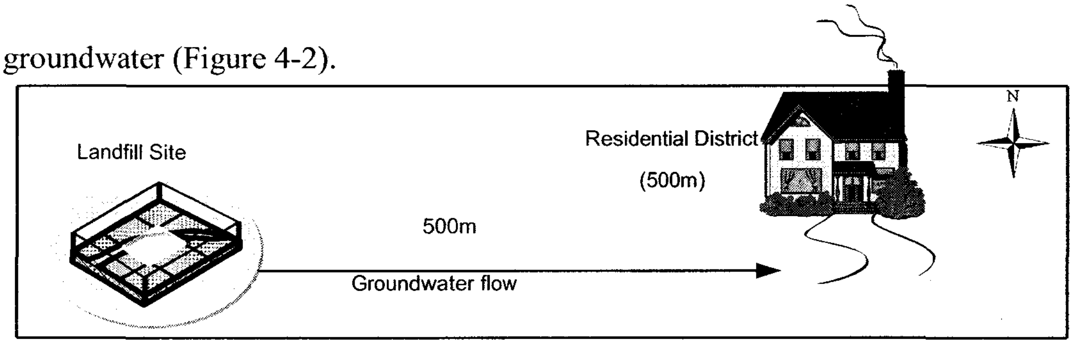

Figure 4-2 Type of site modeled

A 0.05 m thick surface cover was constructed to control volatile gas emissions, but no liner system was installed at the landfill's base. The landfill is located in an urban region where precipitation levels produce a 5-mm d^{-1}-bulk leachate velocity in the landfill zone. The soil beneath the landfill site is composed of sand, clay and gravel. Thus, the bulk density of the unsaturated and the saturated zone is 1.59 mg m^{-3}. The groundwater level is 3.5 meters beneath the landfill bottom and flows underneath the landfill in an eastern direction with a velocity of 0.03 m d^{-1}. The porosity of the soil and the groundwater near the landfill site is 0.4. Benzene was chosen as the contaminant as it is harmful to human health. The input parameters (Tables 4-1, 4-2) include the landfill characteristics, chemical properties, and soil properties of landfill, the unsaturated zone's characteristics, chemical properties and saturated zone's characteristics. Bulk gas velocity and leachate velocity are 0.05 m d^{-1} and 0.05 m d^{-1} for the simulation of benzene concentration in the soil.

Table 4-1 Input parameters for air module (Stephenw and Karsten, 2003)

Parameters	Symbol (units)	Value
Coefficient of transverse dispersion	D_E (m^2 d^{-1})	1×10^{-6}
Half-life	$t_{1/2}$ (day)	365
Henry's law constant (dimensionless)	K_H	0.22
Retardation (dimensionless)	R	1
Air height	Z (m)	5

Table 4-2 Input parameters for landfill module (Lin and Hildemann, 1995)

Parameters	Symbol (units)	Value
Gaseous diffusion coefficient	D_g (m^2 d^{-1})	0.752
Henry's law constant (dimensionless)	K_H	0.22
Half-life	$t_{1/2}$ (day)	365
Diffusion coefficient	D_l (m^2 d^{-1})	88.1×10^{-6}
Bulk density	P_b (kg m^{-3})	1350
Landfill depth	Z (m)	1
Volumetric air content of the soil	a	0.2
Volumetric water content at field capacity	n	0.3

Table 4-3 Input parameters of unsaturated zone module (Domenico, 1987)

Parameters	Symbol (units)	Value
Coefficient of transverse dispersion	D_T (m^2 d^{-1})	2.7×10^{-3}
velocity	v (m d^{-1})	5×10^{-3}
Porosity of unsaturated zone	φ_{un}	0.4
Bulk density of unsaturated zone	ρ_{unsat} (kg m^{-3})	1590
Half-life in unsaturated zone	$t_{1/2\ unsat}$ (d)	365
Water table depth	z_{wt} (m)	3.5

Table 4-4 Input parameters of saturated groundwater module (Carnahan and Remer, 1984)

Parameters	Symbol (units)	Value
velocity	v (m d^{-1})	0.03
Bulk density	ρ_{sat} (kg m^{-3})	1590
Organic carbon fraction	f_{ocsat} (dimensionless)	0.0125
Half-life	$t_{1/2\ sat}$ (d)	365

Both numerical and analytical results are obtained and compared in Figure 4-3. It shows that pollutant concentration profiles along the depth are well simulated using both analytical and numerical method in this example to solve Equations 3.11, 3.16, 3.21, and 3.27. They are in accordance with analytical solutions given by similar examples in Carnahan and Remer (1984), Domenico (1987), and Lin and Hildemann (1995).

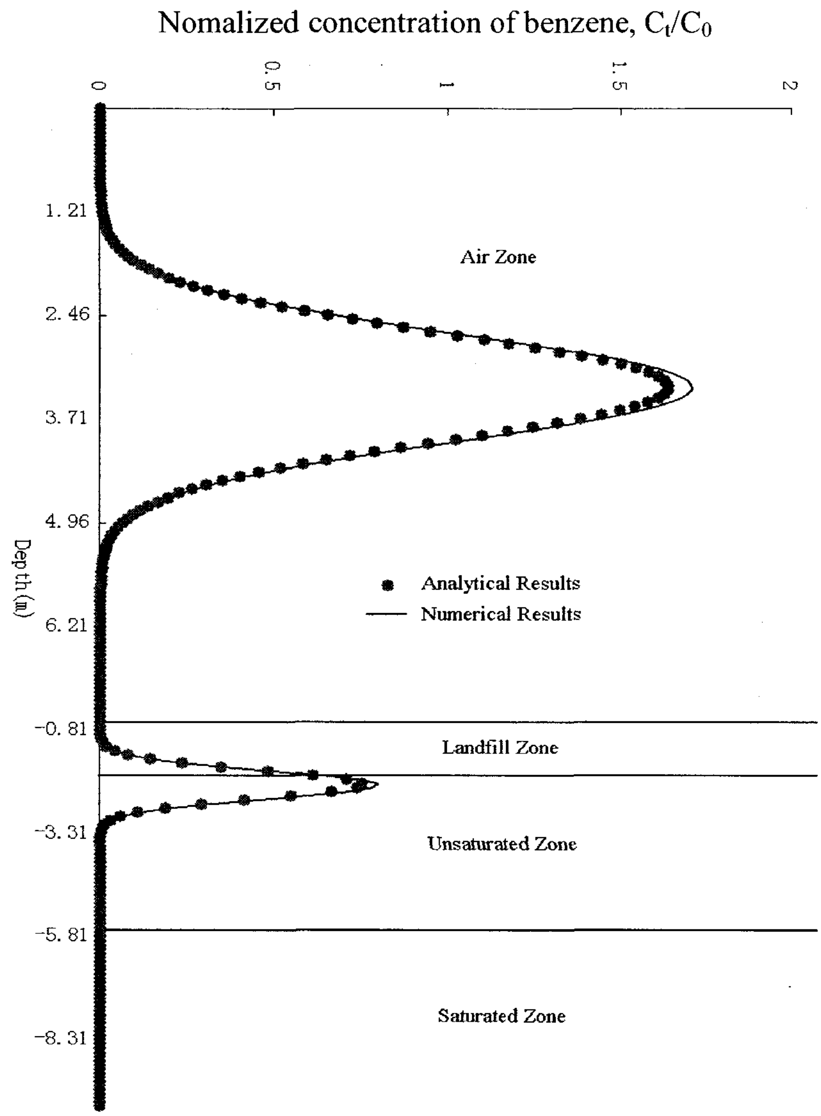

Figure 4-3 EEMMS numerical and analytical solutions in four zones

4.1.2 Modeling Flux Results

All input parameters are entered into the two systems; sequentially, the modeling system runs in a designed order to read the corresponding parameters into the air module, landfill module, the unsaturated zone module, and the saturated zone module. Finally, once the calculated results are output from the modeling system, the values are stored in the categorized output files, including air dispersion file, landfill file, unsaturated zone file, and saturated zone file. The flux computation comparisons results are shown in Table 4-5.

Table 4-5 Modeling flux outputs results to compare the traditional and new EEMMS

(Evaluation time (d), depth (m))	Traditional EMMS uniform total flux ($mg \cdot m^{-2} \cdot d^{-1}$)	EEMMS non-uniform total flux ($mg \cdot m^{-2} \cdot d^{-1}$)	(Evaluation time (d),depth(m))	Traditional uniform total flux ($mg \cdot m^{-2} \cdot d^{-1}$))	EEMMS non-uniform total flux ($mg \cdot m^{-2} \cdot d^{-1}$)
Landfill zone output			Unsaturated zone output		
(0,0)	0.0176	0.0176	(0,1)	0.0176	1.286×10^{-7}
(200,0)	1.549×10^{-3}	1.549×10^{-3}	(200,1)	1.085×10^{-3}	6.08×10^{-8}
(200,1)	1.123×10^{-3}	1.123×10^{-3}	(200,4)	1.1×10^{-3}	1.335×10^{-8}
(365,1)	7.63×10^{-4}	7.63×10^{-4}	(365,4)	1.02×10^{-3}	6.61×10^{-9}
Saturated zone output			Air zone output		
(0,5)	1.154×10^{-5}	8.861×10^{-11}	(0,0)	-	1.5985×10^{-2}
(200,5)	1.419×10^{-7}	8.672×10^{-11}	-	-	-
(200,8)	1.737×10^{-10}	9.27×10^{-12}	-	-	-
(365,8)	1.0×10^{-10}	6.5×10^{-13}	-	-	-

The Traditional EMMS uniform total phase flux simulation results were compared with the newly developed EEMMS' non-uniform total phase flux. The comparisons between uniform and non-uniform distributions of flux transport are illustrated in Figures 4-4 and 4-5. Usually, one should assume that the non-uniform distribution is the "standard" and the uniform distribution is the "approximation." The error arises from the solution of the governing equations for the uniform conditions. The limitation of former landfill and unsaturated modules in this case is the key assumption that all the compartments in the unsaturated zone are uniformly mixed. Such an assumption is not correct when the effect of variation in the spatial and temporal scale of the model is important for the risk assessment.

Figure 4-4 shows the distribution of the magnitude of simulated liquid mass flux within the time vs. concentration domain under uniform conditions. It shows the mass flux changing uniformly along horizontal and vertical axes at different elevations. The flux is decreased with increasing depth. Figure 4-5 shows the distribution of the magnitude of simulated liquid mass flux under non-uniform conditions. Here mass flux is predominantly vertically decreased with increasing depth over the entire model domain. The first sharp decrease is located at the bottom of the landfill zone, which will enter into the unsaturated zone and the saturated zone. The second one is at the top of the landfill zone, at which the flux will be transported into the air zone. At both elevations, Figure 4-5 shows a significant variability in flux with values ranging from almost 0.0176 mg m^{-2} d^{-1} to almost 1.5×10^{-7} mg m^{-2} d^{-1}. The results indicate the output of new EEMMS is less in the unsaturated zone and the saturated zone as compared with the traditional EEMMS. Furthermore, about 90% of the total benzene flux was distributed to the air zone from the landfill sources and only 10% of the total flux emitted into the unsaturated, saturated zones in non-uniform conditions. However, the flux would not change significantly in a uniform domain. Considering the fact that benzene is a volatile, highly flammable material means that most of the benzene would volatize into the air, which coincide with the non-uniform model results.

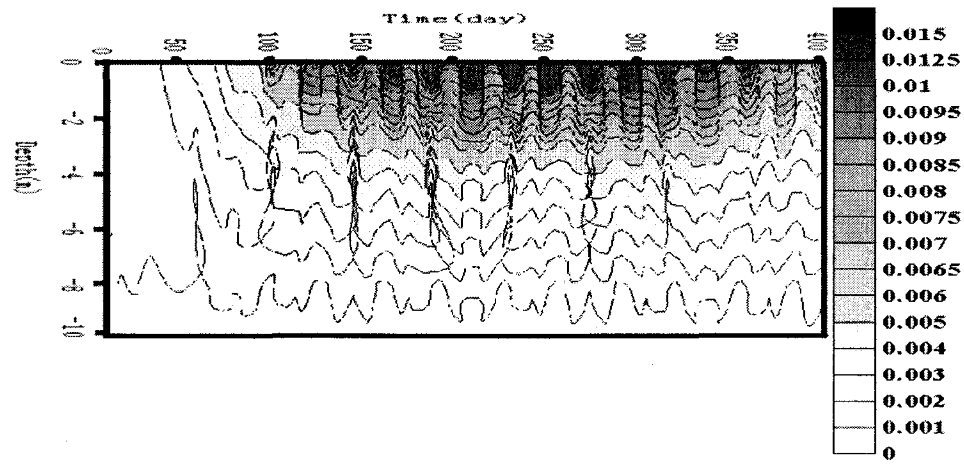

Figure 4-4 Distribution of uniform vertical fluxes (mg m^{-2} d^{-1})

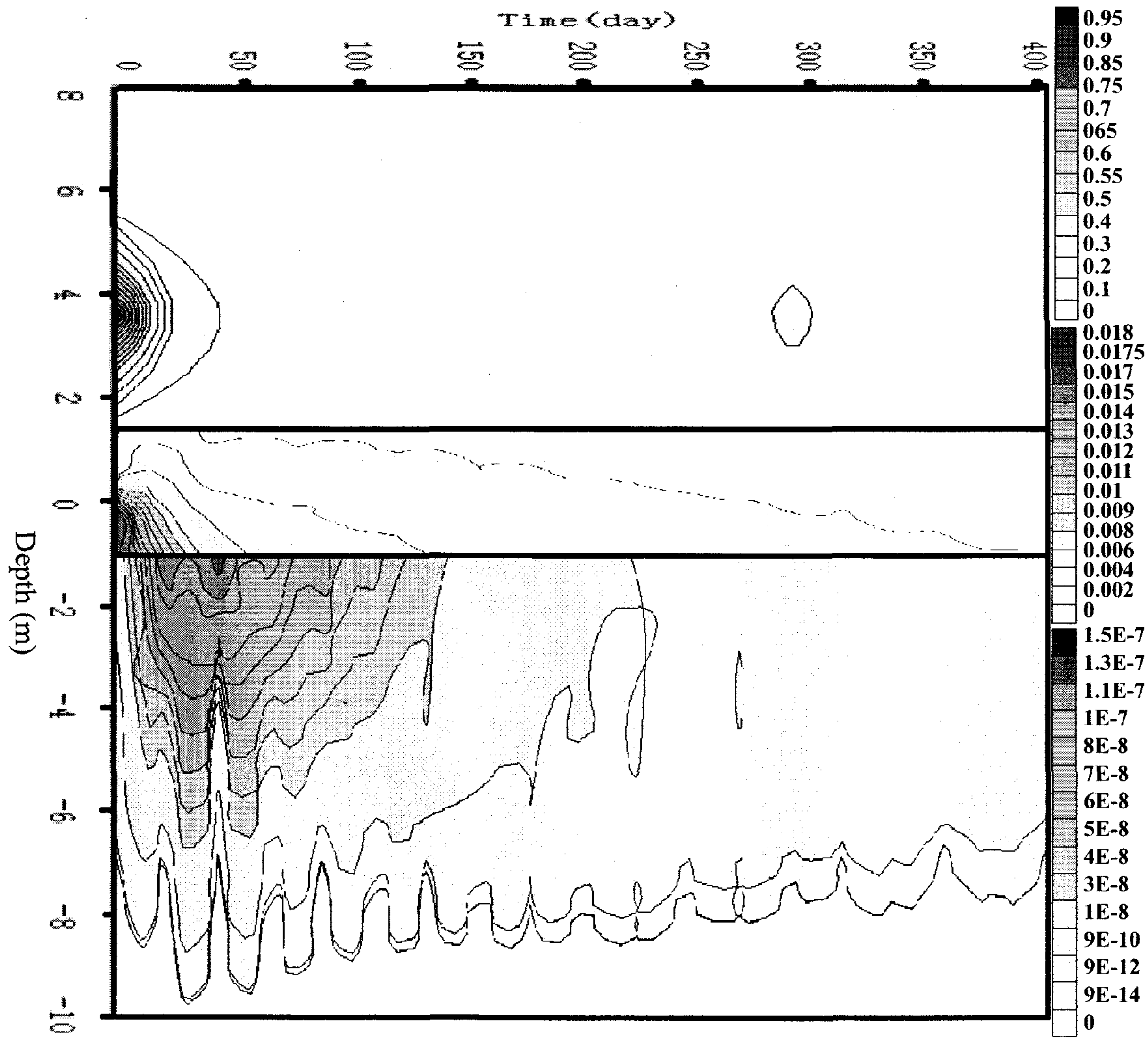

Figure 4-5 Distribution of non-uniform vertical fluxes (mg m^{-2} d^{-1})

As initially stated in the methodology sections, traditional EMMS modules assume the zones are uniform, especially for the unsaturated and saturated zones. As a result, they will input the same input parameters (diffusion coefficient, transverse dispersion, bulk density and porosity, etc) into the governing equations. However, the new EEMMS perceives the different layers as having different input factors, boundary conditions and initial conditions.

4.1.3 Comparison with Literature Data

Finally, to examine how the flows affect benzene, emission fluxes were plotted against time. Figure 4-6 presents the distribution of benzene flux presented by Lin and Hildemann (1995), analyzed solutions and numerical solutions of the present study. Numerical and analytical results closely matched the physical analytical results.

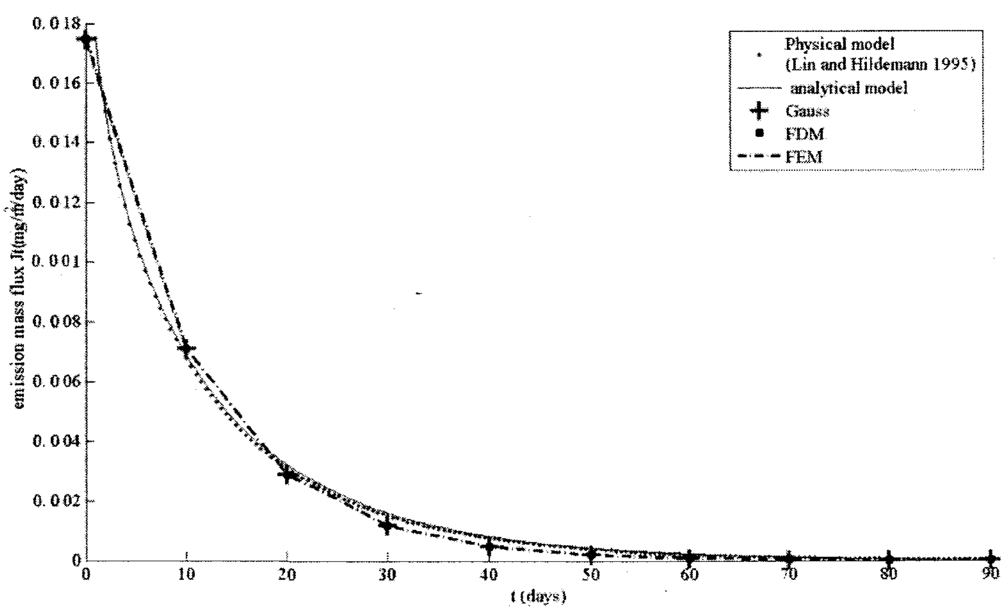

Figure 4-6 Comparison of different models' prediction of subsurface flux for benzene

Figure 4-7 compares the benzene concentration profile at the bottom of the unsaturated zone between the analytical and numerical methods. The numerical results are in agreement with the analytical results. The pollutant concentration at the unsaturated zone boundary varies from an initial concentration of 0 g m^{-3} to 2.895×10^{-3} g m^{-3}. In other words, the clean soil was contaminated by the leachate flowing downward. Under the conditions in which the pollutant from the landfill is released with an exponential decrease, the concentration front will take a relatively longer time to move downward through the unsaturated zone to the division boundary between the unsaturated zone and the saturated zone. The peak concentration occurred at the end of the year. With increasing years, the concentrations will stabilize.

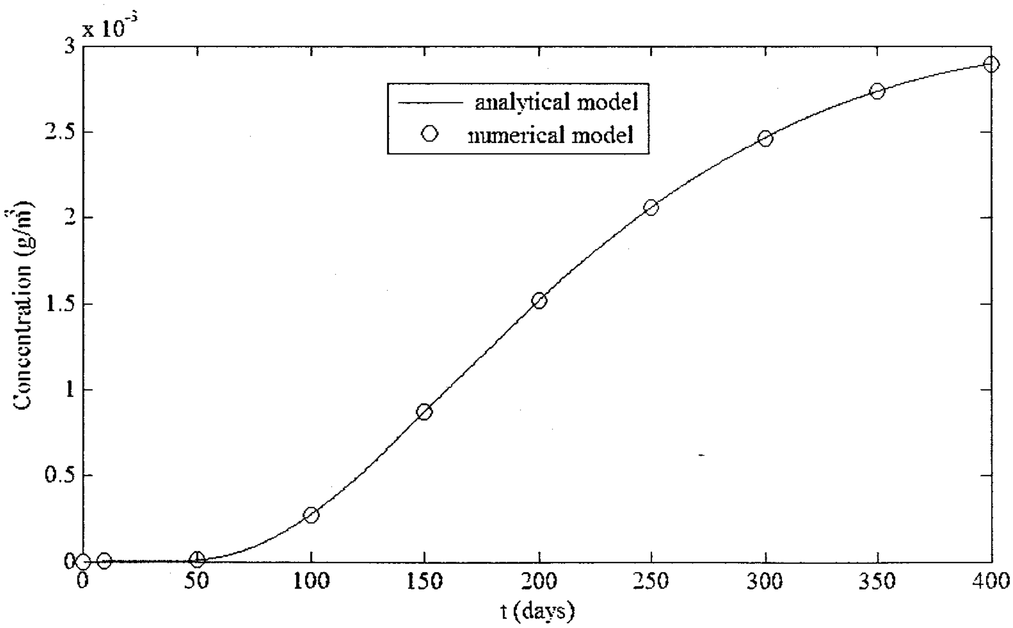

Figure 4-7 Benzene concentration profile at the bottom of the unsaturated zone

Figure 4-8 represents the relationship between the time and the predicted benzene concentration distribution in the groundwater. The predicted concentration at groundwater is 6.5×10^{-4} g m^{-3} at the end of the evaluation period. The concentration slowly decreases to the down gradient of the groundwater flow, due to contaminant dispersion and diffusion in the groundwater.

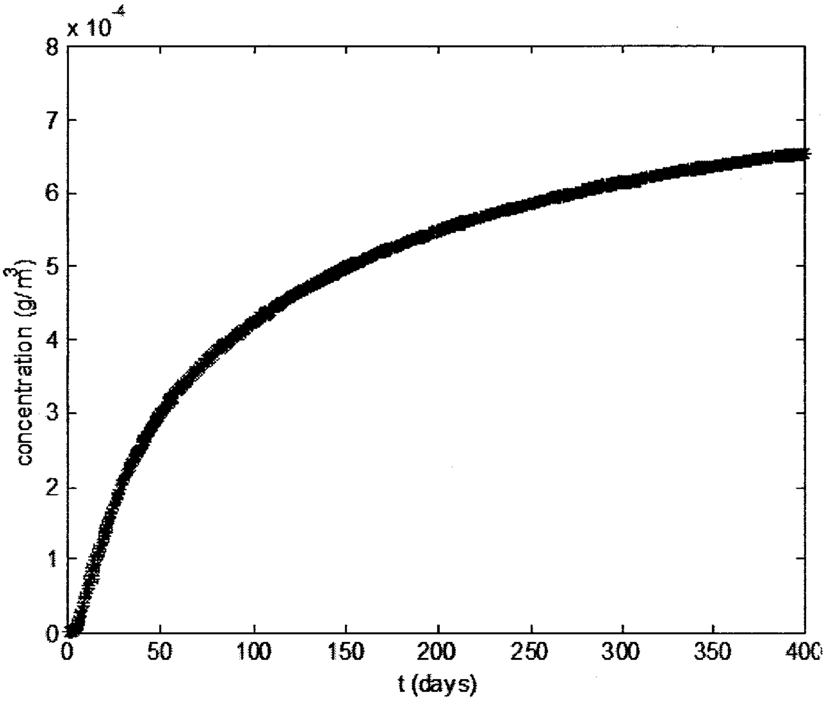

Figure 4-8 Benzene concentration profile at the bottom of the saturated zone

4.2 Model Validation

The landfill module is the core and critical component of the developed EEMMS. The strength of emissions (i.e., emission mass flux) out of a landfill influences its subsequent impacts on the surrounding soil, water, and air environment. Preliminary validation of the EEMMS focusing on the landfill module is presented in this section.

Data from an experiment landfill site (Figure 4-9), which are adapted from the study conducted by Rickabaugh (1990), were used to validate the model's predicted gaseous emission rate from a landfill cover. Subject to a rigorous sorting technique, the landfill waste was divided into 12 categories to ensure that the waste was "typical municipal refuse." Following the sorting, the waste was shredded and then loaded into the landfill cell lift by lift; it was finally compacted to a density of 0.474 mg m^{-3} (wet weight). Waste composition, landfill configuration and operational parameters are presented in Table 4-6. The prepared spike chemical was placed between the first and the second lift. A water distribution ring was positioned above the refuse surface, with gravel underlying the ring for the purpose of simulating water infiltration. The gas collection apparatus was installed on the refuse surface.

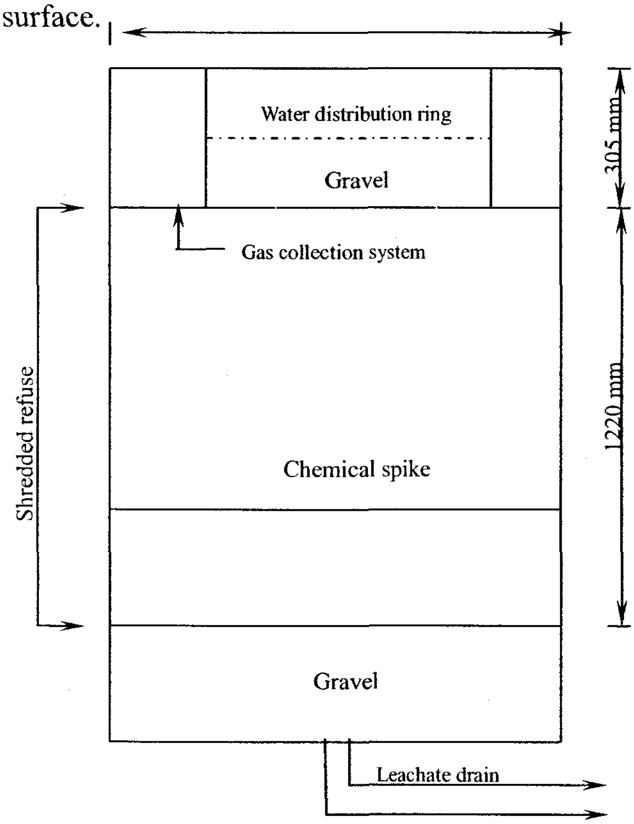

Figure 4-9 Landfill leachate and gas composition experimental setup

Table 4-6 Input parameters for modeling the mass flux of benzene (Rickabaugh, 1990)

The gaseous diffusion coefficient in air	D_g^a (m^2 d^{-1})	0.752	Length orthogonal to groundwater flow.	A_y (m)	1.435
Organic carbon partition coefficient	K_{oc} (m^3 kg^{-1})	0.083	Length parallel to groundwater flow	A_x (m)	0.457
Henry's law constant, dimensionless	K_H	0.22	The volumetric air content of the soil	a	0.15
Half-life	$t_{1/2}$ (d)	300	The volumetric water content at field capacity	n	0.4
Organic carbon fraction	f_{oc}	0.0125	Bulk density	ρ_b (kg m^{-3})	474
Cover thickness	d (m)	0.305	Landfill depth	L (m)	1.22
Gaseous velocity	v_G (m d^{-1})	0.0005	Liquid velocity	v_L (m d^{-1})	5×10^{-4}
The liquid diffusion coefficient in water	D_l^w (m^2 d^{-1})	8.81×10^{-5}	-	-	-

The leachate, gas production, and gas composition were monitored for 5 years. The initial concentration of benzene in the landfill was 83 mg kg^{-1} (per kg wet refuse). Monitoring data of benzene emission fluxes from this landfill cell, as reported by Rickabaugh (1990), were used to validate the developed numerical model.

Both analytical and numerical approaches (FDM and FEM) were used to analyze the experimental input data reported in Rickabaugh (1990). The analytical solutions for the gaseous benzene flux were based on Equation (3.12) and on the numerical solution of Equations of Appendices. Particularly, unsteady flow effects are addressed in the numerical models. Table 4-7 shows the results that we obtained using the three approaches shown in Figure 4-10, together with the experimental results reported by Rickabaugh

(1990). Also in order to show how accurately the model results are, the relative error between mean experimental and FEM model results are listed in Table 4-7. This is done by minimizing the sum of the squares of the differences in logarithms of the experimental values and predicted model values divided by the difference-squared value between experimental and predicted model. The more minimized the relative error, the more matched between the two compared value. This is equivalent to maximizing the correlation coefficient R, Thus, for example, $R^2 = 1$ signifies the best that best fit the data, the error equal to 0 are the best fit data.

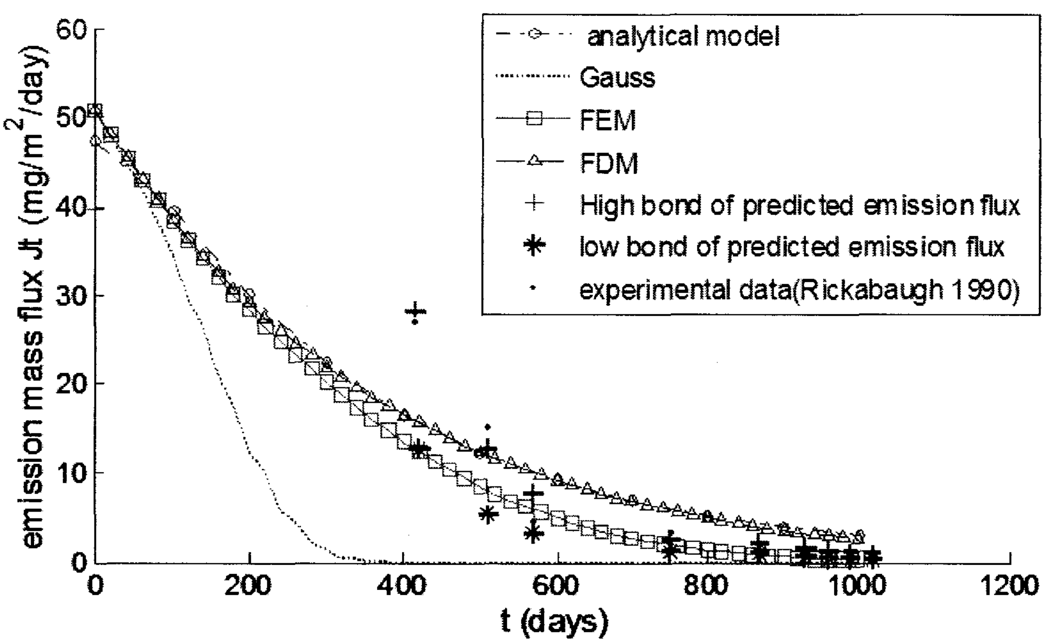

Figure 4-10 Comparisons between numerical, analytical, and experimental results

Table 4-7 Comparison of the flux results generated from the EEMMS using the numerical (FEM and FDM) and analytical approaches and Rickabough's(1990) experimental results

Time (days)	Data from Rickabaugh (1990)			EEMMS/ FEM model results (mg m^{-2} d^{-1})	Relative error between mean experimental and FEM model results
	Lower boundary experimental results (mg m^{-2} d^{-1})	Mean experimental results (mg m^{-2} d^{-1})	Upper boundary experimental results (mg m^{-2} d^{-1})		
420	12.7	29.34	29.7	15.7	-
510	5.4	15.7	12.7	14.9	0.003425
570	3.3	4.5	7.8	4.4	0.000054
750	1.1	3.3	2.6	3.2	0.000054
870	1.0	1.89	2.3	1.7	0.000193
930	0.7	1.0	1.7	1.0	0.000000
960	0.6	1.1	1.3	0.9	0.000214
990	0.5	1.03	1.2	0.8	0.000283
1020	0.4	0.6	1.0	0.5	0.000054

As shown in Table 4-7, except for the Gauss results, analytical and numerical results based on EEMMS provide good simulations compared to the experimental results. Furthermore, as shown in Figure 4-9, all the EEMMS/FEM predictions were in the range (between the high and low boundaries) of the experimental results. In contrast, the majority of the EEMMS/FDM and analytical predictions (shown in italic font) were too high and fell outside the high boundary of the experimental results, particularly for tests done at later times (570-1020 days). The outputs from the EEMMS/FEM method are in the best agreement with the experimental results; the relative error between mean experimental and FEM model results are from 0.003425 to 0.000054 during later times

(510-1020 days). The maximum difference between the mean experimental and FEM modeled results are 0.34%. The minimum difference between the FEM model results and the observed data is 0 from 510 to 1020 days.In conclusion, as shown in Table 4-7 and Figure 4-9, the EEMMS/FEM results of the developed EEMMS provided the more accurate prediction of the complex unsteady landfill gas mass flux.

4.3 Discussion

Case studies show that numerical analysis not only gets the better simulation results to improve EEMMS, but also is effective in the environmental assessment of the complex environmental multimedia system. Both FEM and FDM are implemented to predict concentration profiles and mass fluxes out and into the interconnected multimedia environment using nonreflecting boundary and interface conditions with hexahedral grids. It is found that analytical solutions and finite difference methods (FDM) approaches to multimedia environment problems are limited, due to the complexity of the problems, the sophistication of the mathematical formulas, as well as difficulty in their implementation. Furthermore, FEM provides better results than FDM under the same condition, which can lead to numerical stability, particularly in multimedia environment and complex boundary conditions.

When the steady and unsteady effects were considered for the same grid size, the computing time required for an unsteady flow simulation was approximately 20 times longer than that of the steady flow analysis. A multi-layer numerical solution was examined in the present study for the developed EEMMS. Although mainly one-dimensional solution has been examined, full three-dimensional (3D) mesh generation can be incorporated into the EEMMS. It is noted that solving 3D EEMMS will impose demanding computational requirements.

4.4 Summary

Preliminary validation in one-dimensional environment has been conducted for the developed EEMMS. It is found that both analytical and numerical models provide well-simulated results compared with observation data in a temporal and spatial scheme. Under the same condition, FEM gives the best results compared to FDM, analytical and Gauss equation outputs. The developed EMMS will be a risk assessment tool for field experiments and for treatment design works to help the subsequent management of the resulting environmental impacts.

Chapter 5: Systematic Model Verification in 2-D through Analytical and Numerical Comparison with Extensive Data from the Literature

In this chapter, the developed EEMMS conducted the 2-D Systematic model verification through analytical and numerical comparison with a 2-D FDM numerical researched literature data given by Zheng and Wang (1998). The verification modeling is tested using a case study. The data sets for the case study are adapted from the dual domain mass transfer model (Feehley et al., 2000), Sudicky (1989), Tsuang and Chao, (1997), and Zheng and Jiao (1998). In the dual domain mass transfer model, only advection and dispersion were considered under steady state conditions. The main contribution of the domain mass transfer model is that the dual domain model minimizes the root mean squared differences between the calculated and observed pressure heads. For the complete case study, EEMMS was used in all zones: saturated zone, unsaturated zone, and air zone. Three different approaches were evaluated for solving the two dimensional coupled advection-diffusion-reaction equations using experimental data from the literature: a) EEMMS/FEM (numerical finite element method); b) EEMMS/FDM (numerical finite difference method); and, c) EEMMS/analytical method.

5.1 Systematic Model Verification in 2-D: Case Study 1

5.1.1 Introduction

The EEMMS was applied to a representative multimedia environment with a 2D steady-state point source in a uniform flow field, assuming a relatively thin aquifer and instantaneous vertical distribution. The 2D FDM numerical approach of Zheng and Wang (1998) was adapted. In this case, there is regional flow from left to right across a 450 m × 300 m aquifer. The fluid moves at a Darcy velocity of 0.5 m d^{-1}. The aquifer has homogeneous and isotropic material properties. A point source releases a small amount of fluid into the aquifer at 0.5 m d^{-1} - a release rate is small enough that the flow field remains uniform. The injected fluid carries a nonreactive solute at a concentration of 1 mg m^{-3}. The detailed domain is shown in Figure 5-1.

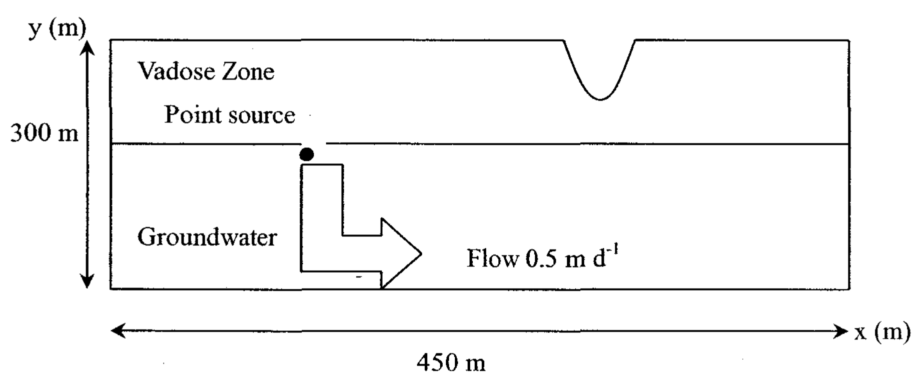

Figure 5-1 Definition of the point source transport problem

The contaminant migrates by advection and dispersion and never reaches a boundary. The aquifer is initially pristine with concentrations everywhere equal to zero. The only source of contaminant is the injection, so flow through the inlet has zero concentration. The period of interest is 100 days. A uniform porosity of 0.2 in the unsaturated zone is assigned, the longitudinal and transverse vertical dispersivity are 10 m and 3 m, respectively. The detailed model parameters of mass balance and its transfer rules used in the simulation are given in Table 5-1, and other initial and boundary conditions are given directly in Figure 5-1.

Further inputs needed for the EEMMS/FEM method include parameters for groundwater table elevation and first-order rate coefficients for dissolution, water gas partitioning and volatilization. The FEM approach generated results for the domain grid nodes and elements, which were then discretized with uniform grid spacing in the x and y directions.

Table 5-1 Input parameters for modeling the mass flux of a point source (Zheng and Wang, 1998)

Item	Value
Groundwater seepage velocity, v	0.5 m d^{-1}
Porosity (%)	0.2
Longitudinal dispersivity	10 m
Ratio of transverse to longitudinal dispersivity	0.3
Volumetric injection rate	0.5 m^3 d^{-1}
Concentration of the injected water	1 mg m^{-3}
Simulation time, t	100 days

5.1.2 Numerical Modeling Approach

In this case study, the 2D EEMMS was solved using FEM software COMSOL Multiphysics 3.4 (COMSOL Inc, Burlington, MA). This software provides an interactive environment for modeling and solving many types of scientific and engineering problems based on partial differential equations (PDEs). The Earth Science module was used because it has functionality optimized for the analysis of transient solute-transport effects, components and systems.

The 2D EEMMS/FEM model equations were arranged into two separate 'General PDE' application modes, the first mode for the mass transport equations, and the second for the flow equations. The earth science module of COMSOL Multiphysics 3.4 was used in the Darcy's law and solute transport application modes. A mesh consisting of 996 quadrilateral elements was constructed. The 2D EEMMS/FEM model took approximately 15 minutes to complete the analysis and post process took a further 10 minutes, with a time step size of 0.1 second on a 3.4 GHz workstation with 2GB RAM. Grid resolution is well documented and FEM models are sensitive to the choice of grid type (Halder et al., 2006). In the case study, memory constraints limited the available grid size. Relatively abrupt changes in grid density may have introduced small instabilities into the solution (Halder et al., 2006). The stabilization parameters used in this study were designed for use with linear Lagrange finite elements and therefore may not be completely suitable for use with Lagrange quadratic triangular elements (Ekrem et al., 2006). The detailed finite elements mesh for this case study is shown in Figure 5-2.

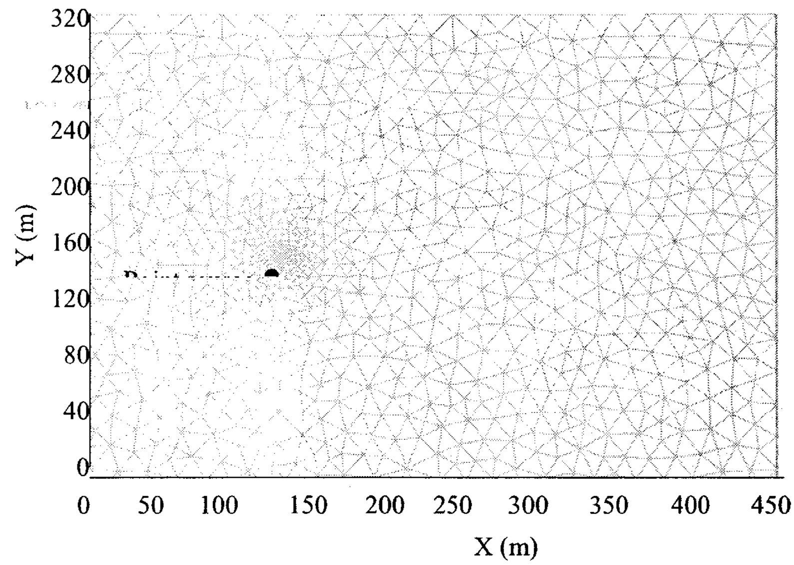

Figure 5-2 Finite element meshes for 2-D point source case study

5.1.3 Results

5.1.3.1 FEM Numerical Results

In order to validate the model, the FEM numerical simulation model shown in Figures 5-3, 5-4, 5-5 was designed using COMSOL Multiphysics. Figure 5-3 shows the x–y plane of the evolution of the contaminant plume at 30 days. The cylinder shown in Figure 5-3 with dark color represents the point source in the computing domain. Figures 5-4 and 5-5 respectively present views of the evolution of the contaminant plume at 60 days and 100 days of the model, whilst Figure 5-6 is a three-dimensional representation of the system geometry at 100 days. Figure 5-6 also shows the solution to the steady-state flow problem. From the bottom of Figure 5-6, it can be noted that the velocity field is near uniform.

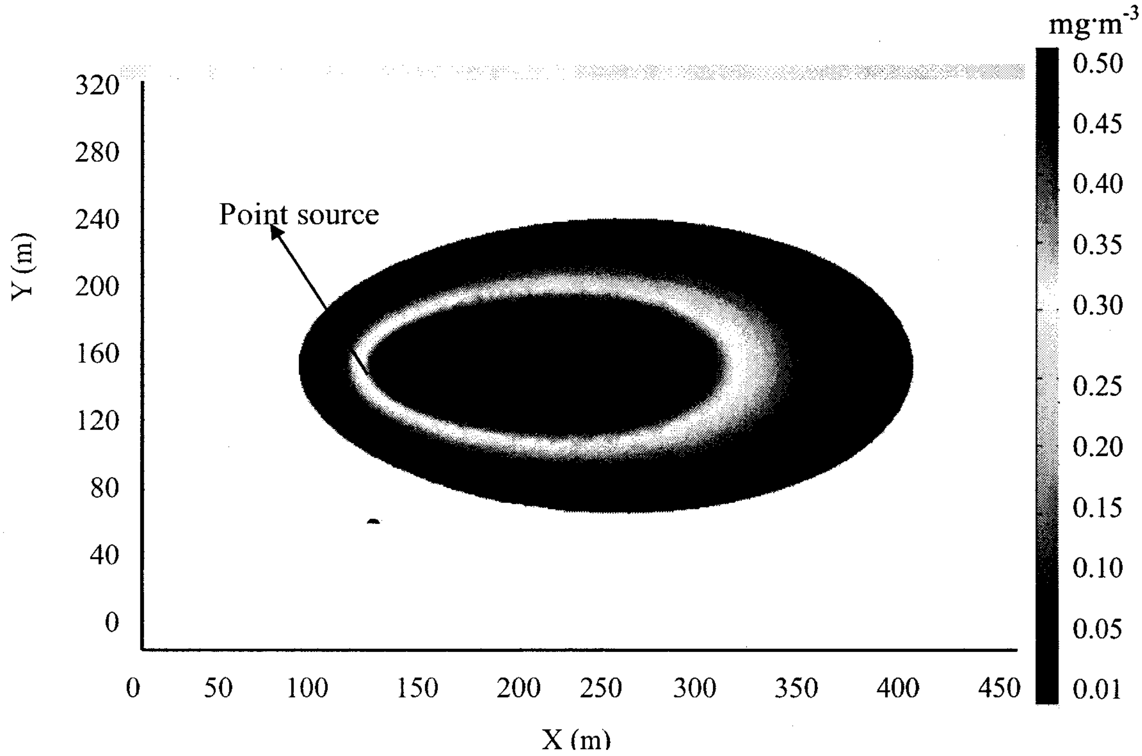

Figure 5-3 2-D point source contaminant plume at time=30 days

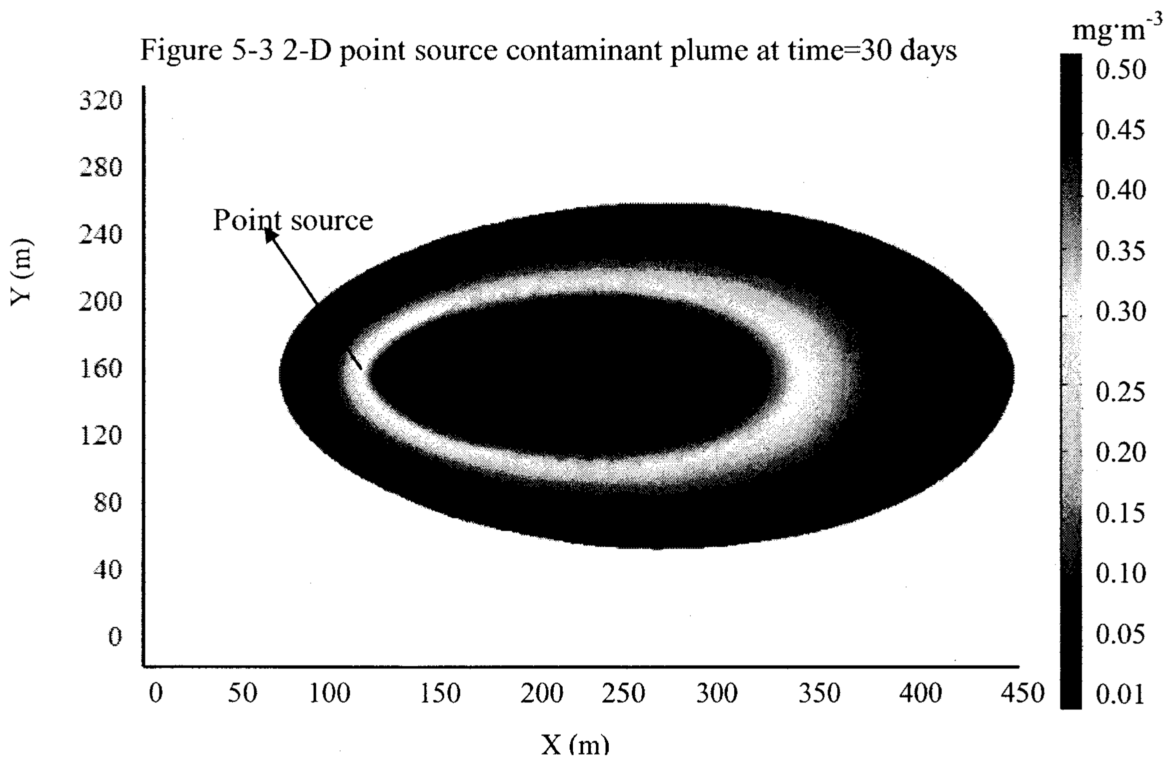

Figure 5-4 2-D point source contaminant plume at time=60 days

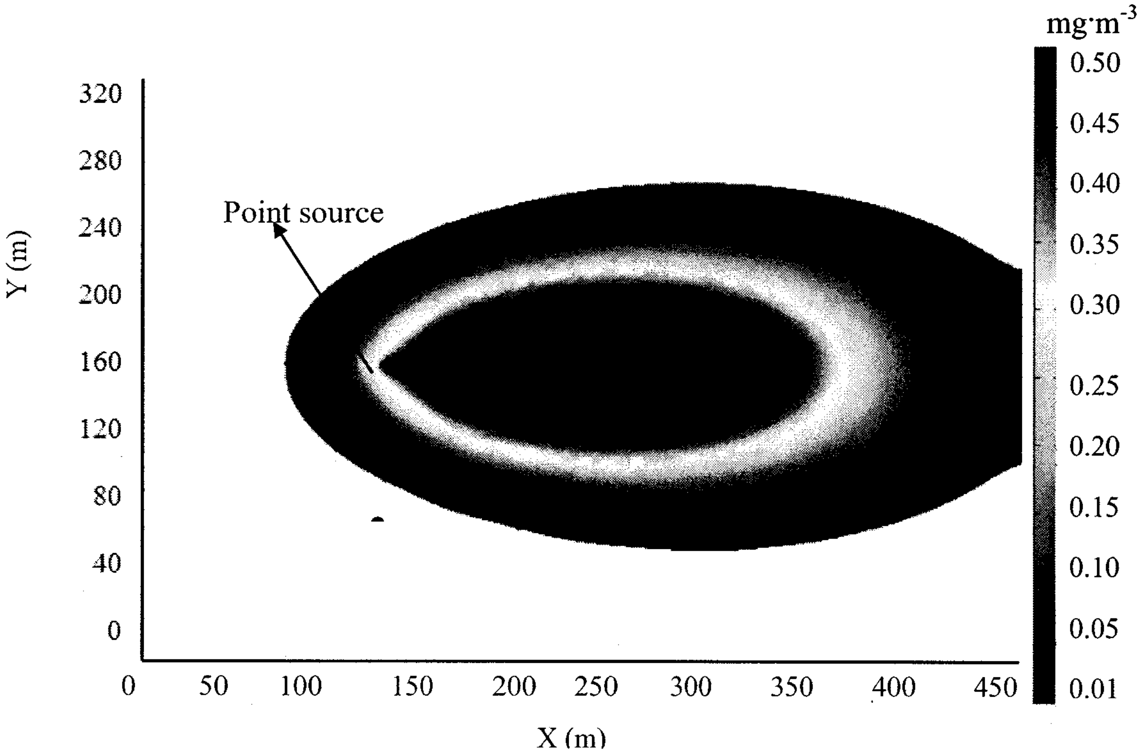

Figure 5-5 2-D point source contaminant plume at time=100 days

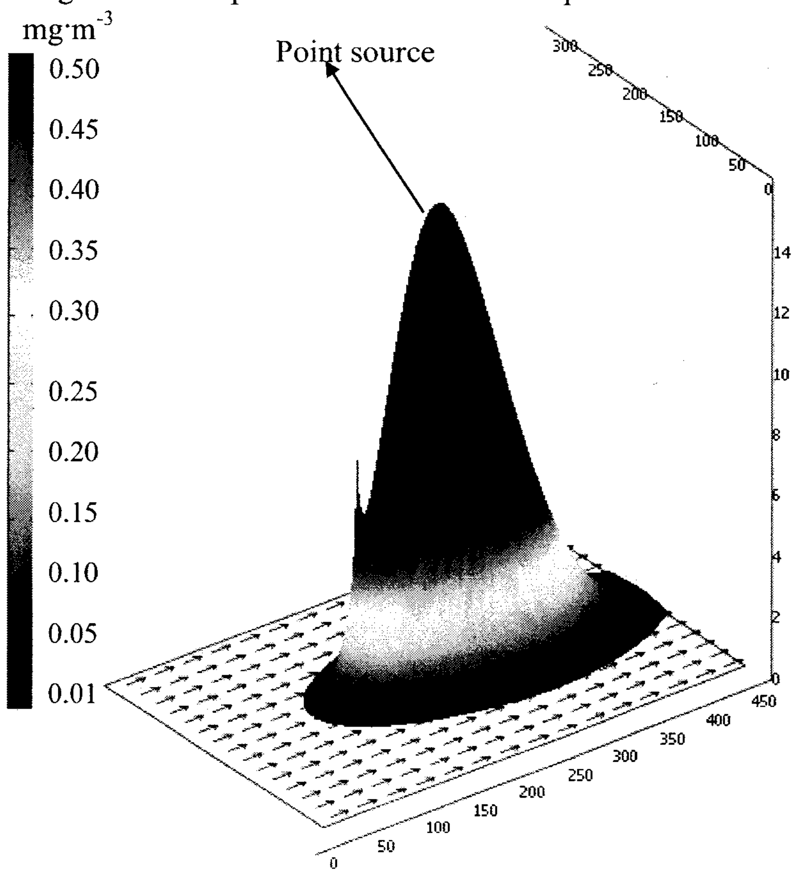

Figure 5-6 3-D point source contaminant plume at time=100 days

5.1.3.2 The Comparison between FEM and FDM, Analytical Results

The case study contaminant transport problem was solved with a high degree of accuracy by all three 2D EEMMS approaches evaluated (FEM, FDM and analytical), and the results are compared in Figures 5-7 to 5-9. The calculated contaminant concentrations (in mg m^{-3}) for the 30, 60, and 100 days simulation periods are shown in Figures 5-7, 5-8 and 5-9 respectively. In Figure 5-7, most of the initial contaminant concentration was found in the central part of the mesh at 0.5 mg m^{-3} as shown in Figure 5-2. With increasing time, the contaminant plume contour expanded and increased slowly along the x-axis. Figures 5-7 to 5-9 show that the EEMMS/FEM and EEMMS/FDM solutions both agreed well with EEMMS/analytical results.

The EEMMS/FEM method: 1) generated numerically simulated values that were similar to the mean of the FDM and the analytical values, 2) was the most accurate of the methods evaluated for the lowest contaminant concentration (0.001 mg m^{-3}), 3) was the most effective for determining the value at different spatial locations in the flow, and, 4) by dividing the flow region into small fluid pixels, generated accurate results for determining the concentration at different positions in the flow cross-section.

Figure 5-9 shows that the results for EEMMS /FEM were similar to the FDM and analytical results reported by Zheng and Wang (1998). Furthermore, the precision of the FEM COMSOL software with a refined mesh is known to be more accurate than that of FDM or analytical solutions with meshes with more degrees of freedom, when calculating low concentrations (COMSOL software product specification sheets). For difficult problems, such as that presented in this case study, the 2D EEMMS/FEM approach was able to calculate low contaminant concentrations (ppb), whereas this was not possible using the EEMMS/FDM or /analytical approaches, no matter how mesh was refined, nor the length of time allowed for the calculations (see discussion for more details).

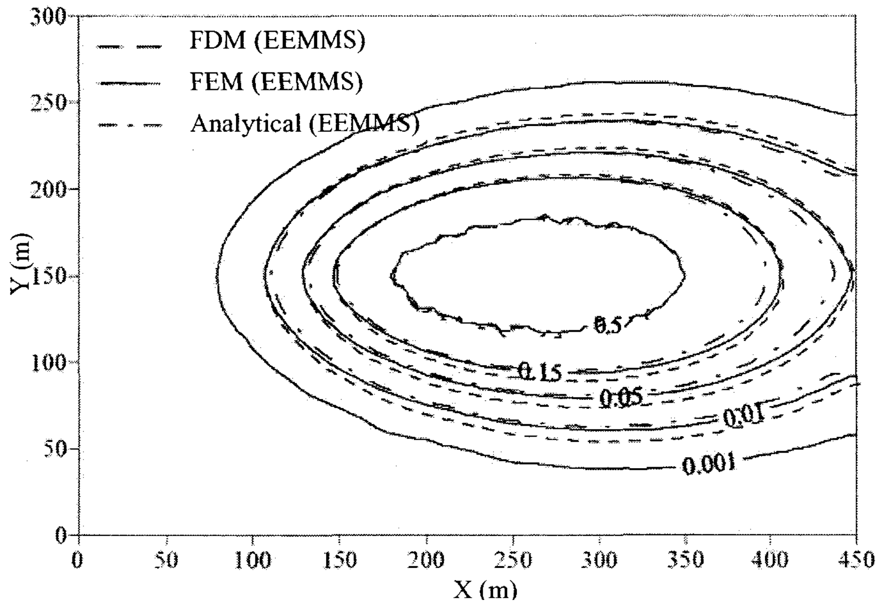

Figure 5-7 Comparison of the 2D EEMMS numerical and analytical concentrations ($mg\ m^{-3}$) results at 30 days from a continuous point source

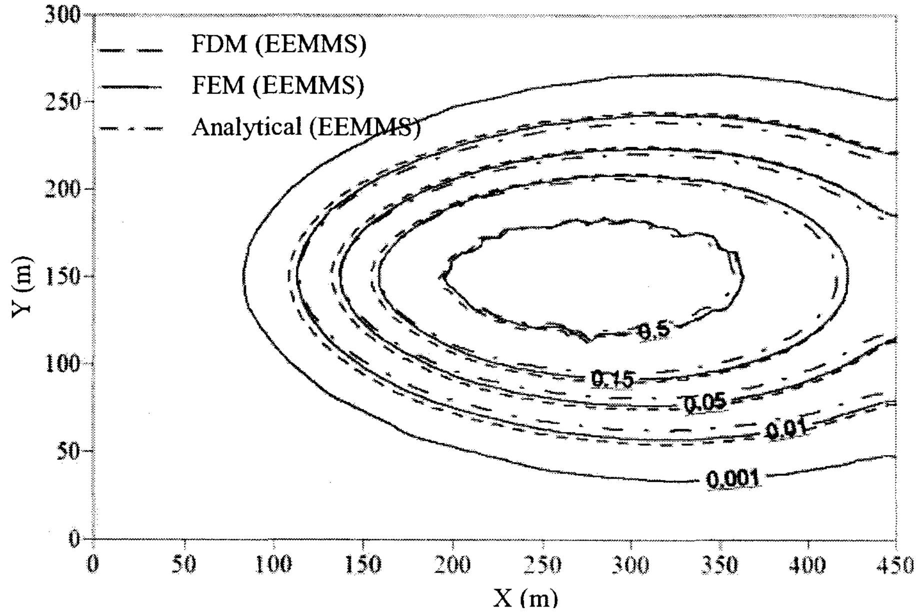

Figure 5-8 Comparison of the 2D EEMMS numerical and analytical concentrations ($mg\ m^{-3}$) results at 60 days from a continuous point source

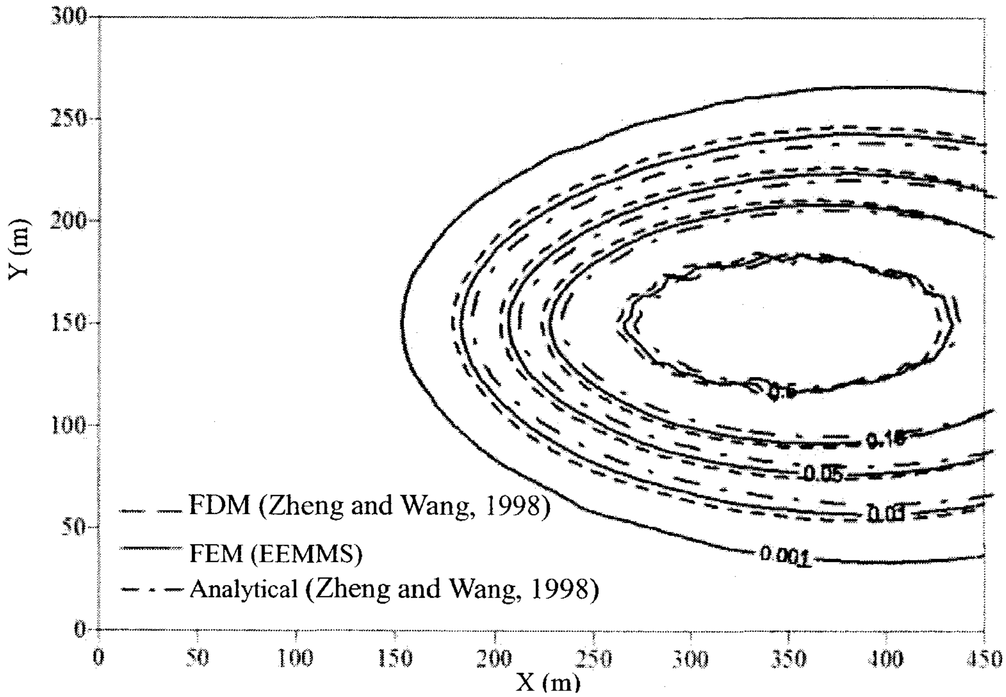

Figure 5-9 Comparison of the 2D EEMMS numerical and analytical concentrations ($mg\ m^{-3}$) results at 100 days from a continuous point source

Interestingly, the 2D EEMMS/FEM model not only accurately simulated case study's experimental results, generated results at the end of analysis (at 100 days) and at low contaminant concentrations, but the model also generated contaminant concentration contours at the different time points. Most importantly, the EEMMS/FEM model shows that the contaminant flux contours emit outward from the point source at different time points (30, 60, 100 days) are at increasing distances from the source. Thus, the model can calculate the concentration and flux changes in a spatial-temporal manner in the 2D multimedia environment.

Details of the 2D EEMMS/FEM model's contaminant flux output are as follows: The cross sections shown in Figure 5-10 illustrate the total flux, which is the sum of the dispersive and advective solute fluxes. The details shown here give results along the y axis equal to 150 m at 10, 30, 60, and 100 days. With increasing time, the total flux output decreases from a peak concentration of 26.5 g m^{-2} d^{-1} (at 10 days) to a peak concentration of 11.7 g m^{-2} d^{-1} (at 100 days) and moved 100 meter along the x axis. Similarly, the dispersive and advective components of the solute flux are illustrated in Figures 5-11 and 5-12 respectively.

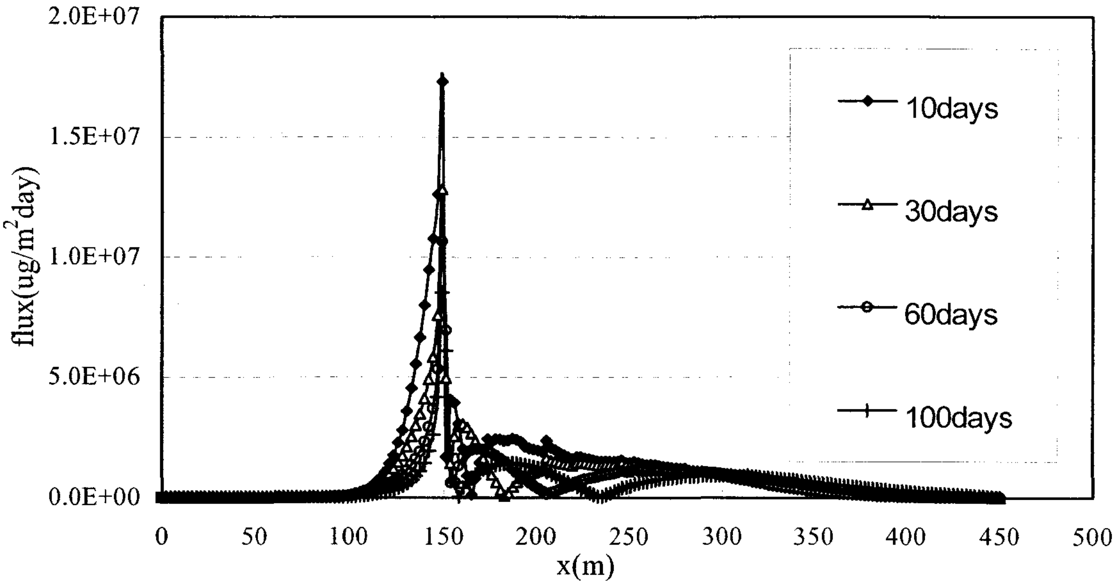

Figure 5-10 2D EEMMS/FEM model calculations of total flux relative to a point source at different times after a spill

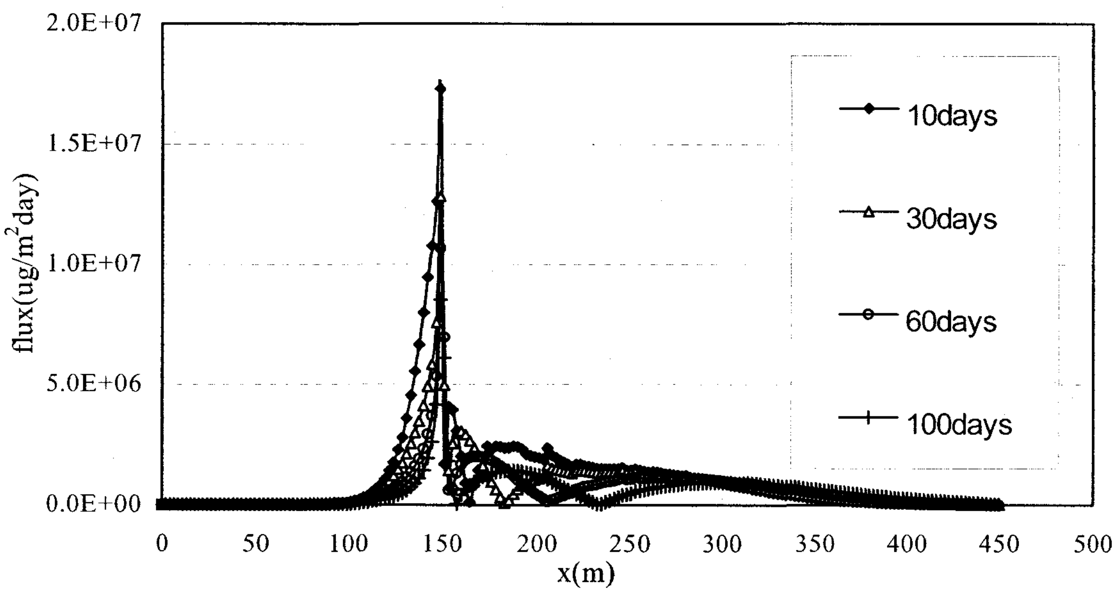

Figure 5-11 2D EEMMS/FEM model calculations of dispersive solute flux relative to a point source at different times after a contaminant spill

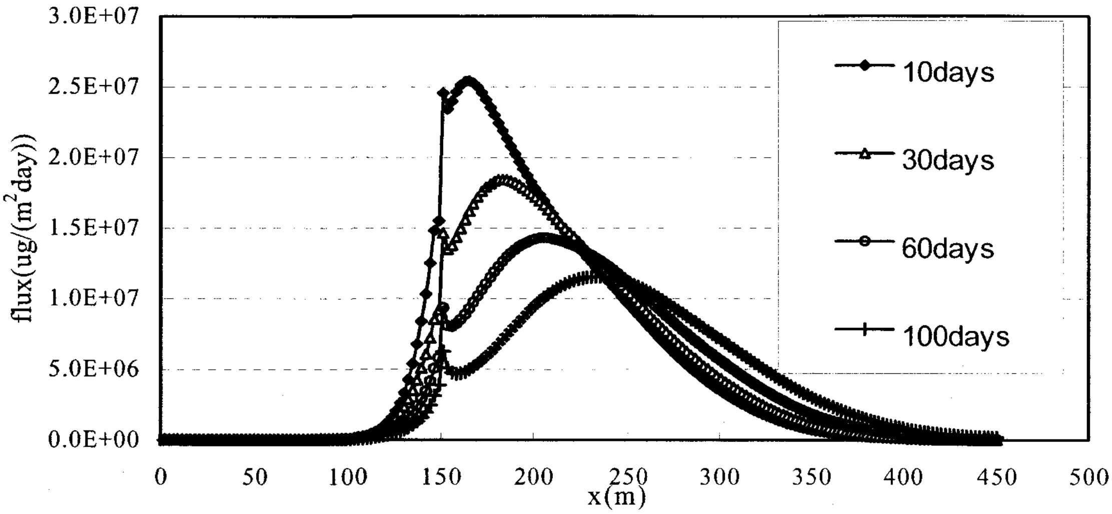

Figure 5-12 2D EEMMS/FEM model calculations of advective solute flux relative to a point source at different times after a contaminant spill

Table 5-2 was generated using the theories of flux transfer described in Equations 3.42 to 3.51, in which one part of the flux is emitted into the air and a second part of the flux is emitted as leachate into the unsaturated zone and enters into the groundwater zone. The total flux equals the sum of the air flux and the leachate flux. Furthermore, Figures 5-10, 5-11 and 5-12 and Table 5-2 show that advection plays an important role in spreading dense chemical pollutants such as those described in this case study (Zheng and Wang, 1998). The results are in agreement with those of Mendoza and Frind (1990a) that suggest that advection is a key parameter for evaluating the effectiveness of pollutant transport and fate in the unsaturated and saturated zones.

Table 5-2 2D EEMMS/FEM model flux results at depth = 200 m at different times after a contaminant spill

Evaluation time (*d*)	Total flux ($\mu g\ m^{-2}\ d^{-1}$)	Air flux ($\mu g\ m^{-2}\ d^{-1}$)	Leachate flux ($\mu g\ m^{-2}\ d^{-1}$)
10 days	1.97×10^7	1.95×10^6	1.78×10^6
30 days	1.83×10^7	1.09×10^6	1.72×10^7
60 days	1.42×10^7	3.74124×10^6	1.38×10^7
100 days	9.551443×10^6	1.23×10^6	8.32×10^6

5.1.4 Discussion

The EEMMS/FEM model showed that the contaminant flux transport mainly depended on the advective flux (leachate flux part). Considering the above case result and the investigation done by Mendoza and McAlary (1990), we suggest that the reason for this is the transport of vaporized chemicals/tritium-radiated contamination due to dissolution of vaporized pollutants. If the unsaturated zone and the saturated zone are treated as a single domain, the potential of advection flux of the gas zone on the contaminants behavior in the subsurface will be evaluated in the entire domain. If the unsaturated zone and the saturated zone are treated as separate domains, advective and dispersive mass transfer of the pollutants at the interface between the two zones will occur.

5.1.5 Summary

Preliminary validation of the proposed EEMMS method has been conducted through a 2-D cases study. In the case study, implementing the EEMMS/FEM solution is found to be better than that of EEMMS/FDM or EEMMS/analytical methods described in the literature (Zheng and Wang, 1998), especially at low concentrations of pollutants. The pollutant fluxes across and distribution in the interconnected compartments are simulated in both numerical spatial and temporal scale for complex multimedia environment.

5.2 Validation in 2-D: Case Study 2

5.2.1 Introduction

The developed new extended environmental multimedia model systems (EEMMS) are applied to a representative multimedia environment with 2-D steady-state subsurface fluid and transient solute transport along a vertical cross section in an unconfined aquifer as shown in Figure 5-13 in this section. It is intended to assess the impact of Tritium on its surrounding soil, air and groundwater system resulted from the emissions. The recent studies in Pennsylvania, California, the United Kingdom, and the study in New York and New Jersey have demonstrated that elevated levels of tritium are quite common in municipal solid waste leachate (Robinson and Grunow, 1996; CSWQB, 2003; PADER, 2006). Consequently, tritium was chosen as the main pollutants in this research section. The site data are adapted from the dual domain mass transfer model (Feehley et al., 2000), , Sudicky (1989), Tsuang and Chao, (1997) and Zheng and Jiao (1998). The domain is the deformed quadrilateral shown in Figure 5-13, with a length of 200 m and a depth ranging from about 65 m along the left boundary and 53.75 m along the right boundary. The flow system is assumed to be at steady state. The left and bottom boundaries are impermeable, and a uniform head of 53.75 m is specified along the right boundary. The water table along the top boundary of the system is represented as a free surface across which a uniform recharge of 1.4×10^{-4}m d^{-1} is applied. The aquifer consists of the fine-grained silty sand (k $=5\times10^{-4}$cm s^{-1}), within which are located two lenses of medium grained sand (k_H=10^{-2} cm s^{-1}). The hydraulic conductivity is assumed to be isotropic. A relative concentration of Tritium 300 pCi mL^{-1} is assigned for the patch extending from x is 40 m to 80 m, and is zero elsewhere. After 5 years the source is removed and the concentration along the top reverts to a uniform value of zero. The domain is initially devoid of contaminants. A uniform porosity of 0.35 is assigned, the longitudinal and transverse vertical dispersivity are 0.1 m and 0.001 m, respectively, and the effective diffusion coefficient is 1.34×10^{-5} cm^2 s^{-1}. In the domain of air zones, D_x, D_y was handled using a constant value (Hanna et al., 1982). A constant value of 10 m^2 s^{-1} for both D_x and D_y is assumed in this study. The letter 'u' is the wind speed, which is shown in the Table 5-4 in this case study. The symbol Λ is a scavenging coefficient (s^{-1}), which ranges from 0.4×10^{-5} to 3×10^{-3} s. since it was with a median value of 1.5×10^{-4} s^{-1} for particle (McMahon and Denison, 1979) and 1.5×10^{-4} s^{-1} is used in this study. The letter 'p' is the proportion of time raining. If wind speed and proportion of time raining did not found in the literature, the assumptions are often made for showing the worst situation and the long distance transport of atmospheric pollutants. Usually wind speed is between 0 -10 m s^{-1}, p is between 0% (rainless time) -100% (raining time) (Ben-jei Tsuang and Jiun-pyng Chao, 1997).

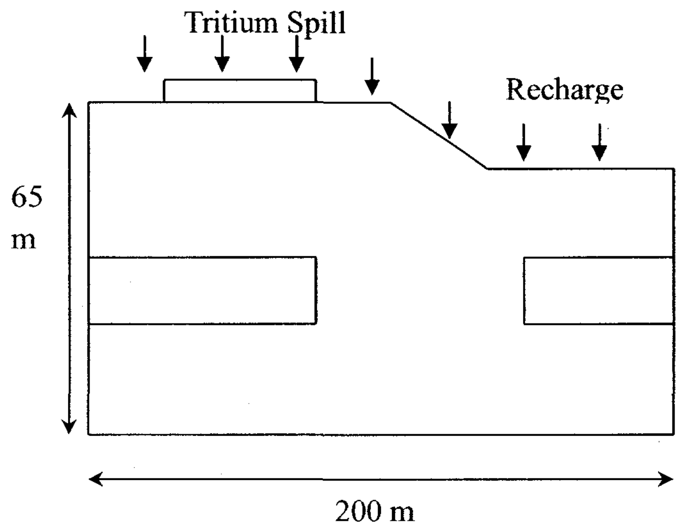

Figure 5-13 Definition of the environmental multimedia transport problem

5.2.2 Problem Description

5.2.2.1 Mesh and Grid

In order to determine the value of the tritium spill transport from top to the bottom, the numerical simulation model was designed using COMSOL Multiphysics, FEM solver. A mesh consisting of 3100 elements was constructed. The model took approximately 15 minutes and post process took approximately 10 minutes to be solved with a time step size of 0.1 second on a 3.4 GHz workstation with 2GB RAM. The details are shown in Table 5-3 and Figure 5-14. From Figure 5-14, it could be noted that mesh resolution is greatest in areas where the pollutants entered into or emitted out of the unsaturated layers are large, for example at the tritium spill of the contraction and close to the air surface. Figure 5-15 shows the geometry used for numerical simulation and the relevant coordinate system. The cylinder shown in Figure 5-15 represents the boundary of the computing domain. Figure 5-15 also presents views of the y–x plane of the model.

Table 5-3 Mesh and grid details

Number of degrees of freedom	13094
Number of mesh points	1724
Number of elements	3100
Triangular	3100
Quadrilateral	0
Number of boundary elements	652
Number of vertex elements	16
Minimum element quality	0.683
Element area ratio	0.005

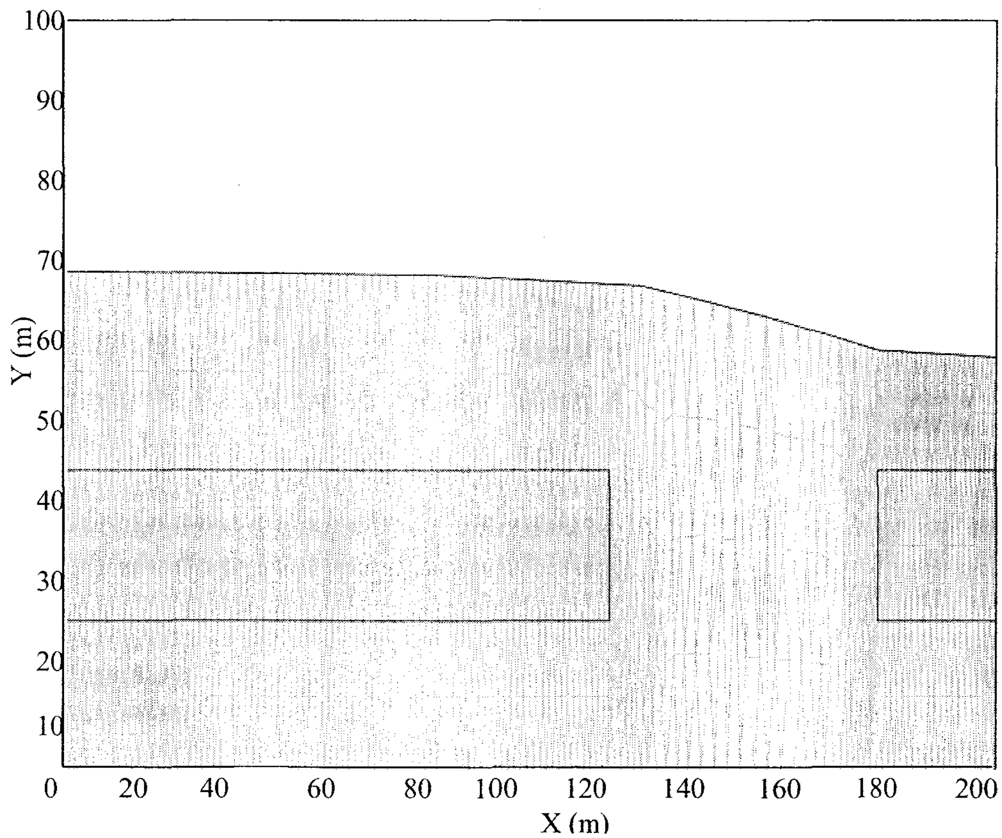

Figure 5-14 Finite element grids for environmental media

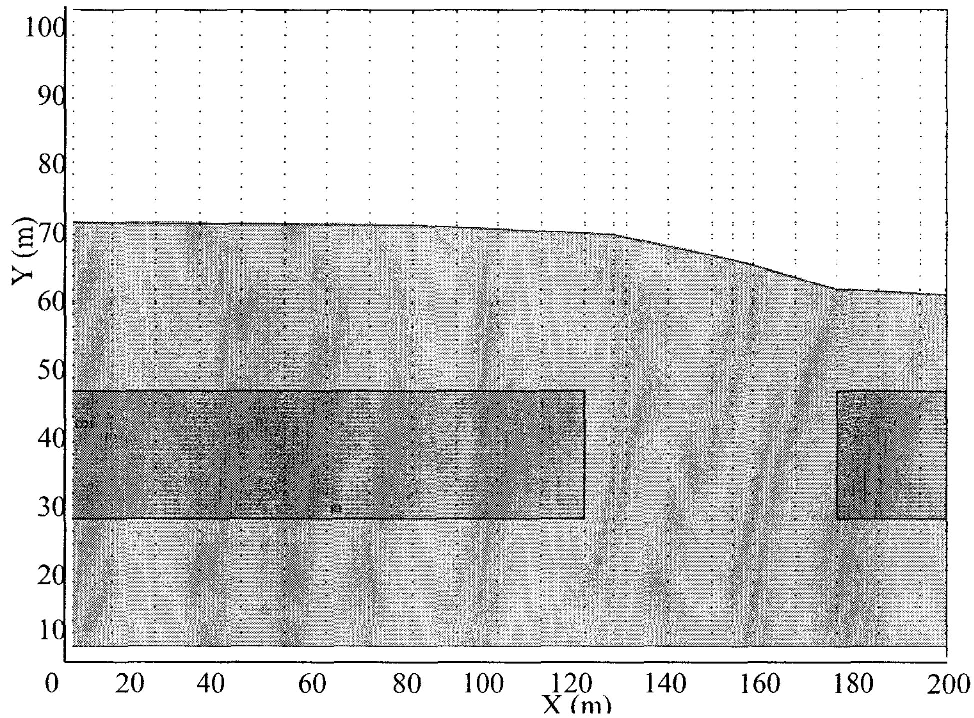

Figure 5-15 Geometry used for numerical simulation and the relevant coordinate system

5.2.3 Basic Results

5.2.3.1 Leachate Concentration Results

Figures 5-16 to 5-19 respectively present views of the evolution of the contaminant plume at 328 days, 1080 days, 1440 days and 1800 days of the model with the EEMMS/FEM solutions whilst Figure 5-20 is simulated tritium plume at 328 days after injection with the analytical solutions at MADE Site (Feehley et al., 2000).

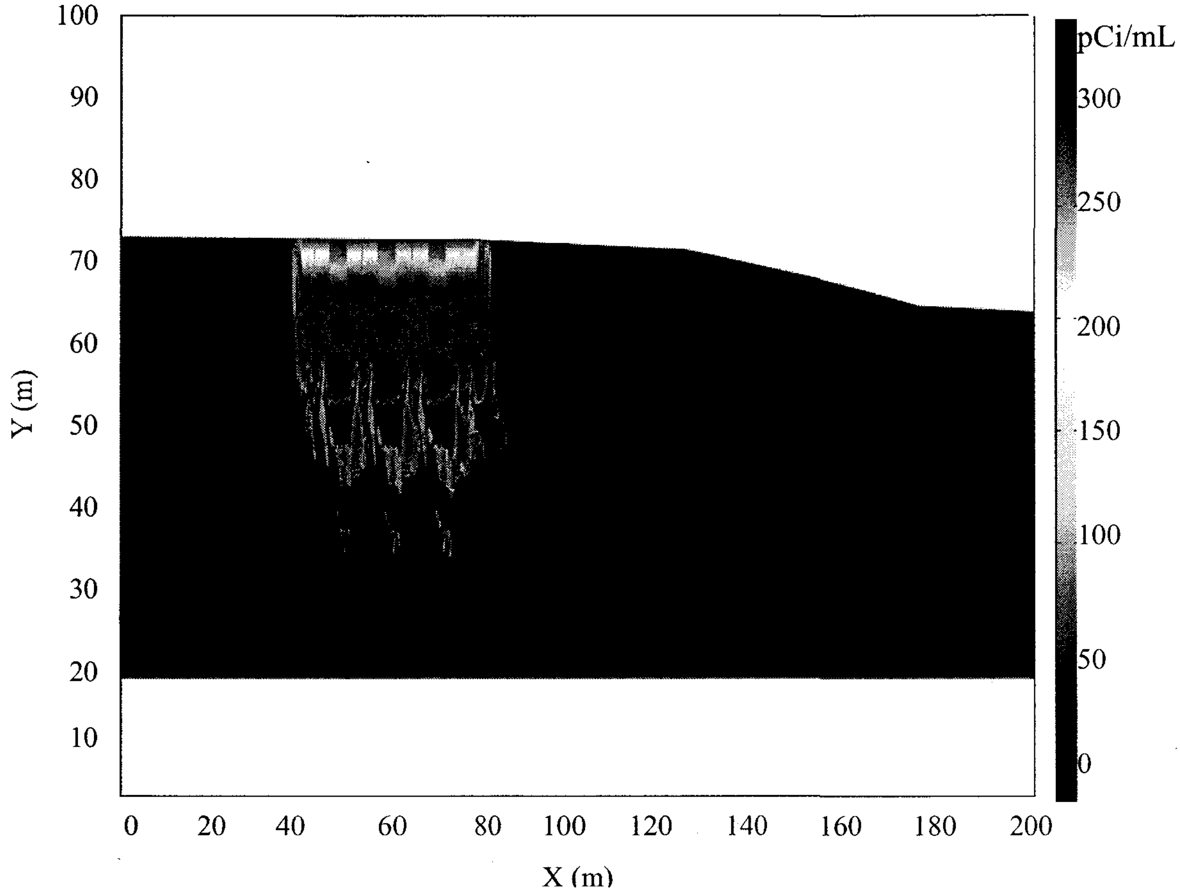

Figure 5-16 2-D EEMMS/FEM point source contaminant plume at time=328 days

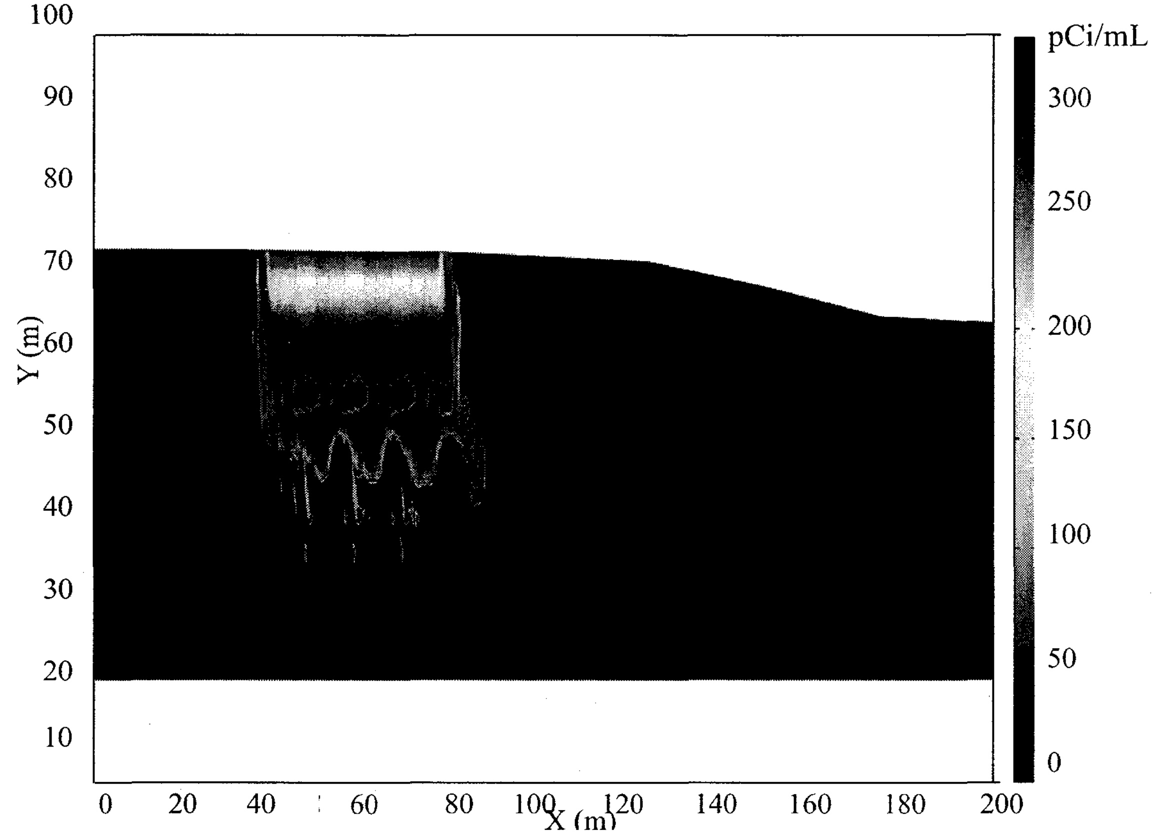

Figure 5-17 2-D EEMMS/FEM point source contaminant plume at time=1080 days

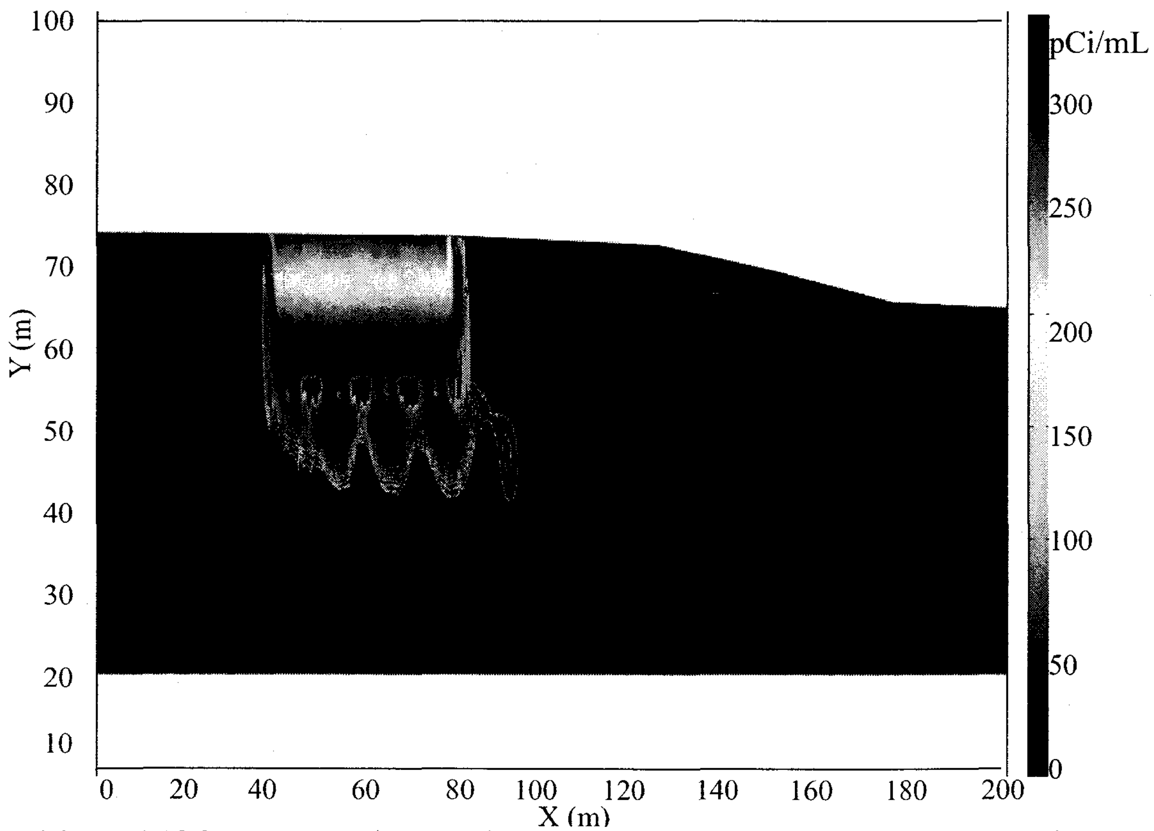

Figure 5-18 2-D EEMMS/FEM point source contaminant plume at time=1440 days

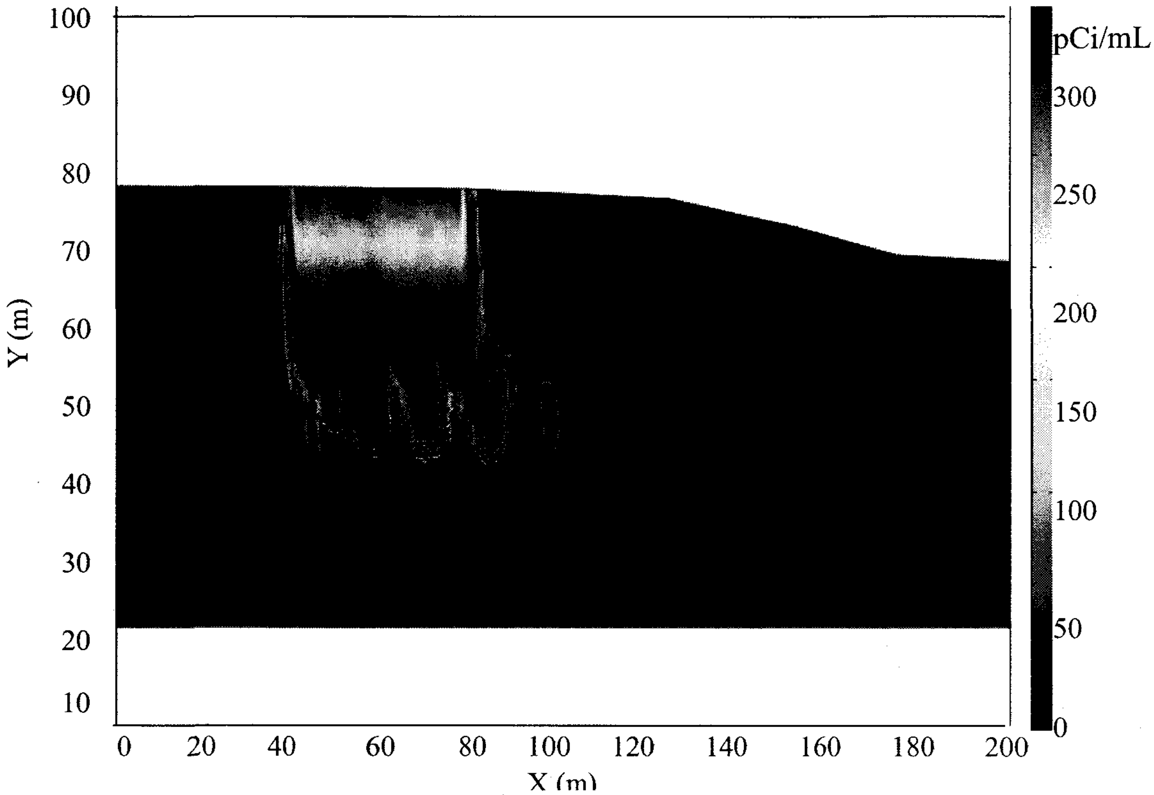

Figure 5-19 2-D EEMMS/FEM point source contaminant plume at time=1800 days

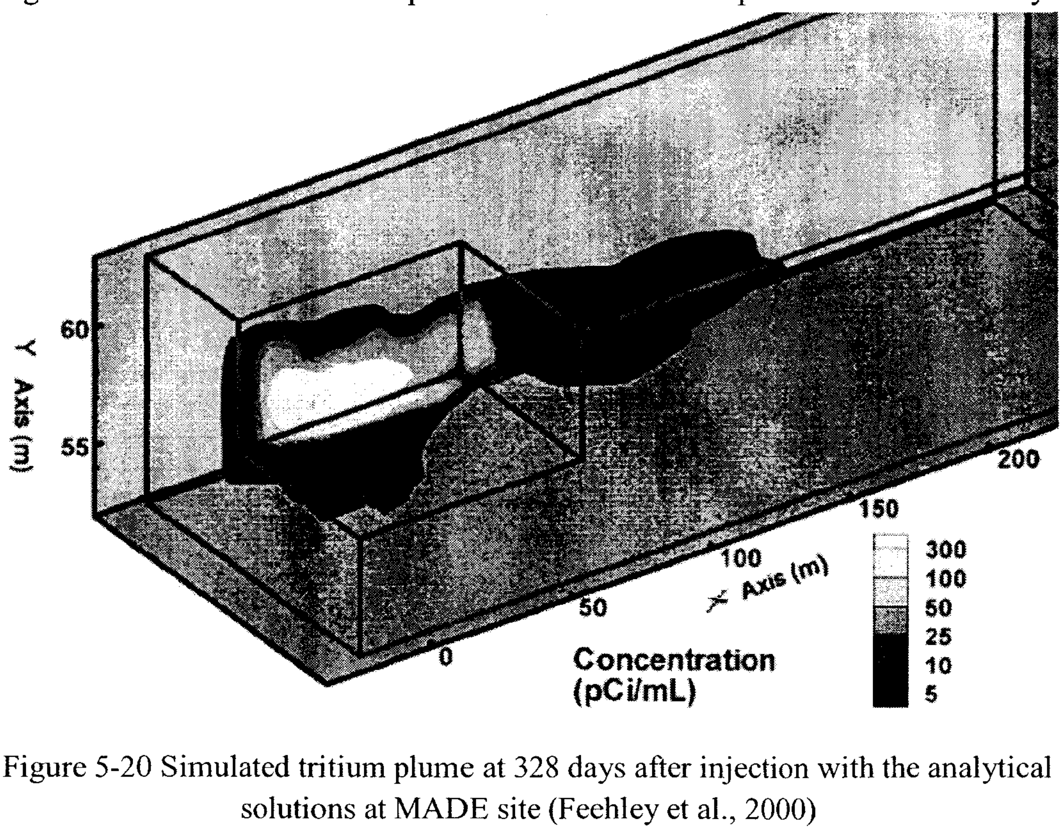

Figure 5-20 Simulated tritium plume at 328 days after injection with the analytical solutions at MADE site (Feehley et al., 2000)

The concentration transport was solved using the finite-element method with the same grid as was used to solve the flow problem. As mentioned in the first 2-D case study, EEMMS/FEM method is well suited for handing problems with relatively small dispersivity. The transport solutions obtained by the EEMMS/FEM and analytical solution done by Feehley et al. (2000) are shown on Figures 5-16, 5-17, 5-18, 5-19 and 5-20 respectively. The agreement between the two solutions is reasonable, in light of the fundamental differences between the transport solution techniques. For the EEMMS/FEM simulation, the transient top boundary condition is modeled using time-varying concentration. The analytical solution option is modeled using the constant concentration. As a consequence, the lowest concentration limit for the analytical solution is 5 pCi mL^{-1} whereas the lowest concentration limit for the EEMMS/FEM could reach 0 pCi mL^{-1}. The key is that the EEMMS/FEM is capable of simulating flow and solute transport in a heterogeneous cross section with the same code together. It could be concluded that the EEMMS/FEM solution is relatively free of numerical dispersion because the concentration contour follows the pattern of the flow lines at the same time. The good agreement between the analytical and EEMMS/FEM solutions suggests that EEMMS/FEM is a correct solution to solve the flow and concentration problems. Furthermore, the results for the EEMMS/FEM simulation are more effective at the end of the 20-year simulation period. The limitation could reach 0 pCi mL^{-1}.

5.2.3.2 Leachate Concentration Results

Figure 5-21 shows the solution to the steady-state flow problem. From the bottom of Figure 5-21, it could be noted that the hydraulic head drops from the inlet to the outlet, and the velocity field is almost uniform.

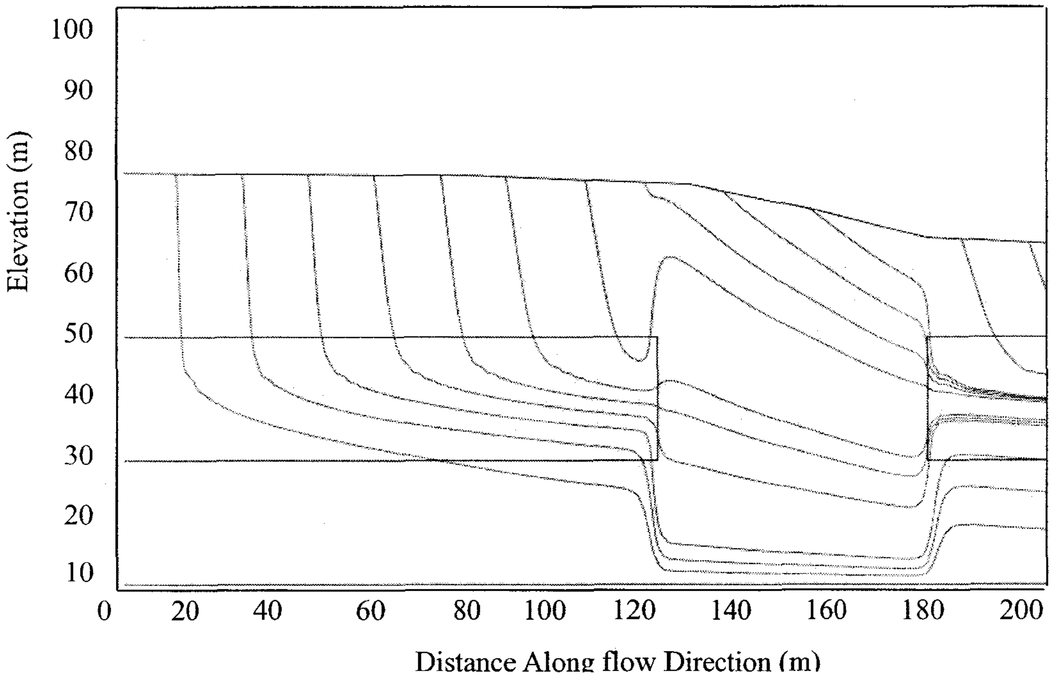

Figure 5-21 2-D point source hydraulic head and stream function solutions (EEMMS/FEM)

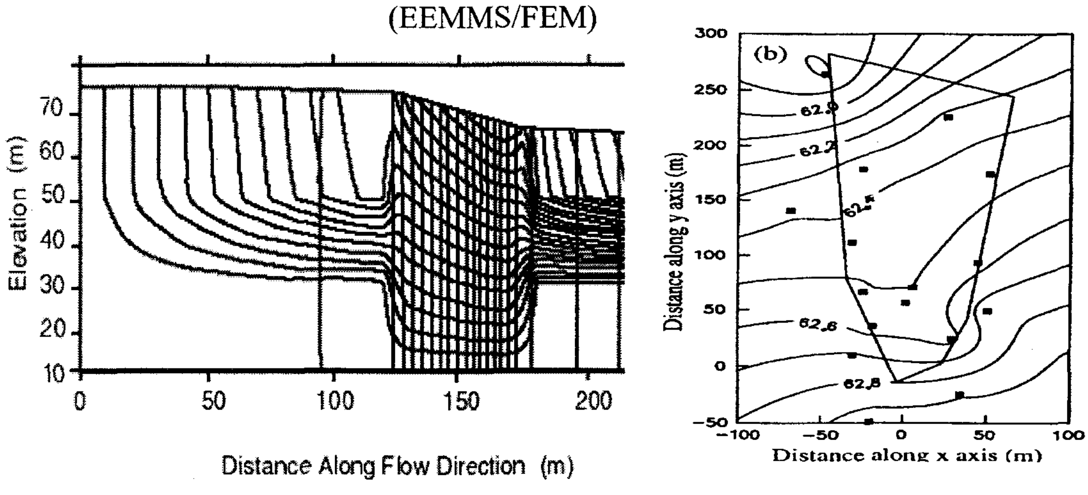

Figure 5-22 Contour of hydraulic head and observed heads at MADE site (Sudicky, 1989; Zheng and Jiao, 1998)

The flow data is adapted from real experimental data collection done by Sudicky (1989), 2-D FDM numerical result was given related to MADE site by Zheng and Jiao (1998). In this research, it was solved using COMSOL multi-physics, FEM solver. The system was discretized into elements using 652 boundary elements nodes in the horizontal direction and 16 vertex elements nodes in the vertical direction. Figure 5-21 shows the hydraulic head and stream function solutions. The elevation of the water table at the left boundary is estimated from Figure 5-21 that is about 6.25 m, which is intended to approximate rather than replicating the data of Sudicky (1989), Zheng and Jiao (1998) shown in Figure 5-22.

5.2.3.3 Air Concentration Results

In order to consider the impaction of wind direction on the tritium gas pollutants, the wind conditions of the MADE site are concerned. Wind direction and the related tritium pollutant coefficient from the MADE site are summarized in Table 5-4. Figure 5-23 and 5-24 illustrates the results more clearly. From Figures 5-23 and 5-24, it could be noted that the southeast wind direction are the main effects to the tritium gas pollutions. The final tritium gas concentration will be effected by this wind direction. Elevated concentration levels contour of tritium have been shown in Figure 5-25, which shows the pollutants will flow mainly to the southeast direction.

Table 5-4 Summary of wind direction and pollutant coefficient

Wind Direction	N	NNE	NE	ENE	E	ESE	SE	SSE	S
Wind Frequency%	2.49	3.33	2.5	6.65	12.5	13.25	14.98	6.65	4.99
Average Velocity $m\ s^{-1}$	1.5833	1.6364	2	2.3077	3.3645	2.2472	1.7881	1.8919	1.6484
Pollutant Coefficient %	1.5726	2.0349	1.25	2.8816	3.7152	5.8962	8.3776	3.5149	3.0272
Relative Coefficient %	3.4908	4.363	2.882	5.9606	7.5334	11.699	16.330	7.1555	6.2351
Wind Direction	SSW	SW	WSW	W	WNW	NW	NNW	C	-
Wind Frequency%	0.83	2.5	2.49	4.15	9.16	3.33	6.66	3.33	-
Average Velocity $m\ s^{-1}$	4	1.3333	1.5	1.4286	1.8598	3.0732	1.8462	0.75	-
Pollutant Coefficient %	0.2075	1.8750	1.66	2.9049	4.9253	1.0836	3.6074	-	-
Relative Coefficient %	0.9151	4.0613	3.6556	6.0045	9.8164	2.568	7.3299	-	-

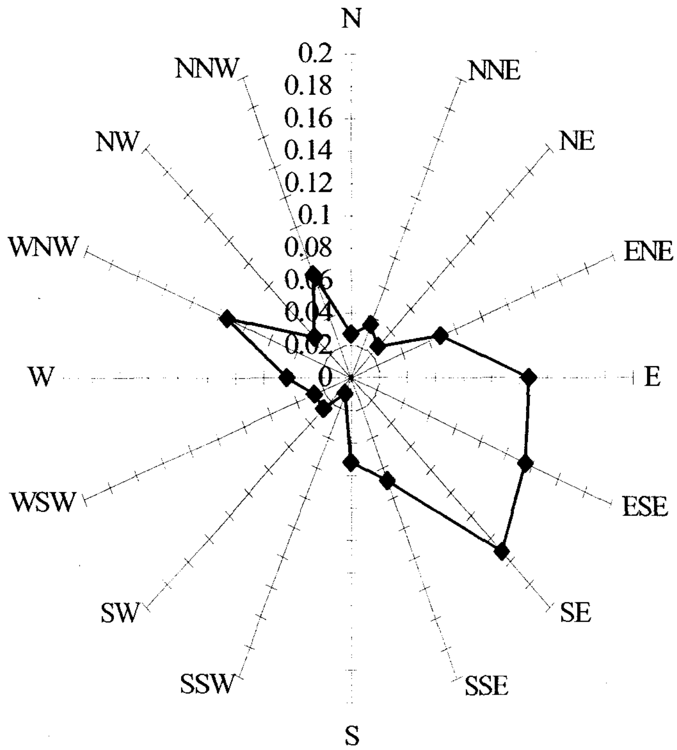

Figure 5-23 Wind direction roses diagram

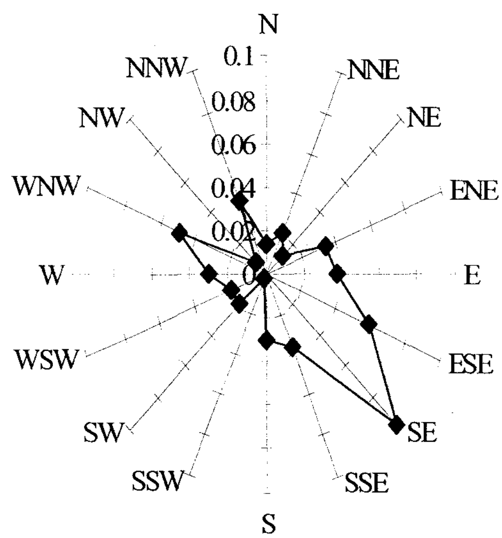

Figure 5-24 Pollutant coefficient roses diagram

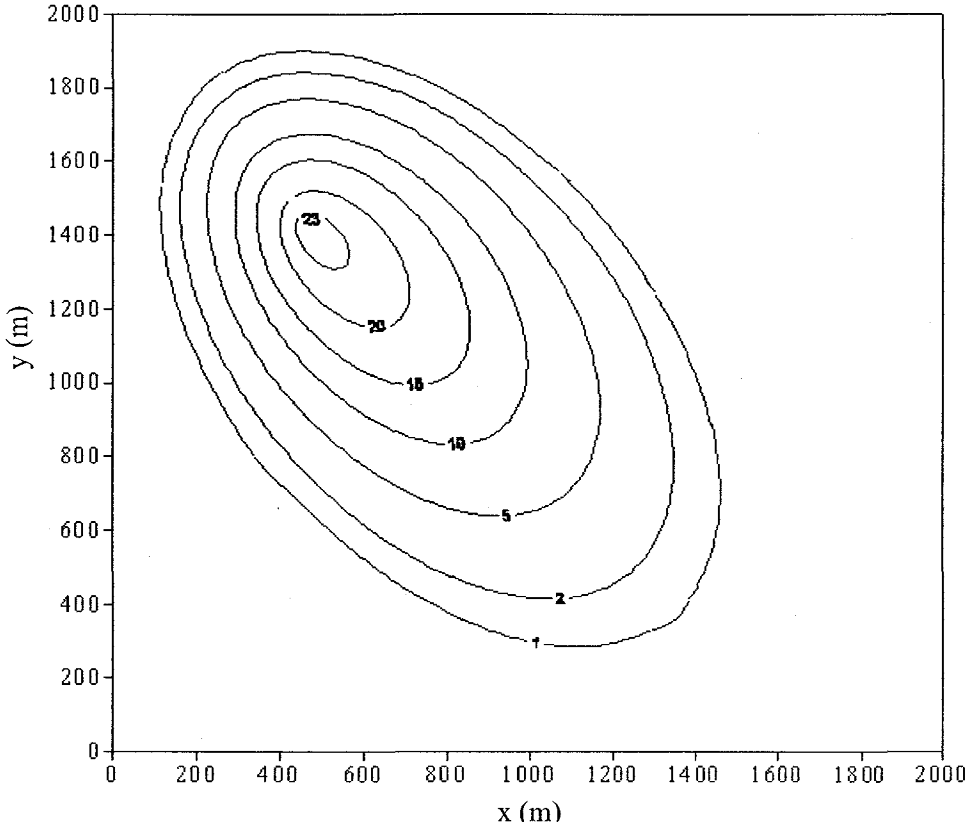

Figure 5-25 Concentration contour of tritium gas from the MADE site (unit: pCi mL^{-1})

Figure 5-25 also shows the concentration in the different years (1, 2, 3, 4, 5, 7.5 and 10). The tritium gas concentrations are 23, 20, 15, 10, 5, 2, 1 pCi mL^{-1} in those different years, separately. When the tritium concentration of the leachate is around 300 pCi mL^{-1}, the tritium gas concentration is around 23 pCi mL^{-1} at the first year, which represents 7% of the whole tritium concentration. This concentration after 10 years is then fit for the Nuclear Regulatory Commission (NRC) recommended maximum annual air concentration for exposure to members of the public living near nuclear power plants of 1×10^6 pCi m^{-3} (USNRC, 2007).

5.2.3.4 The Whole Flux Outputs

Given the above characteristics, the flux of tritium in the leachate is 7.7 curies per year emitted into the unsaturated zone and enters into the groundwater zone. In contrast, the tritium gas from the example MADE would contribute a flux of 0.59 curies per year emitted into the air. According to the theories of flux transfer mentioned in Chapter 3, Equations 3.42-3.51, the total flux equals to the sum of the air flux and the flux to the leachate. The total flux of tritium would, therefore, be 8.3 curies per year with leachate representing 93 percent of the tritium flux. EPA set a maximum contaminant level of 20,000 picocuries per liter (pCi L^{-1}) for tritium (EPA, 2006a). This standard was expected to be exceeded only in extraordinary circumstances (EPA, 2006a). That means this level is assumed to yield a dose of 1000 curies per year of tritium, which many nuclear reactors are permitted to discharge into large bodies of receiving water. They have usable life spans of 10-12 years due to the relatively short 12.32-year half-life of tritium. It follows then that the total flux in this case study is not particularly high, the whole tritium fluxes are shown in Table 5-5.

Table 5-5 Modeling tritium flux outputs results of EEMMS at different times

Evaluation time (year)	The total flux (curies per year)	The air flux (curies per year)	The flux to the leachate (curies per year)
1	8.3	0.59	7.7
3	5.4	0.38	5.02
5	1.8	0.13	1.67
10	0.36	0.03	0.33

5.2.4 Discussion

The model was evaluated using a complete case study chosen from the literature representative of typical two dimensional (2D) pollution transport problems through the whole three zones: the unsaturated zone, saturated zone and the air zone (Feehley et al., 2000; Zheng and Jiao, 1998; Sudicky, 1989; Tsuang and Chao, 1997). Several numerical approaches (FEM) and analytical simulation approaches were compared. The EEMMS/FEM model was found to be more accurate than that of the EEMMS/FDM or EEMMS/analytical methods described in the literature (Sudicky, 1989; Tsuang and Chao, 1997; Zheng and Jiao, 1998; Feehley et al., 2000), particularly for low concentrations of tritium-radiated pollutants.

The research in the second complete case study has demonstrated that elevated levels of tritium in the gas are of the same important as in the leachate even if it is in low concentration. Predictably, the tritium also manifests itself in MADE site both as tritiated water vapor and as tritiated gas. Nonetheless, further study of this issue seems warranted given the public's well-documented concern over exposure to radiologic agents. Although data is lacking, preliminary calculations suggest that tritium released from this MADE Site could, under some circumstances, pose a risk to workers. Even if the above described case study demonstrates that leachate tritium associated with gas tritium poses no significant risk to public health or the environment in the long run, results suggest that a perception of risk may still pose a problem for many facilities at the beginning period.

5.2.5 Summary

The research has demonstrated that elevated levels of tritium in the gas are of the same important as in the leachate even if it is in low concentration. Predictably, the tritium also manifests itself in MADE site both as tritiated water vapor and as tritiated gas. This case suggests that the issue of risk perception can best be overcome by a careful analysis of the real risk together with well planned and managed risk communication.

5.3 Discussion

The advantages of the EEMMS/FEM model are that it: (i) generates fine spatial and temporal concentration profiles, allowing estimation of time-varying and space-varying pollutant concentrations in multimedia environments, and thus significantly assisting in the evaluation of biological risk level for exposure to hazardous contaminants, and (ii) provides several assumptions to simplify problems. These include the following assumptions: (1) the aquifer is infinite in area extent and relatively thin in vertical extent, so that instantaneous vertical mixing can be assumed; and, (2) the contaminants input rate is insignificant compared with the ambient uniform flow.

When the steady and unsteady effects were considered for the same grid size, the computing time required for an unsteady flow simulation was approximately 20 times longer than that for the steady flow analysis. Future work will thus be directed towards examining a mainly multi-layer numerical solution, full three-dimensional (3D) mesh generation, and an EEMMS/numerical solution algorithm. Solving 3D EEMMS will require additional computational resources. Both EEMMS/FEM and /FDM approaches were taken to predict concentration profiles and mass fluxes out of and into the interconnected multimedia environment using nonreflecting boundary and interface conditions and hexahedral grids. FEM provided better results than FDM and analytical solutions under the same condition when the model mathematical equations become more complicated and highly non-linear (particularly for boundary conditions). Simple FDM and analytical solutions to such problems do not exist. It requires many assumptions to be made and these assumptions generated low accuracy results and excessively long execution times with lengthy simulations.

5.4 Summary

The general EEMMS using experimental data was evaluated from two case studies (representative of two dimensional pollutant transport problems), using three different approaches: a) EEMMS/FEM (numerical finite element method); b) EEMMS/FDM (numerical finite difference method); and, c) EEMMS/analytical method numerical finite element method. The results indicated that the EEMMS/FEM model provided improved accuracy of results compared to the other methods and also compared to previous models that have been described in the literature, particularly for low concentrations of contaminants (Sudicky, 1989; Tsuang and Chao, 1997; Zheng and Jiao, 1998; Zheng and Wang, 1998; Feehley et al., 2000).

The EEMMS/FEM model described in this communication was developed with the goal of being able to effectively solve complex pollution transport problems in multimedia environments. At present, the model appears to be more accurate than other current models for solving two-dimensional problems. Ultimately, we hope to be able to solve three-dimensional problems and to validate the model for contaminant/pollutant environmental risk assessment and management.

As far as we know, the EEMMS/FEM model is the first model that accurately addresses multi-dimensional multimedia environment pollution problems. The model generates predictions of spatial and temporal concentration profiles of contaminants/pollutants in the different environmental media of complex environments, and integrates air, unsaturated and saturated groundwater domains based on mass conservation, mass flux, and transient non-uniform initial and boundary conditions.

Based on the two case studies, we suggest that the general EEMMS may provide a useful risk assessment tool to assess and predict the fate and transport of chemical contaminants/pollutants in complex multimedia environments. Due to the complexity of the problems encountered, the general EEMMS requires optimization for each case studied, by testing the numerical and analytical approaches with field data and then choosing the most accurate approach. The optimized EEMMS (for example, EEMMS/FEM) is expected to provide to a fast and cost effective project decision making tool for assessing, predicting and comparing the effects of various strategies in a given multimedia environment, particularly for low levels of pollutants.

Relations between gas and leachate tritium are often contentious and should have the solid waste management according to the different tritium pollutants. The topic associated with tritium used to be reserved for nuclear power plants.

Chapter 6 Validation of EEMMS through Analytical and Numerical Comparison with Field-Scale Data for Benzene Dispersion

Field studies have played a pre-eminent role in efforts to better understand and characterize solute transport processes. In this section, the Trail Roadsanitary landfill site would be used to verify the EEMMS. The sites have provided new insight and extensive data sets for development and testing of EEMMS. Validation should provide useful information regarding the range of model applicability to various problem contexts such as different chemicals, geographic conditions, climatic conditions, sizes of the compartments used, and so on. Detailed analysis and comparison with the field observation data will be shown in the sections to follow.

6.1 Introduction the Dispersion of Benzene at Trail Road Landfill Site

6.1.1 Site Information of the Trail Road Landfill Site

This site, which includes the Nepean and Trail Road landfills, is located within the Ottawa-Carleton region, which houses a population of 750,000. The site, approximately

200 ha in area, is surrounded by light industry and farmland. Highway 416, Moodie Drive, and Cambrian Road bound the site, to the east, west and north, respectively, and at some distance from the landfills, Barnsdale Road to the south. (see Figure 6-1).

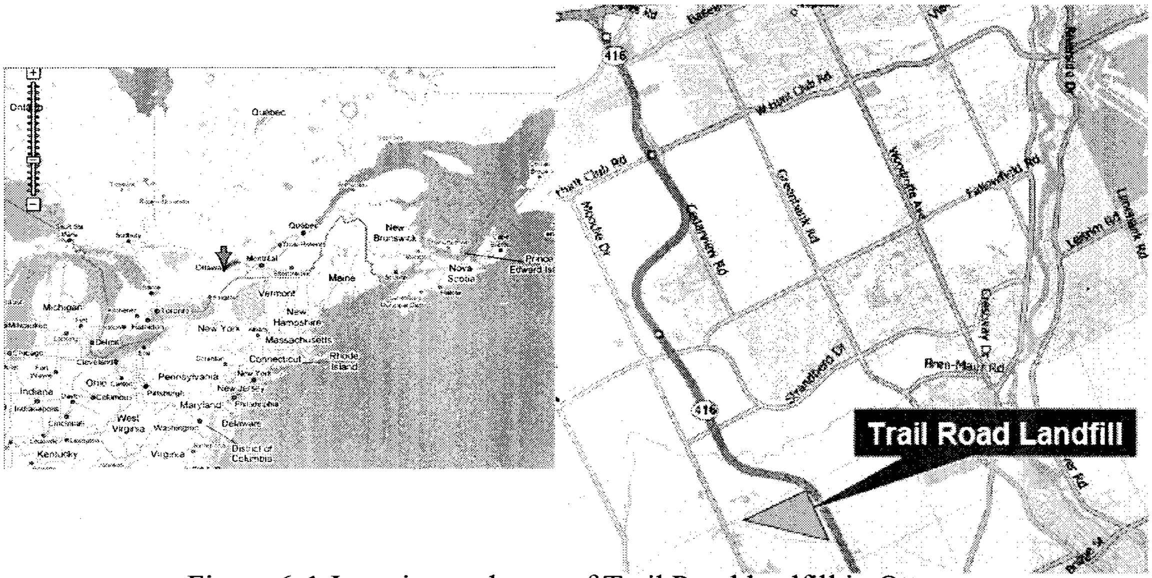

Figure 6-1 Location and map of Trail Road landfill in Ottawa

The Trail Road landfill was opened in 1980 and has been continuously operated in stages. Stage 1, approximately 25 ha, was opened in 1980, and stopped receiving waste in 1986. Stage 2, about 16 ha, received waste from 1986 and was completed in 1991(Dillon et al., 1995, 2002 and 2005). The first two stages of the Trail Road landfill are now closed and capped with polyethylene and soil but are not lined and do not have leachate collection systems. Stage 3 was constructed with a 60 cm thick clay and a high-density polyethylene (HDPE) liner. The third stages, which opened in 1991, are nearly full, and will be capped with a polyethylene liner and soil. Stages 3 and 4 have leachate collection systems (Dillon et al., 2002; Dillon et al., 2005;)(Figure 6-2) .

Figure 6-2 Leachate collection systems of Trail Road landfill in Ottawa

6.1.2 Geological Condition of the Trail Road Landfill Site

The Jock River is located approximately 1km from the north of the landfill, the landfill site is positioned on a glacial outwash plain, which has a complex mixture of sands, gravels, cobbles, clays and silt (Figure 6-3). A discontinuous dense layer of silt and clay (approximately two meters in thickness) separates two aquifers. The silt and clay layer is complete under the Nepean landfill but not under all of the Trail Road landfill and acts as an aquitard to a perched aquifer.

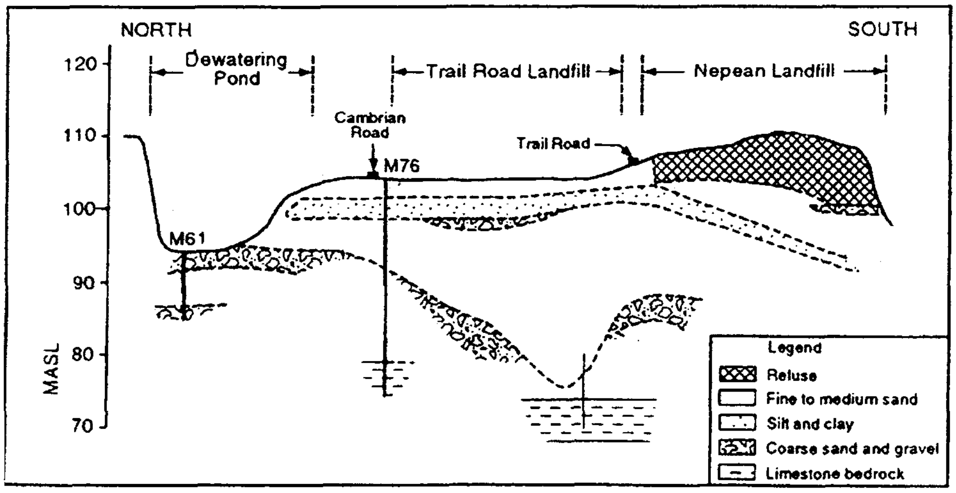

Figure 6-3 North to south cross section of site (Dillon et al., 2002 and 2005)

Approximately 500 meters from the northern boundary of Trail Road landfill on the north side of Cambrian Road is a large de-watering pond used to catch the local groundwater discharge. The pond water eventually discharges into the Jock River, which is located approximately 1 km to the north. Southwest of Trail Road is the Nepean landfill which has been closed now. Surface water runoff flows in a south to southwesterly directly from Trail Road. There are two aquifers, separated by clay, underlying the entire site. A shallow sand aquifer flows in a north to northeasterly direction under the Trail Road landfill. Surface water penetration creates a shallow groundwater flow in a south to southwesterly direction under the Nepean landfill. The deep aquifer, located in a layer of bedrock at a depth ranging from 10-30 meters flows in a south to north direction.

6.1.3 Climate Conditions of the Trail Road Landfill Site

The temperature of Ottawa region where Trail Road landfill is located, significantly changes between summer and winter, and is subject to unpredictable weather conditions

(Table 6-1). Winters are generally with snow and ice. Temperatures in winter can drop as low as -25°C at night. Summer weather in Ottawa is warm and humid, with temperatures exceeding 30 °C fairly often, sometimes as early as April and as late as October. Summers are usually short though, and spring and autumn are unpredictable with early or late snowfalls possible or even unseasonably heat waves.

The weather statistics given in Table 6-1 represent the mean value of each meteorological parameter for each month of the year. The sampling period for this data covers 30 years from 1961 to 1990.

Table 6-1 Climate information of landfill site

Month	1	2	3	4	5	6	7	8	9	10	11	12
Rainfall (mm)	58	59	65	69	76	77	88	92	83	75	86	83
Mean Temp (°C)	-10	-8	-2	6	13	18	21	19	14	8	1	-7
Wind speed (km h^{-1})	16	16	16	16	14	13	11	11	12	13	15	15
Wind Direction	W	W	W	NW	SW	SW	SW	SW	SW	SW	E	W

6.2 Data Collections

6.2.1 Collections and Estimation of Model Data

Imprecise and inaccurate input parameters are the primary source of modeling error in environmental risk assessment. Measured data may even prove to be incorrect due to errors in sampling and analysis errors. For example, as a pollutant's half-life is concerned, there may be significant discrepancy between its value measured in the laboratory and the actual value on site. On the other hand, determination of a parameter values itself carries inherent uncertainty since the processes simulated by the model have a large natural variability in time and space. Moreover, such values are often derived from the experimental data that refer to only a few discrete points in time and space (USEPA, 1996).

Selecting or estimating important parameters has a relatively large potential influence on modeling outputs. These parameters may not be suitable for the other sites where environmental conditions are different. The input parameters related to environmental conditions and the physical properties of the site are given in Table 6-2.

Table 6-2 Physical properties and environmental conditions in the landfill site

Parameters		Value	
Layer 1		Layer 2	Layer 3
Materials	Fine to medium sand	Silt and clay	Coarse sand and gravel
Total porosity (%)	30	46	42
Effective porosity (%)	27	30	27
Bulk density (g cm^{-3})	1.5	1.8	1.5
Horizontal hydraulic conductivity *Kx* (m s^{-1})	4×10^{-5}	4×10^{-5}	6×10^{-3}
Horizontal hydraulic conductivity *Ky* (m s^{-1})	4×10^{-5}	4×10^{-5}	6×10^{-3}
Vertical hydraulic conductivity *Kz*(m s^{-1})	1.4×10^{-6}	4×10^{-6}	6×10^{-4}
Rain Recharge (mm per year)	91.1	-	-
Specific storage, *Ss* (m^{-1})	0.00003	0.00003	0.00003
Specific yield, *Sy* (%)	27	18	27
Recharge (mm per year)	1825		
Year	20		

In Table 6-2, the parameters are mainly decided according to the materials of the various layers. Porosity is a measure of the void spaces in a material and is measured as a fraction, between 0-1 or as a percentage between 0 ~ 100%. Different soils have different porosity. The referential values of porosity for various materials shown in Table 6-2 are from Allen et al. (1997). Effective porosity is an indication of how much of the void space within the soil is capable of transmitting water. This is important because some rock formations may have considerable pore (or void) space, but because the pores are not interconnected, the rock or soil may have difficulty transmitting water. The effect of porosities is different in different regions and soils. No field porosity data is available in the study area and the following generic values were used, silt and clay: 0.27; sand: 0.30 (Nastev et al., 2004). Bulk density is a measure of the weight of the soil per unit volume (g cm^{-3}), usually given on an oven-dry (110°C) basis. Variation in bulk density is attributable to the relative proportion and specific gravity of solid organic and inorganic particles and to the porosity of the soil. Most mineral soils have bulk densities between 1.0 and 2.0 (Nastev et al., 2004). Hydraulic conductivity, symbolically represented as K, is a property of soil or rock, which describes the ease with which water can move through pore spaces or fractures. It depends on the intrinsic permeability of the material and on the degree of saturation. Different soils have different hydraulic conductivity; the hydraulic conductivity depends on the soil grain size, the structure of the soil matrix, the type of soil fluid, and the relative amount of soil fluid (saturation) present in the soil matrix. The important properties relevant to the solid matrix of the soil include pore size distribution, pore shape, tortuosity, specific surface, and porosity (Fredrick et al., 2006). In this project, recharge was used 10%

of the average yearly rainfall being 91.1mm yr^{-1}. Specific yield is a ratio, less than or equal to the effective porosity, indicating the volumetric fraction of the bulk aquifer volume that a given aquifer will yield when all the water is allowed to drain out of it under the forces of gravity. It is primarily used for unconfined aquifers, since the elastic storage component, *Ss*, is relatively small and usually has an insignificant contribution. Specific yield can be close to effective porosity, but there are several subtle things that make this value more complicated than it seems. Some water always remains in the formation, even after drainage. It clings to the grains of sand and clay in the formation. The value of specific yield may not be fully realized until later in time due to complications caused by unsaturated flow. In this project, values of specific yield are taken from Johnson (2003). The specific storage is the amount of water, which a given volume of aquifer will produce, provided a unit change in hydraulic head is applied to it (while it still remains fully saturated). It has units of inverse length, $[L^{-1}]$. It is the primary mechanism for storage in confined aquifers. It can be expressed as the volume of water released from storage per unit decline in hydraulic head in the aquifer, per unit volume of aquifer. The value of specific storage is typically very small, generally 0.00003 m^{-1} or less. In this project, the value of specific storage is 0.00003 m^{-1}. According to Dillon et al. (2002, 2005), the vertical hydraulic conductivity beneath Trail Road Landfill is 1.4× 10-6 m s^{-1}, and the average hydraulic gradient under the site is 0.008 with a porosity of 0.3. Thus the average velocity of fluid is 3.23×10^{-3} m d^{-1} according to the Darcy's Law mentioned in the former sections. Similarly, according to the Dillon et al. (1995, 2002 and 2005), the average horizontal hydraulic gradient under Trail landfill site is approximated 0.05, and the average horizontal hydraulic conductivity is estimated as 4E-5 m s^{-1} with a porosity of 0.3. Thus, by using the Darcy's law, the seepage velocity in groundwater is 0.576 m s^{-1}. Furthermore, based on the data from Dillon et al. (1995, 2002 and 2005), the rate of refuse annually disposed in landfill is estimated as 287,000 tones per year.

6.2.2 Collections of Pollutants' Physical-Chemical Properties

The biodegradation of benzene occurs both in soil and groundwater. In Howard (1990) and Howad et al. (1991), the degradation rate of benzene ranges from a few hours and hundreds of hours in soil and in groundwater and it is much shorter in soil than in groundwater. That means, it will decay from an initial concentration to zero in a few days in soil, but it will take almost two years to complete this process in the groundwater. Such a discrepancy between two degradation rates is primarily because of the chemical half-life in soil in which the literature refers to in near-surface soil, leading to the chemical degrading faster under aerobic condition. In comparison, due to anoxic conditions typically found in organic contaminated aquifers, anaerobic degradation of aromatic hydrocarbons plays an important role in degradation processes occurring in groundwater (Jahn et al., 2005).

Concerning the soil in a landfill and underlying the landfill, it is obvious that it cannot be treated as near-surface soil as it can be distributed to tens meters beneath the ground surface. Therefore, it is more suitable to consider that the degradation compound occurs mainly under anaerobic condition in landfill and the same happens in groundwater.

Environmental half-lives of benzene in air, water, and soil are all 6.97× 10^{-7} days in MEPAS, which means the first order decay rates are around 0 in those media. In MMOSILS, the first order decay rate of 0 is used for waste management union, unsaturated zone, groundwater, and air medium. Totally, benzene has a very low rate of biodegradation in this project.

Table 6-3 Input parameters related to pollutants' chemical properties

Property	Symbol	Benzene
Gaseous diffusion coefficient in air	D_g^a ($m^2\,d^{-1}$)	0.756
Liquid diffusion coefficient in water	D_l^w ($m^2\,d^{-1}$)	8.81×10^{-5}
Organic carbon partitioning coefficient	K_{oc} ($m^3\,kg^{-1}$)	0.347
Henry's law constant,	K_H	0.225
Half-life in landfill	τ (d)	-

6.3 Simulation Results of Benzene and Comparison with Observed Data at Trail Road Landfill Site in 3D

6.3.1 Model Setting and Topography

A large-scale area of about 4 km × 3 km with the Trail Road landfill site is shown in Figure 6-5. The left boundary is the Cambrian road which is a large de-watering pond used to catch the local groundwater discharge. The pond water eventually discharges into the Jock River, which is located approximately 1 km to the north. Approximately 500 meters from the northern boundary of Trail Road landfill on the north side of southwest of Trail Road is the Nepean landfill. The model grid and bottom topography are shown in Figures 6-4 and 6-5. Figure 6-5 shows that surface water runoff flows in a south to southwesterly directly from Trail Road. There are two aquifers, separated by clay, underlying the entire site. A shallow sand aquifer flows in a north to northeasterly direction under the Trail Road landfill.

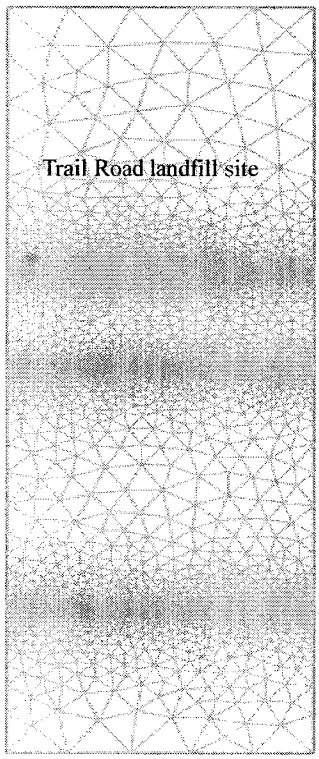

Figure 6-4 3D model grid of the site in study area

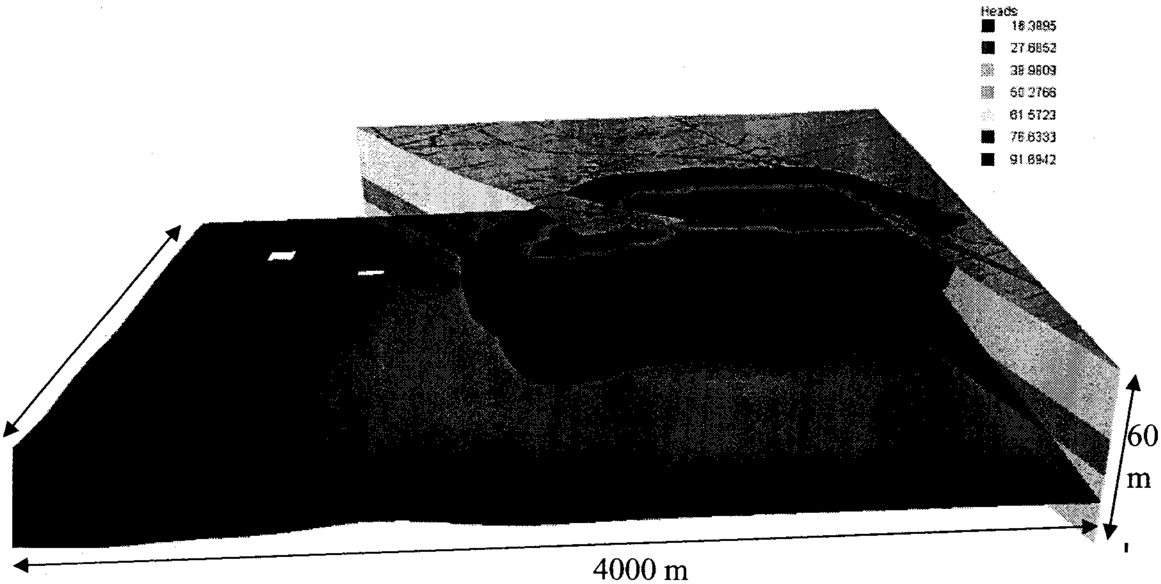

Figure 6-5 3D bottom topography of the site in study area

6.3.2 Current Groundwater Flow Direction and Water Table

As shown in Figure 6-6, the study area has a depth of between 40 m to 17 m distributed in the area of about 39 meters at the Trail Road landfill site. The water depth in the whole large-scale area extends from the value of 40 m in the Trail Road landfill to the value of 17 m in south and west of the trail landfill, which is near the dewatering pond. It is also found that the groundwater flow direction in the upper/middle part of the deep aquifer is northwest, generally directing to the dewatering pond, and is northwards immediately in south and west of the Trail Road landfill. Water levels in the area typically range from near surface to about 2 meter below ground surface. Surface water flows in a south to southwesterly directly from Trail Road landfill. In the areas of continuity, horizontal and vertical groundwater flow gradients change rapidly.

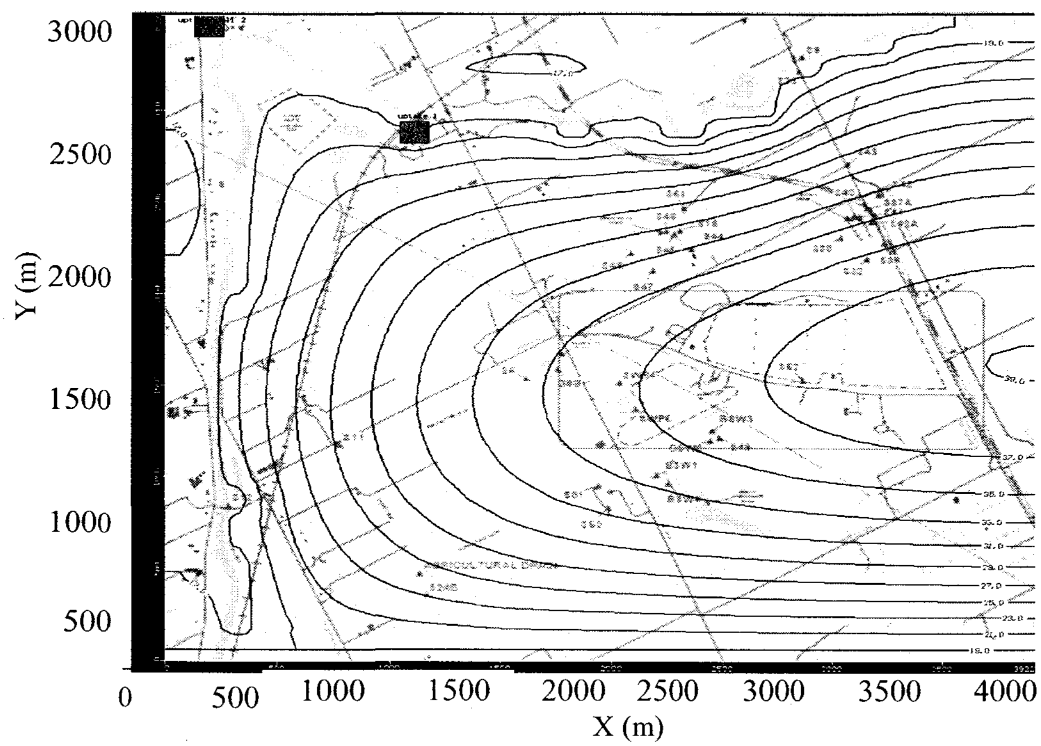

Figure 6-6 Contour of flow on the Trail Road landfill (EEMMS/FEM)

Figures 6-7 is the contour of water table, velocity vector and its cut-section velocity. As shown, the flow directions are clearer than that given in Figure 6-6. Ground water flow is not found in the upper/middle deep aquifer in the vicinity immediately northeast of the trail landfill due to the absence of the upper/middle deep aquifer in this area. Beneath the Trail landfill site, the groundwater flow direction in the upper/middle part of the deep aquifer is northwest, in the general direction of the dewatering pond. Immediately south and west of the Trail landfill, groundwater flow is northwards.

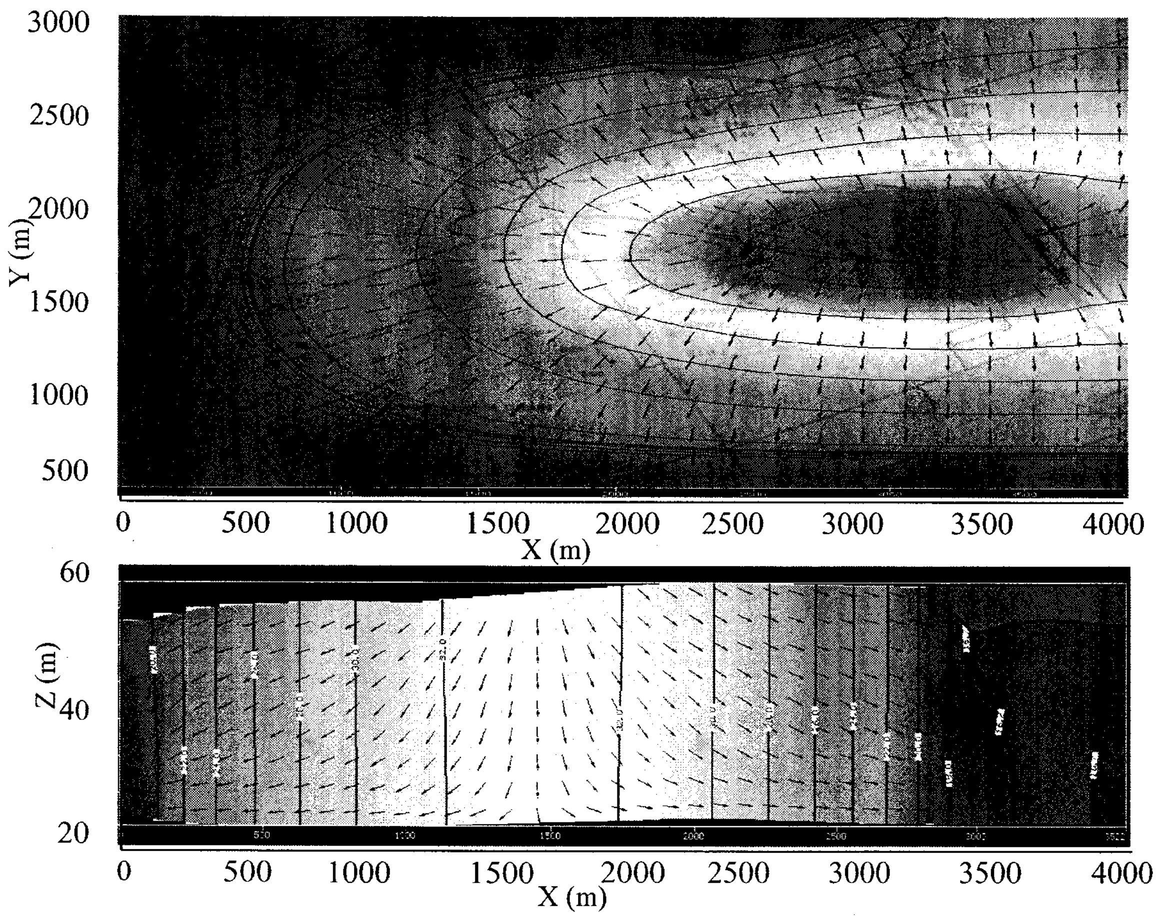

Figure 6-7 Contours of water table, velocity vector and its cut-section velocity

6.3.3 Concentration Comparison Based on Current Data

Table 6-4 shows the comparison of the average concentrations between the modeled and observed current data of the different years. All sampled data are from Accutest laboratories Ltd. (Accutest) of Ottawa, Ontario. Accutest is certified by the Canadian Association for Environmental (analytical laboratories (CAEAL). CAEAL is a non-profit organization who, in partnership with the standards council of Canada (SCC). All laboratory data for the 2002-2005 Trail Road and Nepean landfill sites annual monitoring and operating program was reported in a consistently thorough manner, ensuring an appropriate level of QA/QC was achieved. Benzene in air cannot be tested, as its value equals to 0. Hence, the air part won't be considered in this research. However, differences between the modeling results and field observations in the other three zones are identified where the comparison is made. Similarly as shown in Table 4-7, the best-fit data was done by minimizing the relative error between observed and predicted EEMMS /FEM modeled concentrations. The differences between the mean concentrations and FEM modeled concentrations are lower than 9%. The minimum difference between the FEM model results and the observed data is 0 during four years. Subsequently, this section of the report interprets the effects from Trail Road landfill leachate on groundwater quality beneath, and in the vicinity of the Trail landfill on the basis of past 2002-2005 monitoring data. The source of leachate's risk impaction will be assessed in the following sections. Figures 6-9 and 6-10 show the EEMMS results using the 3-D FEM solver (COMSOL code) as compared to observed concentrations to confirm model accuracy.

Table 6-4 Comparison of modeling results and observed benzene

Year	Lower bound of concentration (mg m^{-3})	EEMMS /FEM modeled concentration (mg m^{-3})	Upper bound of concentrations (mg m^{-3})	Observed concentration (mg m^{-3})	Relative error between observed and predicted EEMMS /FEM
2002	3.4	6.3	8.8	6.3	0.0000
2003	3.3	4	8.7	6.2	0.0908
2004	3.2	3	8.5	9.8	-
2005	3.1	2	8.3	3.5	0.0422
2006	-	1	-		-

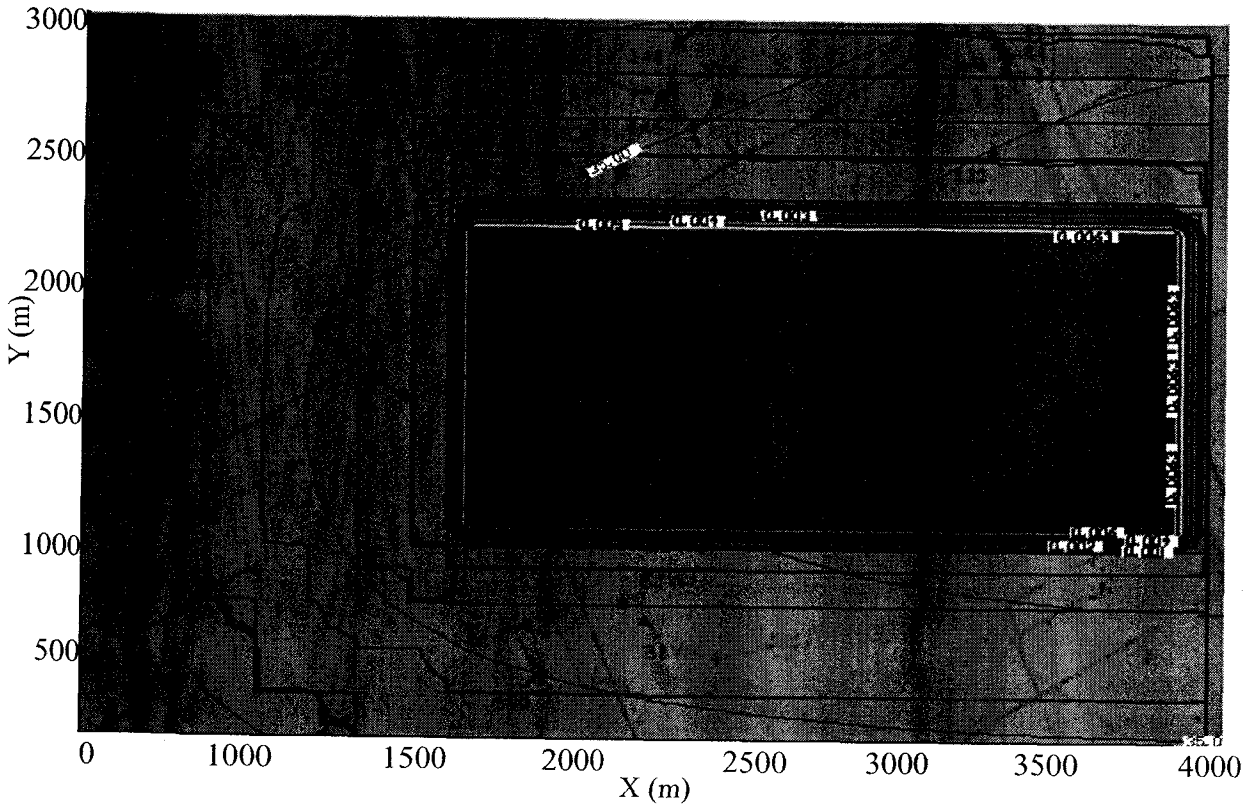

Figure 6-8 Concentration EEMMS /FEM contours of benzene from 2002-2006 (g m^{-3})

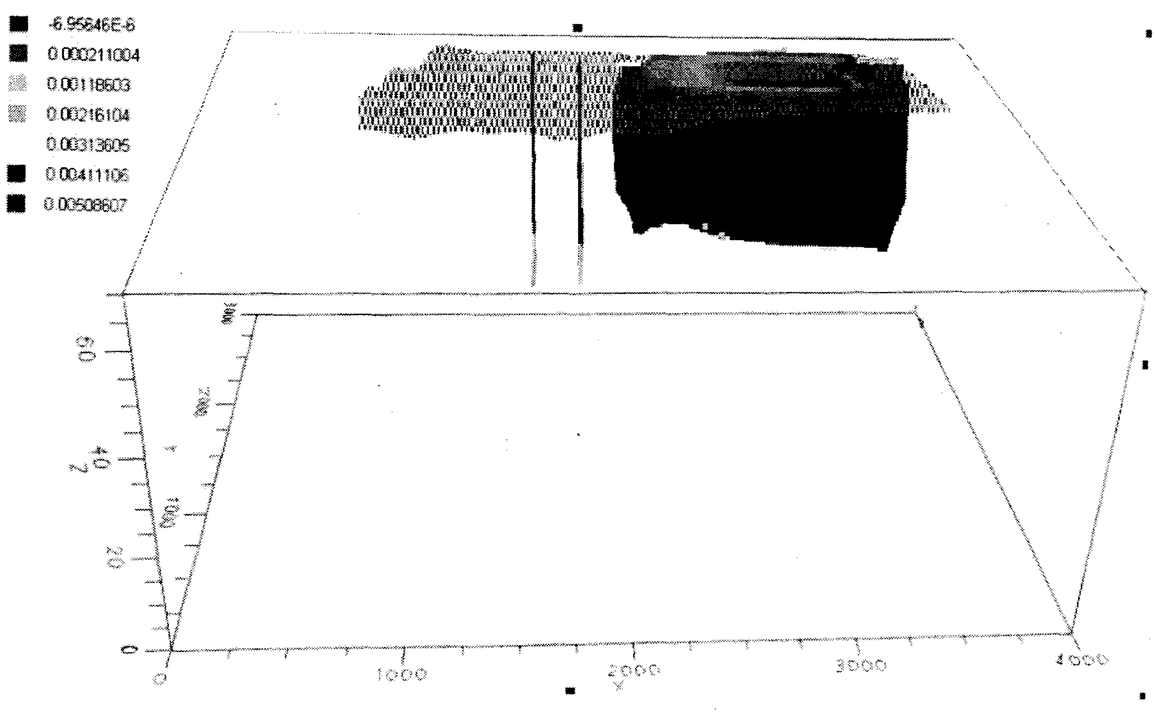

Figure 6-9 Concentration of 3D EEMMS /FEM contours of benzene (g m^{-3}, 10 years)

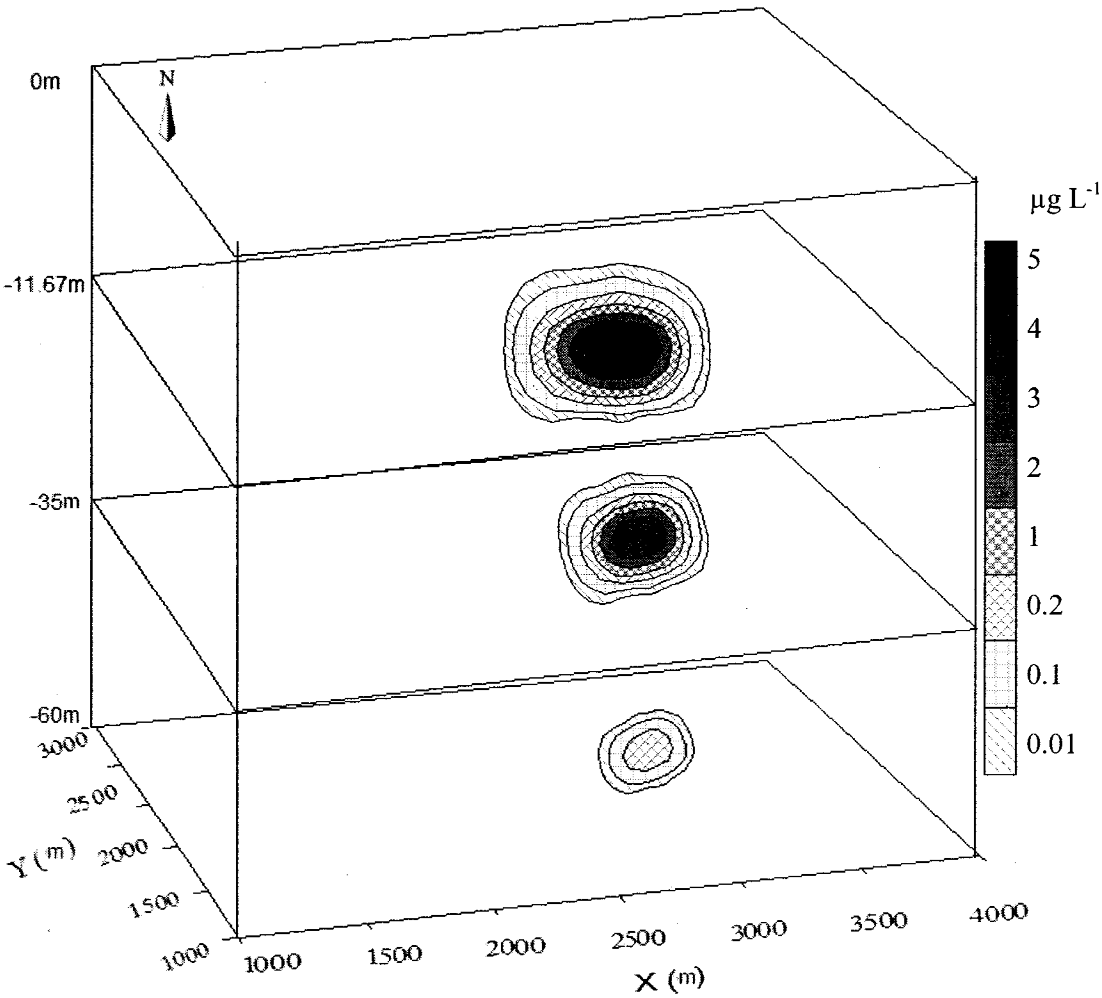

Figure 6-10 Concentration 3D EEMMS /FEM contours of benzene ($\mu g\ L^{-1}$, 10 years)

6.4 Discussion

Health Canada, as secretariat to the federal provincial territorial committee on drinking water is posting the guideline of 0.001 mg L^{-1} (1 $\mu g\ L^{-1}$) for benzene in drinking water (Health Canada, 2007). According to the basic environment law issued by Health Canada, the groundwater quality standard, and the average concentration of the benzene contaminants shown in Table 6-5 does not exceed the standard after 5 years.

Table 6-5 Groundwater quality standard for benzene

Contaminants	Maximum concentration of layer 1 (after 5 years)	Standard
Benzene	1 μg L^{-1}	$\leq$ 1 μg L^{-1}

6.5 Summary

An EEMMS/FEM modeling has been developed and validated by the use of field data and investigation to simulate 3D current conditions of the Trail Road landfill area. The validation of the 3D average flow and concentration modeling indicates that EEMMS can, for the Trail Road landfill region, provide satisfactory simulations. In conjunction with the flow and concentration contour described in this chapter, the pollutant dispersion of benzene and risk assessment for Trail Road landfill site are investigated by using EEMMS risk assessment methods in the following chapter.

Chapter 7 Sensitivity Analysis and Integrated Risk Assessment

7.1 Introduction

Input parameter variability is described by statistical distributions. The variability in model output, also called uncertainty, is typically captured through a statistical representation (typically probability density or a cumulative density plot) of the model output. There are many input parameters that will affect the uncertainty of the output. Required input for flow analyses consists of initial conditions, soil hydraulic properties, fluid properties, time integration parameters, boundary condition data and mesh geometry. For transport analyses, additional input data are porous media dispersivity, initial concentrations, equilibrium partition coefficients, component densities, diffusion coefficients, first-order decay coefficients, mass transfer coefficients (for non equilibrium analyses) and boundary condition data. All of those input parameters required for the EEMMS simulation comprised environmental properties, chemical properties, chemical releases, and background concentrations. Environmental properties included landscape parameters, hydrological flow rates, and meteorological data. Compared to the air and surface water, porous compartments of soil and sediment showed larger uncertainties in the predicted pollutants concentrations (Cohen and Cooter, 2002a). Parameters such as hydraulic conductivity, bulk density and porosity are mainly targeted.

In this chapter, sensitivity analysis was conducted using Pe number and retardation factors to evaluate the uncertainty analysis techniques to the new EEMMS. Furthermore, an integrated risk assessment - MCM and uncertainty analysis are used to estimate total variance associated with the model outcome, and to evaluate the variability of model predictions.

7.2 Sensitivity Analysis

A sensitivity analysis was performed to understand which input parameters were important to the output by characterizing the degree of monotonic relationship between the model prediction and uncertain inputs. Sensitivity analysis investigates how the variation in the output of a model can be apportioned either qualitatively or quantitatively to different sources of variation. A parametric uncertainty analysis is the process of propagating parameter variability through a model to quantify the uncertainty introduced in the model output by input parameter variability. It can include all manner of variability and uncertainty in inputs, and combinations of both.

7.2.1 Peclet Number (Pe)

When the transport problem is advection-dominated, the grid Peclet number can measure the sharpness of the concentration front, or the degree to which the transport problem is dominated by advection. The Peclet number in a one-dimensional uniform flow field is given as:

$$Pe = \frac{V\Delta x}{D} = \frac{\Delta x}{\alpha_L} \qquad (7.1)$$

As physical dispersion becomes larger, the Peclet number becomes smaller. The Peclet number is also dependent on the grid spacing. When grid spacing, Δx, decreases, so does the Peclet number. Taking $\Delta x = 1$, and only considering the relationship between Pe, V and D, V is the velocity and D is the dispersion, one finds that smaller Peclet numbers are associated with finer spatial discretization. This implies that using finer grids spacing can reduce artificial oscillation. For those scenarios, comparisons were further performed for five different Peclet numbers (Pe=0.1 0.5, 5, and 10) that correspond to various diffusion/dispersion coefficients (Figure 7-1). The contaminant load rate was 0.3 g m^{-2}. Retardation was 1, and decay was not considered. Figure 7-1 illustrates the analytical and numerical solutions at four different Peclet numbers, indicates that oscillatory behavior was eliminated when Pe was reduced.

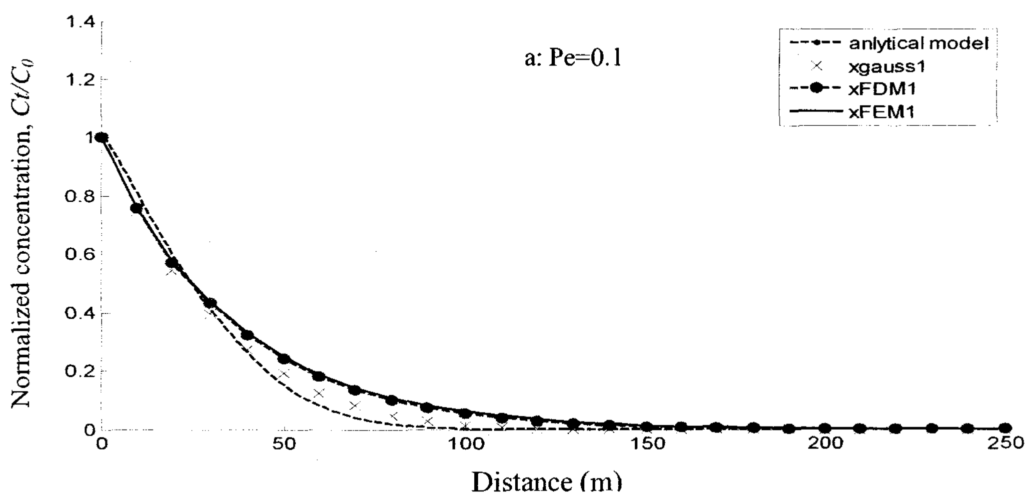

Figure 7-1a Comparison, at indicated times, of the performance of multimedia models using different numerical and mathematical solutions for Pe=0.1

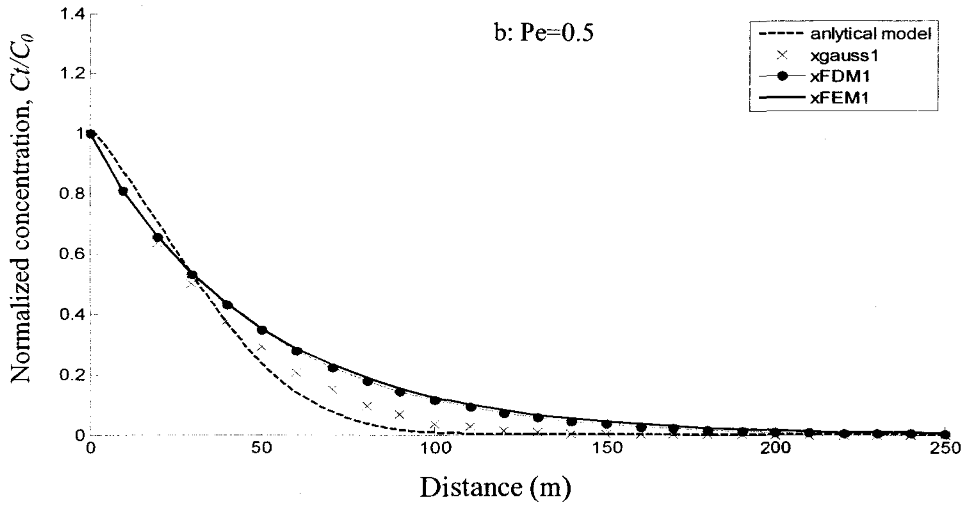

Figure 7-1b Comparison, at indicated times, of the performance of multimedia models using different numerical and mathematical solutions for Pe =0.5

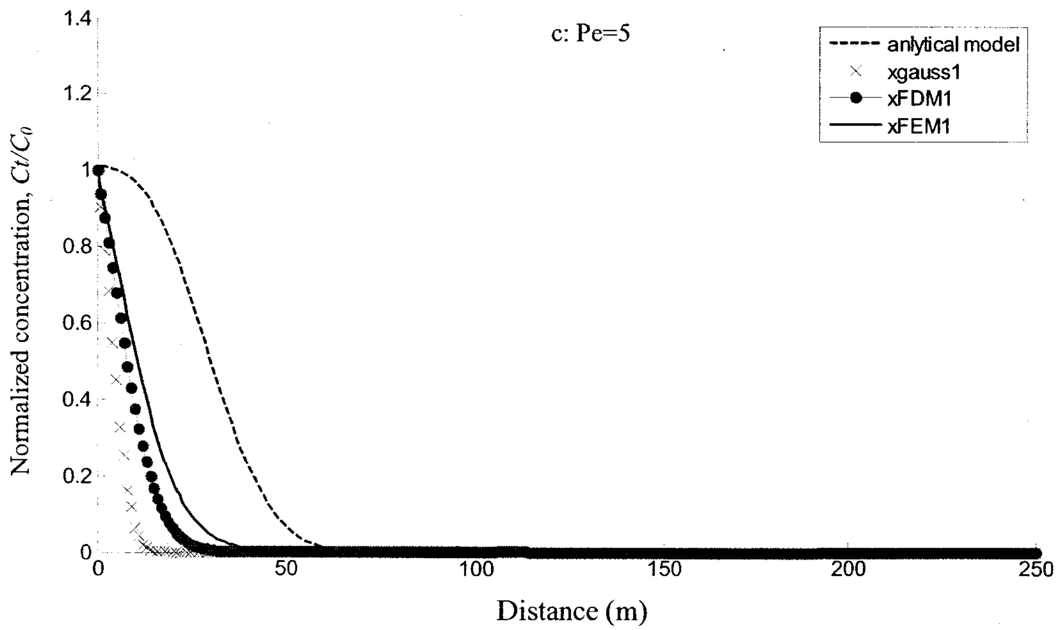

Figure 7-1c Comparison, at indicated times, of the performance of multimedia models using different numerical and mathematical solutions for Pe =5

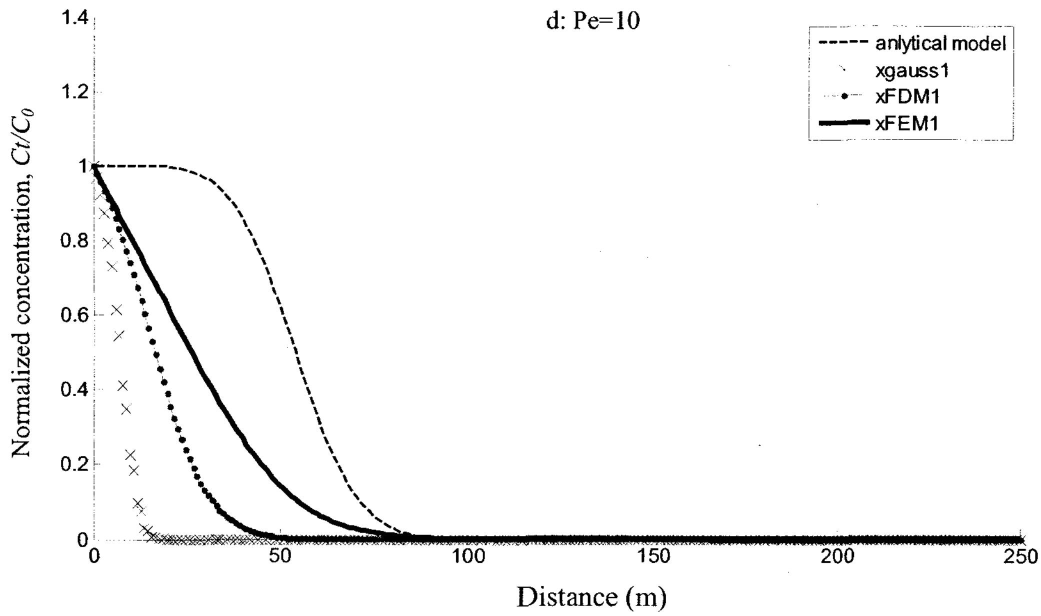

Figure 7-1d Comparison, at indicated times, of the performance of multimedia models using different numerical and mathematical solutions for for Pe =10

Figure 7-1 also shows that when the advective and diffusion factors decreased (Pe number), the three numerical models gave similar results. If the analyzed results were right, the FEM would have more accurate results than the FDM or Gauss model. That infers the FEM solution is more effective when oscillatory behavior is significant since oscillatory behavior is eliminated as the Pe decreases. The FDM and analytical solutions are not so accurate due to their own limitations. The major limitation of the finite-difference model is itself, that is, finite-difference grids do not conform to boundaries that are not parallel to the coordinate axes. Stair-step approximations to angular boundaries are inconvenient to specify and can cause local variations in the multimedia or contaminant plume that are not realistic.

7.2.2 Retardation Factor

Basically, when a contaminant compound is released to the environment, it will partition onto soils or subsurface solids as water moves through the system. The degree to which the contaminant is distributed between the absorbed and aqueous phases is described by the appropriate sorption isotherm for the compound and its concentration in the system. *R*, the retardation factor, will reflect these parameters. It is the most fundamental parameter in transport simulation, affecting the pollutant's transfers time and peak. It is calculated as:

$$R = 1 + k_d \frac{\rho_b}{\theta} \tag{7.2}$$

where,

k_d is the distribution coefficient,

ρ_b is the bulk density (kg m^{-3}), and

θ is the porosity(%).

The soil distribution coefficient is the more general expression for contaminant sorption. The distribution coefficient (k_d) is defined as:

$$k_d = \frac{C_a}{C_d} \tag{7.3}$$

where,

C_a is the mass of contaminant absorbed (mg g^{-1}), and

C_d is the mass of contaminant dissolved in the aqueous phase (mg ml^{-1}).

In order to evaluate the retardation's effect on transport, a plot of a pulse throughput, using the analytical and numerical methods is shown in Figure 7-2. The retardation factor was given values of 1.4776, 2.9552, and 4.4328. At each value of the retardation, a match was obtained with the analytical and numerical solution. The time for the concentration peak to appear in the throughput is roughly the same, but the value of the peaks changes significantly (Figure 7-2). The greater the retardation, the smaller the peak concentrations tend to be. The long tail illustrates the increase in retardation ability as concentration decreases.

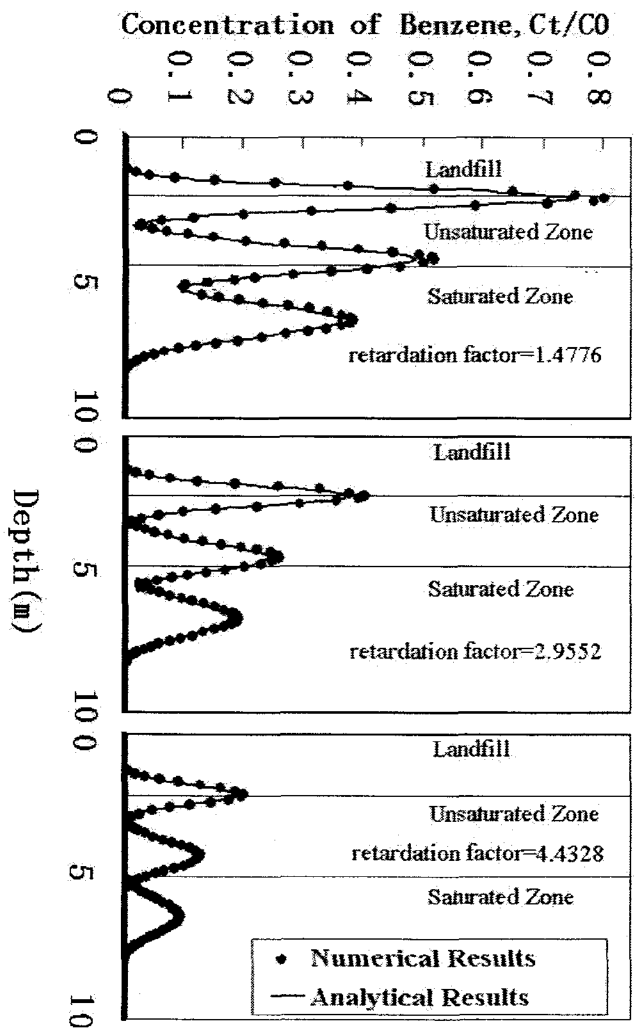

Figure 7-2 EEMMS numerical and analytical solutions in four zones for different

retardation factor values.

7.3 Integrated Risk Assessment for the Trail Road Landfill Site

In this section, two future emission rates are examined for risk assessment of Trail Road landfill site area in the years of 2016 and 2026; the data are predicted base on the trend of known production from 2001 to 2006 shown in Chapter 6. Uncertainties in the system are examined by means of MCM. The risk quotient (RQ) factors combined with the present and future rates of chemical pollutant will provide the spatial and temporal assessment of risk from the leachate in Trail Road landfill site.

7.3.1 Monte Carlo Simulation for Uncertainty Analysis and Risk Assessment

MCM for uncertainty analysis is a method used to ascertain the dependency of a given model output (for example, water level or concentration) upon model input parameters (for example, hydraulic conductivity, bulk density and mass loading rate). Uncertainty analysis is important for checking the quality of the calibration of a given model, as well as a powerful tool for checking the robustness and reliability of model simulations. Thus, uncertainty analysis provides a method for assessing relations between information provided as input to a model, in the form of model input parameters, and information produced as output from the model. Numerous methods are described in the literature for conducting uncertainty analysis (Saltelli et al., 2000). For the EEMMS, selected model parameters were varied one at a time from their respective calibrated values, and the corresponding effect of this variation on the change in the benzene concentration at the Nepean landfill was assessed. Contaminant fate and transport model parameters that were subjected to the uncertainty analysis were: hydraulic conductivity of the aquifers, storage coefficients (includes specific yield), bulk density, effective porosity, and infiltration (recharge) rate.

In conducting the uncertainty analysis, all calibrated model parameters were increased and decreased by factors ranging from 50% to 400% of their calibrated values. For example, horizontal hydraulic conductivity for model was varied by 90%, 110%, 150%, and 250% of its calibrated value; dispersivity was varied by 50%, 200%, and 400% of its calibrated value. The detailed hydrogeology and contaminant transport data have already been listed in Table 6-2 in the last chapter. Once the input data are entered using the MCM, parameters probability density functions (PDFs) are generated and simulated results are provided in a MCM output according to Figures 3-7 and 3-8. PDFs are mathematical functions that express the probability of a random variable (model input) falling within some interval value, such as horizontal hydraulic conductivity, is obtained multiple times assuming the spatially interpolated values follow a Gaussian (normal) distribution. This kind of probabilistic analysis is used to generate uncertainties in model inputs so that estimates of uncertainties in model outputs can be made. Although the uncertainty analysis provided some insight into the relative importance of selected model parameters, a probabilistic analysis provides quantitative insight about the range and likelihood (probability) of model output.

Figure 7-3 to Figure 7-5 shows the detailed output for three of the five variants: horizontal hydraulic conductivity, bulk density and recharge. For horizontal hydraulic conductivity that related to the groundwater velocity, a probability distribution was assumed (Figures 7-3a).A normal complementary cumulative probability distribution was then assumed (Figures 7-3a). These graphs are fully customizable such as being able to modify the number of classes or bins that describe the simulated PDFs. Once the PDF for each variant has been generated, two options are available to complete the fate and transport simulation. The option is to select the PDFs for the variants. In this manner, EMMS uses the entire range of simulated values for each parameter variant, randomly selected, for the fate and transport simulation. Each of the aforementioned model parameters can be represented by a PDF such as a normal, lognormal, triangular, or uniform distribution. In the current analysis, a normal distribution was chosen to represent each uncertain parameter (or variant) with the exception of dispersivity. The examples of PDFs generated for hydraulic conductivity of the aquifers, bulk density and recharge compared with the appropriate theoretical distribution are shown in Figures 7-3, 7-4, and 7-5 respectively. Two points are noteworthy: (1) for a normal distribution (Figures 7-3a, 7-4a, and 7-6a), values for the mean, mode, and median are equal, whereas for a lognormal distribution (Figures 7-3b, 7-4b, and 7-6b), the values for the mean, mode, and median are not equal; and (2) because the mean value of recharge varies yearly, the generated values of concentration output associated with the PDF also will vary yearly, but the type of PDF will always be the same.

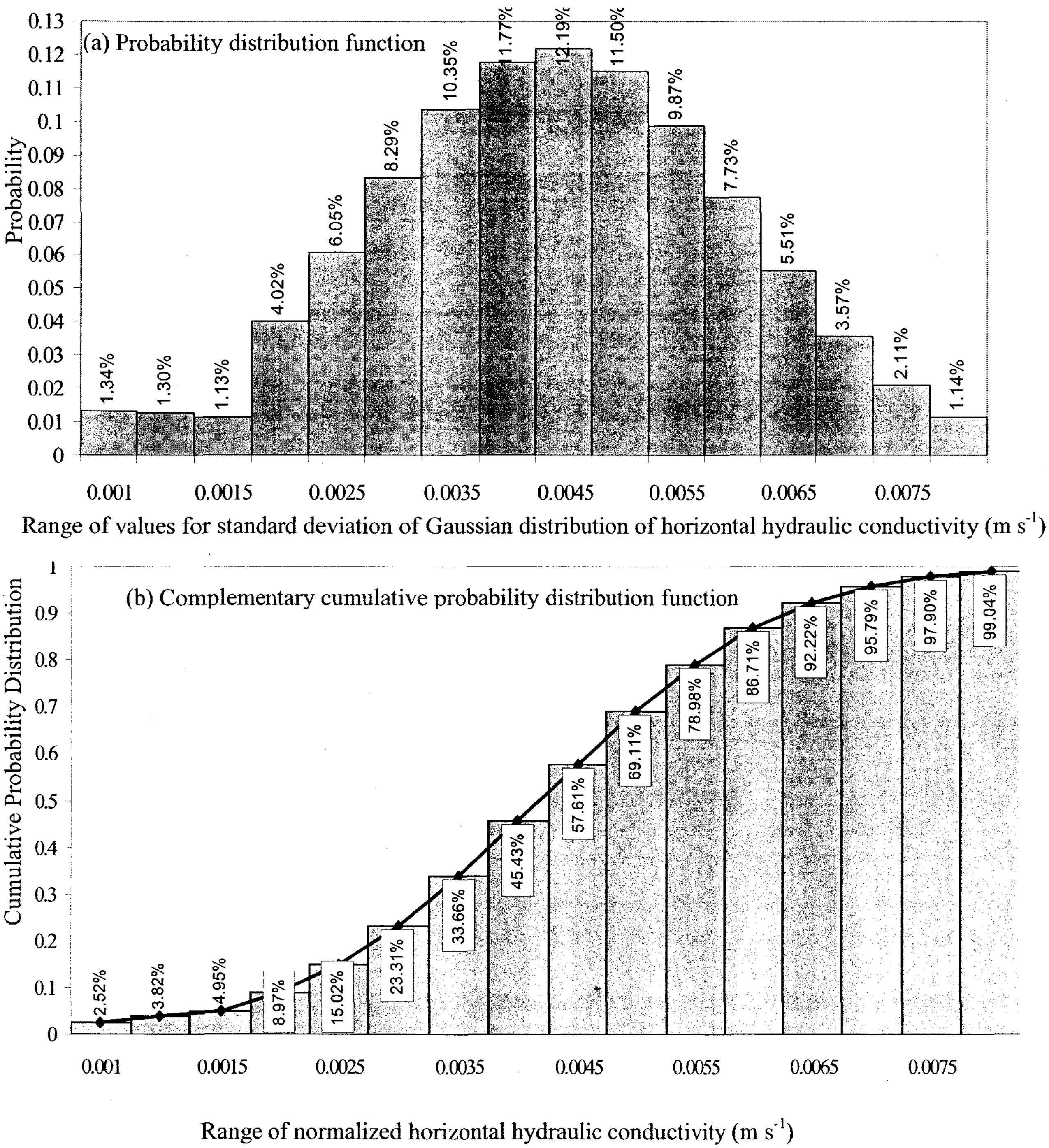

Figure 7-3 Graphical output from EEMMS probabilistic analysis of hydraulic conductivity at (1400m, 1800m) in 2016: (a) probability distribution and (b) cumulative probability distribution

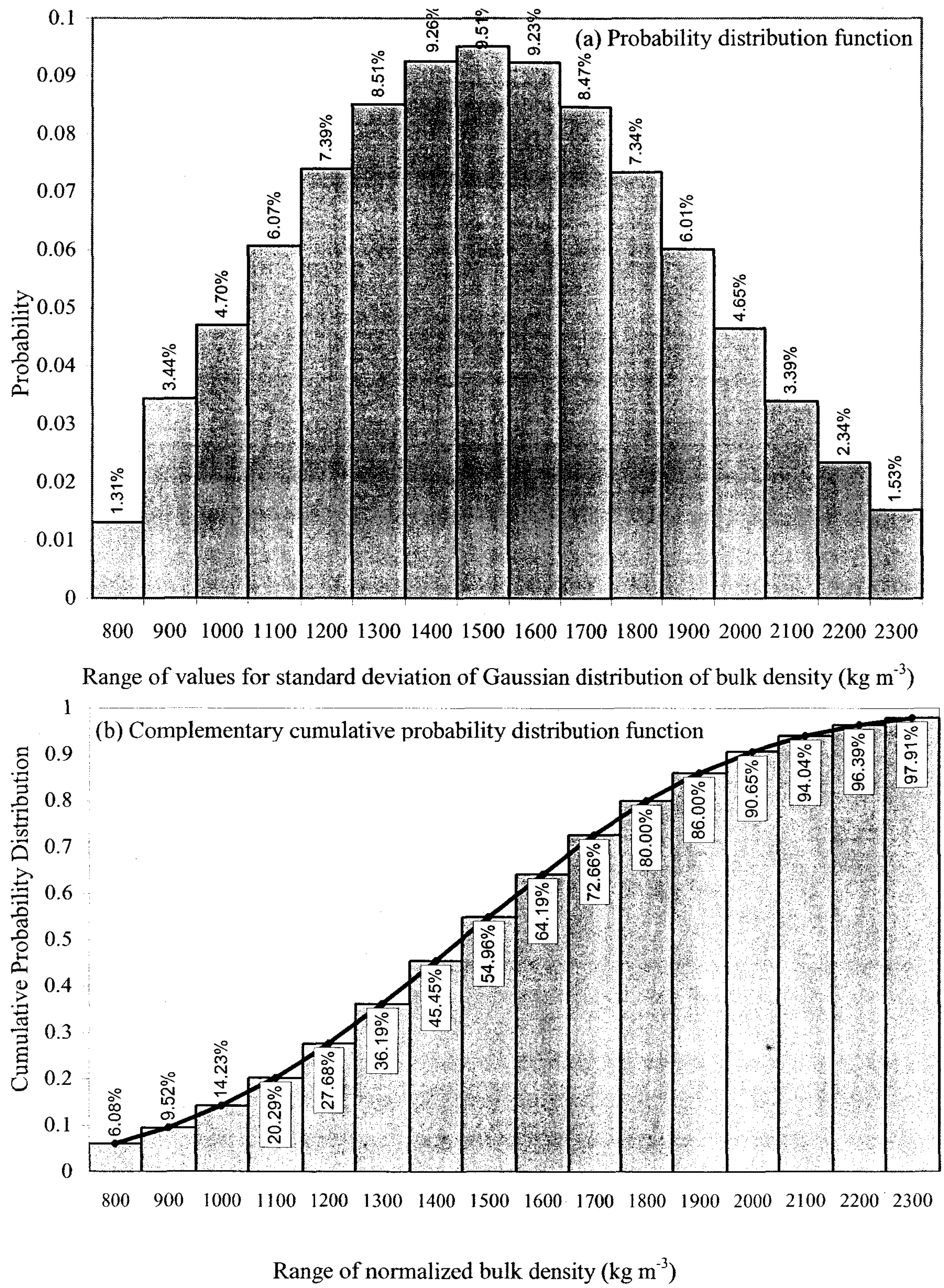

Figure 7-4 EEMMS probabilistic analysis of bulk density at (1400m, 1800m) in 2016: (a) probability distribution and (b) cumulative probability distribution

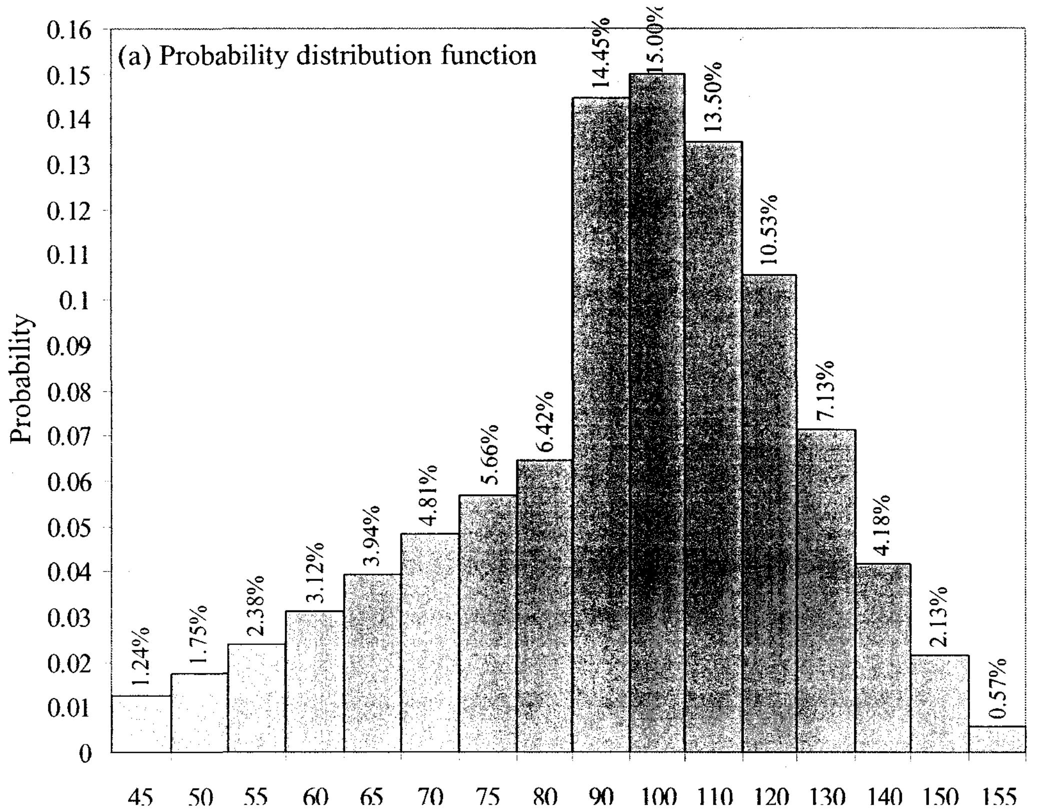

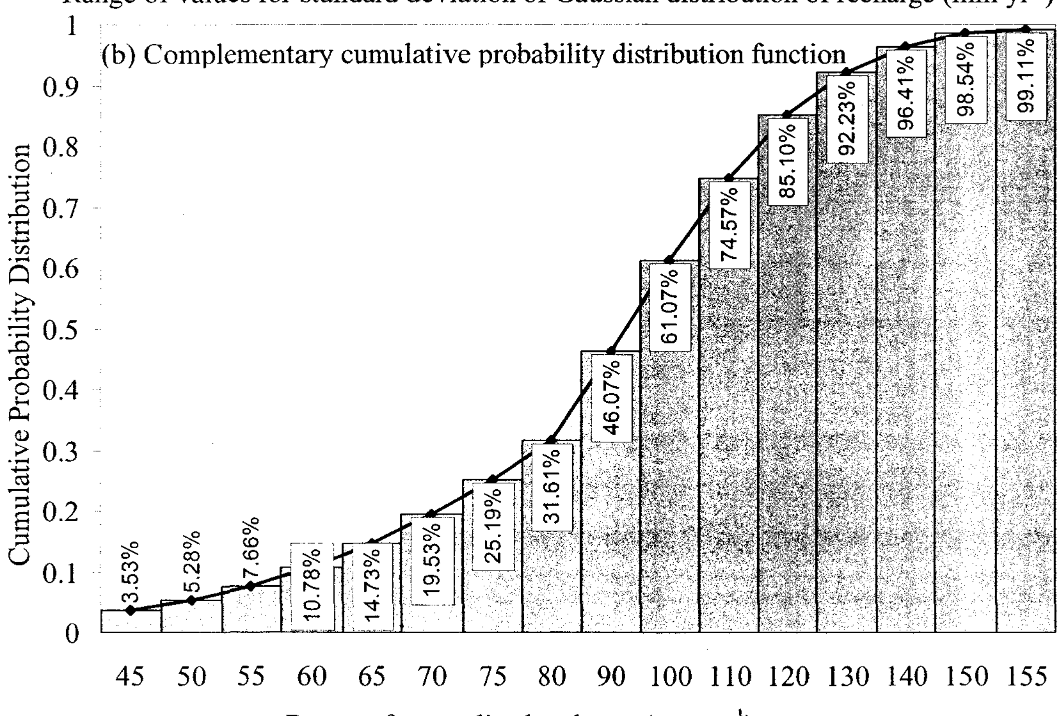

Figure 7-5 EEMMS probabilistic analysis of recharge at (1400m, 1800m) in 2016: (a) probability distribution and (b) cumulative probability distribution

The values of hydraulic conductivity of the aquifers and storage coefficients (includes specific yield) are selected to be normally distributed (Riddle et al., 2001). Statistics associated with the normal and lognormal distributions for the hydraulic conductivity such as the mean, standard deviation, minimum, and maximum, are expressed in detail in Figure 7-3. The maximum value is 0.006997 m s^{-1}, the minimum value is 0.00103 m s^{-1}, the mean value is 0.0042 m s^{-1} and the deviation value is 0.0016 m s^{-1}. Similarly, Figure 7-3 shows that the bulk density is specified from a uniform distribution from the minimum 769 to the maximum 2241 kg mg^{-3}, the mean value is 1447.8 kg $mg^{-3}$and the deviation value is 418.5 kg mg^{-3}. As shown in Figure 7-5, the recharge is from a normal distribution from the minimum 43.97 to the maximum 137.3 mm per year with mean 92.6 mm per year and standard deviation of 26.3 mm per year.

7.3.2 Risk Quotient (RQ) Evaluation

Risk quotient (RQ) evaluation will be derived from the CHARM (chemical hazard assessment and risk management) model. It is a primary tool to support the environmental evaluation of the use of production chemicals on the basis of available data about these chemicals and platform-related conditions (Thatcher et al., 1999, 2001). The RQ quotient evaluation is carried out based on the comparison of the predicted environmental concentration (PEC) to the known environmental criteria (KEC), which refer to local environmental guidelines for a species. The RQ can be viewed as the "severity measures" of risks. The higher the value of RQ above 1, the greater the possibility of environmental risks is. When RQ > 1 adverse environmental effects may be expected. To evaluate the probability of RQ exceeding 1, the probabilistic distribution for each point of concern resulting from the MCM is taken into account for the quantification of the risk quotient. For example, the RQ distribution under 95 percentile concentrations, which present the "worst case" section, will be performed to show the severity risk levels.

7.4 Integrated Risk Assessment Results

Once the input data are entered using the MCM, parameters probability density functions (PDFs) are generated and simulated results are provided in a MCM output. The following Figures 7-6 and 7-7 (a) and (b) show the probability distribution of benzene concentration that is located in the site (1400m, 1800m) in 2016 and 2026.

Table 7-1 shows the overall risk assessment results for Trail Road Landfill Site. Based on the drinking water for benzene criterion issued by the Health Canada, 0.001 mg L^{-1} (1 $\mu g\ L^{-1}$), in 2016, the RQ of the percentiles of 5% is of the order of 0.0002 - 0.793; the probabilistic risk levels are zero, indicating that negligible risk is associated with present benzene dispersion in the Trail Road landfill site within 10 years for typical locations indicated in Table 7-1. However, with the benzene concentration towards its end, the concentration will exceed the criterion. In 2016, the probabilistic risk level within 16 m of the source is from 9.91×10^{-10} to 7.55×10^{-6} kg m^{-3}; the RQ of the percentiles of 95% is of the order of 0.00099 -7.55 for typical locations indicated in Table 7-1.

Table 7-1 Summary of risk assessment results

X (m)	Y (m)	Depth (m)	Probability (100%)	Mean concentration (kg m^{-3})	Standard deviation (kg m^{-3})	0.95 (kg m^{-3})
1162.641	1573.6195	16	0.531197	3.38E-06	2.54E-06	7.55×10^{-6}
1248.506	1554.1785	11	0.471316	1.69E-06	1.27E-06	3.78×10^{-6}
1248.506	1554.1785	9	0.357247	3.92E-10	3.64E-10	9.91×10^{-10}
X (m)	Y (m)	Depth (m)	0.05(kg m^{-3})	RQ (0.05) (100%)	RQ (0.95) (100%)	-
1162.641	1573.6195	16	7.93×10^{-7}	0.793	7.55	-
1248.506	1554.1785	11	3.96×10^{-7}	0.396	3.78	-
1248.506	1554.1785	9	2.07×10^{-10}	2.07×10^{-4}	9.91×10^{-4}	-

Figure 7-6 shows that about 60% of the predicted concentrations fall in the range of 1.15×10^{-6} to $2.65\times10^{-}$ kg m^{-3}. The maximum concentration is only 1.08085×10^{-5} kg m^{-3}. The percentiles of 5% and 95% of benzene concentration are 1×10^{-6} kg m^{-3}and 3.67×10^{-6} kg m^{-3} respectively. The minimum value is 1.10963×10^{-6} kg m^{-3}, the mean value is 3.37875×10^{-6} kg m^{-3} and the deviation value is 2.53609×10^{-6} kg m^{-3}; Similarly, as shown in Figure 7-7, the recharge is from a normal distribution from the minimum 1.08807×10^{-10} to the maximum 9.84547×10^{-10} kg m^{-3} with mean 3.92235×10^{-10} kg m^{-3} and standard deviation of 3.64115×10^{-10} kg m^{-3}.

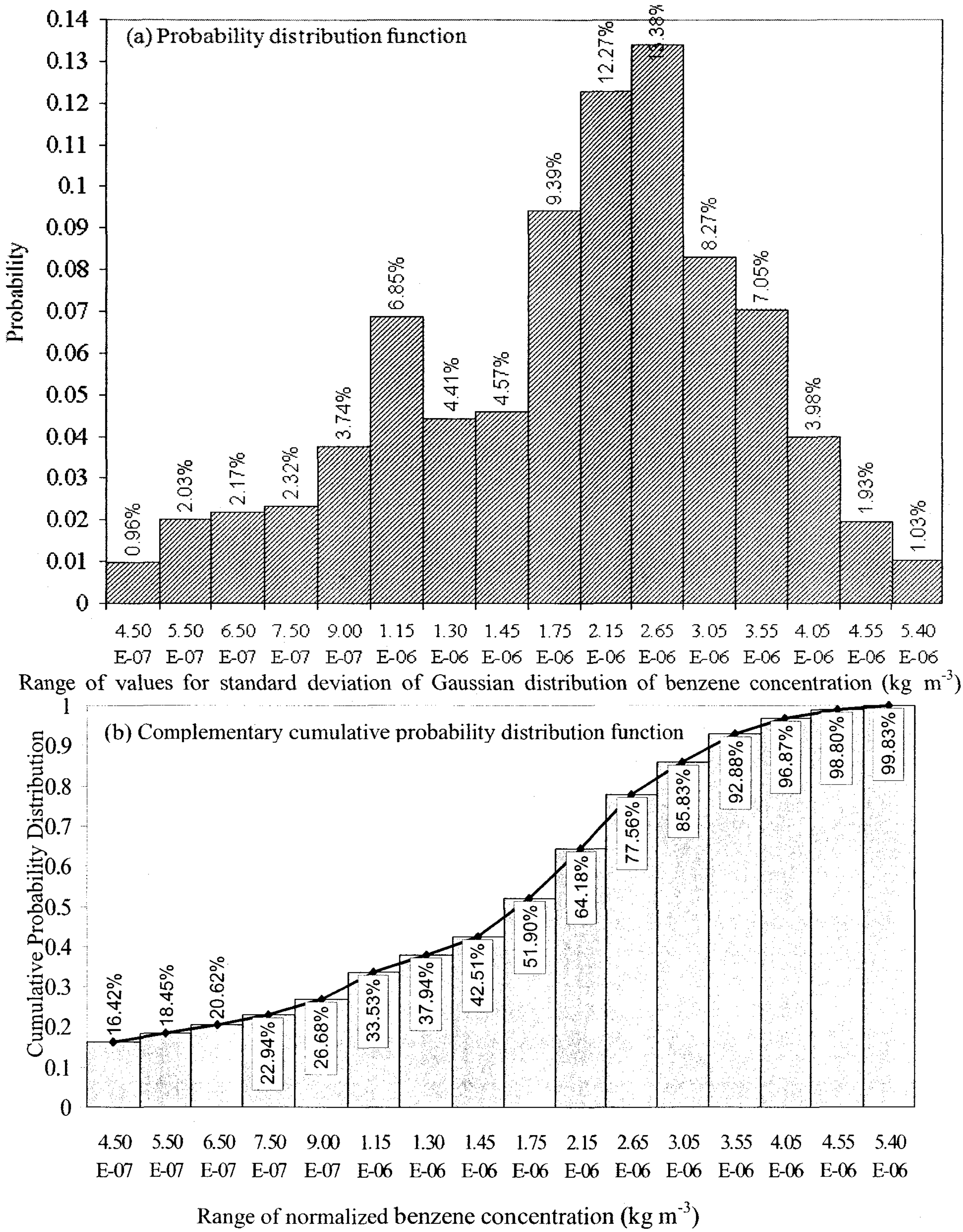

Figure 7-6 EEMMS output probabilistic analysis of benzene concentration (kg m^{-3}) at (1400m, 1800m) in 2016

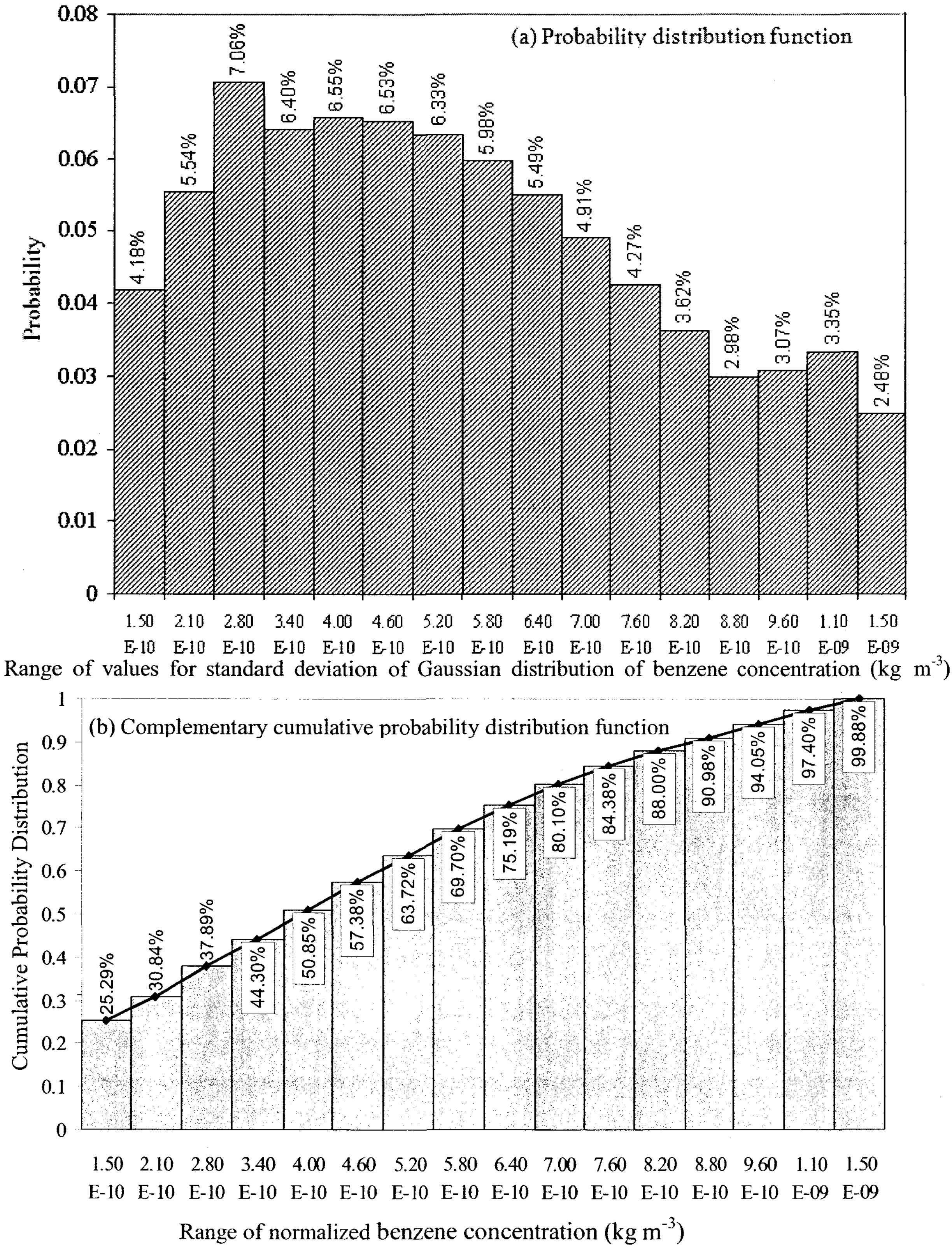

Figure 7-7 EEMMS output from probabilistic analysis of benzene concentration (kg m^{-3}) at (1400m, 1800m) in 2026

The 95 and 5 percentile concentration contour maps in 2016 are prepared as shown in Figures 7-8 and 7-9. It should be noted that the plots in Figure 7-8 (95 percentile concentration) necessarily represent an instantaneous concentration distribution that could occur because the 95-percentile concentration distribution may represent a "worst case" prediction. The 5 percentile concentrations are generally low. The percentiles predicted 95 percentile concentrations in 2016 are of the order of 12.5-6.2 $\mu g\ L^{-1}$, and the corresponding 5 percentile concentrations in 2016 are of the order of 1.2-0.4 $\mu g\ L^{-1}$. The 95 and 5 percentile concentration contour maps in 2026 are too small compared to the criterion issued by the Health Canada; the risk is the zero probability, as shown in Figures 7-6 and 7-7.

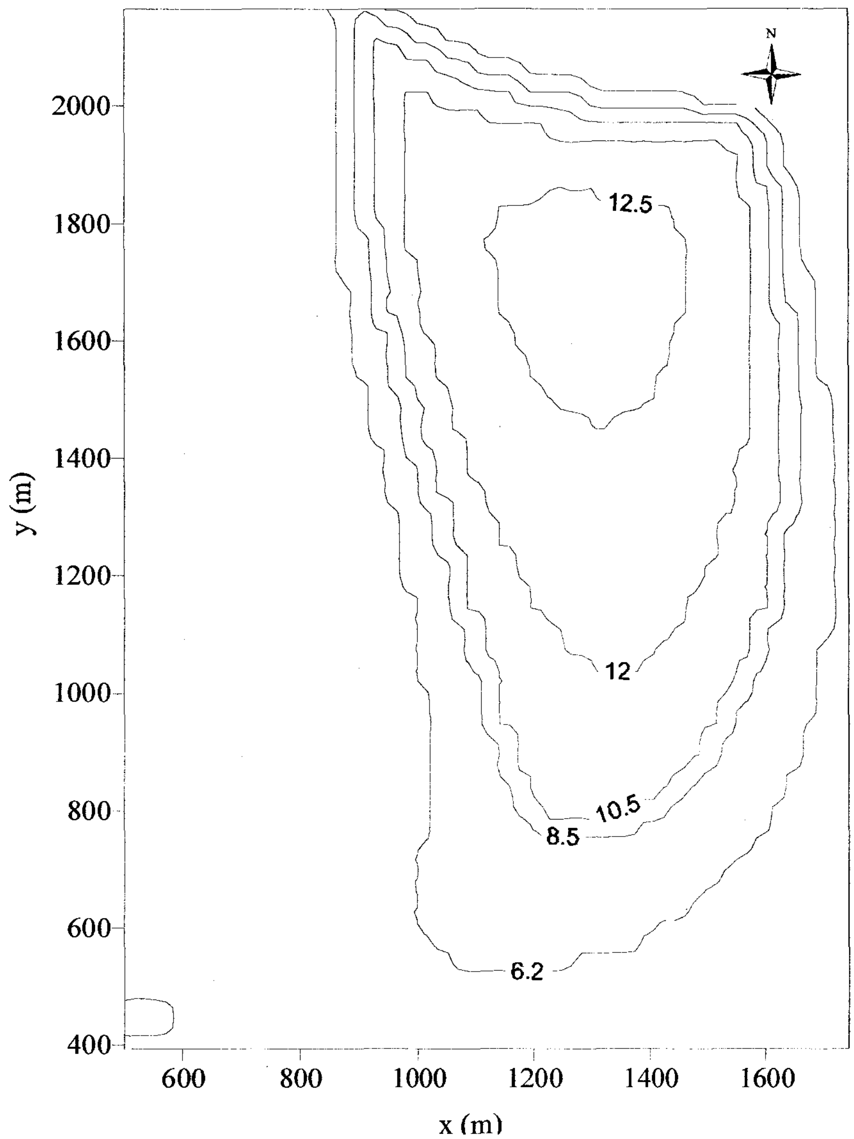

Figure 7-8 Uncertainty predictions contour maps of 95 percentile concentrations in 2016

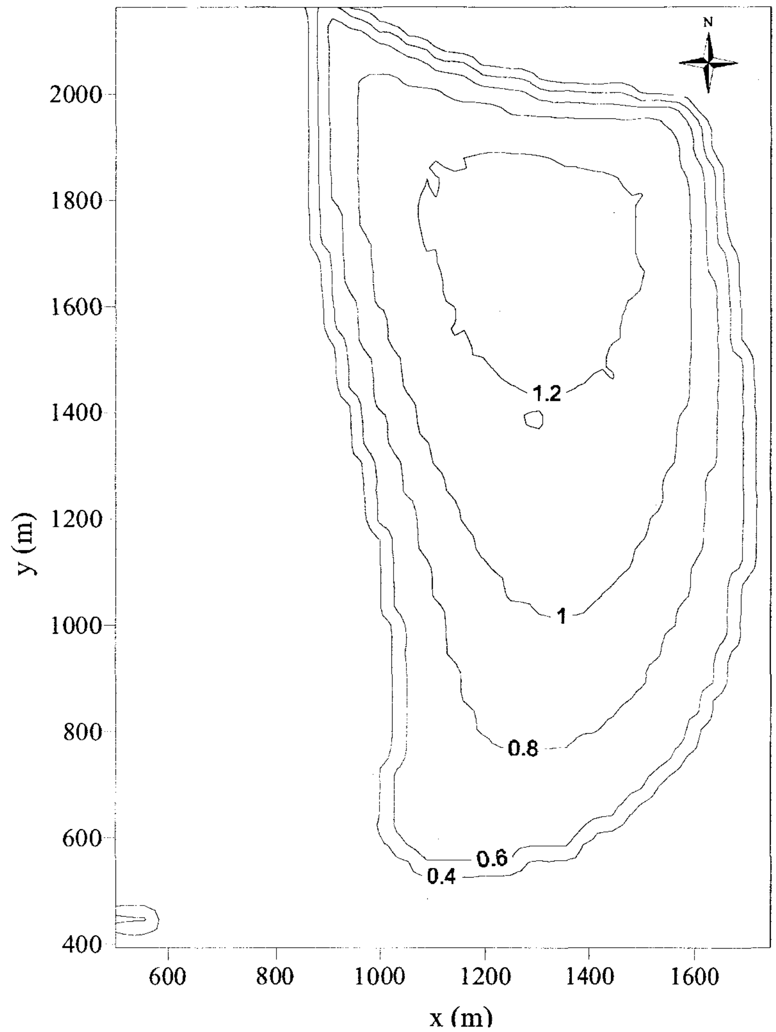

Figure 7-9 Uncertainty predictions contour maps of 5 percentile concentrations in 2016

7.5 Summary

The sensitivity analysis and integrated risk assessment results have been presented in this chapter. The sensitivity analysis was also conducted using Pe number and retardation factors to evaluate the applicability and performance of various uncertainty analysis techniques to this new EEMMS system. Oscillatory behavior was shown to be eliminated when the Peclet number (Pe) decreased. The FEM and FDM are more accurate than the Gauss model when the Peclet number (Pe) increased. For the retardation, the long tail for the retardation curve illustrates that an increase in retardation ability occurs when concentration decreases. The results indicate that towards its depleted stage of waste pollutants such as in the landfill, adverse effects of contaminant benzene on the drinking water would reveal and the potential risk zone may cover approximate 20000 m^2 area with the Trail Road landfill site being the center. Other areas are the zero risk zones after 10 years. The integrated risk assessment results and sensitivity discussion indicate that the improved multimedia model system can be used as a tool in a field experiment and in future treatment design works. Further discussion related to the uncertainty analysis is conducted in the next chapter.

Chapter 8 Discussion

This chapter presents more discussions about the developed EEMMS system, model validation and its numerical method's sensitivity, and integrated risk assessment. The discussions mainly deal with the methodologies described in Chapter 3 and the results analysis presented in Chapters 4, 5, 6 and 7.

8.1 Discussion of Numerical Method's Sensitivity

The EEMMS was applied to perform the simulations of pollutants' concentrations and flux in multimedia environmental media. Both uncertainty in chemical properties such as chemical emission velocity and variability in environmental parameters such as the time changes were included in the general governing equations in Chapter 3. Other parameters such as compartmental dimensions, densities, emissions, and background concentrations were assumed to be constant in this research. Figure 8-1 gives the detailed results (data sources: Lin and Hildemann, 1995).

In the first case study of 1-D, Figure 8-1 shows the mathematical results of benzene at different times. The times are taken as 5 days, 100 days and 200 days, respectively. When it is with 5 days, peak concentration appears at the depth of 0.7m when time increases to 100 days, peak concentration is around 55% of C_0 at a depth of

2.8m; and peak concentration with value of a little more than 40% of C_0 moves downwards to a depth of 5m at a time up to 200 days.

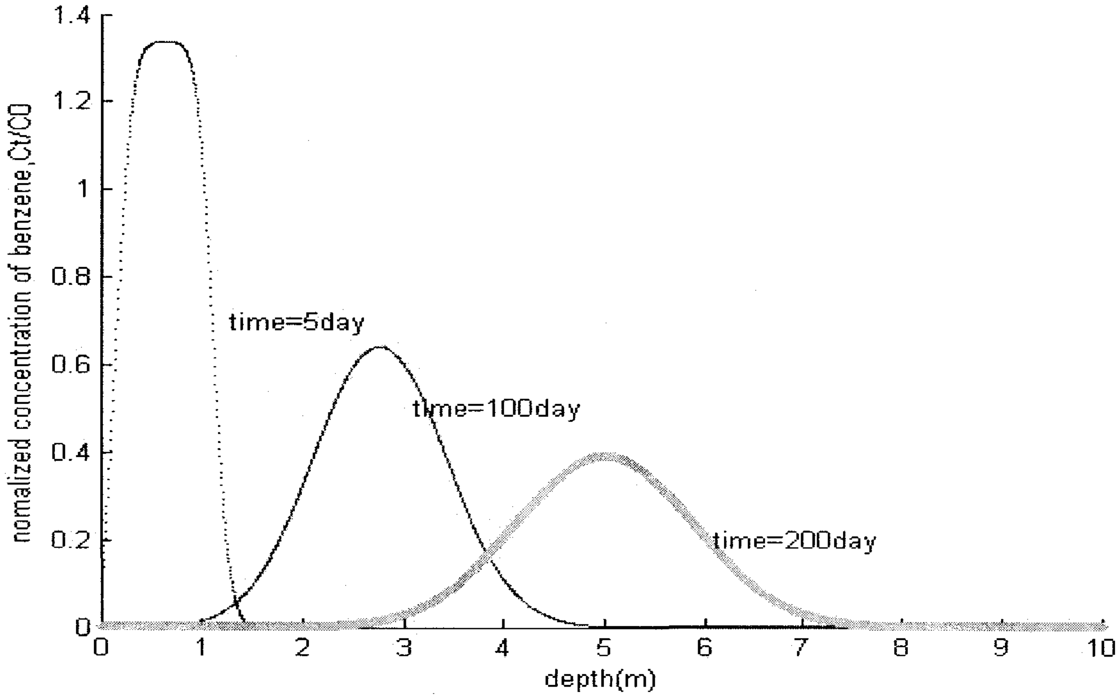

Figure 8-1 Subsurface concentration profile of benzene as function of depth

The proposed model carries the advantages of both the analytical methods and numerical methods, which were absent in the conventional model. However, the complexity of calculation is considered a major shortcoming. Based on the comparison of analytical methods and numerical methods, a sensitivity analysis was conducted to determine the influence of individual input parameters on the output variance for concentration in multi environmental media. Results of model validation indicated that the model predictions were in reasonable agreement with spatial and temporal distribution patterns, among the 1-D and 2-D case studies in Chapter 4 and 5, of reported data in the literature. The results of sensitivity analysis in this study also indicate that the model sensitivity to an input parameter might be affected by the methods, which was used in the research. Therefore, uncertainty and sensitivity analyses of the different methods for models were suggested to be conducted after the model output was validated based on appropriate case studies. The detailed results will be shown in Figures 8-2 and 8-3 (data sources: Lin and Hildemann, 1995), and Figures 8-4 and 8-5(data sources: Zheng and Wang, 1998).

In the present study, there is an improvement from previous models. Commonly, analytical linear equilibrium results ignore many potential temporal and spatial effects. The analyzed results sometimes cannot obtain the correct results due to calculation errors or being out of the boundary being modeled. For example, comparing Figure 8-2 with Figure 8-3, it is found that if it needs to analyse the pollutant transport within 1 meter depth, the analyzed model will give erred results as it only gets to the zero result as time increases. In Figure 8-3, we get the accurate results at times 100 days and 200 days using numerical model though they are close to zero, they are not to be neglected.

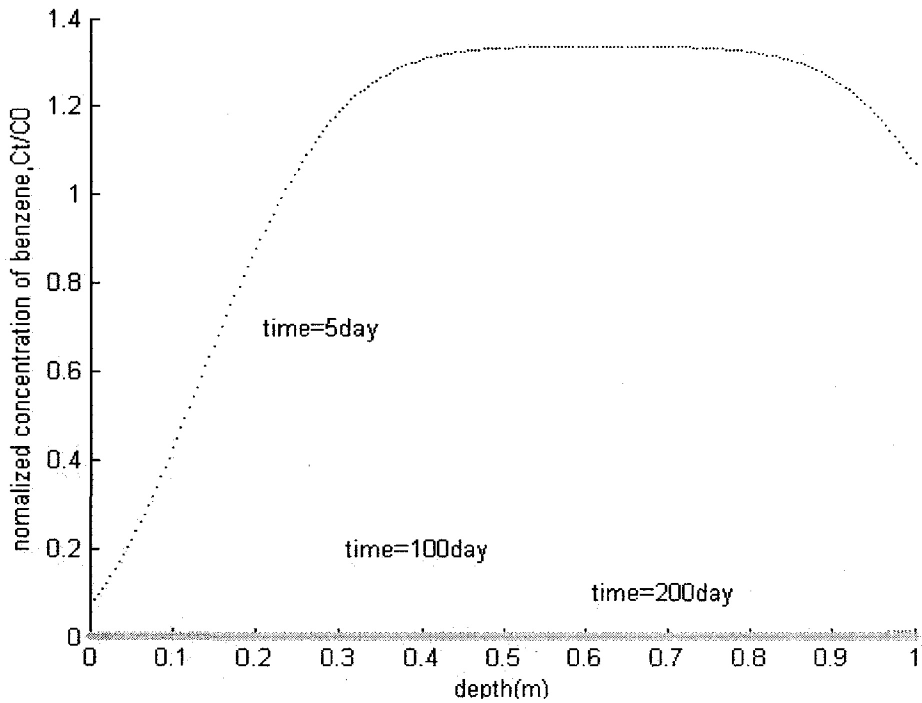

Figure 8-2 Analytical concentration results of benzene as function of depth

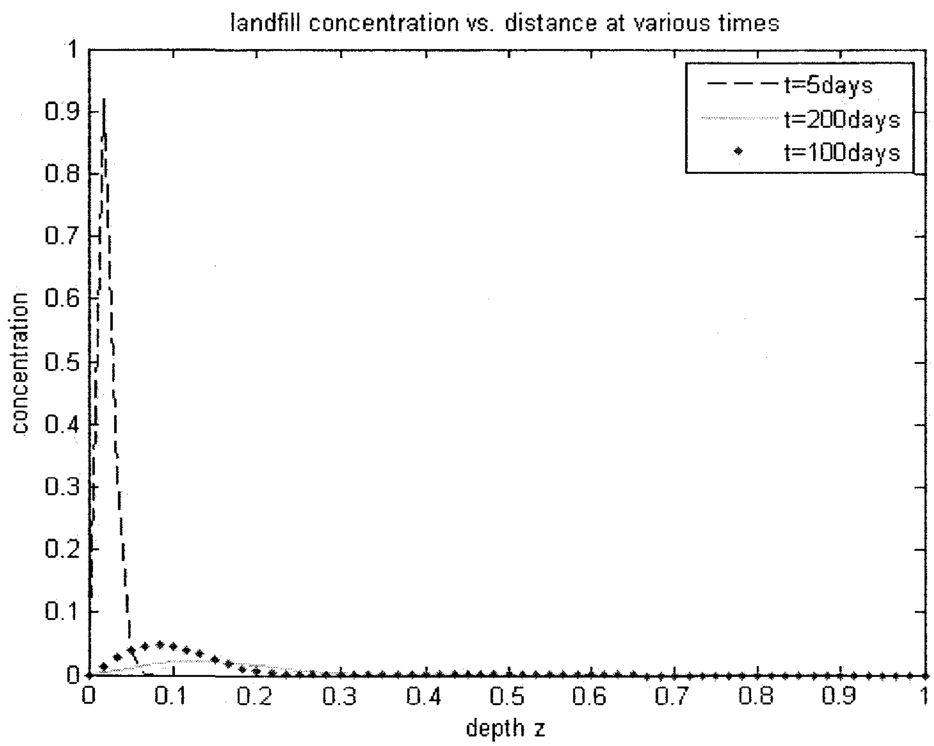

Figure 8-3 Numerical concentration results of benzene as function of depth

Numerical analysis not only get the accurate results, but it is also an effective way to deal with real variable or complex variable questions, numerical linear over the real or complex fields, the solution of differential equations are the study of algorithms for the problems of continuous mathematics. The proposed numerical model (FDM and FEM) carries the advantage of considering more accurate results, which was ignored by the analytical model. However, the complexity of calculation is considered as a major shortcoming, it requires large data storage for three-dimensional. For example, in Chapter 5, it is worth mentioning that both the FEM and FDM analyses in 2-D case study, carried out on the same grid size, have the same memory requirements as well as the same computing cost per iteration. This implies that the computing time required for an FDM analysis is approximately 20 times longer than that of the FEM analysis. The major limitation of the FDM is that finite-difference grids do not conform to boundaries that are not parallel to the coordinate axes. Stair-step approximations to angular boundaries are inconvenient to specify and can cause local variations in the contaminant plume that are not realistic, as well as the uncertainty concerning the correlation EEMMS. This FDM requires large data storage for the multi-dimensional (2-D and 3-D) real case study applications. The advantage of the FEM is that equations are solved on a finite element basis and the solution is intended to represent the real boundaries and so the results are more accurate than the FDM, which are proved in Figures 8-4 and 8-5. As one may clearly see that, when FEM is used, stability improved considerably (Figure 4-6, Figure 8-2 to Figure 8-5). Also, from the detailed case studies mentioned in Chapter 4 and 5, one may observe that that a decrease of step sizes of grid spacing (or using smaller Δt) result in an improvement of stability of the tool systems. So, the FEM is seen as an improvement to the FDM. This method couples the 3-D solutions of COMSOL very quickly. In this approach, the smaller Δx and Δt in the proper interface boundary conditions are specified. The above procedure is repeated at each decreased element grid (e.g., FEM grid Figures) until the equations are appropriately converged. The advantages of this method include its ability to represent a multistage environment, while solving for a multimedia problem and the iterative determination rather than sequential imposition. The disadvantages of the FEM include the complexity, which requires specific knowledge.

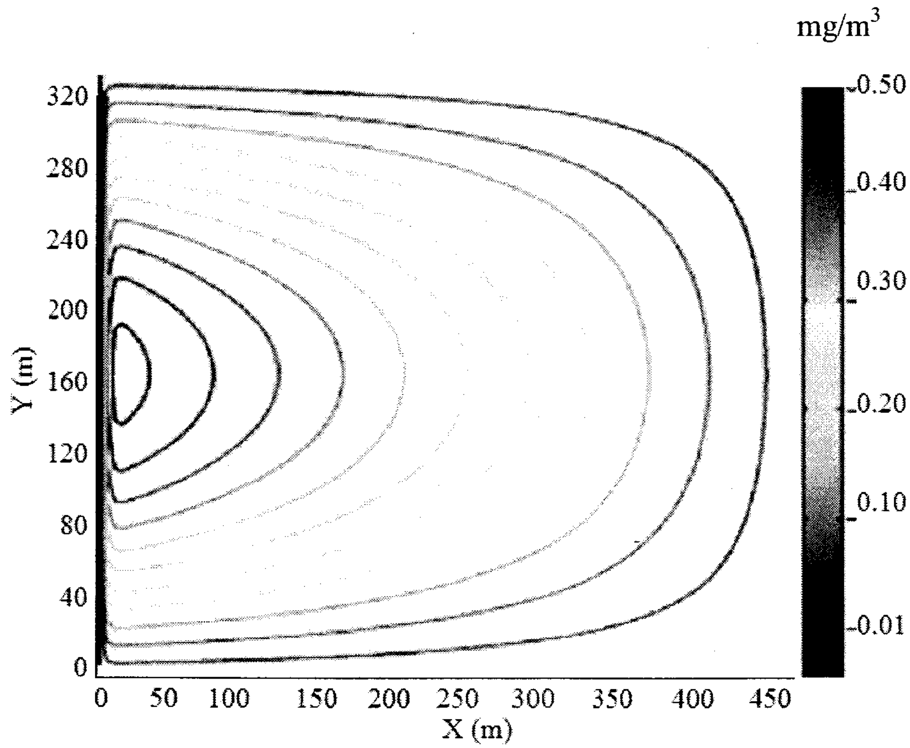

Figure 8-4 FEM concentration contour when solving the problems in point sources

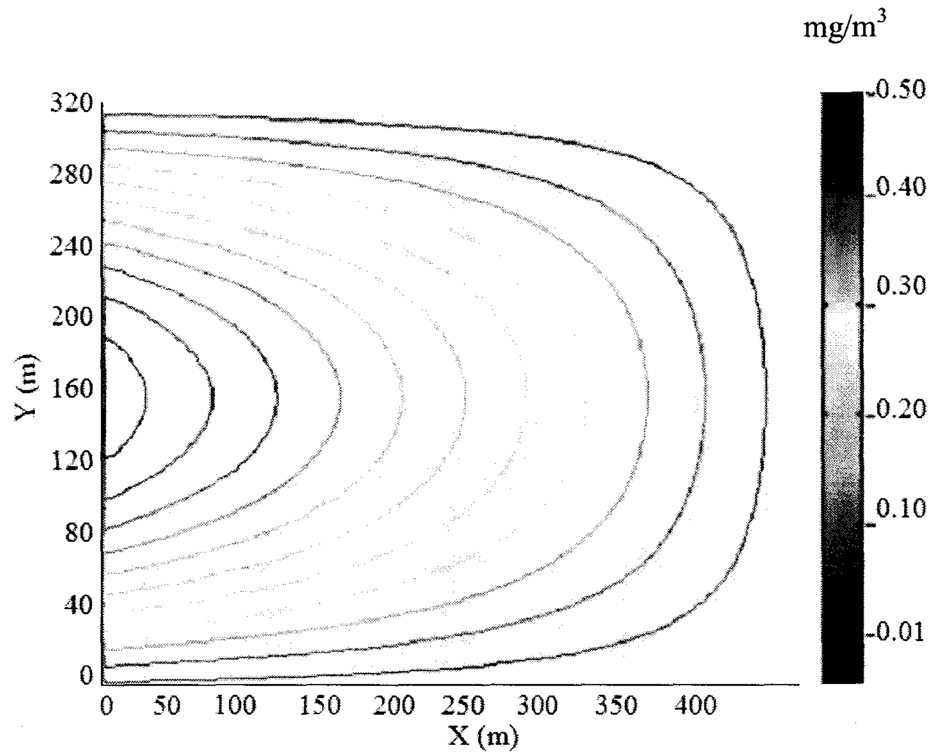

Figure 8-5 FDM concentration contour when solving the problems in point sources

Except the method or basis parameters of the governing equations sensitivity analysis, there are some other parameters' sensitivity analyses in Chapter 7; it was found that there are many factors that impact on the contaminants in moving downwards. There are other factors such as depth; materials of aquifer media and soil media, and mobility of organic and inorganic pollutants, which affect the transport of contaminants through the unsaturated zone to the saturated zone. This would eventually affect the quality of the plume to move downwards. Those factors have been researched and some literature was found on them (Anderson, 1979; Rea and Upchurch, 1980; Reinhard et al., 1984). Dispersion causes the s-shaped breakthrough curve to broaden. The characteristic depth of the media, which is known as the dispersive length, when multiplied with the unsaturated zone velocity, is used to determine the flux due to the dispersive effects. How fast pollutants can travel through the soil depends on the soil itself. Different materials of soil will affect porosity and permeability and ultimately plume movement. For example, pollutants can travel very quickly in porous and permeable materials such as sandy soils, gravel or limestone, but for other materials of soil, such as clay soils do not let pollutants move that fast. Mobility and sorptive capacity of organic and inorganic pollutants will decide whether the pollutants can freely or are difficult to move further downwards. Since the mechanics of organic and inorganic pollutants are complex functions of flow dynamics, oxidation and reduction, as well as soil adsorption reactions and microbial activity, some pollutants are retained by sorption and cause the long-term impact of their belated release to the groundwater. Since all the factors can either affect the pollutant's transfer time or affect the s-shaped curve peak, retardation also will affect both.

8.2 Discussion of Integrated Risk Assessment

Leachates beneath (or immediately downgrading of) the fill area have high concentrations of dissolved constituents. These chemical concentrations are typically ten to several hundred times higher than those measured at reference monitoring locations due to varying leachate generation rates and the age and composition of waste. An effective integrated risk assessment could provide a systematic procedure for predicting potential risks to the environment. This chapter shows if a chemical can be used as intended without causing detrimental effects to the environment. In Chapter 5, the real 2-D case studies related to the simulated tritium plume at 100 days after injection at MADE site (Feehley et al., 2000) were presented. Further in Chapter 6, comparing the dispersion results of benzene for the Trail Road landfill site did a real field-scale validation through analytical and numerical. Leachate integrated risk effects of several years later at the MADE site and at the Trail landfill site are modeled by the EEMMS, and presented in Figures 8-6 and 8-7. As shown in Figure 8-6, Tritium leachate originating from the MADE site is represented by groundwater quality immediately down the east gradient of the aquifer. If a pumping well is set to the down gradient of the aquifer, the potential impaction of the tritium leachate at different temporal period will be shown in Figure 8-8. According to the tritium leachate regulatory criteria (EPA, 2006b), after 5 years, no tritium leachates maximums exist in the aquifer in excess of reference criteria (20 pCi mL^{-1}) immediately east of the MADE site. Benzene is a good indicator of leachate impact at the Trail landfill because it occurs in the source of contamination near the Trail landfill other than in leachate. Groundwater in the shallow aquifer from beneath the Trail landfill flows mainly in a southward direction, generally following the slope of the underlying clay layer surface (refer to Figure 6-7 in Chapter 6). A pumping well was set in the southwest of the trail site, as the topography declines and the shallow aquifer pinches out to the southwest of the site and the clay becomes the surface unit. As shown in Figure 8-7, benzene leaving this area is in compliance with the appropriate regulatory criteria (Health Canada, 2007) after diluting for five years. Dilute leachate effects of benzene will be observed in the southwest portion of the Trail landfill area in the lower deep aquifer at multi-level monitor pumping well. Leachate effects were also observed to the north of the landfill site in the upper/middle and lower parts of the deep aquifer in the southern portion of Trail landfill area similarly. In conclusion, using those kinds of integrated risk assessment methods, the adverse effects on the environment caused by certain kinds of chemical substances will be easily modeled temporal and spatially. It is anticipated that the most significant leachate impact generated by the sources is located somewhere and possibly when the pollutants reach the regulatory criteria.

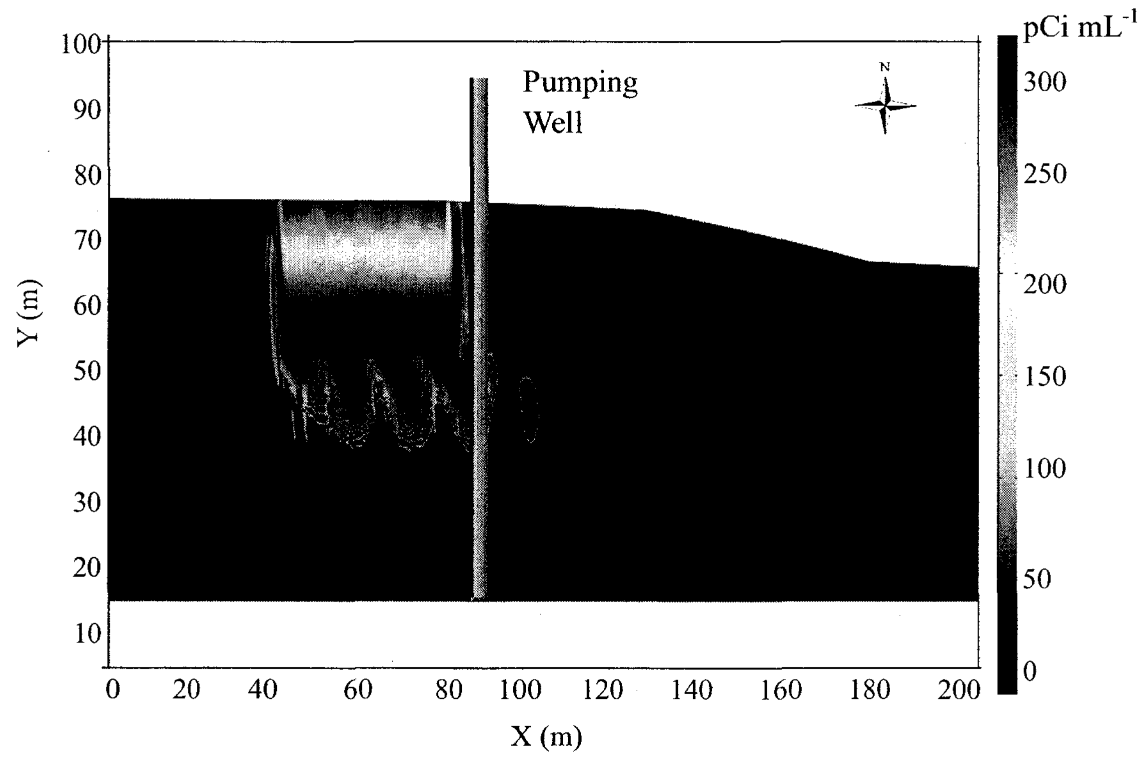

Figure 8-6 Concentration contour for standard C=20 (pCi mL^{-1}) for tritium after 1800 days

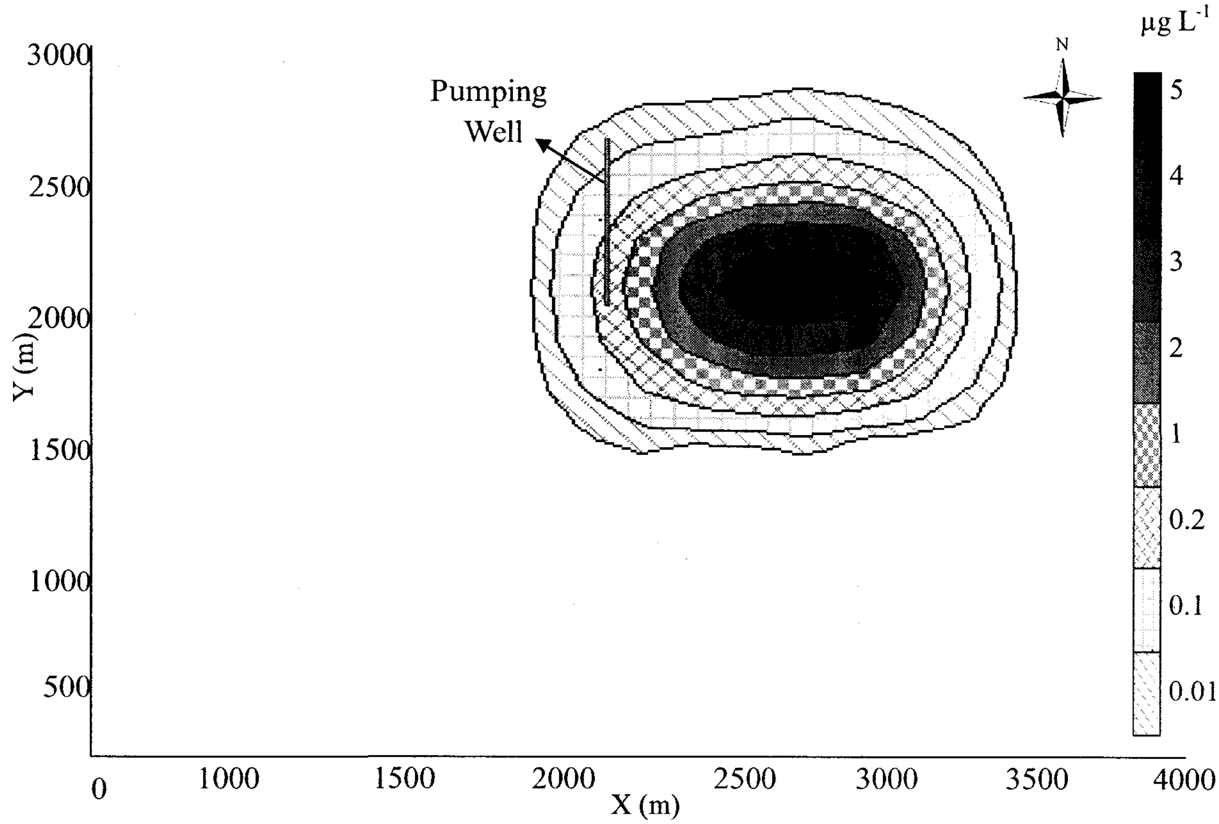

Figure 8-7 Concentration contour for standard C=1 $\mu g\ L^{-1}$ after five years

Integrated risk assessment analysis techniques, as MCM analysis, with adequate supporting data and credible assumptions, can be viable statistical tool for analyzing variability and uncertainty in risk assessments to the environment. Thus, the decision to utilize a MCM will need to be determined on a case-by-case basis, depending upon financial, time, and personnel constraints. Since there is both a financial and time cost associated with conducting a MCM, it may be counterproductive to perform such an analysis for sites where the estimated remediation costs are low. On the other hand, there will be situations where a probabilistic approach may have a great deal of value. For example, for the MADE or Trail landfill sites, if the estimated cost of remediation is high, conservative terms can be used in deterministic modeling, a MCM may be warranted. There may also be times where other evidence (e.g., biological surveys and toxicity testing) indicates that the effects to environment will probably be localized and the use of a MCM can help evaluate the likelihood of negative site-wide effects. The following Figures 8-8 and 8-9 give a detailed example of how this MCM effectively works for the EEMMS.

Figure 8-8 shows that the area of RQ larger than 6.2 covers the high and medium risk zone and small part of the low risk zone. In this study, a severity scale is constructed as high-risk level ($P(C>C_{standard})$ > 6.2). Figure 8-8 shows the severity scale map associated with the probabilities of exceeding the standard (1 μg L^{-1}). As shown in the Figure 8-8, the high-risk zone is located within an area of approximately 200000 m^2 around the Trail Road landfill site. Comparing Figure 8-8 with Figure 8-9 shows the 5% RQ distribution map in 2016 associated with the criterion issued by the Health Canada (1 μg L^{-1}). The inside shaded area indicates the RQ factor larger than 1, which indicate medium risk level (10% < $P(C>C_{standard})$ < 20%) and low risk level (($P(C>C_{standard})$ < 10%)). The medium risk zone is between 90 m to 100 m away from the source, which shows a very thin ring area with a mean concentration of around 1.2 μg L^{-1}. The low risk zone covers 10000 m^2 in area outside the medium risk zone, which has the concentration between 1 to 1.2 μg L^{-1}. The rest of the area will have a zero probability of violating the benzene criteria. This area covers approximately 180000m^2 (about 400 m in radius). As mentioned before, RQ larger than 1 generally correspond to over 5% probability of exceeding the chosen criterion. This MCM is simple and effective to visually rank the possible risk zone relating to the potential benzene risk to the groundwater and could give the decision maker a more comprehensive view of the risks involved in landfill or oil drill waste management.

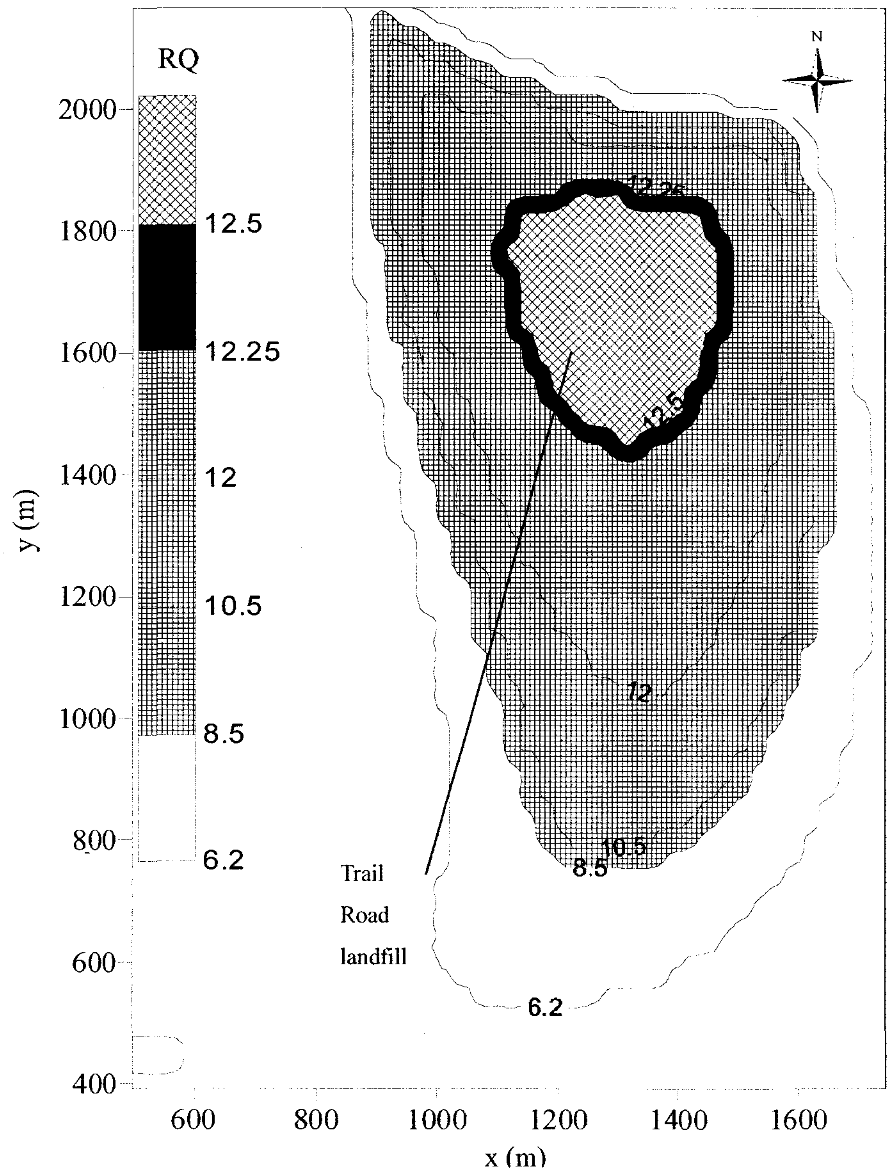

Figure 8-8 95-percentile risk quotients associated with the benzene criterion issued by the Health Canada (1 μg L^{-1}) in 2016, the shaded area is RQ $\geq$ 6.2

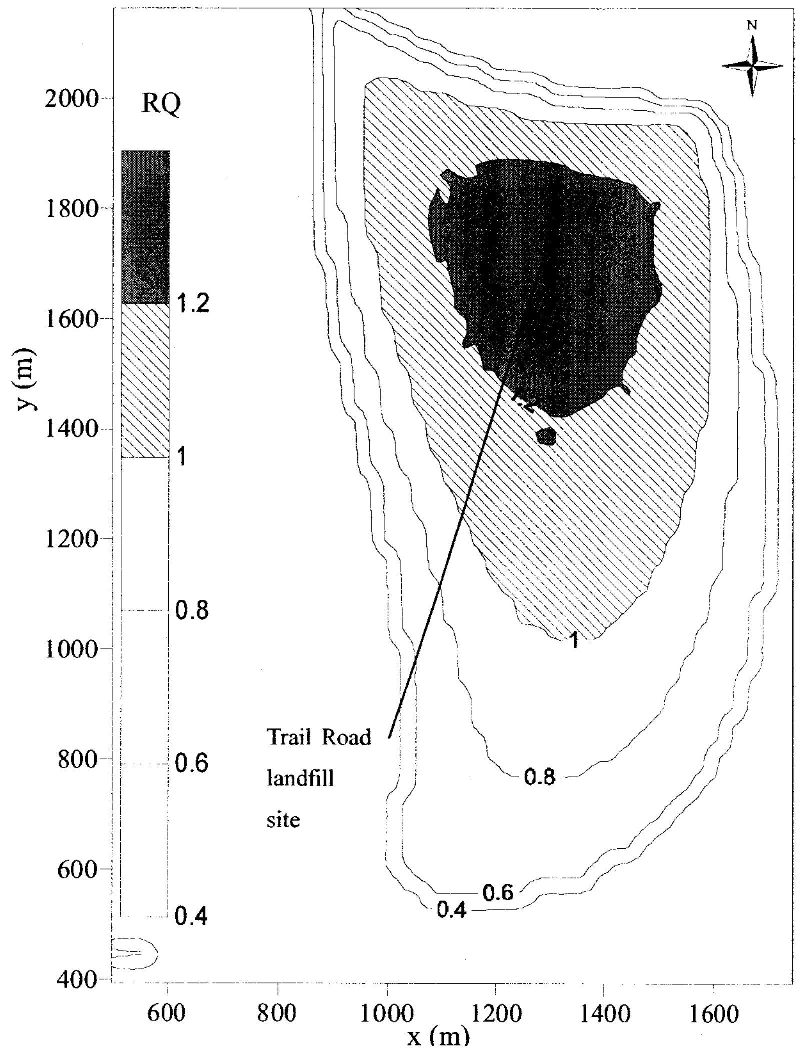

Figure 8-9 5-percentile risk quotients associated with the criterion issued by the Health Canada (1 μg L^{-1}) in 2016, the shaded area is RQ ≥ 1

8.3 Other Factors Affecting the Pollutants' Transport

Temperature is the main factor since it will affect the other parameters. When the temperature changes, other factors such as diffusion coefficient, vapor pressure and solubility will change too. For example, as discussed in Chapter 6, in Ottawa, the annual average temperature is 12.3°C. The hottest month is July during which the average temperature is 12°C. January is the coldest month and its average temperature being -15°C. Whereas in California, the average temperature can reach 24°C, the lowest temperature is 12°C and the highest temperature is around 36°C. For benzene, the vapor pressure increased from 47 mmHg to 185 mmHg as temperature declined from 10°C to 40°C. The results show that the average benzene concentration is around 932 ppb in California in winter. However the average benzene concentration is zero in winter in Ottawa atmosphere.

Chapter 9 Conclusion, Contribution and Future Work

9.1 Conclusions

1. In the present study, a new tool as an extended environmental multimedia modeling system (EEMMS) and an integrated risk assessment approach based on EEMMS and MCM (Monte Carlo Method) have been developed. It improves the previous EMMS on:

(1). Considering the unsteady flow effects of pollutant sources and leachate emissions;

(2). Integrating air modules, source module (eg. landfill), unsaturated media modules, and groundwater media modules within an EMMS framework based on mass conservation, mass flux, and transient non-uniform initial and boundary conditions;

(3). Introducing numerical solutions based on FEM and FDM. The model has been developed to address multi-dimensional multimedia environmental pollution problems;

(4). The optimized EEMMS (for example, EEMMS/FEM) is expected to provide a fast and cost effective project decision making tool for assessing, predicting and comparing the effects of various strategies in a given multimedia environment, particularly for low levels of pollutants.

2. Secondly, due to the complexity of the problems encountered, the general EEEMMS required optimization for each case studied, by testing the numerical and analytical approaches with field data and then choosing the most accurate approach. Finite element (FEM) methodology for the analysis of the EEMMS has been presented for multidimensional unsteady pollutant transport. Two other methodologies (FDM and analytical solutions) were described for comparison and their advantages and shortcomings were discussed.

3. Thirdly, based on the consideration of boundary conditions and the above four items of improvements, the methodology has been validated through five test cases in a temporal and spatial scheme using Matlab and COMSOL, with hexahedral grids.

(1). The first two test cases involved the preliminary 1-D systematic model verifications. The result obtained from the EEMMS showed good agreement with field and experimental data in the literature. The modified unsaturated zone and saturated zone transport equations were verified using numerical techniques of FEM and FDM. The FEM and FDM were more accurate than the Gauss model, and FEM was the most accurate numerical model overall. The 1-D model validations generate predictions of spatial and temporal concentration profiles of contaminants/pollutants in the different environmental media of complex environments. The accuracy of simulation assuming non-uniform conditions was compared to that of a traditional, uniform EEMMS, which the mass flux transportation changes uniformly along horizontal and vertical axes at different elevations and the flux decreased with increasing depth. This numerical result corrects the key assumption in the previous EMMS, which assumed that all the compartments in the unsaturated zone are uniformly mixed. Such an assumption is obviously not correct when the effect of variation in the spatial and temporal scale of the model is accrued.

(2). The third and fourth test cases considered 2-D complete case studies validations comparing with the dual domain mass transfer model and 2-D analytical model, involving the correct choice of the parameters peculiar of the numerical model (stabilization technique, a mesh that minimizes the error or even a faster FEM solver - i.e., COMSOL). In contrast with first two 1-D case studies, the 2-D numerical predictions agree well with experimental observations from the literatures. These test cases highlighted the high stability and accuracy of FEM, as indicated by the high time step sizes allowed. As a comparison, typically 50 to 70 time-steps per period are required with this method whereas 1000 to 3000 time-steps may be taken with FDM methods. It was found that numerical results, especially the FEM, obtained for both cases compare well with the literature data, indicating that the FEM method is more accurate for those complicated multimedia environment. This finding is an important contribution of this thesis.

(3). The fifth test case dealed with a real field-scale validation through analytical and numerical comparison with experiment of the dispersion of benzene for the Trail

Road landfill site. The results of the field site obtained from EEMMS showed good agreement with the field observations. The comparison indicates that the EEMMS can achieve good simulations in the near area, but much smaller concentrations than observations in the far areas.

4. Furthermore, impacting factors such as Peclet number (Pe) and retardation, hydraulic conductivity, bulk density and porosity are used to calibrate sensitivity analysis of the model. It was found again that FEM and FDM were more accurate than a Gauss model when the Peclet number (Pe) increased; the larger the retardation, the lower the concentration in multimedia system.

5. At last, the MCM (Monte Carlo Method) was integrated to EEMMS to reflect uncertainties and to conduct the long-term risk assessment associated with the evaluation criteria for pollutants dispersion in the multimedia environment. The benzene concentration results from the MCM for the Trail Road landfill site revealed that there was a negligible risk associated with the concentration dispersion of benzene in the Trail Road landfill site within 10 years. However, towards its depleted stage, adverse effects on the groundwater associated with benzene concentration were revealed, and the potential risk zone might cover an area of approximately 20000 m^2 with a risk quotient (RQ) larger than 1 and 5% to 25% probability of violating the chosen environmental endpoint (1 $\mu g\ L^{-1}$). Results also imply that there is a possibility that the dispersion of a large volume of pollutants from the landfill or the oil drill could have adverse impacts on a relative

large area based on a well-defined endpoint, which may be selected depending on a specific problem under investigation.

6. Finally, considering the three-dimensional EEMMS as inputs to the mass transport model and to examine the dispersion of toxic components on a regional spatial scale, integrated with MCM risk assessment approach, the integrated risk assessment results and risk discussion indicated that the improved multimedia model system could be used as a tool in a field experiment and in future treatment design works.

7. This research would contribute to the development of an effective decision tools for the assessment and management of the dispersion of a large volume of pollutants in the regional multimedia environment.

9.2 Research Contributions

In addition to the conclusions in Section 9.1, the contributions coming out of present study are summarized below:

1. A new modeling approach (EEMMS) including an air dispersion module, a source module, an unsaturated module and a saturated module have been developed on a regional spatial-temporal scale, with the mass balance in the whole multimedia in the non-uniform conditions. Specifically:

(1). The developed EEMMS corrects the key assumption in the previous EMMS, which assumed that all the compartments in the unsaturated media are uniformly mixed. Such an assumption is obviously not correct when the effect of variation in the spatial and temporal scale of the model is accrued;

(2). Its governing equations and computational scheme with much more full consideration of initial conditions were presented in the non uniform multimedia conditions;

(3). The method of FEM and FDM were first time applied to pollutant dispersion model using Matlab and COMSOL;

(4). The above model has been first time integrated with the Monte Carlo risk assessment method in the non-uniform multimedia conditions.

2. The EEMMS is only tool that generates predictions of multidimensional, spatial and temporal concentration profiles of contaminants/flux in the different environmental media of complex environments, and integrates source, air, unsaturated and saturated groundwater domains based on mass conservation, mass flux, and transient non-uniform initial and complicated environmental and site conditions.

3. Using three different approaches: a) EEMMS/FEM (numerical finite element method); b) EEMMS/FDM (numerical finite difference method); and, c) EEMMS/analytical method numerical finite element method, the developed EEMMS first performed validation through typical landfill or/and oil spill case studies of typical contaminants. The EEMMS/FEM model demonstrated the improvement of results accuracy comparing to other methods and to previous

experimental and literature data, particularly for contaminants at low concentrations.

4. EEMMS was applied for first time to model multi-dimensional contaminant dispersion in a temporal and spatial scheme in conjunction with the flow. The validation results based on real site observation data at a landfill showed that the developed EEMMS could provide a realistic, complex field assessment of the toxic components dispersion activities. Then, EEMMS is a new tool in addressing the long term environmental risks associated with dispersion of toxic components.
5. The developed EEMMS is only tool that deals in such extend with vague or imprecise site conditions. Then EEMMS embedded uncertainty quantification sensitivity analysis techniques that optimize model parameters such as retardation factor, Peclet number (Pe), hydraulic conductivity, bulk density and porosity. The perfection of this tool permitted to eliminate an oscillatory behavior when the Peclet number (Pe) decreased. Furthermore, it permitted for first time assess retardation ability in 3D in multimedia system.
6. An integrated risk assessment approach based on an EEMMS and the Monte Carlo Method (MCM) has been developed. Two methods of quantifying the risk levels, which are probabilistic risk assessment (PRA) and the risk quotient (RQ) factor, have been used to map the possible environmental risk severities in a temporal and spatial scheme.
7. Integration of EEMMS and MCM is a first tool that permits on quick and more

precise assessment of long term risks associated with the dispersion of contaminants into the regional multimedia environment. It was demonstrated that the developed approach could contribute extensively to environmental risk assessments and to effective pollution control decisions in a field experiment and in future engineering works.

9.3 Recommendations for Future Work

In spite if the results presented in the previous chapters, there are still limitations relating to the new EEMMS approach. Future studies recommended are as follows:

1. Extension of EEMMS to more complex considerations; introduction of some other complex physical processes (e.g. temperature and pressure effects) or biodegradation to the general governing equations.
2. In the present research, only a single source has been considered in the modeling; the simulation of the concentrations of pollutants from multiple sources can be established in the future.
3. The large site experiment validations in the present research were conducted for one real case study - Trail Road landfill site. Therefore, more tests and validations can be expected based on the real site sampling experiment results for other periods of time or/ and on other real sites or platforms.
4. In the present uncertainty analysis, the uncertainty parameters such as retardation

factor, Peclet number (Pe), hydraulic conductivity, bulk density and porosity have been specified in a relatively high mixing range. In the ongoing studies, these parameters can be measured through experimental investigation and can be combined with sensitive analysis to understand more about important modeling uncertainties in the long run.

References

Al_Yousfi, A.B., and Pohland, F.G., 1998. Strategies for simulating, Design, and management of solid wastes disposal sites as landfill bioreactors. *Practice periodical of hazardous, toxic and radioactive waste management,* 2(1): 13-21.

Allen, D.J., Brewerton, L.J., Coleby, L.M., Gibbs, B.R., Lewis, M.A., MacDonald, A.M., Wagstaff, S.J. and Williams, A.T., 1997. *The physical properties of major aquifers in England and Wales.* BGS Technical Report WD/97/34 (equivalent to Environment Agency.

Al-Thani, A.A., Beaven, R.P., and White, J.K., 2004. Modelling flow to leachate wells in landfills. *Waste Management,* 24(3): 271-276.

Anderson, M.P. 1979. Using Models to Simulate the Movement of Contaminants through Groundwater Flow Systems. *CRC Critical Reviews in Environmental Control,* 9: 97-156.

Arystanbekova, N.K., 2004. Application of Gaussian plume models for air pollution simulation at instantaneous emissions. *Mathematics and Computers in Simulation,* 67(4-5): 451-458.

Aulisa, E., Ibragimov, A., Valko, P., and Walton, J., 2006. *Mathematical Frame-Work For Productivity Index of The Well for Fast Forchheimer (non-Darcy) Flow in*

Porous Media. Excerpt from the Proceedings of the COMSOL Users Conference, Boston.

Bachmat, Y., and Bear, J., 1964. The general equation of hydrodynamic dispersion in homogeneous isothopic mediums. *J. Geophys. Res.*, 69(12): 2561-2567.

Ball, W.P., 1989. *Equilibrium sorption and diffusion rate studies with halogenated organic chemicals and sandy aquifer material.* Stanford, Stanford University.

Batelaan, O. and Smedt, De.F., 2004 SEEPAGE, a new MODFLOW DRAIN package. *Groundwater,* 42 (4): 576–588.

Bear, J., 1960. On the tensor form of dispersion in porous media. *J. Geophys. Res.*, 66(4): 1185-1197.

Beck, M.B., Ravetz, J.R., Mulkey, L.A., and Barnwell, T.O., 1997. On the problem of model validation for predictive exposure assessments. *Stochast. Hydrol. Hydraulics*, 11(1): 229–254.

Bennett, D.H., Kastenberg, W.E., and McKone, T.E., 1999. A multimedia, multiple pathway risk assessment of atrazine: the impact of age differentiated exposure including joint uncertainty and variability. *Reliab. Eng. Syst. Safe.,* 63: 185–198.

Bird, R.B., W.E. Stewart, and Lightfoot, E.N., 2002. *Transport phenomena.* John Wiley & Sons, New York.

Brusseau, M.L, 1994. Transport of reactive contaminants in heterogeneous porous media. *Rev. Geophys.,* 32: 285–313.

Brusseau, M.L. and Rao, P.S.C., 1989. Sorption nonideality during organic contaminant transport in porous media. *CRC Crit. Rev. Environ. Control,* 19(1): 33–99.

Brusseau, M.L. and Rao, P.S.C., 1990. Modeling Solute Transport in Structured Soils: A Review. *Geoderma,* 46(1-3): 169-192.

Brusseau, M.L., 1998. Nonideal transport of reactive solutes in heterogenous porous media: 3. Analyzing field data with mathematical models. *Journal of Hydrology,* 209(1-4): 147-165.

Brusseau, M.L., Jessup, R.E., and Rao, P.S.C., 1989. Modeling the Transport of Solutes Influenced by Multi Process Nonequilibrium. *Water Resources Research,* 25(9): 1971-1988.

Carnahan, C.L., and Remer, J.S., 1984, Nonequilibrium and equilibrium sorption with a linear sorption isotherm during mass transport through an infinite porous medium: Some analytical solutions, *J. Hydrol.*, 73: 227-258.

Carroll, K.M., Harkness, M.R., Bracco, A.A. and Balcarcel, R.R., 1994. Application of a permeant/polymer diffusional model to the desorption of polychlorinated biphenyls from Hudson river sediments. *Environ. Sci. Technol.,* 28: 253–258.

Chen, Y.C., and Ma, H.W., 2006. Model comparison for risk assessment: A case study of contaminated groundwater. *Chemosphere*, 63: 751–761.

Citra, M.J., 2004. Incorporating Monte Carlo analysis into multimedia environmental fate models. Environ. *Toxicol. Chem.*, 23: 1629–1633.

Clark, K.E., 1990. Model of Organic Chemical Uptake and Clearance by Fish from Food and Water. *Environmental Science and Technology,* 24: 1203-1213.

Coats, K.H., and Smith, B.D., 1964. Dead-end pore volume and dispersion in porous media. *J. Soc. Petrol. Eng.*, 4: 73-84.

Cohen, Y., and Cooter, E., 2002. Multimedia environmental distribution of Toxics (Mend-Tox) I: hybrid compartment-spatial modelling framework. *Hazardous, Toxic, and Radioactive Waste Management*, 6(2): 70-86.

Cohen, Y., and Cooter, E.J., 2002. Multimedia environmental distribution of toxics (Mend-Tox). II: Software implementation and case studies. *Hazardous, Toxic, and Radioactive Waste Management*, 87-101.

Cohen, Y., and Ryan, P.A., 1985. Multimedia modeling of environmental transport: trichloroethylene test case. Environ. Sci. Technol., 9: 412-417.

Cooke, A.J. and Kerry, R., 2008. 2D modelling of clogging in landfill leachate collection systems. *Can. Geotech.,* 45: 1393–1409.

Coulibaly, L., Mohamed, E.L., and Robert, H., 2004. A GIS-based multimedia watershed model: development and application. *Chemosphere,* 55: 1067–1080

Cowan, C.E., Mackay, D., Feijtel, T.C.J., Van De Meent, D., and Di Guardo, A., 1995. *The Multi-Media Fate Model: A Vital Tool for Predicting the Fate of Chemicals*. Society of Environmental Toxicology and Chemistry, Pensacola, USA.

CSWQB, 2003. California State Water Quality Board.

Delshad, M., Pope, G.A., and Sepehrnoori, K., 1996. A compositional simulator for modeling surfactant enhanced aquifer remediation. *J. Contamin. Hydrol.*, 23(1-2): 303-327.

Detwiler, R.L., Glass, R.J., and Bourcier, W.L., 2003. Experimental observations of fracture dissolution: The role of Peclet number on evolving aperture variability. *Geophys. Res. Lett.*, 30(12): 1648-1652.

Devillers, J., Bintein, S., and Karcher, W., 1995. ChemFrance: A regional level III fugacity model applied to France. *Chemosphere*, 30(1): 457–476.

Di Guardo, A., Williams, R.J., Matthiessen, P., Brooke, N., and Calamari, D., 1994b. Simulation of pesticide runoff at Rosemaund Farm (UK) using the soil fug model. *Environ. Sci. Pollut. Res.*, 1(1): 151-160.

Di Toro, D.M., and Horzempa, L.M., 1982. Reversible and Resistant Components of PCB Adsorption-Desorption: Isotherms. *Environ. Sci. Technol.,* 16: 594-602.

Diersch, H. J., and Kolditz, O., 2002. Variable-density flow and transport in porous media: Approaches and challenges. *Adv. Water Res.,* 25: 899–944.

Dillon, M.M., 2005. Trail Road and Nepean landfill sites monitoring and operating report: final report. Dillon Consulting Limited. *Transportation, Utilities and Public Works Department, Utilities Services Branch, Sold Waste Services Division.* City of Ottawa.

Dillon, M.M., and Gartner, L., 1995. *TRNL: Trail Road and Nepean landfill Sites Final Report for the 1995 Monitoring and Operation Program.* Environment and Transportation Department, Solid Waste Division.

Dillon, M.M., and Gartner, L., 2002. *TRNL: Trail Road and Nepean landfill Sites Final Report for the 2002 Monitoring and Operation Program.* Environment and Transportation Department Solid Waste Division.

Dmitry, V., and Victor, C., 1999. Analytical modeling of aquifer pollution caused by solid waste depositories. *Groundwater*, 37(3): 352-357.

Doherty, S.T., 2005. How far in advance are activities planned? Measurement challenges and analysis. *Journal of the Transportation Research Board,* 1926: 41-49.

Domenico, P.A., 1987. An analytical model for multidimensional transport of a decaying contaminant species. *J. of Hydrol.*, 91: 49-58.

Droppo, J.G., Buck, J.W., Strenge, D.L., and Hoopes, B.L., 1993. Risk computation for environmental restoration activities. *Journal of Hazardous Materials,* 35: 341-352.

Droppo, J.G., Strenge, D.L., Buck, J.W., Hoopes, B.L., Brockhaus, R.D., Walter, M.B., and Whelan, G., 1989. *Multimedia environmental pollutant assessment System (MEPAS) Application Guidance Volume 1-User's Guide*. Pacific Northwest Laboratory, Richland, WA.

Eisenbud, M., 1987. *Environmental Radioactivity from Natural, Industrial, and Military* Sources. Academic, 3rd ed. New York.

Fadel EI, M., Findikakis, N., and Leckie, J.O., 1996. Biochemical and physical processes in landfills. *Solid Waste Technology and Management*, 23(3): 131-143.

Faye, R.E., and Valenzuela, C., 2007. *Analyses of Groundwater Flow, Contaminant Fate* *and Transport, and Distribution of Drinking Water at Tarawa Terrace and Vicinity, U.S. Marine Corps Base Camp Lejeune, North Carolina: Historical Reconstruction and Present-Day Conditions—Chapter C: Simulation of Groundwater Flow.* Atlanta, GA: Agency for Toxic Substances and Disease Registry.

Feehley, C.E., Zheng, C., and Molz, F., 2002. A dual-domain mass transfer approach for modeling solute transport in heterogeneous aquifers: application to the MADE site. *Water Resour. Res.*, 36(9): 2501-2516.

Fenner, K., Scheringer, M., and Hungerbuhler, K., 2004. Prediction of overall persistence and long-range transport potential with multimedia fate models: robustness and sensitivity of results. *Environ. Pollut.,* 128:189–204.

Ferguson, W.J., and kaddouri, A., 2004. A mass conservative non-isothermal subsurface three-phase flow model: formulation and application. *Water, Air, and Soil Pollution,* 153: 269–291.

Ferguson, W.J., and Kaddouri, A., 2004. A Mass Conservative Non-Isothermal Subsurface Three-Phase Flow Model: Formulation and Application. *Water, Air, and Soil Pollution,* 153(1-4): 269-291.

Fredrick, B.S., Linard, J.I., and Carpenter, J.L., 2006. *Environmental Setting of Maple Creek Watershed, Nebraska.* US Geological Survey. Scientific Investigations Report 2006-5037.

Freeman, D.H., and Cheung, L.S., 1981. *A gel partition model for organic desorption from a pond sediment.* Science, 214: 790–792.

Garg, A., Achari, G., and Joshi, R.C., 2006. A model to estimate the methane generation rate constant in sanitary landfills using fuzzy synthetic evaluation. *Waste manage. Res.*, 24(4): 263-375.

Garg, A., Achari, G., and Joshi, R.C., 2007. Application of fuzzy logic to estimate flow of methane for energy generation at a sanitary landfill. *J. energy eng.,* 133(4):212-223.

Gobas F., Pasterna J., Lien, K., and Duncan, R., 1998. Development and field validation of multimedia exposure assessment model for waste load allocation in aquatic ecosystems: Application to 2, 3, 7, 8-tetrachlorodibenzo-*p*-dioxin and 2, 3, 7, 8-tetrachlorobenzofuran in the Fraser River watershed. *Environ Sci Technol.* 32:2442–2449.

Halder, A., Dhall, A., and Datta, A.K., 2006. *Modeling of Frying and Related Processes Involving Strong Evaporation: A Porous Media Approach.* Excerpt from the Proceedings of the COMSOL Users Conference, Boston.

Hanna, S., Briggs, G.A., and Hosker, R.P., 1982. *Handbook on Atmospheric Diffusion,* DOE/TIC-11223, U.S. Department of Energy, pp. 102.

Harbaugh, A.W., Banta, E.R., Hill, M.C., and McDonald, M.G., 2004. *MODFLOW-2004, the u.s. geological survey modular ground-water model-user guide to modularization concepts and the ground-water flow process, Open file report 00-92.* U.S. Geological Survey.

Harleman, D.R.E., and Rumer, R.R., 1962. *The Dynamics of Salt-Water Intrusion in Porous Media, report 55.* Hydrodynamic Lab., MIT, Cambridge, MA.

Harmon, T.C., 1992. *Determining and modeling diffusion-limited desorption rates in heterogeneous aquifer solids.* Standford, CA, Standford University.

Harper, B.M., Stiver, W.H., and Zytner, R.G., 2003. Nonequilibrium nonaqueous phase liquid mass transfer model for soil vapor extraction systems. *J. of Environ. Eng.*, 129(8): 745-753.

Health Canada, 2007. www.hc-sc.gc.ca,

Healy, R.W., and Ronan, A.D., 1996. *Documentation of computer program VS2DH for simulation of energy transport in variably saturated porous media -- modification of the U.S. Geological Survey's computer program VS2DT: report 96-4230.* Geological Survey Water-Resources Investigations Agency, U.S.

Helmig, R., 1997. Multiphase Flow and Transport Processes in the subsurface - A contribution to the Modeling of Hydrosystems. Springer (Environmental Engineering), Berlin, Heidelberg .

Howard, P.H., 1990. *Handbook of Environmental Fate and Exposure Data for Organic Chemicals.* Vol. II. Lewis Publishers, Chelsea, MI.

Howard, P.H., Boethling, R.S., Jarvis, W.F., Meylan, W.M., and Michalenko, E.M., 1991. *Handbook of Environmental Degradation Rates.* Printup, H.T., Lewis Publishers, Chelsea, MI.

HSDB. 1995. *Hazardous Substances Data Bank.* National Library of Medicine, Bethesda, MD (TOMESÒ CD-ROM Version). Micromedex, Inc., Denver, Colorado (Edition expires 1/31/95).

Hsieh, C.R., and Ouimetter, J.R., 1994. Comparative study of multimedia modelling for dynamic partitioning of fossil fuels-related pollutants. *Hazardous Materials*, 37: 489-505.

Islam, J., and Singhal, N., 2002. A one-dimensional reactive multi-component landfill leachate transport model. *Environmental Modelling & Software,* 17 (6): 531–543.

Jahn, M.K., Haderlein, S.B., and Meckenstock, R.U., 2005. Anaerobic degradation of benzene, toluene, ethylbenzene, and o-xylene in sediment-free iron-reducing enrichment cultures. *Appl. Environ. Microbiol.,* 71: 3355–3358.

Jang, W., and Aral, M.M., 2005. *Three-Dimensional Multiphase Flow and Multi-Species Transport Model, TechFlowMP. Atlanta, GA: Multimedia Environmental Simulations Laboratory (MESL), Report No. MESL-02-05.* School of Civil and Environmental Engineering, Georgia Institute of Technology, U.S.A.

Jang, W., and Mustafa, M.A., 2007. Density-driven transport of volatile organic compounds and its impact on contaminated groundwater plume evolution. *Transp Porous Med.,* 67: 353–374.

Johnson, S.J., Woolhouse, K.J., Prommer, H., Barry, D.A., and Christofi, N., 2003. Contribution of anaerobic microbial activity to natural attenuation of benzene in groundwater. *Eng. Geol.*, 70: 343–349.

Johnston, J.M., Novak, J.H., and Kraemer, S. R., 2000. Multimedia integrated modeling for environmental protection: Introduction to a collaborative framework. *Environ. Monit. Assess.,* 63(1): 253–263.

Jury, W.A., Russo, D., Strelie, G., and Abd, H.E., 1990. Evaluation of volatilization by organic chemicals residing below the soil surface. *Water Resource Research*, 26(1): 13-20.

Kamboj, S., Gnanapragasam, E., LePoire, D., Biwer, B.M., Cheng, J., Arnish, J., Yu, C., Chen, S., Mo, Y.T., Abu-Eid, R., and Thaggard, M., 2002, Probabilistic Approach to identify sensitive parameter distributions in multimedia pathway analysis. *Hazardous, Toxic, and Radioactive Waste Management*, 6(1): 158-174.

Karickoff, S.W. and Brown, D.S., 1978. Paraquat sorption as a function of particle size in natural sediments. *Journal of Environmental Quality,* 7(2): 246-252.

Kindlein, J., Dinkler, D., and Ahrens, H., 2006. Numerical modeling of multiphase flow and transport processes in landfills. *Waste Manage Res*: 24(4): 376-387.

Kling, T., and Korkealaakso, J., 2004. Application of nonisothermal multiphase modeling to in situ soil remediation in Soderkulla. *Vadose Zone*, 3: 901-908.

Labieniec, P.A., Dzombak, D.A., and Siegrist, R.L., 1996a. Soil Risk: Risk Assessment Model for Organic Contaminants in Soil. *Journal of Environment Engineering,* 122(7): 388-398

Labieniec, P.A., Dzombak, D.A., and Siegrist, R.L., 1996b. Risk variability due to uniform soil remediation goals. *Journal of Environmental Engineering,* 122(7): 612-621.

Lansana, C., Mohamed, E.L., and Robert H., 2004. A GIS-based multimedia watershed model: development and application. *Chemosphere,* 55: 1067–1080

Lee, H.M., 1996. Applying fuzzy set theory to evaluate the rate of aggregative risk in software development. *Fuzzy Sets and Systems,* 26: 1182-1191.

Lehmann, F., and Ackerer, P.H., 1998. Comparison of iterative methods for improved solutions of the fluid flow equation in partially saturated porous media. *Transp. Porous Media,* 31: 275–292.

Lin, J.S. and Hildemann, L.M., 1995. A non-steady-state analytical model to predict gaseous emissions of volatile organic compounds from landfills. *Hazardous Materials*, 40: 271-295.

Liu Zhiquan, 2007. Sensitivity of key factors and uncertainties in health risk assessment of benzene pollutant, *J. Environ. Sci.*, 19: 1272–1280.

Liu, C., Bennett, D.H., Kastenberg, W.E., McKone, T.E., and Browne, D., 1999. A multimedia, multiple pathway exposure assessment of atrazine: fate, transport and uncertainty analysis. *Reliab. Eng. Syst. Safe.,* 63:169–184.

Lowrance, W.W., 1976. Of Acceptable Risk, William Kaufmann, Inc., Los Altos, CA.

Luo,Yuzhou, and Yang, Xiusheng, 2007. A multimedia environmental model of chemical distribution: Fate, transport, and uncertainty analysis. *Chemosphere,* 66:1396–1407.

Mackay, D., 1991. *Multimedia environmental models: The fugacity approach*. Lewis Publishers, Chelsea, Michigan.

Mackay, D., and Paterson, S., 1982. Fugacity Revisited. *Environ. Sci. Technol.*, 16:

654-660.

Mackay, D., and Paterson, S., 1991. Evaluating the multimedia fate of organic chemicals: A level III fugacity model. *Environ Sci Technol.* 25: 427–436.

Mackay, D., Di Guardo, A., Paterson, S., and Tam, D.D., 2003. *ChemCAN: Level III fugacity model of regional fate of chemicals version 6.00.* Canadian Environmental Modelling Centre, Trent University, Peterborough, Ont., Canada.

MacLeod, M., Fraser, A.J., and Mackay, D., 2002. Evaluating and expressing the propagation of uncertainty in chemical fate and bioaccumulation models. *Environ. Toxicol. Chem.,* 21: 700–709.

Maslia, M.L., Sautner, J.B., Faye, R.E., Suárez-Soto, R.J., Aral, M.M., Grayman, W.M., Jang, W., Wang, J., Bove, F.J., Ruckart, P.Z., Valenzuela, C., Green, J.W.J., and Krueger, A.L., 2007a. *Analyses of Groundwater Flow, Contaminant Fate and Transport, and Distribution of Drinking Water at Tarawa Terrace and Vicinity, U.S. Marine Corps Base Camp Lejeune, North Carolina: Historical Reconstruction and Present-Day Conditions—Chapter K: Supplemental Information.* Atlanta, GA: Agency for Toxic Substances and Disease Registry.

Masters, G.M., 1998. *Introduction to Environmental Engineering and Science*. 2nd ed. Prentice Hall.

McCoy, B.J., and Rolston, D.E., 1992. Convective transport of gases in moist porous media: Effect of absorption, adsorption, and diffusion in soil aggregates. *Environ. Sci. Technol.*, 26: 2468-2476.

McDonald, J.P., and Gelston, G.M., 1998. Description of the multimedia environmental pollutant assessment system (MEPAS, Version 3.2), with application to a hypothetical soil contamination scenario. *Soil Contaminant*, 7(3): 283-300.

McKone, T.E., and Enoch, K.G., 2002. *CalTOX, A multimedia toal exposure model spreadsheet user's guide Version 4.0.* Ernest Orlando Lawrence Berkeley National Laboratory.

McMahon, T.A., and Denison, P.J., 1979. Emperical Atmospheric Deposition Parameters - A survey. *Atmos. Environ.,* 13(5): 571–585.

Mendenhall, W., and Sincich, T., 1994. *Statistics for engineering and the sciences. Prentice Hall,* Inc. Upper Saddle River, NJ 07458.

Mendoza, C.A., and Frind, E.O., 1990. Advective-dispersive transport of dense organic vapors in the unsaturated zone. 1. Model development. *Water Resources and Research,* 26: 370-379.

Mendoza, C.A., and Mcalary, T.A., 1990. Modeling of groundwater contamination caused by organic-solvent vapors. *Ground Water,* 28: 199–206.

Michael, M., Volker, B., and Andreas, B., 2004. Probabilistic Uncertainty Analysis Of The European Union System For The Evaluation Of Substances Multimedia Regional Distribution Model. *Environmental Toxicology and Chemistry,* 23(10): 2494–2502.

Millington, R.J., and Quirk, J.P., 1961. Permeability of porous solids. *Transactions of the Faraday Society*, 57(7): 1200-1207.

Morris, L.M., and Mustafa, M.A., 2004. Analytical Contaminant Transport Analysis System (ACTS) —Multimedia Environmental Fate and Transport. *Hazardous, Toxic, and Radioactive Waste Management*, 8(3): 181-198.

Mulligan, C.N., and Yong, R.N., 2004. Natural attenuation of contaminated soil. *Environmental International,* 30: 587-601.

Nastev, M., Savard, M., Lapcevic, P., Lefebvre, R., and Martel, R., 2004. Hydraulic properties and scale effects investigation in regional rock aquifers, south-western Quebec, Canada. *Hydrogeology Journal,* 12(3): 257-269

NRC, 2007. Nuclear Regulatory Commission.

OEHHA, 1996a. *OEHHA, Evidence on Developmental and Reproductive Toxicity of Cadmium, Office of Environmental Health Hazard Assessment, Sacramento, California.* http://www.oehha.ca.gov/prop65/pdf/CD-HID.pdf.

PADER, 2006. *Radiological Investigation Results for Pennsylvania Landfill Leachate Fall 2005 Tritium Update,* April 7, 2006.

Parker, J.C., 1989. Multiphase flow and transport in porous media. *Reviews of Geophysics*, 27: 311-328.

Pohland, F.G., and Al-Yousfi, A.B. (1994). Design and Operation of landfills for optium stabiliztion and biogas production. *Water science and technology journal,* 30(12): 117-124.

Rathfelder, K., and Abriola, L.M., 1994. Mass conservative numerical-solutions of the head-based Richards equation. *Water Resour. Res.,* 30: 2579–2586.

Rea, R.A. and Upchurch, S.B., 1980. Influence of Rego-lith Properties on Migration of Septic Tank Effluent. *Ground Water,* 18: 118–125.

Reinhard, M., Goodman, N.L., and Barker, J.F., 1984. Occurrence and distribution of organic chemicals in two landfill leachate plumes. *Environment Science Technology,* 18: 953-961.

Rickabaugh, J.F., 1990. *Evaluation of Trace VOC Emissions from Sanitary Landfills. Ph.D. dissertation.* Department of Civil and Environmental Engineering of the College of Engineering, University of Cincinnati.

Riddle, A.M., Beling, E.M., and Murray-Smidth, R.J., 2001. Modeling the uncertainties in predicting produced water concentrations in the North Sea. *Environmetal Modelling & Software,* 16: 659-668.

Robinson, H.D. and Gronow, J.R., 1996. Tritium Levels in Leachates and Condensates from Domestic Wastes in Landfill Sites. *Journal of the Chartered Institution of Water and Environmental Management,* 10 (6): 391-398.

Rong, R.Zh., 2006. *Development of a Fuzzy-Set Enhanced Environmental Multimedia Modelling System.* M.A.Sc., Civil Engineering. Concordia University.

Rossman, L.A., 2000. *EPANET 2 Users Manual, report No.: EPA/600-R-00/057.* Cincinnati: U.S. Environmental Protection Agency, National Risk Management Research Laboratory.

Saltelli, A., Ratto, M., and Tarantola, S., 2001. *Model-free importance indicators for dependent input.* In: Prado, P., Bolado R. (Eds.), Proceedings of SAMO 2001, Third International Symposium on Sensitivity Analysis of Model Output, Madrid, 3-7.

Sautner, J.B., Valenzuela, C., Maslia, M.L., and Grayman, W.M., 2007. *Analyses of Groundwater Flow, Contaminant Fate and Transport, and Distribution of Drinking Water at Tarawa Terrace and Vicinity, U.S. Marine Corps Base Camp Lejeune, North Carolina: Historical Reconstruction and Present-Day Conditions—Chapter J: Field Tests, Data Analyses, and Simulation of the Distribution of Drinking Water.* Atlanta, GA: Agency for Toxic Substances and Disease Registry.

Scheringer, M., Stroebe, M., and Held, H., 2002. *Chemrange 2.1- a multimedia transport model for calculating persistence and spatial range of organic chemicals.* Swiss Federal Institute of Technology Zurich.

Schnoor, J.L., 1996. *Environmental Modeling, John Wiley and Sons*, New York, 682.

Schroeder, P.R., Dozier, T.S., Zappi, P. A., McEnroe, B. M., Sjostrom, J. W., and Peyton, R.L., 1994b. *The Hydrologic Evaluation Of Landfill Performance (HELP) Model: Engineering Documentation for Version 3.* EPA/600/R-94/168b, U.S. Environmental Protection Agency Risk Reduction Engineering Laboratory, Cincinnati, OH.

Schroeder, P.R., Dozier, T.S., Zappi, P.A., McEnroe, B.M., Sjostrom, J.W., and Peyton, R.L., 1994a. *The Hydrologic Evaluation Of Landfill Performance (HELP) Model:*

User's Guide for Version 3. EPA/600/R-94/168a, U.S. Environmental Protection Agency Risk Reduction Engineering Laboratory, Cincinnati, OH.

Schuhmacher, M., Meneses, M., Xifro, A., and Domingo, J.L., 2001. The use of Monte-Carlo simulation techniques for risk assessment: study of a municipal waste incinerator. *Chemosphere*, 43: 787-799.

Solhotra, A.M., Mineart, P., Sharp-hansen, S., Allison, T., John, R., and Mills, W.B., 1995. *Multimedia exposure assessment model (MULTIMED 2.0) for evaluating the land disposal of waste-model theory*. EPA, Athens, Environmental Research Lab, U.S.

Spectrum Laboratories online datasheet: http://www.speclab.com/compound/c108883.htm

Stephenw, W., and Karsten, P., 2003. The Use of Fick's Law for Modeling Trace Gas Diffusion in Porous Media. *Transport in Porous Media*, 51: 327–341.

Sudicky, E.A., 1989. The Laplace transform Galerkin technique: A time-continuous finite element theory and application to mass transport in groundwater. *Water Resour. Res.,* 25(8): 1833-1846.

Sun, N., Wood, N.B., Hughes, A.D., Thom, S.A.M. and Xu, X.Y., 2006. Fluid-wall modeling of mass Transfer in an Axisymmetric Stenosis: Effects of Shear-Dependent Transport Properties. *Annals of Biomedical Engineering,* 34(7): 1119–1128.

Thatcher, M., Robson, M., and Henriquez, L.R., 1999. *A CIN revised CHARM III report. A user guide for the evaluation of chemicals used and discharged offshore, version 1.0.*

Netherlands Ministry of Transportation, The Netherlands.

Thatcher, M., Robson, M., Henriquez, L.R., and Karman, C.L., 2001. *An user guide for the evaluation of chemicals used and discharged offshore: version 1.2. CIN revised CHARM III Report.* Charm Implementation Network (CIN), Eurpean Oilfield Speciality Chemicals Association (EOSCA).

The Weather Network: http://www.theweathernetwork.com/weather/cities/can/Pages/CAON0512.htm

Thibodeaux, L.J., 1996. *Environmental Chemodynamics – Movement of Chemicals in Air, Water, and Soil.* John Wiley & Sons Inc., New York, USA.

Thomson, N.R., Sykes, J.F., and Van Vliet, D., 1997. A numerical investigation into factors affecting gas and aqueous phase plumes in the subsurface. *J. Contamin. Hydrol.,* 28: 39–70.

Tompson, A.F. B., and Gelhar, L.W., 1990. Numerical simulation of solute transport in three-dimensional, randomly heterogeneous porous media. *Water Resour. Res.*, 26(10): 2541-2562.

Tsuang, B.J., and Chao, J.P., 1997. Development of a circuit model to describe the advection–diffusion equation for air pollution. *Atmospheric Environment,* 31: 639–657.

Urquiza, J.M., N'Dri, D., Garon, A., and Delfour, M.C., 2008. Coupling Stokes and Darcy equations. *Appl. Numer. Math.,*58: 525-538.

USEPA (U.S. Environmental Protection Agency), 1988. *Methodology for estimating* *multimedia exposures to soil contamination (MMSOIL).* Office of Health and Environmental Assessment, Exposure Assessment Group, Washington, D.C.

USEPA (U.S. Environmental Protection Agency), 1992. Definitions. Heterogeneous wastes characterization: methods and recommendations. USEPA, Washington, DC. EPA- -600-R-92-033.

USEPA (U.S. Environmental Protection Agency), 1994a. *Proposed Rule: Addition of Certain Chemicals; Toxic Chemical Release Reporting; Community Right to Know.* USEPA, Washington, DC. EPA- 59 FR 1788.

USEPA (U.S. Environmental Protection Agency), 1996. *Three multimedia models used at hazardous and radioactive waste sites.* Environmental Protection Agency, Washington, D.C., U.S.

USEPA (U.S. Environmental Protection Agency), 1996a. *Summary report for the workshop on Monte Carlo Analysis risk assessment forum.* USEPA, Washington, DC. EPA-630-R-96-010.

USEPA (U.S. Environmental Protection Agency), 1999. *US-EPA Documentation for the FRAMES-HWIR Technology Software System.* vol 1: System Overview, Pacific Northwest National Laboratory.

USEPA (U.S. Environmental Protection Agency), 2002. *US-EPA Total Risk Integrated Methodology. TRIM.FaTE Technical Support Document.* Vol I: Description of Module. USEPA, Washington, DC. EPA- 453/R-02-011a.

USEPA (U.S. Environmental Protection Agency), 2003. *A framework for finite-source multimedia, multipathway and multireceptor risk assessment: 3MRA.* U.S. Environmental Protection Agency, Office of Solid Waste

USEPA (U.S. Environmental Protection Agency), 2006a. *Ecological risk assessments.* http://www.epa.gov/pesticides/ecosystem/ecorisk.htm,1-2.Environmental Protection Agency.

Vogel, J.E., 1970. ERF and ERFC: *Mathematical Routines for Computing the Error Function and Complementary Error Function*, SC-M-70-275.

Wang, J, and Aral, M.M., 2007. *Effect of Groundwater Pumping Schedule Variation on Arrival of Tetrachloroethylene (PCE) at Water-Supply Wells and the Water Treatment Plant, Report No.: MESL-01-07.* Atlanta, GA: Multimedia Environmental Simulation Laboratory (MESL), School of Civil and Environmental Engineering, Georgia Institute of Technology.

Wang, X. and Pepper, D., 2007. Application of an hp-adaptive FEM for solving thermal flow problems. *AIAA Journal of Thermophysics and Heat Transfer,* 21(1): 190-198.

Weber, W.J. and DiGiano, F.A., 1996. *Process dynamics in environmental systems.* New York, John Wiley & Sons Inc.

Weber, W.J. and Huang, W., 1996. A Distributed Reactivity Model for Sorption by Soils and Sediments. 4. Intraparticle Heterogeneity and Phase-Distribution Relationships under Nonequilibrium Conditions. *Environmental Science and Technology,* 30(3): 881-888.

Weber, W.J., and McGinley, P.M., 1991. Sorption phenomena in subsurface systems: concepts, models and effects on contaminant fate and transport. *Water Research,* 25(5): 499-528.

Werth, C.J. and Hansen, K.M., 2002. Modeling the effects of concentration history on the slow desorption of trichloroethene from a soil at 100% relative humidity. *Journal of Contaminant Hydrology,* 54(4): 307-327.

Werth, C.J. and Reinhard, M., 1997. Effects of temperature on trichloroethylene desorption from silica gel and natural sediments. 1. Isotherms. *Environmental Science and Technology,* 31(3): 689-696.

Whicker, F.W., and Kirchner, T.B., 1987. Pathway: a dynamic food-chain model to predict radionuclide ingestion after fallout deposition. *Health Physics*, 52: 717–737.

Yeh, G.T., 1987. *FEMWATER: A Finite Element Model of WATER Flow through Saturated- Unsaturated Porous Media—First Revision, ORNL-5567/R1*. Oak Ridge National Laboratory, Oak Ridge, TN.

Yeh, G.T., 1990. A Lagrangian-Eulerian Method with zoomable hidden fine-mesh approach to solving advection-dispersion equations. *Water Resour. Res.*, 26(6): 1133-1144.

Zacharof, A. I. and Butler, A. P., 2004b. Stochastic modelling of landfill processes incorporating waste heterogeneity and data uncertainty. *Waste Management,* 24: 241-250.

Zacharof, A.I., and Butler, A.P., 2004. Stochastic modelling of landfill leachate and biogas production incorporating waste heterogeneity: Model formulation and uncertainty analysis. *Waste Management*, 24(5): 453-462.

Zhang, Q., John, C.C., David, S., James, R.M., 2003. Development and evaluation of an environmental multimedia fate model CHEMGL for the Great Lakes region. *Chemosphere*, 50: 1377–1397.

Zheng, C., and Jiao, J.J., 1998. Numerical simulation of tracer tests in a heterogeneous aquifer. *Journal of Environmental Engineering,* 124(6): 510-516.

Zheng, C.M., and Wang, P.P., 1998. *MT3DMS: A Modular Three-Dimensional Multi-Species Model for Simulation of Advection, Dispersion and Chemical Reactions of Contaminants in Groundwater Systems: Documentation and User's Guide, SERDP-99-1*, 98-101. U.S. Army Engineer Research and Development Center, Vicksburg, MS.

Appendix.

A: Finite-Difference Method (FDM)

One of the widely used numerical techniques to solve partial differential equations is the finite-difference method. It proceeds by replacing the derivatives in the equation by finite differences and involves an initial discretization of domain. It is a simple and efficient method for solving ordinary differential equations (ODEs) in problem regions with simple boundaries. The method requires the construction of a mesh defining local coordinate surfaces. For each node of this mesh, the unknown function values are found, replacing the differential equations by difference equations,

Suppose we are interested in solving a continuity equation over the space interval $0<Z<L$ (depth of the landfill) and the time interval $0<t<T$. We compute a numerical solution by estimating C (t, z) over a uniform grid consisting of m+1 values of t and n+2 values of z as shown in Figure A-1.

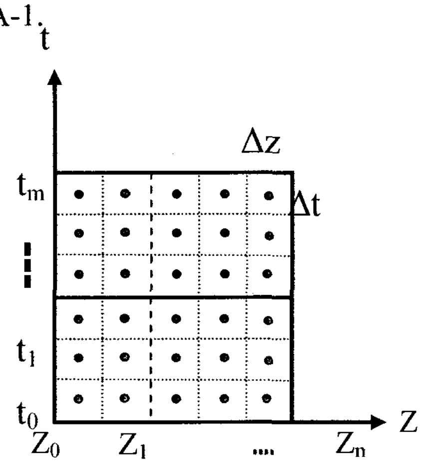

Figure A-1 Grid used to obtain a numerical solution to the continuity equation

For simplicity's sake, let Δt and Δz denote the step sizes of the variables t and z, respectively.

$$\Delta t = T/m \text{ and } \Delta = L/(n+1) \tag{A.1}$$

To simplify the final equations, let t_k and z_j denote the values of z at the grid points. That is,

$$t_k = k\Delta t, \quad 0 \leq k \leq m \tag{A.2}$$

$$z_j = k\Delta z, \quad 0 \leq j \leq (n+1) \tag{A.3}$$

Let C_j^k denote the computed value of C (t_k, z_j). We need initial and boundary condition to get unique solution to the problem. The initial and boundary conditions will be of the form:

$$C\ (0,\ z) = f\ (z),\quad 0<z<L \tag{A.4}$$

$$C\ (t,\ 0) = g1\ (t),\quad t>0 \tag{A.5}$$

$$C\ (t,\ L) = g2\ (t),\quad t>0 \tag{A.6}$$

There are several finite difference methods. Each method has some advantages and disadvantages in term of stability, convergence and required time for calculation. We mainly consider the explicit forward Euler method. This method states that the first-order derivative can be approximated with a two point forward Euler difference, while the second-order derivative can be approximated with a three-point central difference. When smooth, we can use a 2nd order central difference, if discontinuity occurs, it must shift to a one–sided difference scheme, because in this advection-dispersion-reaction equation, it is smooth in the procedure, so we could use the following derivatives.

$$\frac{\partial^2 C}{\partial z^2} = \frac{C_{j+1} - 2C_j + C_{j-1}}{\Delta z^2} + O(\Delta z^2) \text{ Central difference} \tag{A.7}$$

$$\frac{\partial^2 C}{\partial z^2} = \frac{C_{k,j} - 2C_{k,j+1} + c_{k,j-2}}{\Delta z^2} + O(\Delta z) \text{ Backward} \tag{A.8}$$

$$\frac{\partial^2 C}{\partial z^2} = \frac{C_{k,j} - 2C_{k,j+1} + C_{k,j+2}}{\Delta z^2} + O(\Delta z) \text{ Forward} \tag{A.9}$$

Here, we choose the central difference, then we get,

$$\frac{C_{k+1,j} - C_{k,j}}{\Delta t} = D_E\left(\frac{C_{k,j+1} - 2C_{k,j} + C_{k,j-1}}{\Delta z^2}\right) - V_E\left(\frac{C_{kj} - C_{k,j-1}}{\Delta z}\right) - \mu C_{k,j} \tag{A.10}$$

The formulation in Equation (A.10) is referred to as the explicit forward Euler method because the time derivative is represented with a forward Euler approximation, and the solution at time t_{k+1} can be solved explicitly as follows:

$$C_{k+1,j} = (\alpha + \gamma)C_{k,j-1} + (1 - 2\gamma - \alpha - \mu)C_{k,j} + \gamma C_{k,j+1} \tag{A.11}$$

Where $\alpha and \gamma$ are positive quantity and are defined as,

$$\gamma = \frac{D_E \Delta t}{\Delta z^2} \qquad \alpha = \frac{V_E \Delta t}{\Delta z} \tag{A.12}$$

B: Finite-Element Method (FEM)

The finite element method has proven to be a powerful technique to solve a variety of science and engineering problems. In recent years, finite element technique has become very popular in the field of engineering to provide solution of various problems. In the present study, finite element technique was mainly used to model multimedia pollutants transport.

We first divide the field into a series of finite line elements of equal length, which join one another at nodal points on the x, y-axis. Both the elements and the nodal points are indexed. We then assume a trial solution of the form as follows:

$$\left.\frac{\partial^r C}{\partial x^r}\right|_{x=x_i} = \sum_{k=1}^{Nx} A_{ik}^{(r)} C_{kj}, i = 1,2,...,N_x;$$
$$\left.\frac{\partial^s C}{\partial x^s}\right|_{y=y_i} = \sum_{l=1}^{Ny} A_{jl}^{(s)} C_{li}, j = 1,2,...,N_y; \tag{B.1}$$

where,

k, l is the node index,

N_x, N_y is the total number of nodes,

C_{li}, C_{kj} are the concentration functions at nodal point k, l., and

A_{ik}, A_{jl} are the interpolation functions, or basis functions, which were calculated according to the following equations: When r=1,

$$A_{ik}^{(1)} = \frac{\Pi(x_i)}{(x_i - x_k)\Pi(x_k)};\ i,k = 1,2,...,N_x\ and\ k \neq i;$$
$$\Pi(x_i) = \prod_{v=1,v\neq i}^{N_x} (x_i - x_v),\quad \Pi(x_k) = \prod_{v=1,v\neq i}^{N_x} (x_k - x_v) \tag{B.2}$$

When $2 \le r \le (N_x-1)$,

$$A_{ik}^{(r)} = r[A_{ii}^{(r-1)} A_{ik}^{(1)} - \frac{A_{ik}^{(r-1)}}{(x_i - x_k)}];\ i,k = 1,2,...,N_x\ and\ k \neq i; \tag{B.3}$$

In this paper, we only consider the one-dimensional model, so we only consider r=1.

$$\frac{\partial C_\alpha}{\partial t} = D_\alpha \frac{\partial^2 C_\alpha}{\partial x^2} - V_\alpha \frac{\partial C_\alpha}{\partial x} - \mu_\alpha C_\alpha \tag{B.4}$$

If the trial solution C (x, t) were exact, it would satisfy equation:

$$D_\alpha \frac{\partial^2 C_\alpha}{\partial x^2} - V_\alpha \frac{\partial C_\alpha}{\partial x} - \mu_\alpha C_\alpha - \frac{\partial C_\alpha}{\partial t} = 0 \tag{B.5}$$

Combining Equation B.5 and Equation B.1, we obtain:

$$\int (D_\alpha \frac{\partial^2 C_\alpha}{\partial x^2} - V_\alpha \frac{\partial C_\alpha}{\partial x} - \mu_\alpha C_\alpha - \frac{\partial C_\alpha}{\partial t}) A_i(x) dx = 0 \tag{B.6}$$

or equivalently,

$$\int D_\alpha \frac{\partial^2 C_\alpha}{\partial x^2} A_i(x) dx - \int V_\alpha \frac{\partial C_\alpha}{\partial x} A_i(x) dx - \int \frac{\partial C_\alpha}{\partial t} A_i(x) dx - \int \mu_\alpha C_\alpha A_i(x) dx = 0 \tag{B.7}$$

where,

$$\int \frac{\partial C_\alpha}{\partial t} A_i(x) dx = \sum \frac{\partial C_\alpha}{\partial t} \int A_i(x) A_j(x) = \frac{\Delta x}{6} \frac{\partial C_{j-1}}{\partial t} + \frac{2\Delta x}{3} \frac{\partial C_j}{\partial t} + \frac{\Delta x}{6} \frac{\partial C_{j+1}}{\partial t} \tag{B.8}$$

$$\int D_\alpha \frac{\partial^2 C_\alpha}{\partial x^2} A_i(x) dx = \frac{D_\alpha}{\Delta x} C_{j-1} - \frac{2D_\alpha}{\Delta x} C_j + \frac{D_\alpha}{\Delta x} C_{j+1} \tag{B.9}$$

$$\int Va \frac{\partial\, C_\alpha}{\partial x} A_i(x) dx + \mu C = \frac{V_a}{2} C_{j+1} - \frac{V_a}{2} C_{j-1} + \frac{\Delta x \mu}{6} C_{j-1} + \frac{2\Delta x \mu}{3} C_j + \frac{\Delta x \mu}{6} C_{j+1} \tag{B.10}$$

Now, combining expressions in Equation B.7-B.9, we obtain the final FEM solutions to Equation B.4 as follows:

$$a_j C_{j-1} + b_j C_j + d_j C_{j+1} = f_j \tag{B.11}$$

where,

$$a_j = \frac{(\Delta x)^2}{6\Delta t} - D - \frac{V_a \Delta x}{2} + \frac{\Delta x \mu}{6} \tag{B.12}$$

$$b_j = \frac{2(\Delta x)^2}{3\Delta t} + 2D + \frac{2\Delta x \mu}{3} \tag{B.13}$$

$$d_j = \frac{(\Delta x)^2}{6\Delta t} - D - \frac{V_a \Delta x}{2} + \frac{\Delta x \mu}{6} \tag{B.14}$$

$$f_j = (\frac{(\Delta x)^2}{6\Delta t} + \frac{\Delta x\mu}{6}) \times C_{j-1} + (\frac{2(\Delta x)^2}{3\Delta t} + \frac{2\Delta x\mu}{3}) \times C_j + (\frac{(\Delta x)^2}{6\Delta t} + \frac{\Delta x\mu}{6}) \times C_{j+1} \qquad \text{(B.15)}$$

The solution of Equation B.11 is subject to the following solutions: Using the fourth-order Runge-Kutta algorithm will solve the equations. The fourth-order Runge-Kutta algorithm is more accurate than the Euler algorithm and permits the use of larger tracking steps. However, the computational effort required by the fourth-order Runge-Kutta algorithm is considerably more than that required by the Euler algorithm, making the former less efficient than the latter for three-dimensional simulations when a very large number of particles are used.

C: Finite-Difference Method (FDM) for Two Dimensional Model

Applying the finite difference algorithm, the first partial derivatives representing the two components of the advection term at any finite difference cell, say *(i, j)* (see Figure C-1) can be approximated by the concentration values at the cell interfaces, as given below:

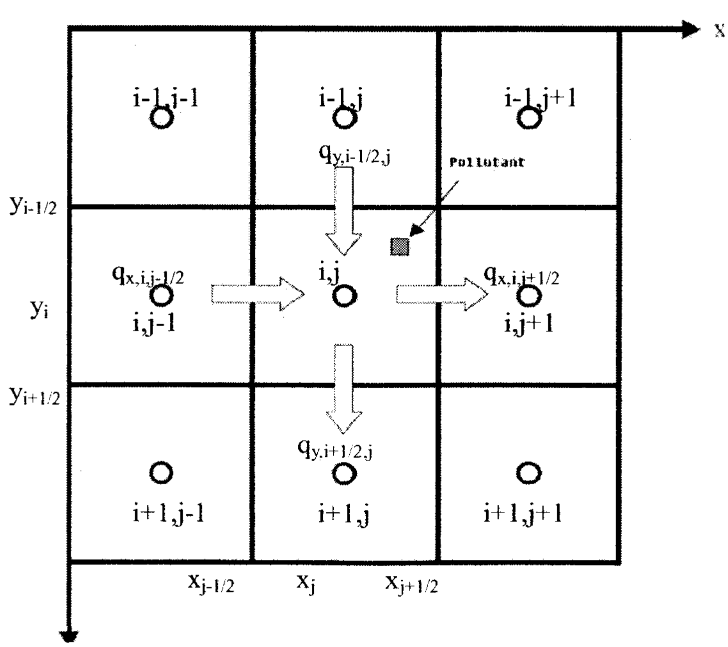

Figure C-1 Finite difference algorithm for two-dimensional equations

As shown in Figure C-1, according to cross derivatives, the first term in Equation 3-19 can be approximated at cell (i, j) as

$$D_{xx}\frac{\partial^2 C}{\partial x^2} = \frac{D_{xx(i,j+1/2)}(C_{i,j+1} - C_{i,j}) - D_{xx(i,j-1/2)}(C_{i,j} - C_{i,j-1})}{\Delta x^2} + O(\Delta x^2)$$

$$D_{xx}\frac{\partial^2 C}{\partial x^2} \approx \frac{D_{xx(i,j+1/2)}(C_{i,j+1} - C_{i,j}) - D_{xx(i,j-1/2)}(C_{i,j} - C_{i,j-1})}{\Delta x^2} \qquad \text{(C.1)}$$

Equation (C.1) represents the net dispersive flux into cell (*i,j*)in the *x* direction due to the concentration gradient in the *x* direction as shown in Figure C-1. The second term on the right-hand side of Equation (3.19) can be approximated as:

$$D_{xy}\frac{\partial^2 C}{\partial x \partial y}$$

$$= \frac{\partial}{\partial x}(D_{xy}\frac{\partial C}{\partial y}) \qquad \text{(C.2)}$$

$$= \frac{\partial}{\partial x}\left[\frac{D_{xy(i,j+1/2)}(C_{i+1,j+1/2} - C_{i-1,j+1/2}) - D_{xy(i,j-1/2)}(C_{i+1,j-1/2} - C_{i-1,j-1/2})}{2\Delta y}\right] + O(\Delta x^2, \Delta y^2)$$

whi

$$\approx \frac{1}{4\Delta x \Delta y}\left[D_{xy(i,j+1/2)}(C_{i+1,j+1} + C_{i+1,j} - C_{i-1,j+1} - C_{i-1,j}) - D_{xy(i,j-1/2)}(C_{i+1,j} + C_{i+1,j-1} - C_{i-1,j} - C_{i-1,j-1})\right]$$

ch represents the net dispersive flux into cell (*i,j*) in the *x* direction due to the concentration gradient in the *y* direction (Figure C-1). Note that the interface concentrations in Figure C-1, from nodal concentrations are:

$$C_{i+1,j+1/2} = \frac{C_{i+1,j+1} + C_{i+1,j}}{2} \tag{C.3}$$

Similarly, we can approximate the net dispersive flux into cell (*i, j*) in the *y* direction due to the concentration gradient in the *y* direction, that is, the third term on the right-hand side of Equation (3.19), as

$$D_{yy}\frac{\partial^2 C}{\partial y^2} = \frac{D_{yy(i+1/2,j)}(C_{i+1,j} - C_{i,j}) - D_{yy(i-1/2,j)}(C_{i,j} - C_{i-1,j})}{\Delta y^2} + O(\Delta x^2) \tag{C.4}$$

and the net dispersive flux into cell(*i,j*) in the *y* direction due to the concentration gradient in the *x* direction, namely, the fourth term on the right-hand side of Equation(3.19), as

$$\begin{aligned}
D_{yx}\frac{\partial^2 C}{\partial y \partial x} &= \frac{\partial}{\partial y}(D_{yx}\frac{\partial C}{\partial x}) \\
&= \frac{\partial}{\partial y}\left[\frac{D_{yx(i+1/2,j)}(C_{i+1/2,j+1} - C_{i+1/2,j-1}) - D_{yx(i-1/2,j)}(C_{i-1/2,j+1} - C_{i-1/2,j-1})}{2\Delta x}\right] + O(\Delta y^2, \Delta x^2) \\
&\approx \frac{1}{4\Delta y \Delta x}\left[D_{yx(i+1/2,j)}(C_{i+1,j+1} + C_{i,j+1} - C_{i+1,j-1} - C_{i,j-1}) - D_{yx(i-1/2,j)}(C_{i,j+1} + C_{i-1,j+1} - C_{i,j-1} - C_{i-1,j-1})\right]
\end{aligned} \tag{C.5}$$

Among them, the values of D_{xx} and D_{xy} at the interface (i, j+1/2) are computed as:

$$\begin{aligned}
D_{xx(i,j+1/2)} &= \frac{\alpha_L V_{x(i,j+1/2)}^{\;2}}{|V|} + \alpha_T \frac{V_{y(i,j+1/2)}^{\;2}}{|V|} \\
D_{xy(i,j+1/2)} &= \frac{(\alpha_L - \alpha_T) V_{x(i,j+1/2)} V_{y(i,j+1/2)}}{|V|} \\
|V| &= \sqrt{V^2_{\;x(i,j+1/2)} + V^2_{\;y(i,j+1/2)}}
\end{aligned} \tag{C.6}$$

where,

α_L and α_T are the dispersivity in the respective coordinate directions (m), and

V_x, V_y are the dispersion coefficient components, which are computed as:

$$V_{x(i,j+1/2)} = \frac{q_{x(i,j+1/2)}}{\theta}$$

$$V_{y(i,j+1/2)} = \frac{1}{2\theta}\left[\frac{(q_{y(i-1/2,j)}+q_{y(i+1/2,j)})+(q_{i-1/2,j+1}+q_{i+1/2,j+1})}{2}\right]+O(V_y^{\,2}) \tag{C.7}$$

$$\approx \frac{1}{2\theta}\left[\frac{(q_{y(i-1/2,j)}+q_{y(i+1/2,j)})+(q_{i-1/2,j+1}+q_{i+1/2,j+1})}{2}\right]$$

The fifth term on the right-hand side of equation represents the net advective flux into cell (i, j) in the x direction, which can be approximated as:

$$V_x\frac{\partial C}{\partial x} = \frac{V_{x(i,j+1/2)}\left\{\left[(1-\alpha)C_{i,j}+\alpha C_{i,j+1}\right]-V_{x(i,j-1/2)}\left[(1-\alpha)C_{i,j-1}+\alpha C_{i,j}\right]\right\}}{\Delta x}+O(\Delta x^2)$$

$$\approx \frac{V_{x(i,j+1/2)}\left\{\left[(1-\alpha)C_{i,j}+\alpha C_{i,j+1}\right]-V_{x(i,j-1/2)}\left[(1-\alpha)C_{i,j-1}+\alpha C_{i,j}\right]\right\}}{\Delta x} \tag{C.8}$$

The sixth term represents the net advective flux into cell (i,j) in the y direction, and can be approximated as

$$V_y\frac{\partial C}{\partial y} = \frac{V_{x(i+1/2,j)}\left\{\left[(1-\alpha)C_{i,j}+\alpha C_{i+1,j}\right]-V_{x(i-1/2,j)}\left[(1-\alpha)C_{i-1,j}+\alpha C_{i,j}\right]\right\}}{\Delta y}+O(\Delta y^2)$$

$$\approx \frac{V_{x(i+1/2,j)}\left\{\left[(1-\alpha)C_{i,j}+\alpha C_{i+1,j}\right]-V_{x(i-1/2,j)}\left[(1-\alpha)C_{i-1,j}+\alpha C_{i,j}\right]\right\}}{\Delta y} \tag{C.9}$$

where,

α is the spatial weighting factor, equal to 0.5 for the central scheme, and 0 or 1 for the upstream scheme depending on the direction of the flow vector at the cell interfaces.

The seventh and eighth terms on the right-hand side of equation are the net mass flux into or out of cell (i,j) resulting from the fluid sink/source term, and the mass lost or gained through the first-order reaction term within the cell(i,j). C, can be expressed as a function of the dissolved concentration.

At last, the left-hand side of Equation (3.19) is the rate of change in mass stored in cell (i, j), which can be approximated as

$$\frac{\partial C}{\partial t} = \frac{C_{i,j}^{n+1} - C_{i,j}^{n}}{\Delta t} + O(\Delta t) \approx \frac{C_{i,j}^{n+1} - C_{i,j}^{n}}{\Delta t} \tag{C.10}$$

When a contaminant compound is released to the environment, it will partition onto soils or subsurface solids as water moves through the system. The degree to which the contaminant is distributed between the sorbed and aqueous phases is described by the appropriate sorption isotherm for the compound and its concentration in the system. In the Equation (C.1), R, is the retardation factor, mentioned in one-dimensional models.

Finally, put Equations (C.1—C.10) into Equation (3.19), and selecting the fully implicit or crank-Nicolson scheme (shown in C-1), the concentrations at the new time level, C^{n+1} — the outcome is a simultaneous system of linear algebraic equations — can be expressed as:

$$\begin{aligned} & a_{i,j}C_{i-1,j-1}^{n+1} + b_{i,j}C_{i-1,j}^{n+1} + d_{i,j}C_{i-1,j+1}^{n+1} + e_{i,j}C_{i,j-1}^{n+1} + f_{i,j}C_{i,j}^{n+1} \\ & + g_{i,j}C_{i,j+1}^{n+1} + h_{i,j}C_{i+1,j-1}^{n+1} + o_{i,j}C_{i+1,j}^{n+1} + w_{i,j}C_{i+1,j+1}^{n+1} = p_{i,j}C_{i,j}^{n} \end{aligned} \tag{C.11}$$

Where,

$$
\begin{aligned}
a_{i,j} &= \frac{D_{xy(i,j-1/2)}}{4\Delta y\Delta x} + \frac{D_{yx(i-1/2,j)}}{4\Delta x\Delta y} \\
b_{i,j} &= \frac{D_{xy(i,j-1/2)}}{4\Delta x\Delta y} - \frac{D_{xy(i,j+1/2)}}{4\Delta x\Delta y} + \frac{D_{yy(i-1/2,j)}}{\Delta y^2} + \frac{V_{y(i-1/2,j)}*(1-\alpha)}{\Delta y} \\
d_{i,j} &= -\frac{D_{xy(i,j+1/2)}}{4\Delta x\Delta y} - \frac{D_{yx(i-1/2,j)}}{4\Delta y\Delta x} \\
e_{i,j} &= \frac{D_{xx(i,j-1/2)}}{\Delta x^2} - \frac{D_{yx(i+1/2,j)}}{4\Delta y\Delta x} + \frac{D_{yx(i-1/2,j)}}{4\Delta y\Delta x} + \frac{V_{x(i,j-1/2)}*(1-\alpha)}{\Delta x} \\
f_{i,j} &= -\frac{R}{\Delta t} - \frac{D_{xx(i,j+1/2)}+D_{xx(i,j-1/2)}}{\Delta x^2} - \frac{D_{yy(i+1/2,j)}+D_{yy(i-1/2,j)}}{\Delta y^2} + \\
&\frac{\alpha V_{x(i,j-1/2)}}{\Delta x} - \frac{V_{x(i,j+1/2)}*(1-\alpha)}{\Delta x} - \frac{V_{y(i+1/2,j)}*(1-\alpha)}{\Delta y} + \frac{\alpha V_{y(i-1/2,j)}}{\Delta y} \\
g_{i,j} &= \frac{D_{xx(i,j+1/2)}}{\Delta x^2} + \frac{D_{yx(i+1/2,j)}}{4\Delta y\Delta x} - \frac{D_{yx(i-1/2,j)}}{4\Delta y\Delta x} - \frac{\alpha V_{x(i,j+1/2)}}{\Delta x} \\
h_{i,j} &= -\frac{D_{xy(i,j-1/2)}}{4\Delta y\Delta x} - \frac{D_{yx(i+1/2,j)}}{4\Delta y\Delta x} \\
o_{i,j} &= \frac{D_{xy(i,j+1/2)}}{4\Delta x\Delta y} - \frac{D_{xy(i,j-1/2)}}{4\Delta x\Delta y} + \frac{D_{yy(i+1/2,j)}}{\Delta y^2} - \frac{\alpha V_{y(i+1/2,j)}}{\Delta y} \\
w_{i,j} &= \frac{D_{xy(i,j+1/2)}}{4\Delta x\Delta y} + \frac{D_{yx(i+1/2,j)}}{4\Delta y\Delta x} \\
p_{i,j} &= -\frac{R}{\Delta t}C^{n}_{i,j}
\end{aligned}
\tag{C.12}
$$

a, b, d, e, f, g, h, o, w on the left side and p, s on the right hand side are all known. Equation can be solved with an interative or direct matrix method. For the 3-dimentional model, the solution will be obtained in a similarity way. We do not mention these in details in the study.

D: Partial Matlab Code

```
% 2-D case study 1

vrsn.ext = ' snapshot';

vrsn.major = 0;

vrsn.build = 201;

vrsn.rcs = '$Name:   $';

vrsn.date = '$Date: 2007/08/03 16:02:35 $';

fem.version = vrsn;

% Constants

fem.const = {'R','3.215e-9', ...

  'Hin','5.3486', ...

  'K1','5e-6', ...

  'K2','0.0001', ...

  'Cin','1', ...

  'n','0.35', ...

  'alphaL','0.5', ...

  'alphaT','0.005', ...

  'Dm','1.34e-9'};

% Geometry

carr={curve2([0,250],[0,0],[1,1]), ...
```

```
  curve2([250,250],[0,5.35],[1,1]), ...
  curve2([250,180],[5.35,5.6000000000000005],[1,1]), ...
  curve2([180,155],[5.6000000000000005,6.045],[1,1]), ...
  curve2([155,127],[6.045,6.455],[1,1]), ...
  curve2([127,80],[6.455,6.6000000000000005],[1,1]), ...
  curve2([80,0],[6.6000000000000005,6.645],[1,1]), ...
  curve2([0,0],[6.645,0],[1,1])};
g1=geomcoerce('solid',carr);
g2=rect2(120,2,'base','corner','pos',[0,2]);
g3=rect2(70,2,'base','corner','pos',[180,2]);
% Analyzed geometry
clear s
s.objs={g1,g2,g3};
s.name={'CO1','R1','R2'};
s.tags={'g1','g2','g3'};
fem.draw=struct('s',s);
fem.geom=geomcsg(fem);
% Initialize mesh
fem.mesh=meshinit(fem, ...
                  'hauto',5);
% Initialize mesh
```

```
fem.mesh=meshinit(fem, ...
                  'hauto',5);
% Refine mesh
fem.mesh=meshrefine(fem, ...
                    'mcase',0, ...
                    'rmethod','regular');
% (Default values are not included)
% Application mode 1
clear appl
appl.mode.class = 'FlPDEC';
appl.dim = {'H','H_t'};
appl.assignsuffix = '_c';
clear bnd
bnd.type = {'dir','neu','neu'};
bnd.r = {'Hin',0,0};
bnd.g = {0,0,'-ny*R'};
bnd.ind = [2,2,2,2,2,2,3,3,2,3,3,2,2,2,3,1,1,1];
appl.bnd = bnd;
clear equ
equ.c = {'-K1','-K2'};
equ.da = 0;
```

```
equ.f = 0;

equ.ind = [1,2,2];

appl.equ = equ;

fem.appl{1} = appl;

% Application mode 2

clear appl

appl.mode.class = 'FlPDEC';

appl.dim = {'C','C_t'};

appl.name = 'c2';

appl.assignsuffix = '_c2';

clear prop

clear weakconstr

weakconstr.value = 'off';

weakconstr.dim = {'lm3','lm4'};

prop.weakconstr = weakconstr;

appl.prop = prop;

clear bnd

bnd.type = {'dir','neu','dir','neu','neu'};

bnd.r = {0,0,'Cin*(40<=x&t<=5*360*86400)',0,0};

bnd.g = {0,0,0,'K1*Hx/n*C','K2*Hx/n*C'};

bnd.ind = [1,2,1,2,1,2,3,1,2,1,1,2,2,2,1,4,5,4];
```

```
appl.bnd = bnd;

clear equ

equ.c = {{{'Dxx';'Dxy';'Dyy'}}};

equ.al = {{{'-vx';'-vy'}}};

equ.f = 0;

equ.ind = [1,1,1];

appl.equ = equ;

fem.appl{2} = appl;

fem.frame = {'ref'};

fem.border = 1;

clear units;

units.basesystem = 'SI';

fem.units = units;

% Subdomain settings

clear equ

equ.ind = [1,2,2];

equ.dim = {'H','C'};

% Subdomain expressions

equ.expr = {'vx',{'-K1*Hx/n','-K2*Hx/n'}, ...

  'vy',{'-K1*Hy/n','-K2*Hy/n'}, ...

  'absv','sqrt(vx^2+vy^2)', ...
```

```
  'Dxx','alphaL*vx^2/absv+alphaT*vy^2/absv+Dm', ...
  'Dyy','alphaL*vy^2/absv+alphaT*vx^2/absv+Dm', ...
  'Dxy','(alphaL-alphaT)*vx*vy/absv'};
fem.equ = equ;
% Multiphysics
fem=multiphysics(fem);
% Extend mesh
fem.xmesh=meshextend(fem);
% Solve problem
fem.sol=femstatic(fem, ...
                  'solcomp',{'H'}, ...
                  'outcomp',{'H','C'});
% Save current fem structure for restart purposes
fem0=fem;
% Plot solution
postplot(fem, ...
         'tridata',{'H','cont','internal'}, ...
         'trimap','jet(1024)', ...
         'title','Surface: H', ...
         'axisequal','off', ...
         'axis',[0,270,-2,10]);
```

```
% 2-D case study 2

% (Default values are not included)

% Application mode 1

clear appl

appl.mode.class = 'FlPDEC';

appl.dim = {'H','H_t'};

appl.assignsuffix = '_c';

clear bnd

bnd.type = {'dir','neu','neu'};

bnd.r = {'Hin',0,0};

bnd.g = {0,0,'-ny*R'};

bnd.ind = [2,2,2,2,2,2,3,3,2,3,3,2,2,2,3,1,1,1];

appl.bnd = bnd;

clear equ

equ.c = {'-K1','-K2'};

equ.da = 0;

equ.f = 0;

equ.ind = [1,2,2];

appl.equ = equ;

fem.appl{1} = appl;

% Application mode 2
```

```
clear appl

appl.mode.class = 'FlPDEC';

appl.dim = {'C','C_t'};

appl.name = 'c2';

appl.assignsuffix = '_c2';

clear prop

clear weakconstr

weakconstr.value = 'off';

weakconstr.dim = {'lm3','lm4'};

prop.weakconstr = weakconstr;

appl.prop = prop;

clear bnd

bnd.type = {'dir','neu','dir','neu','neu'};

bnd.r = {0,0,'Cin*(40<=x&t<=5*360*86400)',0,0};

bnd.g = {0,0,0,'K1*Hx/n*C','K2*Hx/n*C'};

bnd.ind = [1,2,1,2,1,2,3,1,2,1,1,2,2,2,1,4,5,4];

appl.bnd = bnd;

clear equ

equ.c = {{{'Dxx';'Dxy';'Dyy'}}};

equ.al = {{{'-vx';'-vy'}}};

equ.f = 0;
```

```
equ.ind = [1,1,1];

appl.equ = equ;

fem.appl{2} = appl;

fem.frame = {'ref'};

fem.border = 1;

clear units;

units.basesystem = 'SI';

fem.units = units;

% Subdomain settings

clear equ

equ.ind = [1,2,2];

equ.dim = {'H','C'};

% Subdomain expressions

equ.expr = {'vx',{'-K1*Hx/n','-K2*Hx/n'}, ...

  'vy',{'-K1*Hy/n','-K2*Hy/n'}, ...

  'absv','sqrt(vx^2+vy^2)', ...

  'Dxx','alphaL*vx^2/absv+alphaT*vy^2/absv+Dm', ...

  'Dyy','alphaL*vy^2/absv+alphaT*vx^2/absv+Dm', ...

  'Dxy','(alphaL-alphaT)*vx*vy/absv'};

fem.equ = equ;

% Multiphysics
```

```
fem=multiphysics(fem);

% Extend mesh

fem.xmesh=meshextend(fem);

% Solve problem

fem.sol=femtime(fem, ...
                'init',fem0.sol, ...
                'solcomp',{'C'}, ...
                'outcomp',{'H','C'}, ...
                'tlist',[0:360*86400:20*360*86400], ...
                'tout','tlist');

% Save current fem structure for restart purposes

fem0=fem;

% Plot solution

postplot(fem, ...
         'tridata',{'H','cont','internal'}, ...
         'trimap','jet(1024)', ...
         'solnum','end', ...
         'title','Time=6.2208e8     Surface: H', ...
         'axisequal','off', ...
         'axis',[0,270,-2,10]);

% Plot solution
```

```
postplot(fem, ...
        'tridata',{'H','cont','internal'}, ...
        'trimap','jet(1024)', ...
        'flowdata',{'Hx','Hy'}, ...
        'flowcolor',[1.0,0.0,0.0], ...
        'flowstart',{[15 30 45 60 75 90 130 145 160 175 190 205 220 235],[5 5 5 5 5 5 5 5
5 5 5 5 5 5]}, ...
        'flowmaxsteps',40000, ...
        'solnum','end', ...
        'title','Time=6.2208e8     Surface: H    Streamline: grad(H)    Streamline Color:
H', ...
        'axisequal','off', ...
        'axis',[-12.5,262.5,-0.3322499990463257,6.977249979972839]);
% Plot in cross-section or along domain
postcrossplot(fem,1,[7,8,10,11,15], ...
            'lindata','(H-y)/y', ...
            'cont','internal', ...
            'linxdata',{'x','unit','m'}, ...
            'solnum','end', ...
            'title','(H-y)/y', ...
            'axislabel',{'x-coordinate [m]','(H-y)/y'}, ...
```

```
            'refine','auto');

% Plot solution

postplot(fem, ...

        'tridata',{'C','cont','internal'}, ...

        'trimap','jet(1024)', ...

        'contdata',{'C','cont','internal'}, ...

        'contlevels',[0.05 0.1 0.15 0.19 0.25 0.30 0.35 0.4 0.45 0.5], ...

        'contlabel','off', ...

        'contmap','cool(1024)', ...

        'solnum',9, ...

        'title','Time=2.48832e8     Surface: C     Contour: C', ...

        'axisequal','off', ...

        'axis',[-12.5,262.5,-0.3322499990463257,6.977249979972839]);

% Plot solution

postplot(fem, ...

        'tridata',{'C','cont','internal'}, ...

        'trimap','jet(1024)', ...

        'contdata',{'C','cont','internal'}, ...

        'contlevels',[0.05 0.1 0.15 0.19 0.25 0.30 0.35 0.4 0.45 0.5], ...

        'contlabel','off', ...

        'contmap','cool(1024)', ...
```

```
        'solnum',13, ...
        'title','Time=3.73248e8    Surface: C    Contour: C', ...
        'axisequal','off', ...
        'axis',[-12.5,262.5,-0.3322499990463257,6.977249979972839]);
% Plot solution
postplot(fem, ...
        'tridata',{'C','cont','internal'}, ...
        'trimap','jet(1024)', ...
        'contdata',{'C','cont','internal'}, ...
        'contlevels',[0.05 0.1 0.15 0.19 0.25 0.30 0.35 0.4 0.45 0.5], ...
        'contlabel','off', ...
        'contmap','cool(1024)', ...
        'solnum','end', ...
        'title','Time=6.2208e8    Surface: C    Contour: C', ...
        'axisequal','off', ...
        'axis',[-12.5,262.5,-0.3322499990463257,6.977249979972839]);
clear vrsn
vrsn.ext = 'a';
vrsn.major = 0;
vrsn.build = 603;
vrsn.rcs = '$Name:  $';
```

```
vrsn.date = '$Date: 2008/12/03 17:02:19 $';

fem.version = vrsn;


% Plot solution

postplot(fem, ...

         'tridata',{'C','cont','internal'}, ...

         'trimap','Rainbow', ...

         'contdata',{'C','cont','internal'}, ...

         'contlevels',[0.05 0.1 0.15 0.19 0.25 0.30 0.35 0.4 0.45 0.5], ...

         'contlabel','off', ...

         'contmap','Rainbow', ...

         'solnum','end', ...

         'title','Time=6.2208e8      Surface: C     Contour: C', ...

         'axisequal','off', ...

         'axis',[-12.5,262.5,2.157145516196295,9.466645495215465]);

%1 D case study 2

% Iterate(A,b,N,Method,w)

%   will implement either Gauss -Seidel method,Finite-difference method(FDM)

%   or Finite-Element mathod(FEM)

%   iterative techniques to solve the problem

%               A x = b
```

```
%   The INPUTS are:
%                 A = nonsingular matrix
%                 b =    any vector (i.e. b=[1;2;3])
%                 N = number of iterations requested
%           Method = a string containing the method name:
%                         Method='Gauss '
%                         Method='FDM'
%                         Method='FEM'
%                 w = relaxation parameter if Method='FEM'
%   There are few built-in safeguards. If method is not
%   declared as one of the above, Fixed Point iteration
%   is used.The seed value is always x=0.
%   The OUTPUT is x. If A is n by n then x is a matrix
%   whose i-th row is the i-th iterate of x.
function [x,ELQ]=Iterate(A,b,N,Method,w)
n=length(b);
switch Method
   case('Gauss '),
   Q=diag(diag(A));
   disp('Gauss    seidel iteration');
   case('FDM'),
```

```
Q=tril(A);
disp('Finite-difference method Iteration');
case('FEM'),
Q=tril(A,-1)+diag(diag(A))/w;
disp('Finite-Element mathod iteration');
otherwise
Q=eye(n,n);
disp('fixed point')
end
LQ=eye(n,n)-inv(Q)*A;
ELQ=eig(LQ);
bQ=inv(Q)*b;
x=zeros(N,n);
x(1,:)=zeros(1,n);
for i=2:N,
y=LQ*x(i-1,:)'+bQ;
x(i,:)=y';
end
close all
clear all
L=1.22;
```

```
C0=1000;

d=0.305;

T=0.3*10^3;

u=log(2)/T;

k=151.5;

vg=0.0005;

vl=0.0005;

Qb=474;

R=27;

Koc=0.083;

foc=0.0125;

Kd=Koc*foc;

Kh=0.22;

sita=0.4;

a=0.15;

fi=sita+a;

Dlw=8.81*10^-5;

Dga=0.752;

Dg=Dga*(a)^(10/3)/fi^2;

Dl=(sita^(10/3)/fi^2)*Dlw;

Rl=Qb*Kd+sita+a*Kh;
```

```
He=(1/(d/Dg+1/k))*Kh/(Rl);

De=(Kh*Dg+Dl)/Rl;

Ve=(-vg*Kh+vl)/Rl;

Ms=0;

a1=Ve*(Ve+He)/(He*De);

a2=(Ve+2*He)*(Ve+He)/(He*De);

t=1:100:1050;

z=1.22;

    b2=He*L/De;

    if b2>709

        s8=exp(709);

    else

        s8=exp(b2);

    end

  m1=erfc((z-L-Ve*t)./(4*De*t).^0.5);

    m2=erfc((z-Ve*t)./(4*De*t).^0.5);

  b5=-u*t+(Ve*z)./De;

  if b5>709

      m3=exp(709);

  else

      m3=exp(b5);
```

```
    end
    m4=erfc((z+L+Ve*t)./(4*De*t).^0.5);
    m5=erfc((z+Ve*t)./(4*De*t).^0.5);
    b6=-u*t+((Ve*He*He^2)*t+(Ve+He)*z)./De;
    if b6>709
        m6=exp(709);
    else
        m6=exp(b6);
    end
    m7=erfc((z+(Ve+2*He)*t)./(4*De*t).^0.5);
    m8=erfc((z+L+(Ve+2*He)*t)./(4*De*t).^0.5);
    aa=Ve/De;
b=Ve*t;
m11=erfc((z-1-b)./(4*De*t).^0.5);
m22=erfc((z-1+b)./(4*De*t).^0.5);
C1=0.5*C0*R*exp(-u*t).*(m1-m2)+0.5*m3.*(m4-m5)+0.5*m6.*(m7-s8.*m8);
J1=He*C1;
hold on; plot(t,J1, 'b-.');
clear all
L=1.22;
d=0.05;
```

```
T0=0.3*10^3;

Rvg=0.05;

Rvl=0.05;

Qb=474;

Koc=0.083;

k=90.5;

foc=0.0125;

Kd=Koc*foc;

Kh=0.22;

sita=0.4;

a=0.15;

fi=sita+a;

Dlw=8.81*10^-5;

Dga=0.752;

Dg=Dga*(a)^(10/3)/fi^2;

Dl=(sita^(10/3)/fi^2)*Dlw;

Rl=Qb*Kd+sita+a*Kh;

He=2400*(1/(d/Dg+1/k))*Kh/(Rl);

r=1+Qb*Kd/sita;

u=log(2)/(r*T0);

De=(Kh*Dg+Dl)/r;
```

```
Ve=(-Rvg*Kh+Rvl)/r;

R=1;

T=0.3*10^3;

u=log(2)/T;

z=1;

T=1000;

m=50;

a1=0.5;

dt=T/m;

dx=z/m;

a=(dt*De/dx^2+(1-a1)*Ve*dt/dx)/R;

b=(-2*dt*De/dx^2-(1-2*a1)*Ve*dt/dx-u*dt)/R-1;

c=(dt*De/dx^2-a1*Ve*dt/dx)/R;

aj=dx^2/(6*dt)-De-Ve*dx/2;

bj=2*dx^2/(3*dt)+2*De-u;

cj=dx^2/(6*dt)-De+Ve*dx/2;

fj1=(dx)^2/(6*dt);

fj2=2*dx^2/(3*dt);

fj3=dx^2/(6*dt);

p=zeros(m,m);

v=zeros(m,1);
```

```
for i=1:m
 for j=1:m
        if (i==j)&(j<=m-1)
        p(i,j)=b;
        elseif (i==j)&(j==m)
        p(i,j)=b+c;
        elseif (i==j+1)
        p(i,j)=a;
        elseif (i==j-1)
        p(i,j)=c;
        else
        p(i,j)=0;
        end;
  end;
end;
for k=1:m
        if (k==1)
               v(k,1)=0-a;
        else
         v(k,1)=0;
        end;
```

```
end;

 [xGauss ,ELQGauss ]=Iterate(p,v,20,'gauss',0);

[xFDM,ELQFDM]=Iterate(p,v,20,'FDM',0);

[xFEM,ELQFEM]=Iterate(p,v,20,'FEM',1.2);

xgauss0=xgauss(20,:);

xgauss1=[1;xgauss0'];

xgauss1=He*xgauss1;

xFDM0=xFDM(20,:);

xFDM1=[1;xFDM0'];

xFDM1=He*xFDM1;

xFEM0=xFEM(20,:);

xFEM1=[1;xFEM0'];

xFEM1=He*xFEM1;

t=[0:dt:T]';

x=[0:dx:z]';

B=[t;xgauss1; xFDM1; xFEM1];

fid=fopen('emission1.txt','at');

fprintf(fid,'%g %e\n',B);

fclose(fid)

plot(t,xgauss1,'-r'); hold on;

plot(t,xFDM1,'m-'); hold on;
```

```
plot(t,xFEM1,'--k');

hold on;

hold on;plot(12*30,39.6,'g*');

hold on;plot(14*30,12.7,'g*');

hold on;plot(17*30,5.4,'g*');

hold on;plot(19*30,3.3,'g*');

hold on;plot(25*30,1.1,'g*');

hold on;plot(29*30,1.0,'g*');

hold on;plot(31*30,0.7,'g*');

hold on;plot(32*30,0.6,'g*');

hold on;plot(33*30,0.5,'g*');

hold on;plot(34*30,0.4,'g*');

hold on;plot(12*30,92.4,'y+');

hold on;plot(14*30,29.7,'y+');

hold on;plot(17*30,12.7,'y+');

hold on;plot(19*30,7.8,'y+');

hold on;plot(25*30,2.6,'y+');

hold on;plot(29*30,2.3,'y+');

hold on;plot(31*30,1.7,'y+');

hold on;plot(32*30,1.3,'y+');

hold on;plot(33*30,1.2,'y+');
```

```
hold on;plot(34*30,1,'y+');
hold on;plot(12*30,61.25,'r.');
hold on;plot(14*30,29.34,'r.');
hold on;plot(17*30,15.7,'r.');
hold on;plot(19*30,4.5,'r.');
hold on;plot(25*30,3.3,'r.');
hold on;plot(29*30,1.89,'r.');
hold on;plot(31*30,1,'r.');
hold on;plot(32*30,1.1,'r.');
hold on;plot(33*30,1.03,'r.');
hold on;plot(34*30,0.6,'r.');
h = legend(' analytical model','Gauss','FEM','FDM','High bound of predicted emission
flux','low bound of predicted emission flux','experimental dat(Rickabaugh 1990)', 10);
set(h,'Interpreter','none')
xlabel('t (days)','FontSize',10);
ylabel('emission mass flux Jt (mg/m^2/day)','FontSize',10);
% 1D case study 1
clear all
close all
% input parameter
z=3.5;
```

```
T=0.365*10^3;
u=log(2)/T;
Ax=100;
Ay=100;
ax=3;
ay=0.3;
az=0.03;
C0=0.001;
Qb=1590;
Qf=1;
Koc=0.082;
foc=0.0125;
Kd=Koc*foc;
Kh=0.22;
sita=0.4;
a=0.2;
v=0.03;
R=Qb*Kd/sita+1;
H=(2*az*Ax)^0.5+R*(1-exp(-Ax*Qf/(v*sita*R)));
for x=1:0.5:40
    for y=-80:2:80
```

```
z=3.5;

t=300;

s=0.5*x/ax*(1-(1+4*u*ax*R/v)^0.5);

b1=0.5*(x-(v*t/R)*((1+4*u*ax*R/v)^0.5))/(ax*v*t/R)^0.5;

if b1>26.5

      s1=erfc(20);

else

    s1=erfc(b1);

end

b2=0.5*(y+Ay/2)/(ay*x)^0.5;

if b2>26.5

      s2=1-erfc(20);

else

    s2=1-erfc(b2);

end

b3=0.5*(y-Ay/2)/(ay*x)^0.5;

if b3>26.5

      s3=1-erfc(20);

else

    s3=1-erfc(b3);

end
```

```
b4=0.5*(z+H)/(az*x)^0.5;
if b4>26.5
        s4=1-erfc(20);
else
      s4=1-erfc(b4);
end
b5=erf(0.5*(z-H)/(az*x)^0.5);
if b5>26.5
        s5=1-erfc(20);
else
      s5=1-erfc(b5);
end
C1=C0*exp(s)*s1*(s2-s3)*(s4-s5)/8;
plot3(x,y,C1,'r-');
hold on;
end;
end;
xlabel('x-distance (m)','FontSize',15);
ylabel('y-distance(m)','FontSize',15);
zlabel('concentration (g/m^3/day)','FontSize',15);
close all
```

```
clear all
L=1;
C0=1;
d=0.01;
T=0.365*10^3;
u=log(2)/T;
k=151.5;
vg=0.16;
vl=0.0005;
Qb=1350;
R=2.7;
Koc=0.083;
foc=0.0125;
Kd=Koc*foc;
Kh=0.22;
sita=0.3;
a=0.2;
fi=sita+a;
Dlw=8.81*10^-5;
Dga=0.752;
Dg=Dga*(a)^(10/3)/fi^2;
```

```
Dl=(sita^(10/3)/fi^2)*Dlw;

Rl=Qb*Kd+sita+a*Kh;

He=(1/(d/Dg+1/k))*Kh/(Rl);

De=(Kh*Dg+Dl)/Rl;

Ve=(-vg*Kh+vl)/Rl;

Ms=0;

a1=Ve*(Ve+He)/(He*De);

a2=(Ve+2*He)*(Ve+He)/(He*De);

t=1:0.5:90;

z=1;

    b2=He*L/De;

    if b2>709

        s8=exp(709);

    else

        s8=exp(b2);

    end

  m1=erfc((z-L-Ve*t)./(4*De*t).^0.5);

    m2=erfc((z-Ve*t)./(4*De*t).^0.5);

  b5=-u*t+(Ve*z)./De;

  if b5>709

      m3=exp(709);
```

```
    else
        m3=exp(b5);
    end
    m4=erfc((z+L+Ve*t)./(4*De*t).^0.5);
    m5=erfc((z+Ve*t)./(4*De*t).^0.5);
    b6=-u*t+((Ve*He*He^2)*t+(Ve+He)*z)./De;
    if b6>709
        m6=exp(709);
    else
        m6=exp(b6);
    end
    m7=erfc((z+(Ve+2*He)*t)./(4*De*t).^0.5);
    m8=erfc((z+L+(Ve+2*He)*t)./(4*De*t).^0.5);
    aa=Ve/De;
b=Ve*t;
m11=erfc((z-1-b)./(4*De*t).^0.5);
m22=erfc((z-1+b)./(4*De*t).^0.5);
C1=0.5*C0*R*exp(-u*t).*(m1-m2)+0.5*m3.*(m4-m5)+0.5*m6.*(m7-s8.*m8);
J1=He*C1;
hold on; plot(t,J1, 'b*');
```

```
C11=0.5*C0*R*(exp(aa*(z)).*m22+m11);

J11=He*C11;

hold on; plot(t,J11, 'g.');

clear all

L=1;

d=0.01;

T0=0.365*10^3;

vg=0.05;

vl=0.05;

Qb=1350;

Koc=0.083;

k=90.5;

foc=0.0125;

Kd=Koc*foc;

Kh=0.22;

sita=0.3;

a=0.2;

fi=sita+a;

Dlw=8.81*10^-5;

Dga=0.752;

Dg=Dga*(a)^(10/3)/fi^2;
```

```
Dl=(sita^(10/3)/fi^2)*Dlw;

Rl=Qb*Kd+sita+a*Kh;

He=(1/(d/Dg+1/k))*Kh/(Rl);

r=1+Qb*Kd/sita;

u=log(2)/(r*T0);

De=(Kh*Dg+Dl)/r;

Ve=(-vg*Kh+vl)/r;

R=1;

T=0.365*10^3;

u=log(2)/T;

z=1;

T=90;

m=9;

a1=0.5;

dt=T/m;

dx=z/m;

a=(dt*De/dx^2+(1-a1)*Ve*dt/dx)/R;

b=(-2*dt*De/dx^2-(1-2*a1)*Ve*dt/dx-u*dt)/R-1;

c=(dt*De/dx^2-a1*Ve*dt/dx)/R;

aj=dx^2/(6*dt)-De-Ve*dx/2;

bj=2*dx^2/(3*dt)+2*De-u;
```

```
cj=dx^2/(6*dt)-De+Ve*dx/2;

fj1=(dx)^2/(6*dt);

fj2=2*dx^2/(3*dt);

fj3=dx^2/(6*dt);

p=zeros(m,m);

v=zeros(m,1);

for i=1:m

  for j=1:m

        if (i==j)&(j<=m-1)

        p(i,j)=b;

        elseif (i==j)&(j==m)

        p(i,j)=b+c;

        elseif (i==j+1)

        p(i,j)=a;

        elseif (i==j-1)

        p(i,j)=c;

        else

        p(i,j)=0;

        end;

   end;

 end;
```

```
for k=1:m
    if (k==1)
        v(k,1)=0-a;
    else
     v(k,1)=0;
    end;
end;
 [xgauss,ELQgauss]=Iterate(p,v,20,'gauss',0);
[xFDM,ELQFDM]=Iterate(p,v,20,'FDM',0);
[xFEM,ELQFEM]=Iterate(p,v,20,'FEM',1.2);
xgauss0=xgauss(20,:);
xgauss1=[1;xgauss0'];
xgauss1=He*xgauss1;
xFDM0=xFDM(20,:);
xFDM1= [1;xFDM0'];
xFDM1=He*xFDM1;
xFEM0=xFEM(20,:);
xFEM1= [1;xFEM0'];
xFEM1=He*xFEM1;
t=[0:dt:T]';
```

```
x=[0:dx:z]';

B=[t;xgauss1; xFDM1; xFEM1];

fid=fopen('emission1.txt','at');

fprintf(fid,'%g %e\n',B);

fclose(fid)

plot(t,xgauss1,'-r'); hold on;

plot(t,xFDM1,'m-'); hold on;

plot(t,xFEM1,'--k');

hold on;

h = legend('Phyical analytical model(Lin and Hildemann 1995)',' anlytical

model','xgauss1','xFDM1', 'xFEM1',10);

set(h,'Interpreter','none')

xlabel('t (days)','FontSize',10);

ylabel('emission mass flux Jt (g/m^2/day)','FontSize',10);
```